



UNIVERSITAT DE
BARCELONA

Metal-dependent 2-oxoacid aldolases as versatile biocatalysts for the synthesis of chiral multifunctional compounds

Roser Marín Valls

ADVERTIMENT. La consulta d'aquesta tesi queda condicionada a l'acceptació de les següents condicions d'ús: La difusió d'aquesta tesi per mitjà del servei TDX (www.tdx.cat) i a través del Dipòsit Digital de la UB (diposit.ub.edu) ha estat autoritzada pels titulars dels drets de propietat intel·lectual únicament per a usos privats emmarcats en activitats d'investigació i docència. No s'autoritza la seva reproducció amb finalitats de lucre ni la seva difusió i posada a disposició des d'un lloc aliè al servei TDX ni al Dipòsit Digital de la UB. No s'autoritza la presentació del seu contingut en una finestra o marc aliè a TDX o al Dipòsit Digital de la UB (framing). Aquesta reserva de drets afecta tant al resum de presentació de la tesi com als seus continguts. En la utilització o cita de parts de la tesi és obligat indicar el nom de la persona autora.

ADVERTENCIA. La consulta de esta tesis queda condicionada a la aceptación de las siguientes condiciones de uso: La difusión de esta tesis por medio del servicio TDR (www.tdx.cat) y a través del Repositorio Digital de la UB (diposit.ub.edu) ha sido autorizada por los titulares de los derechos de propiedad intelectual únicamente para usos privados enmarcados en actividades de investigación y docencia. No se autoriza su reproducción con finalidades de lucro ni su difusión y puesta a disposición desde un sitio ajeno al servicio TDR o al Repositorio Digital de la UB. No se autoriza la presentación de su contenido en una ventana o marco ajeno a TDR o al Repositorio Digital de la UB (framing). Esta reserva de derechos afecta tanto al resumen de presentación de la tesis como a sus contenidos. En la utilización o cita de partes de la tesis es obligado indicar el nombre de la persona autora.

WARNING. On having consulted this thesis you're accepting the following use conditions: Spreading this thesis by the TDX (www.tdx.cat) service and by the UB Digital Repository (diposit.ub.edu) has been authorized by the titular of the intellectual property rights only for private uses placed in investigation and teaching activities. Reproduction with lucrative aims is not authorized nor its spreading and availability from a site foreign to the TDX service or to the UB Digital Repository. Introducing its content in a window or frame foreign to the TDX service or to the UB Digital Repository is not authorized (framing). Those rights affect to the presentation summary of the thesis as well as to its contents. In the using or citation of parts of the thesis it's obliged to indicate the name of the author.



**METAL-DEPENDENT 2-OXOACID ALDOLASES AS
VERSATILE BIOCATALYSTS FOR THE SYNTHESIS OF
CHIRAL MULTIFUNCTIONAL COMPOUNDS**

UNIVERSITAT DE BARCELONA
FACULTAT DE FARMÀCIA I CIÈNCIES DE L'ALIMENTACIÓ
Programa de doctorat en Biotecnologia

INSTITUT DE QUÍMICA AVANÇADA DE CATALUNYA (IQAC)
CONSELL SUPERIOR D'INVESTIGACIONS CIENTÍFIQUES (CSIC)

**Roser Marín Valls
2021**

UNIVERSITAT DE BARCELONA
FACULTAT DE FARMÀCIA I CIÈNCIES DE L'ALIMENTACIÓ
Programa de doctorat en Biotecnologia

INSTITUT DE QUÍMICA AVANÇADA DE CATALUNYA (IQAC-CSIC)

**METAL-DEPENDENT 2-OXOACID ALDOLASES AS
VERSATILE BIOCATALYSTS FOR THE SYNTHESIS OF
CHIRAL MULTIFUNCTIONAL COMPOUNDS**

Memòria presentada per Roser Marín Valls per optar al títol de doctora per la
Universitat de Barcelona

Directors:

Tutora:

Dr. Pere Clapés Saborit
Dr. Karel Hernández Sánchez

Dra. Josefa Badia Palacín

Doctoranda:

Roser Marín Valls

Roser Marín Valls
2021

Als meus pares

Cover design by Clara Borràs Eroles

lacienciaclara@gmail.com

AGRAÏMENTS

M'agradaria poder donar les gràcies a totes les persones que m'han ajudat en la realització d'aquesta tesi, que després de quatre anys de feina, no en son poques.

Primerament, i com no pot ser d'altra manera, m'agradaria mencionar als Drs. Pere Clapés i Karel Hernández, els meus directors, per confiar en mi per dur a terme aquest projecte i per acompanyar-me en aquest procés. Pere, moltes gràcies per totes les hores que m'has dedicat, analitzant complicats espectres d'RMN, organitzant resultats, escrivint els articles i revisant-me aquesta tesi. La passió que tens per la investigació s'encomana i això fa que hagi estat un plaer formar part del teu grup de recerca. Karel, gracias por la infinita paciencia que has tenido, por todas las clases de teoría, por sentarte conmigo a discutir resultados cada vez que te lo he pedido, por preocuparte por mí y darme buenos consejos. Creo que no hubiera podido tener a nadie mejor a mi lado para enseñarme cómo trabajar en un laboratorio de química. També vull donar les gràcies al Dr. Jordi Bujons, que ha fet una gran feinada construint meticulosament els models computacionals i donant explicació als resultats obtinguts, i al Dr. Jesús Joglar per assistir a tots els seminaris i fer preguntes que obliguen a qüestionar-t'ho tot.

En segon lloc m'agradaria mencionar a tots els companys de laboratori que he tingut, alguns dels quals s'han convertit en molt bones amistats. Carlos, sin ti el trabajo en el laboratorio no hubiera sido lo mismo. Hemos aprendido juntos a manejar complicadas reacciones químicas con mil globos y cánulas, nos hemos podido hacer todas las confianzas del mundo en momentos difíciles y nos hemos reído de las situaciones absurdas. Ànims, que ja et queda poc! Mercè, gràcies per l'acollida del principi, per tots els moments divertits viscuts i per convertir-te en essencial els primers mesos de tesi. No menys importants son la Raquel, la Mireia, l'Ana, la Cristina i en Pol, que, com que ja han passat per aquesta etapa, estan sent els millors consellers del món. Sense ells els dinars no haurien estat el moment de desconexió i de diversió que esperava amb ganes cada dia. Tampoc em vull oblidar d'en Mathias, amb qui vam coincidir

poc temps però vam treballar colze a colze, i de l'Àngela, que s'ha convertit en la meua companya d'escriptori durant aquest últim any i m'ha animat i ajudat en aquesta recta final.

També vull agrair a la família i amics per aquest paper tant difícil que els ha tocat. Als meus pares pels valors transmesos, pels consells i el recolzament incondicional durant totes les etapes de la meua vida que m'han dut fins aquí. També a la meua germana Núria, a qui admiro per seguir sempre les seves idees i estar compromesa amb els seus. A la meua àvia, a la Laura, i a tots els meus tiets i cosins, perquè sense entendre ben bé el que faig sempre m'han donat el seu suport. Finalment donar les gràcies als amics que m'han acompanyat durant molts anys: Núria, Deya, Txema, Laia, companys de la universitat, companys de rem, Gerard... tot i que amb alguns no coincidim tant com voldríem, gràcies per aguantar-me el rotllo cada vegada que us he vist.

A tots vosaltres, moltes gràcies!

The work reported in this Doctoral Thesis has given rise to the following publications:

- 1) Marín-Valls, R., Hernandez, K., Bolte, M., Joglar, J., Bujons, J., & Clapes, P. (2019). Chemoenzymatic hydroxymethylation of carboxylic acids by tandem stereodivergent biocatalytic aldol reaction and chemical decarboxylation. *ACS Catalysis*, 9(8), 7568-7577.
- 2) Marín-Valls, R., Hernández, K., Bolte, M., Parella, T., Joglar, J., Bujons, J., & Clapés, P. (2020). Biocatalytic Construction of Quaternary Centers by Aldol Addition of 3, 3-Disubstituted 2-Oxoacid Derivatives to Aldehydes. *Journal of the American Chemical Society*, 142(46), 19754-19762.

TABLE OF CONTENTS

ABBREVIATIONS	1
SUMMARY	3
1 INTRODUCTION.....	5
1.1 Enzymes	7
1.2 Enzymes in organic synthesis	9
1.3 Protein engineering of enzymes	11
1.3.1 Rational design: structure guided protein engineering.....	11
1.3.2 Directed evolution.....	13
1.3.3 Semi-rational design.....	14
1.3.4 Approaches for protein sequence modifications	16
1.4 Aldol reactions	19
1.4.1 Aldolases	24
1.5 Ketopantoate hydroxymethyltransferase (EC 2.1.2.11)	27
1.5.1 Structure and catalytic mechanism of KPHMT.....	28
1.6 2-Keto-3-deoxy-L-rhamnonate aldolase (EC 4.1.2.53)	33
1.6.1 Structure and catalytic mechanism of YfaU.....	34
1.6.2 Biocatalytic applications of YfaU	37
1.7 Synthesis and applications of relevant chiral building blocks.....	40
1.7.1 Synthesis and applications of Roche esters derivatives	40
1.7.2 Synthesis and applications of compounds bearing quaternary centers	45
1.7.3 Synthesis and applications of nucleoside analogues	51
2 OBJECTIVES	57

3	RESULTS AND DISCUSSION.....	61
3.1	Chemoenzymatic synthesis of Roche ester derivatives.....	63
3.1.1	Introduction.....	65
3.1.2	KPHMT as biocatalyst in aldol additions of 2-oxoacids to formaldehyde.....	67
3.1.3	Study of the aldol addition of 2-oxobutanoate to formaldehyde catalyzed by MBP-YfaU or KPHMT.....	72
3.1.4	Synthesis and screening of a panel of 2-oxoacids.....	80
3.1.5	Construction of enzyme variants and screening with different nucleophiles.....	85
3.1.6	Preparative synthesis of Roche ester derivatives.....	93
3.1.7	Absolute stereochemistry determination.....	96
3.1.8	Summary.....	99
3.2	Biocatalytic construction of quaternary centers.....	101
3.2.1	Introduction.....	103
3.2.2	Synthesis of 3,3-disubstituted 2-oxoacids.....	104
3.2.3	Construction of new variants of KPHMT.....	108
3.2.4	Screening with formaldehyde.....	109
3.2.5	Study of KPHMT catalyzed aldol addition of 2-oxoacids to other aldehydes.....	113
3.2.6	Preparative synthesis and characterization of products obtained with aldehydes 2a,b,d.....	118
3.2.7	Preparative synthesis and characterization of products obtained with α -hydroxy aldehydes.....	131
3.2.8	Enzymatic cascade reactions.....	134
3.2.9	Summary.....	139

3.3	Preliminary studies of the application of KPHMT and MBP-YfaU on the synthesis of nucleoside analogues.....	141
3.3.1	Introduction	143
3.3.2	Enzymatic synthesis of lactone precursors using (<i>R</i>)-3-(benzyloxy)-2-hydroxypropanal as an electrophile in aldol reactions .	145
3.3.3	Use of D-glyceraldehyde as electrophile in aldol reactions..	150
3.3.4	Synthesis of α,α -disubstituted- α -hydroxy aldehydes	152
3.3.5	Enzymatic synthesis using aldehydes 2n-q as electrophiles in aldol reactions	157
3.3.6	Determination of the stereochemistry of 12c	160
3.3.7	Future perspectives.....	168
3.3.8	Summary	172
4	CONCLUSIONS.....	175
5	EXPERIMENTAL SECTION	179
5.1	Biological materials.....	181
5.1.1	Microorganisms.....	181
5.1.2	Vectors	181
5.1.3	Oligonucleotides.....	183
5.1.4	Culture media and solutions	184
5.2	Molecular biology techniques	184
5.2.1	Isolation and purification of plasmid DNA (Miniprep)	184
5.2.2	Agarose gel electrophoresis of DNA.....	185
5.2.3	Quantification of nucleic acids.....	185
5.2.4	Mutagenesis techniques.....	185
5.2.5	Heat shock transformation of the competent cells	191

5.2.6	Analysis of the DNA sequences.....	191
5.3	KPHMT expression and purification	191
5.3.1	Protein electrophoresis (SDS-PAGE)	192
5.3.2	Electrospray mass spectrometry of proteins.....	193
5.4	Chemical and analytical materials.....	194
5.5	Chemical and analytical general methods	194
5.5.1	Activity assay of KPHMT.....	195
5.5.2	Determination of the initial reaction rates	196
5.5.3	Determination of the effect of formaldehyde on the conversion of the aldol addition.....	196
5.5.4	2-Oxoacid stock solution preparation.....	197
5.5.5	Crystallization for X-ray structure determination	197
5.6	Synthesis and characterization of products from section 3.1	197
5.6.1	Synthesis of substrates	197
5.6.2	Enzymatic synthesis of phenacyl ester derivatives	202
5.6.3	Enzymatic synthesis of benzyl and 4-nitrobenzyl ester derivatives	212
5.6.4	Synthesis of derivatives for absolute stereochemistry determination.....	214
5.6.5	Catalytic hydrogenation of compounds <i>S</i> -6d and <i>R</i> -5c	216
5.6.6	Synthesis of racemic mixtures of products.....	217
5.7	Synthesis of compounds from section 3.2.....	217
5.7.1	Synthesis of 2-oxoacids.....	217
5.7.2	Synthesis of hydroxyaldehydes	220
5.7.3	Enzymatic synthesis of products 7a–j	221

5.7.4	Enzymatic synthesis of products 8a–g	226
5.7.5	Enzymatic synthesis of products 9a–q	229
5.8	Synthesis of compounds from section 3.3.....	239
5.8.1	Synthesis of intermediates C11–16	239
5.8.2	Synthesis of aldehydes 2m–q	246
5.8.3	Enzymatic synthesis of products 11a–d	247
5.8.4	Enzymatic synthesis of products 12a–e.....	249
5.8.5	Synthesis of intermediates C17–21	251
BIBLIOGRAPHY		257

ABBREVIATIONS

α-KIV	α -Ketoisovalerate
ACN	Acetonitrile
BTMA-ICl₂	Benzyltrimethylammonium dichloriodate
DCM	Dichloromethane
DHA	Dihydroxyacetone
DIBAL	Diisobutylaluminium hydride
DMF	<i>N,N</i> -Dimethylformamide
DMAP	4-Dimethylaminopyridine
DNA	Deoxyribonucleic acid
dr	Diastereomeric ratio
EC	Enzyme Commission number
ee	Enantiomeric excess
eq	Equivalent(s)
er	Enantiomeric ratio
Et₃N	Triethylamine
EtOAc	Ethyl acetate
Et₂O	Diethyl ether
FSA	D-Fructose-6-phosphate aldolase
HA	Hydroxyacetone
HPLC	High-performance liquid chromatography
IPTG	Isopropyl- β -D-1-thiogalactopyranoside
KP	Ketopantoate
KPHMT	Ketopantoate hydroxymethyltransferase
MBP	Maltose binding protein
MCPBA	<i>meta</i> -Chloroperoxybenzoic acid
MTBE	Methyl <i>tert</i> -butyl ether
MTHF	Methylene tetrahydrofolate

NBS	<i>N</i> -Bromosuccinimide
NMR	Nuclear magnetic resonance
OTf	Trifluoromethanesulfonate
PCR	Polymerase chain reaction
PDB	Protein data bank
PFPA	Pentafluoropropionic anhydride
PIDA	(Diacetoxyiodo)benzene
PMBCl	4-Methoxybenzyl chloride
rt	Room temperature
TCC	Trichloroisocyanuric acid
TEA	Triethanolamine
TFA	Trifluoroacetic acid
THF	Tetrahydrofuran
TLC	Thin layer chromatography
TMDMS	<i>tert</i> -Butyldimethylsilyl
Tris	Tris(hydroxymethyl)aminomethane
TsOH	<i>para</i> -Toluenesulfonic acid
YfaU	2-Keto-3-deoxy-L-rhamnonate aldolase
wt	Wild-type

SUMMARY

Biocatalysis gained importance in the latter half of the 20th century and its application in the pharmaceutical, food and chemical industries continues to expand nowadays. Enzymes catalyze chemical reactions in a highly selective manner, achieving high molecular complexity without the need of protection and deprotection steps and usually under mild reaction conditions. Particularly important classes of enzymes are aldolases, which catalyze stereoselectively carbon-carbon bond formation between a nucleophilic donor and an electrophilic acceptor. The aldol adducts are usually typified as β -hydroxycarbonyl compounds, a structural element that is frequently found in the framework of complex molecules. For this reason, advances in this field are focused on finding new aldolases with unprecedented activities and engineering those available for improved substrate tolerance and stereoselectivity.

In this thesis, we exploited the potential capacities of two Class II aldolases that utilize 2-oxoacids and aldehydes as substrates, to furnish different chiral molecules that are used as building blocks in organic chemistry. These are YfaU (2-keto-3-deoxy-L-rhamnonate aldolase, EC 4.1.2.53), which was used as a robust biocatalyst in previous investigations in our group, and KPHMT (ketopantoate hydroxymethyltransferase, EC 2.1.2.11), which was employed with synthetic applications for the first time in this present work.

In **chapter 3.1** MBP-YfaU and KPHMT were applied to the synthesis of 2-substituted 3-hydroxycarboxylate esters (i.e., Roche ester, 3-hydroxy-2-methylpropanoate), which are an important class of chiral building blocks widely used in organic synthesis. To do this, KPHMT from *E. coli* was cloned, expressed, and characterized (e.g., metal cofactor, nucleophile substrates, tolerance to formaldehyde). Then, a panel of different 2-oxoacids was synthesized, and based on molecular models, four variants of KPHMT were constructed to increase the substrate scope of this catalyst. Finally, the aldol addition of different 2-oxoacids to formaldehyde catalyzed by KPHMT and MBP-YfaU wild-type and variants was deeply studied and it was determined

that they generated stereocomplementary aldol adducts. Oxidative decarboxylation and esterification of the aldol adducts led to the formation of Roche ester derivatives with high isolated yields and excellent enantiomeric excesses.

In **chapter 3.2** KPHMT was used in the synthesis of compounds bearing quaternary carbon centers. To this end, 3,3-disubstituted 2-oxoacid nucleophiles and a panel of selected aldehydes were used as substrates. Based on molecular models, residue V214 was targeted for site directed mutagenesis and five new variants that were useful for the synthesis of these congested compounds were produced. Different methodologies on the aldol adducts rendered 2-oxolactones (including a bicyclic lactone), 3-hydroxyacid derivatives and ulosonic acid type products, all of them bearing *gem*-dialkyl, *gem*-cycloalkyl and spirocyclic quaternary centers.

In **chapter 3.3** preliminary studies for the application of KPHMT and MBP-YfaU to the synthesis of nucleoside analogues were performed. As substrates we selected 2-oxoacids and D-glyceraldehyde derivatives, including *O*-protected D-glyceraldehyde and α,α -disubstituted- α -hydroxy aldehydes. The subsequent oxidative decarboxylation of the aldol adducts rendered diverse lactones and carboxylic acids. These products with different substituents at C2 and at C4 can be used as precursors for the synthesis of nucleoside analogues.

1 INTRODUCTION

1.1 Enzymes

The rate of chemical reactions that occur within all living organisms are mostly regulated by enzymes. Without them, many of these reactions would not take place at a perceptible rate. Hence, an *enzyme* is a biological catalyst present in living organisms that regulates the rate at which chemical reactions proceed without itself being altered in the process.^{1,2} A paradigmatic example is the *de novo* biosynthesis of pyrimidines that requires the formation of uridine monophosphate (UMP) via the decarboxylation of orotidine monophosphate (OMP). The half-life of this chemical reaction is approximately 78 million years, which is not a rate that can sustain life on earth without some very significant enhancement. The enzyme OMP decarboxylase (EC 4.1.1.23) enhances the rate of decarboxylation by some 10^{23} -fold so that the reaction half-life of the enzyme-catalyzed reaction (0.018 seconds) displays the rapidity necessary for living organisms (Figure 1.1).

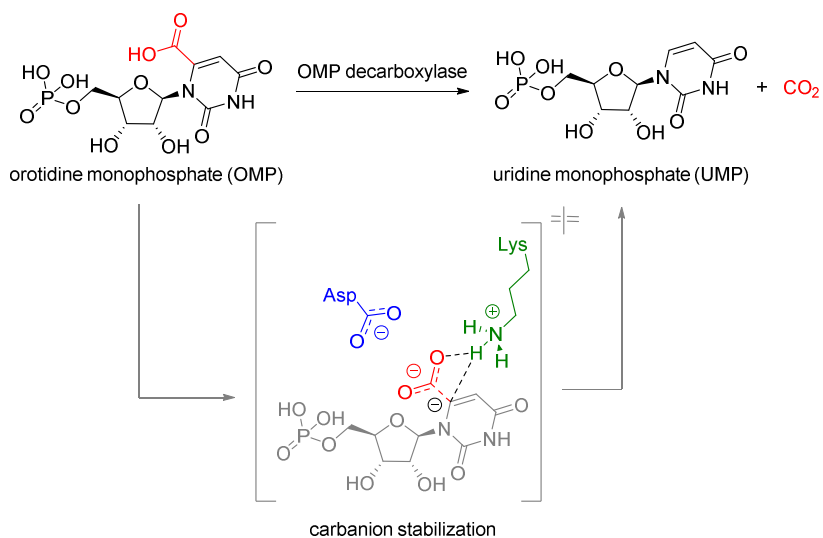


Figure 1.1 Synthesis of uridine monophosphate catalyzed by OMP decarboxylase. The enzyme stabilizes the carbanion and enhances the rate of OMP decarboxylation by a factor of 2×10^{23} over that of the non-catalyzed reaction, making it the most catalytically proficient enzyme known.

Introduction

Nearly all known enzymes are proteins (catalytically active RNA molecules are an exception) with a complex tertiary and quaternary structure determined by its primary amino acid sequence.³ Catalysis usually takes place in infoldings or pockets on the surface of the enzymes, known as *active sites*, with preferential transition state binding. In this way, enzymes catalyze reactions by decreasing the energy of transition states, the highest-energy species in reaction pathways.^{2,4}

The activity of many enzymes depends on the presence of small molecules called *cofactors*, which are able to execute chemical reactions that cannot be performed by the standard set of twenty amino acids. Among them, there are metal cations (e.g., Fe^{2+} , Mg^{2+} , Mn^{2+} , or Zn^{2+}) or complex organic or metalloorganic molecules called *coenzymes* (e.g., Coenzyme A, NAD^+ , PLP or ThDP). When a coenzyme or metal ion is very tightly or even covalently bounded to the enzyme is called a *prosthetic group*. A complete, catalytically active enzyme together with its bound cofactor is called *holoenzyme*. The protein part of such an enzyme is called the *apoenzyme* or apoprotein.¹

Enzymes are classified into six major groups based on the type of reaction catalyzed: i) *Oxidoreductases* (EC 1.x.x.x): oxidation-reduction reactions; ii) *Transferases* (EC 2.x.x.x): intermolecular transfer of a functional groups; iii) *Hydrolases* (EC 3.x.x.x): hydrolytic reactions; iv) *Lyases* (EC 4.x.x.x): breaking and formation (synthase) of various chemicals bounds by means other than hydrolysis and redox reactions; v) *Isomerases* (EC 5.x.x.x): isomerization by intramolecular transfer of functional groups and vi) *Ligases* (EC 6.x.x.x): bond formation coupled with ATP hydrolysis.^{2,5}

Many enzymes retain their catalytic potential after extraction from the living organism, and it did not take long for mankind to recognize and exploit the catalytic power of enzymes for commercial purposes. In fact, enzymes were early applied in the manufacture of cheeses, breads, and alcoholic beverages. As of today enzymes continue to play key roles in many food and chemicals manufacturing processes.

1.2 Enzymes in organic synthesis

Biocatalysis refers to the use of whole cells and enzymes, which may be purified or used as a cell-free extract, to catalyze chemical reactions.⁶ Advances in chemical catalysis and biocatalysis are determinants in reducing the environmental footprint of chemical processes. Biocatalytic transformations have emerged as a viable alternative to other asymmetric chemical methods due to the intrinsic high stereoselectivity of the enzymes and the mild reaction conditions.⁷⁻⁹

Enzymes differ from ordinary chemical catalysts in several important aspects. The rates of enzymatically catalyzed reactions are typically 10^6 to 10^{12} times higher than those of the corresponding non-catalyzed reactions and are at least several orders of magnitude greater than the chemically catalyzed. Moreover, enzymes have an elevated degree of specificity, regio-, stereo- and enantioselectivity, and, as a result, enzymatic reactions rarely produce side products. Finally, enzymatic catalysis operates under relatively mild conditions: room temperatures (typically around 25 °C and at most 37 °C), atmospheric pressure, aqueous solvent or green solvents, and nearly neutral pH. In contrast, chemical catalysis often requires anhydrous organic solvents, elevated pressures, extreme temperatures, and the presence of strong acids or bases.^{5,10-12}

However, enzymes have some limitations in *in vitro* reactions. They display their highest activity in water but usually this is the least suitable solvent for most organic reactions. The presence of organic solvents in the reaction media, high temperature, pH, or salt concentration may lead to the deactivation of some enzymes. For this reason, enzymatic processes require restricted operation parameters and there is a narrow window for alteration. Moreover, enzymes are prone to substrate and/or product inhibition phenomena, which can limit the efficiency of the process.^{5,6}

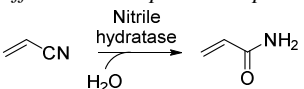
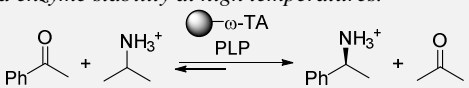
Introduction

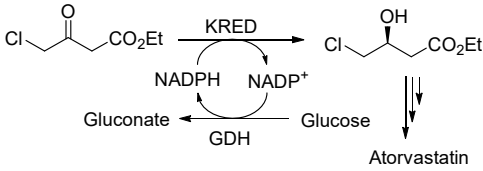
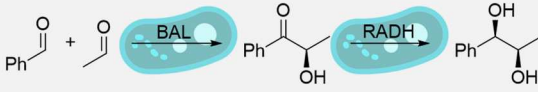
The fact that some enzymes are exclusively bound or activated by their natural cofactors is also a limitation. Cofactors such as NAD(P)H (shuttle of redox equivalents) or ATP (storage of chemical energy) are relatively unstable and prohibitively expensive to use in stoichiometric amounts. Cascade reactions have been envisaged to recycle these compounds and made possible the full substrate conversion using under stoichiometric cofactor concentrations. Therefore, biocatalysis is usually accepted for new products for which a chemical process is difficult or does not yet exist.^{5,9}

Nowadays, advances in molecular biology, biotechnology and genetic engineering can overcome some of these limitations (Table 1.1). For instance, the use of immobilized enzymes is now a routine process for the manufacture of many industrial products as it brings important advantages, such as simplified downstream processing or continuous process operations.^{12, 13}

The increasing knowledge into the understanding of protein structure and function, and the recent advances in high-throughput screening techniques and computational design, has made protein engineering an important tool for the development of new enzymes.

Table 1.1 Problem statements and solutions for the use of enzymes in organic synthesis.

Problems	Solutions
Price and availability	<p><u>Recombinant expression in a suitable host:</u></p> <p><i>Ex.: The efficient overexpression of nitrile hydratase (EC 4.2.1.84) in a suitable host offered a novel process to produce acrylamide.¹⁴</i></p>  <p><chem>C=CC#N.O>>C=CC(=O)N</chem></p>
Instability	<p><u>Immobilization to enhance stability and facilitate re-use</u></p> <p><i>Ex.: ω-Transaminases (EC 2.6.1.1) immobilized on different carriers allowed re-use of the enzyme for 8 cycles, with 250 h of operation retaining more than 50% initial activity and with increased enzyme stability at high temperatures.¹⁵</i></p>  <p><chem>CC(=O)c1ccccc1.N>>CC(N)c1ccccc1.CC(=O)C</chem></p>

<p>Dependency on expensive cofactors</p>	<p><u>Efficient recycling systems for NADH, NADPH and for ATP are available</u></p> <p><i>Ex.: Ketoreductase (KRED, EC 1.1.1.184), coupled with glucose 1-dehydrogenase (GDH, EC 1.1.1.47) for NADPH sub-stoichiometric regeneration, was applied in the first step to produce atorvastatin (drug that blocks the cholesterol synthesis in the liver). This multi-enzyme process makes it environmentally attractive and economically viable.¹⁴</i></p> 
<p>Difficulty on downstream processing</p>	<p><u>Use of whole cells in biocatalysis facilitates the downstream process</u></p> <p><i>Ex.: Application of lyophilized E. coli whole cells expressing benzoin aldolase (BAL, EC 4.1.2.38) and alcohol dehydrogenase (RADH, EC 1.1.1.71) for the synthesis of vicinal diols facilitates downstream process by easily removing of the catalyst and unreacted substrates.¹⁶</i></p> 

1.3 Protein engineering of enzymes

Protein engineering uses molecular biology techniques, to produce enzymes with optimized features such as activity, enantio-, regio- and chemo-selectivity, stability, substrate and cofactor specificity, tolerance of co-solvents and pH optimum among others. This facilitates biocatalyst applications expanding the toolbox of enzymes that can be used for organic synthesis.^{17, 18} There are three main approaches for enzyme engineering: rational design, directed evolution and semi-rational design.

1.3.1 Rational design: structure guided protein engineering

Rational design or structure guided protein engineering was the earliest developed approach to protein engineering since 1978 and has remained useful over decades. The strategy is mainly completed *in silico* and requires information on the amino acid sequence, three-dimensional structure, and catalytic mechanisms of the protein.¹⁸ This knowledge is used to make targeted

Introduction

amino acid mutations, usually by *site-directed mutagenesis*, which is predicted to affect enzymatic properties vital for the desired reaction (Figure 1.2).

In a sequence-based approach, systematic comparisons of homologous protein sequences are pursued to identify possible residues that could alter protein activity. When the three-dimensional crystal structure of the target enzyme is available, a more direct structure–function relationship study of residues within the active site can be investigated. Through this visualization, the active site structure can be redesigned, for example, mutating large residues to smaller hydrophobic residues, thus enlarging the active site allowing a larger substrate to accommodate.¹⁹

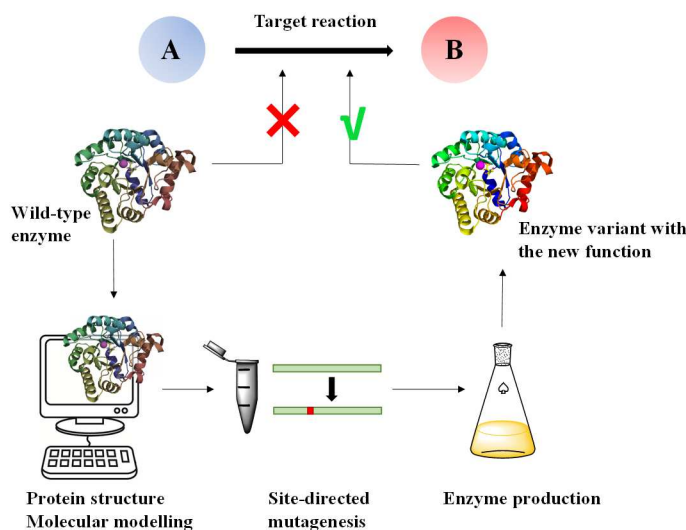


Figure 1.2 Workflow diagram of rational design approach.

Rational design is not only used to modify existing enzymes, it can also create new ones (*de novo* protein design). A detailed understanding of the desired catalytic mechanism and its associated transition states and reaction intermediates is typically required for this method.¹⁹

The creation of enzymes capable of catalyzing any desired chemical reaction is a great challenge combining computational protein design, rational design and directed evolution approaches.

1.3.2 Directed evolution

Directed evolution has become one of the most powerful tools in protein engineering. The process mimics Darwinian evolution in a test tube and involves iterative rounds of creating genetic diversity followed by selection or screening.¹⁹ This approach comprises three main steps: *i*) Construction of mutant library, *ii*) high throughput screening (HTS)/selection of mutants with improved function, and *iii*) isolation of improved genes (Figure 1.3).

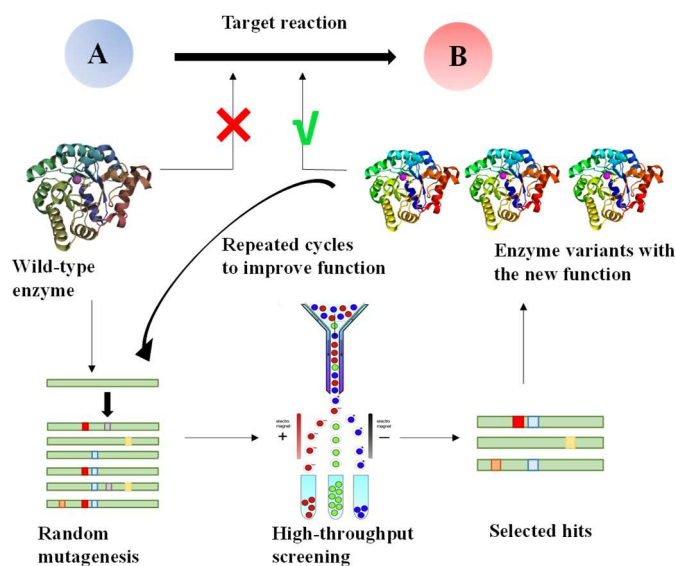


Figure 1.3 Workflow diagram of directed evolution approach.

The challenge of creating a library of mutants has been overcome with the development of several robust techniques for producing genetic diversity such as *error-prone PCR* or *DNA shuffling*. Through these strategies, the creation of a large mutant library displaying a high level of sequence diversity is achieved.

Introduction

This library is then explored by *high-throughput screening* (HTS) to identify and select for those mutations, which produce the desired phenotype. This selection procedure is repeated several times to produce the final biocatalyst with the desired traits. Numerous screening methods have been developed such as colorimetric assays, colony size-based growth assays and fluorescence activated cell sorting (FACS).^{18, 20}

Some advantages of directed evolution are that no prior knowledge of the enzyme structure or mechanism is required and the ability to mutate the entire enzyme, thus identifying residues distant to the active site that could improve enzymatic properties. However, a serious limitation on this method is that the larger the library size the greater the chance of selecting the desired mutant. Consequently, testing large number of mutants (10^3 – 10^6 mutants) is needed and developing a HTS method for a target enzyme property can be extremely laborious and time consuming.^{19,21}

For example, Hilvert *et al.* used 13 rounds of directed evolution to improve the activity of an aldolase by a factor of 30. To prepare the mutant, the encoding gene was diversified by a combination of error-prone PCR, cassette mutagenesis and DNA shuffling. In each round, they sorted 10^6 – 10^7 library members using a novel microfluidic device that integrate droplet generation, incubation and sorting on a single chip.²²

Nevertheless, the creation of smaller, high-quality libraries containing more mutants displaying the target function, would be a more practical approach to avoid the screening bottleneck. With this aim, researchers have embarked upon the path of semi-rational design of biocatalysts.

1.3.3 Semi-rational design

In the *semi-rational design*, a specific domain or a targeted residue that is suspected to have critical function is mutagenized. This requires some degree of understanding of the mechanism by which the enzyme catalyzes a reaction, as well as prior knowledge of either the sequence or the three-dimensional

structure of the enzyme. These requirements immediately limit the use of semi-rational design to only those enzymes which have been previously characterized. On the other hand, semi-rational design is powerful because it can reduce the library size to be screened ($10\text{--}10^3$ mutants) and can enhance the success rate of identifying positive hits (Figure 1.4).²³

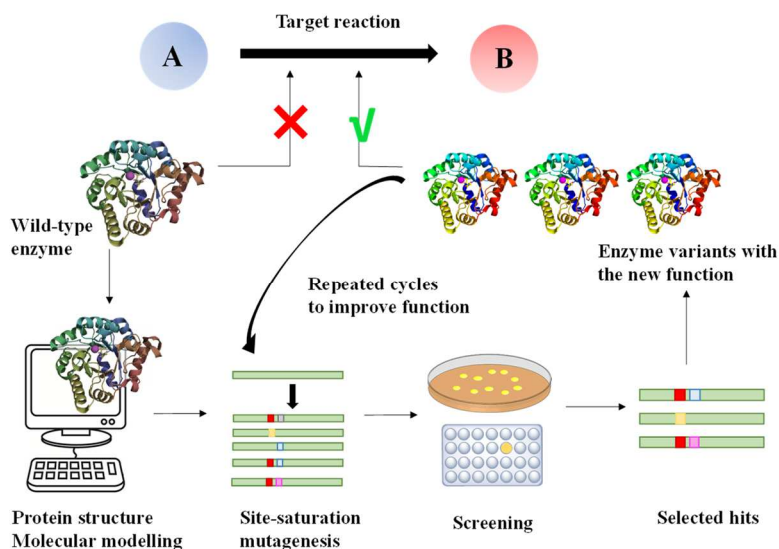


Figure 1.4 Workflow diagram of semi-rational design approach.

For example, Arnold *et al.* reported an engineered β -subunit of tryptophan synthase (TrpB, EC 4.2.1.20) for selective quaternary carbon bond formation. Six generations of site-saturation mutagenesis and random mutagenesis were needed producing almost 5000 mutants. These were screened by HPLC in 96-well plates, obtaining a TrpB Pf_{quat} with a 400-fold improvement activity.²⁴

As introduced in the previous sections, researchers have developed many methods for gene diversification. In rational design, specific residues are mutated by site-directed mutagenesis. For directed evolution random mutagenic techniques that affect all the gene are needed; whereas for semi-rational design, focused mutagenesis techniques that introduce diversification in one specific region of the gene are used.²⁵

1.3.4 Approaches for protein sequence modifications

The most employed techniques nowadays for random mutagenesis are *error-prone PCR*,²⁶ which inserts mutations randomly across genes because the Taq polymerase lacks 3'-5' exonuclease proofreading activity; and *DNA shuffling*,²⁷ which involves the recombination of homologous sets of genes. Other techniques to introduce sequence diversity include the use of *mutator strains*,²⁸ which lack one or more DNA repair pathways such as *E. coli* XL-red; and *sequence saturation mutagenesis* (SeSaM),²⁹ which generates random mutations across each nucleotide within a given sequence. Random mutagenesis can also be performed through *chemical methodologies*, although these are quite obsolete nowadays. One example is the growth of cells harboring a plasmid encoding for the gene of interest in the presence of chemical mutagens such as ethyl methanesulfonate (EMS) or ultraviolet irradiation.²⁵

Focused mutagenesis techniques to apply in semi-rational design are based on PCR and can be achieved by *site-directed saturation mutagenesis* in which synthetic DNA oligonucleotides contain one or more degenerate codons at specific residues. Thus, sampling all possible amino acids at a given position can be accomplished.²⁵

Finally, in rational design, specific targeted residues are mutated by *site directed mutagenesis* in a PCR based approach. There are different described methods for site-directed mutagenesis, classified according to the desired position of the mutation in the PCR product.

a) Inverse PCR method over an entire plasmid

Using this technique, the gene of interest and the entire plasmid are amplified by PCR by using two mutagenic primers (one forward and one reverse) without the need of further steps.^{30, 31} One specific example is *QuikChange®* methodology that uses two complementary mutagenic primers to amplify the DNA template on opposing strands around the circular construct (Figure 1.5). Usually, larger times of denaturation, annealing and extension are needed to

efficiently amplify the whole construct. Moreover, *DpnI* digestion is needed to remove parental sequences, which improves the selection of the mutated template. Finally, the final PCR product, which is a double stranded linear DNA, is used to directly transform the cells that generate an intact circular plasmid.³²

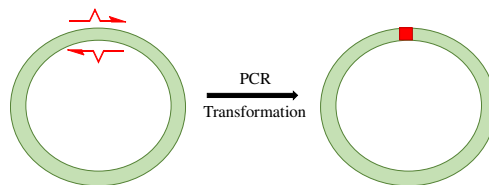


Figure 1.5 Site-directed mutagenesis by inverse PCR method over an entire plasmid.

b) Introducing mutations in the extreme of a gene

Mutations into the terminus of a PCR product are simply introduced by modifying one of the outside primers, which may contain restriction sites to easily clone the resulting PCR product into a vector (Figure 1.6).³³

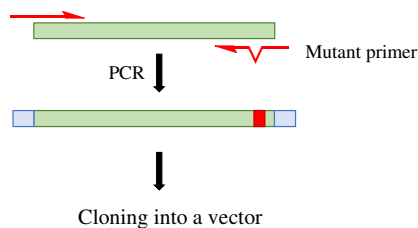


Figure 1.6 Mutation in the extreme of a PCR product by site-directed mutagenesis.

c) Introducing mutations in the middle of a gene

When the mutation is located in the middle of a DNA sequence, two separate PCRs and four primers are needed to amplify two halves of the complete gene. In the first PCR, an outside-forward primer is paired with a middle-reverse primer; and in the second one the outside-reverse primer is paired with the middle-forward primer. Then, the two PCR products must be assembled in order to obtain the whole construct (Figure 1.7A).^{34,35} If the two fragments do not overlap, these are aligned in “tail-to-tail” fashion and ligated. This *blunt-end ligation* is no longer widely used as it is very inefficient and there is no control of the orientation of the fragments to be ligated.³⁶ Alternatively, a common restriction site can be built in the end of both middle primers and the two PCR products can then be digested and ligated.³⁷

When the two PCR products have a longer overlapping sequence, these can be fused *in vivo*³⁸ (by homologous recombination) or *in vitro*³⁹ (by overlap-extension PCR or Gibson assembly). The *Gibson assembly* is a quite recent developed technology that allows the fusion of up to 15 DNA fragments with overlapping sequences. The resulting product can be either a linear or a closed circular molecule ready for cell transformation. The main advantage of this methodology is that it requires few components and minor manipulations making it faster and simpler than the traditional cloning schemes.⁴⁰

A specific methodology for mutations in the middle of a gene is the *megaprimer* PCR method that is based in the fact that a double-stranded DNA of several hundred base pairs can also serve as a primer.^{41, 42} Using this method, two outside primers, one middle mutagenic primer and two PCRs are needed. The first PCR involves one outside primer and the middle mutagenic primer that can be reverse or forward whichever direction makes the megaprimer smaller. The PCR product is purified and used as a megaprimer in a second PCR with the other outside primer and the wild-type template (Figure 1.7B).⁴² Working with megaprimer may imply PCR optimization to speed up the process and

improve the yields of final products (e.g., lengthening the times for denaturation and particularly annealing).³⁵

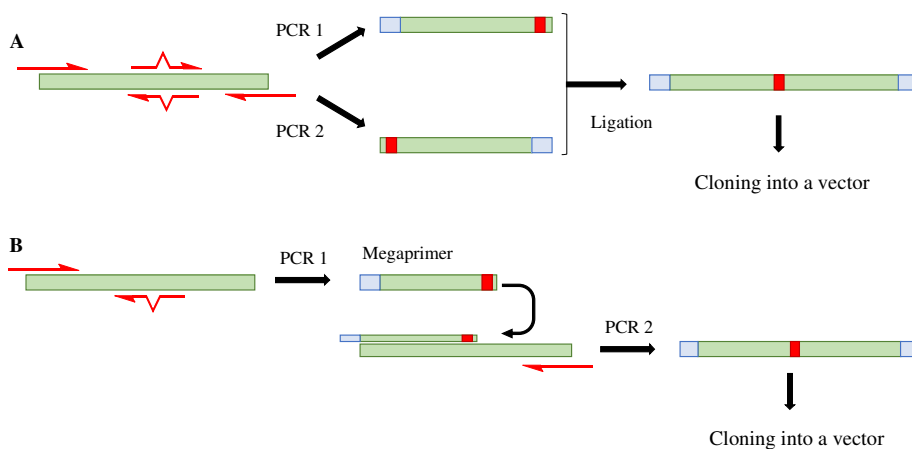


Figure 1.7 Mutation in the middle of a PCR product by **A** site-directed mutagenesis or by **B** megaprimer PCR method.

Some of these methodologies (e.g., QuikChange® or megaprimer approaches) have been applied in this present thesis to modify the protein sequence of a particular type of enzymes called aldolases, which catalyzes the formation of carbon-carbon bonds through aldol addition.

1.4 Aldol reactions

The formation of carbon-carbon bonds is one of the most important cornerstone reactions in synthetic organic chemistry, as it is in nature. One of the most commonly used methods for this purpose is the *aldol reaction*, which is a powerful strategy that also enables the installation of functionality and the creation of stereogenic centers.^{8, 43} In 1864, Charles Wurtz and Alexander Borodin (the famous Russian composer) were the firsts to describe the most simple traditional aldol reaction, which runs under thermodynamic control. The reaction was performed in the presence of sodium as a base, which is not the method of choice nowadays, and furnishing the aldol addition product, the

Introduction

aldol condensation product and several side products that were not identified (Figure 1.8).^{44, 45}

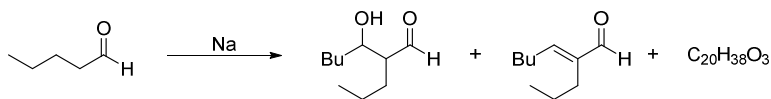


Figure 1.8 First described aldol reaction.

Formally, the aldol addition reaction consists of the addition of an enolizable carbonyl compound (nucleophile) to an aldehyde or ketone (electrophile) under acid or basic conditions giving an aldol product.⁴⁶ This transformation is usually reversible, and dehydration can occur losing the stereogenic centers formed (Figure 1.9).⁴⁷

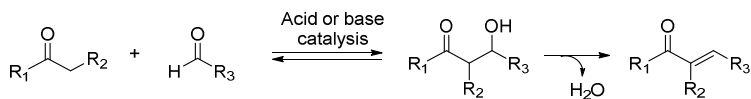


Figure 1.9 Typical aldol reaction followed by dehydration of the aldol adduct.

When the two carbonyl compounds are different (i.e., mixed or *crossed aldol reactions*), they can generally serve both as donors and acceptors and this give complex mixtures of homo and crossed aldol adducts. Success on obtaining the desired product would imply using reactive aldehydes or carbonyl compounds without acidic protons that can only act as acceptors or electrophiles (e.g., formaldehyde or benzaldehyde).^{46, 47}

Other strategies have been developed to avoid undesirable side reactions and induce chirality. One of the firstly developed methods is the generation of a lithium *preformed enolate* followed by the slow addition of the electrophile at low temperatures (Figure 1.10A).⁴⁸ Through this strategy, the reaction runs under kinetic control producing a well-defined aldol adduct. Later, lithium and also magnesium preformed enolates were substituted by other metals such as boron, silicon or titanium enolates. For example, the Mukaiyama reaction is an

aldol addition between a silyl enolate and an aldehyde mediated by a Lewis acid (Figure 1.10B).^{49,50} Zimmerman proposed a chair transition state model to explain why the *Z*- or *E*- preformed enolates preferentially generate *syn*- or *anti*-aldol products, respectively (Figure 1.10C).⁵¹

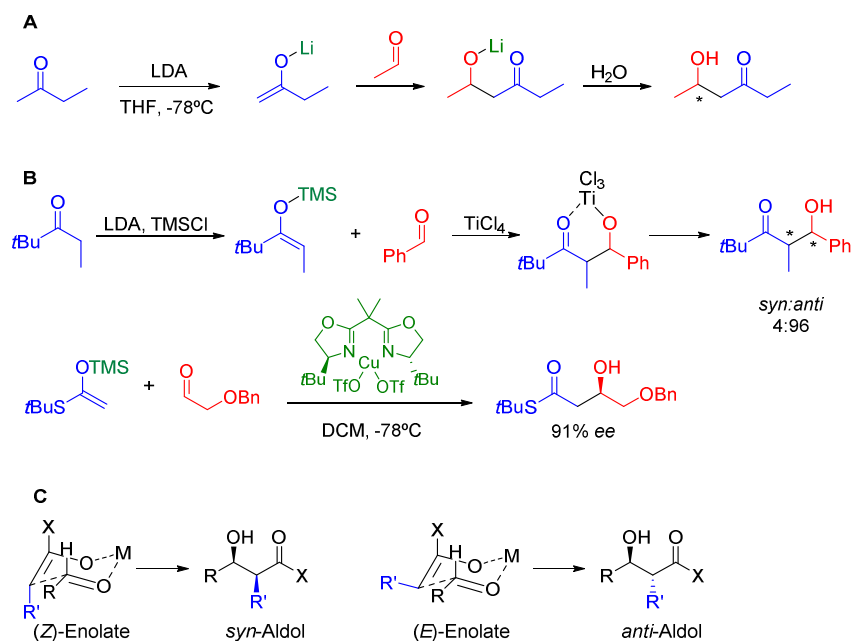


Figure 1.10 Aldol additions with preformed enolates. **A** Preformed lithium enolate followed by the slow addition of the electrophile, **B** Mukaiyama reactions with silicon derived preformed enolates⁵² and **C** Zimmerman model for the stereoselective aldol reaction of preformed (*Z*) and (*E*) enolates.⁵¹

A different strategy to enhance selectivity and induce chirality is by using *chiral auxiliaries*. These are enantiopure chiral molecules used in stoichiometric amounts which attach to the substrate to induce chirality to the resulting compound.⁴⁷ For example, α -amino acid derived oxazolidin-2-ones developed by Evans are chiral auxiliaries that have been widely used for more than 40 years because they are easily removable and very effective for the stereoselective formation of carbon-carbon bonds.^{53, 54} Moreover, a wide variety of transformations have been developed to generate different useful

Introduction

functional groups upon removal of the chiral auxiliary moiety (e.g., primary alcohols, carboxylic acids, benzyl esters or Weinreb amides) (Figure 1.11).⁵⁵

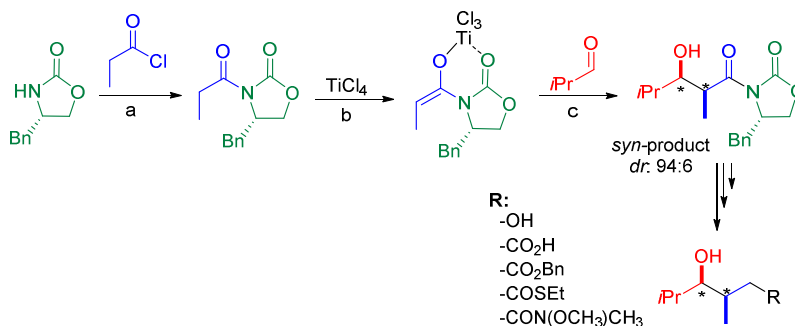


Figure 1.11 Stereochemical control in aldol additions using Evans oxazolidinone chiral auxiliary. Reagents and conditions: a) *n*BuLi, THF, -78 °C; b) DIPEA, DCM, 0 °C; c) DCM, -78 °C → 0 °C. Adapted from literature.^{55, 56}

Furthermore, catalytic methods to perform *direct aldol reactions* with higher atom economy had been developed. These consist of generating the active nucleophile in the reaction. They can be classified in three main types: metal catalyzed reactions, organocatalysis, and biological processes using enzymes or catalytic antibodies (i.e., biocatalysis).

Metal catalysts are based on Lewis acidic metal complexes and are designed to activate the electrophile and facilitate enolate formation from an aldol donor. Moreover, the chiral environment surrounding the metal–ligand complex controls the enantioselectivity of the aldol reaction (Figure 1.12A).^{57, 58} Catalytic activation of the donor rather than the acceptor provides an alternative to the asymmetric Mukaiyama aldol reaction. Numerous approaches have been developed that incorporate a variety of catalysts from organometallic reagents to phosphoramidate Lewis bases.⁵⁹ As well, some catalysts have been developed to activate both the donor and the acceptor (*bifunctional catalysts*). These contain Lewis acidic and Brønsted basic sites that participate in the reaction, which catalyze the aldol addition of unmodified ketones with aldehydes. For example, LaLi₃ tris(binaphthoxide) (LLB) incorporates a central lanthanum

atom, which serves as a Lewis acid, and a lithium binaphthoxide moiety, which serves as a Bronsted base (Figure 1.12B).⁶⁰

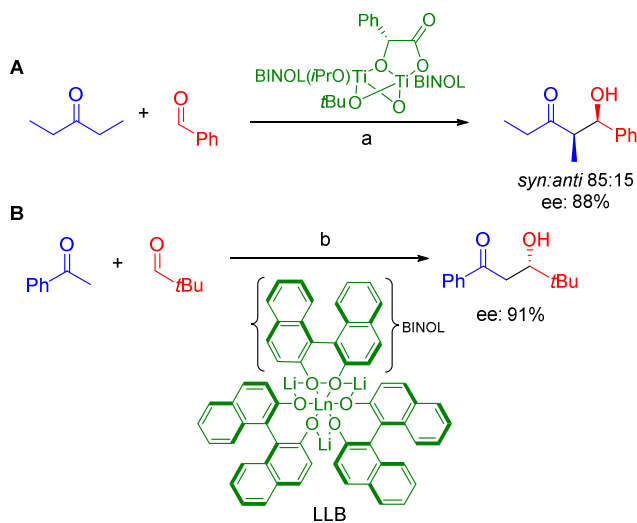


Figure 1.12 Examples of **A** metal catalyzed direct aldol reaction using a titanium(IV) alkoxide/mandelic acid complex⁵⁷ and **B** bifunctional catalyst applied in an aldol reaction.⁶⁰ Reagents and conditions: a) Catalyst 1 mol%, rt; b) Catalyst 20 mol%, THF, $-20\text{ }^{\circ}\text{C}$.

Organocatalysis has emerged as a powerful synthetic strategy to make diverse chiral molecules. Proline, sometimes named as the simplest enzyme, is the cornerstone in the field of organocatalysis because it has been used in a wide range of asymmetric reactions with excellent results (Figure 1.13).⁶¹ A part from proline, several different types of organocatalysts have been developed including primary amino acid and non-enamine based organocatalysts.^{62, 63}

Introduction

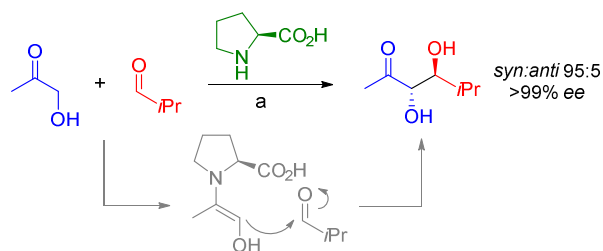


Figure 1.13 Organocatalyzed aldol reaction using L-proline. Reagents and conditions:
a) Catalyst 20 mol%, DMSO, rt.⁶⁴

The mechanisms through which these catalytic methods proceed are also found in nature. As it will be detailed in the next section, the mechanism of metal-enolate based methods resemble the one used by Class II aldolases, which usually possess a zinc ion cofactor; and the one of organocatalyzed aldol reactions is the same as the one of Class I aldolases, through the formation of an enamine intermediate.

1.4.1 Aldolases

Direct aldol additions mediated by *aldolases* are finding increasing acceptance in chemical research and production of asymmetric compounds due to its high selectivity and catalytic efficacy. Aldolases are enzymes that reversibly catalyze the aldol addition reaction with, in most cases, unparalleled stereoselectivity and unbiased control of the two newly formed stereogenic centers.⁶⁵ The aldol adducts formed are usually typified as β-hydroxycarbonyl compounds, a structural element that is frequently found in the framework of complex molecules.⁶⁶

At the beginning of their discovery and synthetic applications, aldolases were classified according to their donor selectivity: pyruvate, dihydroxyacetone phosphate (DHAP), dihydroxyacetone (DHA), glycine and acetaldehyde dependent aldolases (Figure 1.14).⁴³ This long-established classification was based on the fact that, most aldolases only tolerate small modifications in the donor substrate structure. Interestingly, they accepted a broad structural variety

of aldol acceptors. Nowadays, advances in screening technologies and protein engineering has revealed the extraordinary malleability of these catalysts towards nucleophile specificity, making this classification useless.⁶⁷

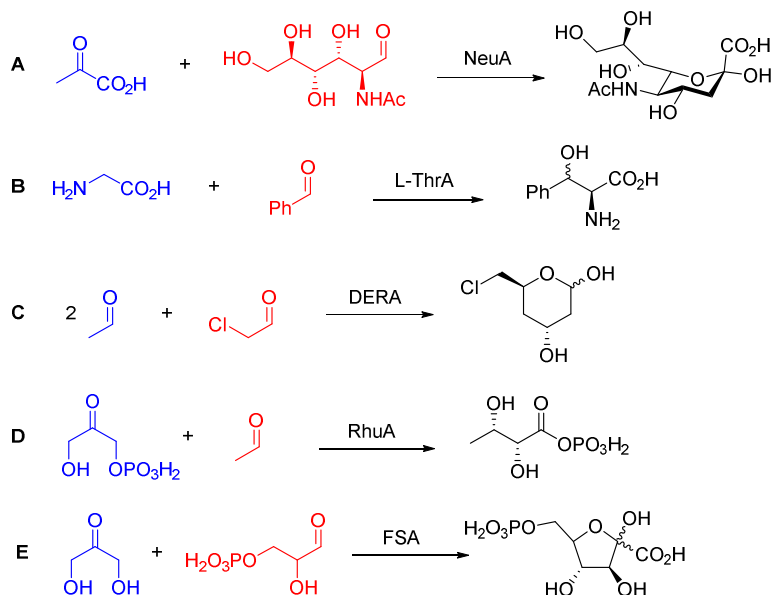


Figure 1.14 Examples of reactions catalyzed by aldolases classified by their donor substrate specificity: **A** pyruvate dependent aldolase NeuA (*N*-acetylneuraminic acid lyase, EC 4.1.3.3), **B** glycine dependent aldolase L-ThrA (threonine aldolase, EC 4.1.2.5), **C** acetaldehyde dependent aldolase DERA (2-deoxy-D-ribose 5-phosphate aldolase, EC 4.1.2.4), **D** dihydroxyacetone phosphate dependent aldolase RhuA (L-rhamnulose-1-phosphate aldolase, EC 4.1.2.19) and **E** dihydroxyacetone dependent aldolase FSA (D-fructose-6-phosphate aldolase, EC 4.1.2.-).

In general, aldolases promote the abstraction of the α proton of the carbonyl compound, thus generating a highly reactive carbon nucleophile in the active site, shielding one of its enantiotopic faces in order to secure correct diastereofacial discrimination. Usually, the approach of the aldol acceptor (electrophile) to the enzyme-bound nucleophile occurs stereospecifically following an overall retention mechanism, while the facial differentiation of the aldehyde carbonyl is responsible for the relative stereoselectivity. In this

Introduction

manner, the stereochemistry of the C-C bond formation is completely controlled by the enzyme, often irrespective of the constitution or configuration of the substrate.^{68, 69} Because of the bimolecular nature of the reaction, the product fraction at equilibrium may be increased in less favorable cases by working at higher substrate concentrations or by driving the reaction with a higher concentration of one of the reactants. Mechanistically, the activation of the aldol donor substrates by stereospecific deprotonation is achieved in two different ways. In the Class I aldolases, the donor substrate binds covalently via imine/enamine to a conserved active site lysine residue. In contrast, Class II aldolases utilize a transition metal cation as a Lewis acid cofactor which facilitates deprotonation by a bidentate coordination of the donor to give the enediolate nucleophile (Figure 1.15).^{70, 71}

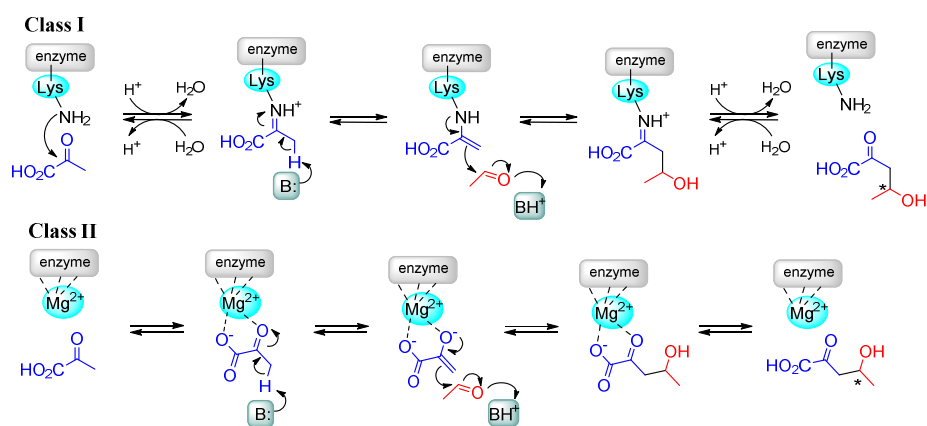


Figure 1.15 Classification of aldolases by their mechanism of enolate stabilization as Class I or Class II aldolases. Both examples show pyruvate aldolases.

As introduced previously, asymmetric aldol addition mediated by aldolases is recognized as a green and sustainable method for carbon–carbon bond formation. In recent years, advances in screening technologies, metagenomics and protein engineering have uncovered a number of novel C–C biocatalysts with high potentiality for the synthesis of diverse new chemical structures and product families.

1.5 Ketopantoate hydroxymethyltransferase (EC 2.1.2.11)

Ketopantoate hydroxymethyltransferase (KPHMT, EC 2.1.2.11) is a transferase encoded by the *panB* gene that catalyzes the first committed step in the biosynthesis of pantothenate, also known as the B₅ vitamin. This vitamin, is a key precursor of two essential cofactors: coenzyme A (CoA) and acyl carrier protein (ACP) that must be synthesized by plants and microorganisms and is obtained from the diet in mammals.^{72,73} Some studies suggest that KPHMT catalyzes, in fact, the rate-limiting reaction in pantothenate biosynthesis and that it might be an attractive target for inhibitor design as antibacterial compounds.⁷⁴

More specifically, KPHMT is a metal cofactor dependent aldolase-like enzyme that utilizes 5,10-methylenetetrahydrofolate (MTHF) to reversibly transfer a hydroxymethyl group to α -ketoisovalerate (i.e., α -KIV, IUPAC name 3-methyl-2-oxobutanoate) to furnish ketopantoate (i.e., KP, IUPAC name 4-hydroxy-3,3-dimethyl-2-oxobutanoic acid) and tetrahydrofolate (Figure 1.16).⁷⁵ In fact, MTHF is used in nature as a carrier of one-carbon units such as formaldehyde enabling its transference during biosynthesis and preventing it to accumulate to toxic levels inside the cells.⁷⁶

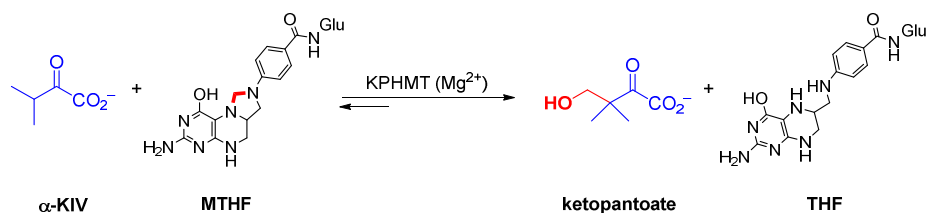


Figure 1.16 Natural reversible reaction of KPHMT that catalyzes the synthesis of ketopantoate, precursor of vitamin B₅. MTHF = *N*⁵,*N*¹⁰-methylenetetrahydrofolate, THF = tetrahydrofolate.

The addition of α -ketoisovalerate to formaldehyde furnishing ketopantoate had been demonstrated using chemical procedures in 1942 but the corresponding enzymatic activity was not detected until 1957. McIntosh *et al.* were the firsts

Introduction

to purify KPHMT from crude extracts of *E. coli* and also to demonstrate its catalytic activity.⁷⁷ The enzyme was purified to a greater level of homogeneity by Teller *et al.*⁷⁵ The activity of this purified enzyme was found to be dependent on *N*⁵,*N*¹⁰-methylenetetrahydrofolate.

More recently, Sugantino *et al.* purified KPHMT from *Mycobacterium tuberculosis* and confirmed that its activity is dependent on the presence of a divalent metal cofactor in the enzyme active site. They found that maximal enolization of the substrate occurred in the presence of Mg²⁺, intermediate activity was found with Co²⁺ and Zn²⁺, and minimal activity with Ni²⁺ and Ca²⁺.⁷³

Moreover, they demonstrated that this catalyst can operate under MTHF-independent mechanism, and perform the synthesis of ketopantoate from formaldehyde and α -ketoisovalerate. This is a major change in the catalytic mechanism of this enzyme, that functions as a Class II aldolase (Figure 1.17).⁷³ A similar promiscuous activity is found in pyridoxal 5'-phosphate dependent serine hydroxymethyl transferases (SHMT, E.C. 2.1.2.1).⁷⁸ It is a remarkable fact that free formaldehyde, which is normally toxic to proteins and deactivates enzymes, even at low concentrations, can be utilized as electrophile with these enzymes at relative high concentrations.

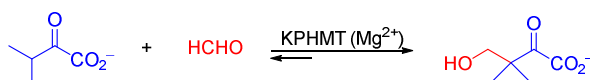


Figure 1.17 Aldol addition of α -KIV to formaldehyde catalyzed by KPHMT *in vitro*.

1.5.1 Structure and catalytic mechanism of KPHMT

Structures of KPHMT from four organisms, *E. coli* (PDB code 1M3U),⁷⁹ *M. tuberculosis*,⁸⁰ *N. meningitides*,⁸¹ and *B. thailandensis*⁸² have been solved by X-ray crystallography. The crystal structure of *E. coli* KPHMT was reported at 1.9 Å resolution, in complex with Mg²⁺ and the product ketopantoate. The

protein adopts a tightly packed homodecameric quaternary structure formed by a pentamer of dimers, with the dimer being the functional unit. Each subunit adopts the classic $(\beta/\alpha)_8$ (or TIM) barrel fold (Figure 1.18).^{79,83}

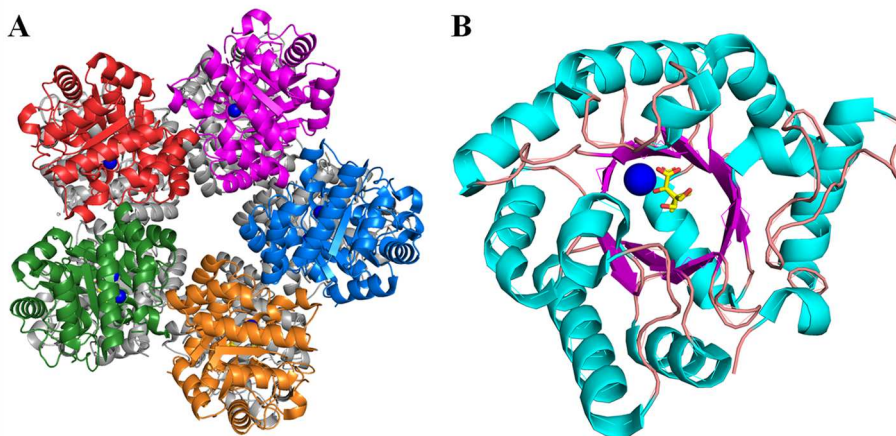


Figure 1.18 Tridimensional crystal structure of KPHMT (PDB code 1M3U). **A** Top view of the protein formed by a pentamer of dimers. **B** KPHMT monomer showing the β strands (purple), α helices (light blue), Mg^{2+} (dark blue) and product ketopantoate (yellow).

In the active site, magnesium is coordinated in an octahedral sphere with the oxygen atoms of the carboxylate and α -ketone of ketopantoate; by the conserved Asp45 and Asp84; and by two structural water molecules. Ketopantoate is additionally bound by hydrogen bonding to Ser46, Lys112 and Glu181. His136 is involved in binding these latter two residues and Glu114 is also involved in binding the structural water molecules (Figure 1.19).^{83,84}

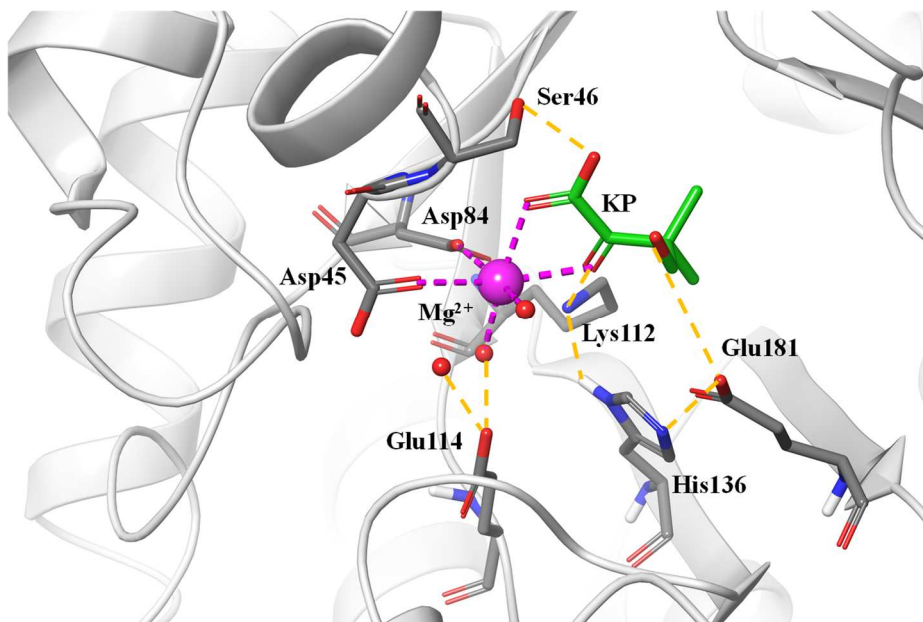


Figure 1.19 Crystal structure of the active site of KPHMT showing the octahedral coordination sphere of magnesium (magenta dashed lines), the hydrogen bonds (yellow dashed lines), the most important residues, water molecules (red), Mg^{2+} (purple) and product ketopantoate (green).

There are several mechanisms proposed for KPHMT, but all are based on the coordination of the carbonyl and carboxyl groups of α -ketoisovalerate to Mg^{2+} , which is presumed to lower the pK_a of the β -proton of the substrate. The substrate-metal complex orients the two methyl groups in the hydrophobic pocket and, consequently, the β -proton towards Glu181, which act as a base forming the enolate (Figure 1.20).^{73, 79}

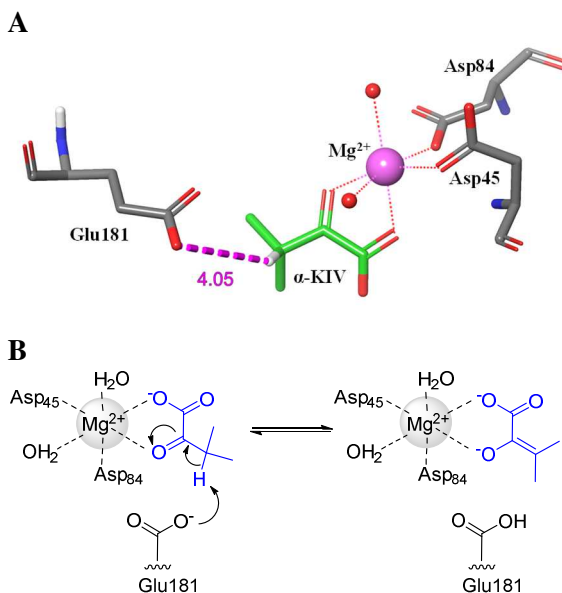


Figure 1.20 **A** Model of the active site of KPHMT showing the distance between the β -proton of α -ketoisovalerate (in green) and the proposed catalytic acid-base residue E181. **B** Mechanism of the enolate formation in the active site of KPHMT.

In the next step, the Glu181 is available to protonate and activate the N10 of MTHF. The difference between the proposed mechanisms relies on the nature of the electrophilic species attacked by the nucleophile. These can be divided in two main explanations. In the first one, the enolate attacks the activated MTHF and, after the hydrolysis of the C-N⁵ bond, the product is released (Figure 1.21A). In the second one, formaldehyde is released by hydrolysis of MTHF and is attacked directly by the enolate to yield the aldol adduct (Figure 1.21B).⁸³

Introduction

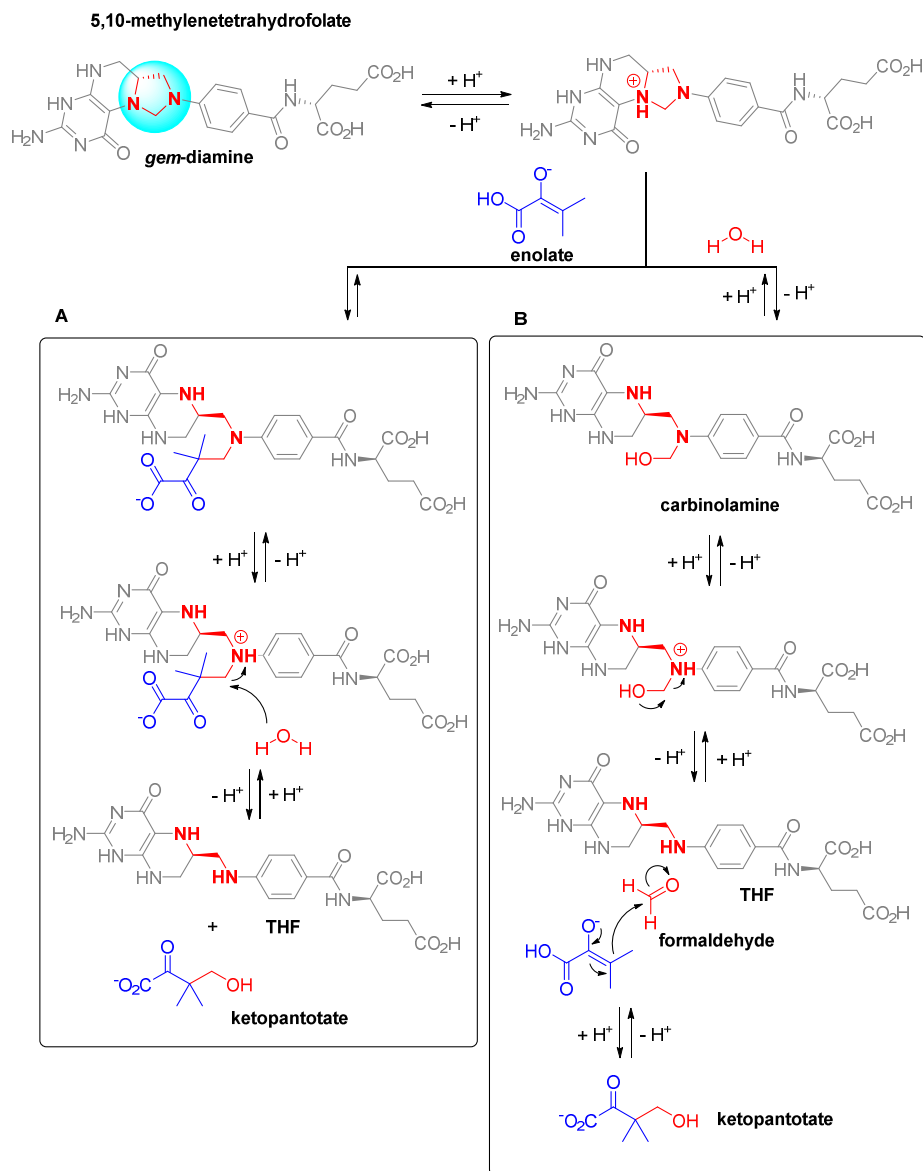


Figure 1.21 Proposed mechanisms for KPHMT. **A** Direct addition of enolate to protonated gem-diamine in 5,10-methylenetetrahydrofolate. **B** Addition of enolate to formaldehyde, formed by hydrolysis of gem-diamine in 5,10-methylenetetrahydrofolate. Adapted from literature.⁸³

Probably, these two processes are undistinguishable in the active site of the enzyme occurring at the same time or as a combination. Moreover, it is

noteworthy that these mechanisms chemically resemble the mechanism of deprotection of a cyclic aminal (in this case the *gem*-diamine between N5 and N¹⁰ of MTHF) to release a diamine and an aldehyde.

Even though KPHMT has been well characterized in the past 10 years, it hitherto has never been applied as biocatalyst in organic synthesis. From reported studies, our research group envisaged that this enzyme has great potential in this field as it possesses some degree of nucleophile promiscuity, which was preliminary uncovered following the rate of deuterium exchange of the β -proton during the enolization of different 2-oxoacids.⁷³

1.6 2-Keto-3-deoxy-L-rhamnonate aldolase (EC 4.1.2.53)

2-Keto-3-deoxy-L-rhamnonate aldolase from *E. coli* (YfaU, EC 4.1.2.53) is a Class II aldolase that catalyzes the reversible cleavage of 2-keto-3-deoxy-L-rhamnonate to furnish L-lactaldehyde and pyruvate (Figure 1.22). The enzyme shows a high degree of acceptor promiscuity for simple and small aldehydes.⁸⁵

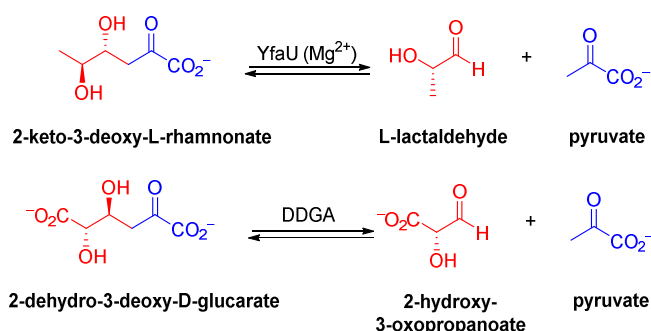


Figure 1.22 Proposed retro-aldol reaction catalyzed by YfaU and DDGA. YfaU is proposed to catalyze the cleavage of 2-keto-3-deoxy-L-rhamnonate furnishing pyruvate and L-lactaldehyde based on the homology with DDGA.

YfaU is encoded by the *rmhA* gene and was first annotated as a putative 4-hydroxy-2-ketoheptane-1,7-dioate aldolase (HpcH, EC 4.1.2.52) in the sequence databases, as they share 53% of sequence identity.⁸⁶ Deeper studies on the gene organization analysis, showed that YfaU is part of an operon related

Introduction

to L-rhamnonate metabolism. This, together with a 43% sequence homology with 2-dehydro-3-deoxygalactarate aldolase (DDGA, EC 4.1.2.20) suggested that YfaU may have a 2-dehydro-3-deoxy aldolase function.^{85, 87} This illustrates the importance of using operon context as well as homology-based approaches for the functional assignment of prokaryotic genes.

1.6.1 Structure and catalytic mechanism of YfaU

Rea *et. al.* determined the crystal structure of *E. coli* K12 YfaU (PDB code 2VWS) by molecular replacement using the coordinates of DDGA (PDB code 1DXE) as a search model.⁸⁸ Refinement resulted in a final model (1.39 Å resolution) in complex with Mg^{2+} and pyruvate. Structurally, YfaU consist of a hexameric assembly comprising a trimer of dimers. All subunits of the hexamer adopt very similar conformations of a classic $(\beta/\alpha)_8$ barrel (Figure 1.23).⁸⁵

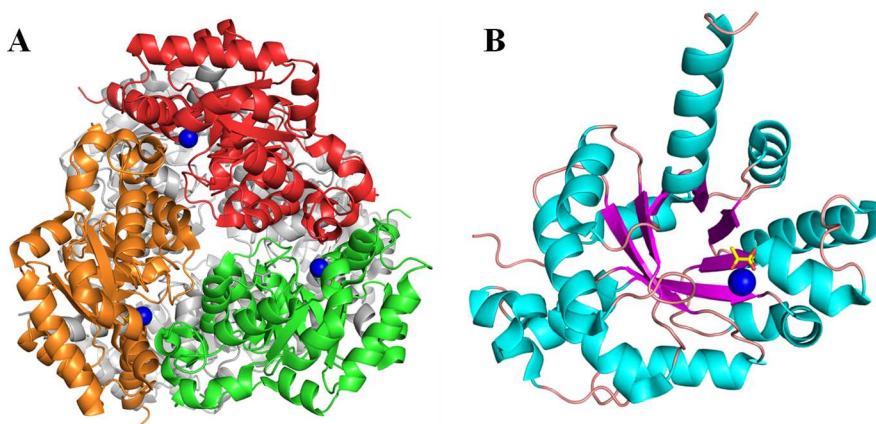


Figure 1.23 Tridimensional crystal structure of YfaU (PDB code 2VWS). **A** Top view of the protein formed by a trimer of dimers. **B** YfaU monomer showing the β strands (purple), α helices (light blue), Mg^{2+} (dark blue) and complexed with pyruvate (yellow).

Magnesium is coordinated in the active site of YfaU by Glu153 and Asp179. The carboxyl group and the carbonyl group of pyruvate provide two further Mg^{2+} ligands, and two water molecules complete the octahedral coordination shell. At the same time, the carboxylate group is bound by hydrogen bonding

to Ala178 and Asp179, and the carbonyl group also has hydrogen bonds to Arg74 and Gln151. Finally, there are three water molecules in the active site that may be catalytically important. Two of these are the metal bound and the third one is bound to Arg74 (Figure 1.24).⁸⁵

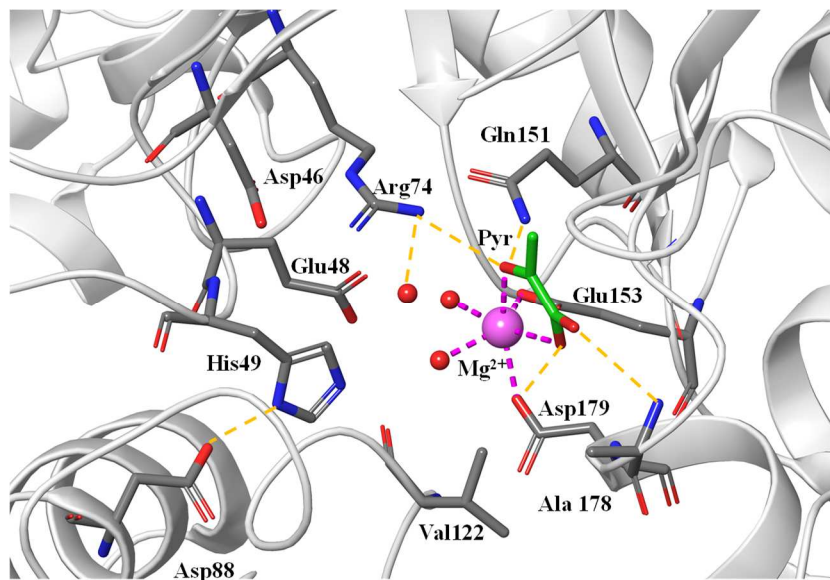


Figure 1.24 Crystal structure of the active site of YfaU showing the octahedral sphere of magnesium (magenta dashed lines), the hydrogen bonds (yellow dashed lines), the most important residues, water molecules (red), Mg^{2+} (purple) and pyruvate (green).

Rea *et al.* also proposed a catalytic mechanism for the retro-aldol reaction catalyzed by YfaU. First, the Asp88-His49 dyad deprotonates a metal-coordinated water molecule that is stabilized as a hydroxide and can deprotonate the C4 hydroxyl of the substrate. This is coupled with the cleavage of the C3-C4 carbon-carbon bond to form the aldehyde product and pyruvate enolate that are stabilized by the metal ion and Arg74. Then, protonation of the enolate at C3 by the Asp88-His49-metal-bound water furnishes the other product pyruvate. The metal-bound water molecule that participates as a base in the first part of the reaction may act as an acid in this step. Finally, the

Introduction

products are released returning the enzyme to the ground state and completing the catalytic cycle (Figure 1.25).⁸⁵

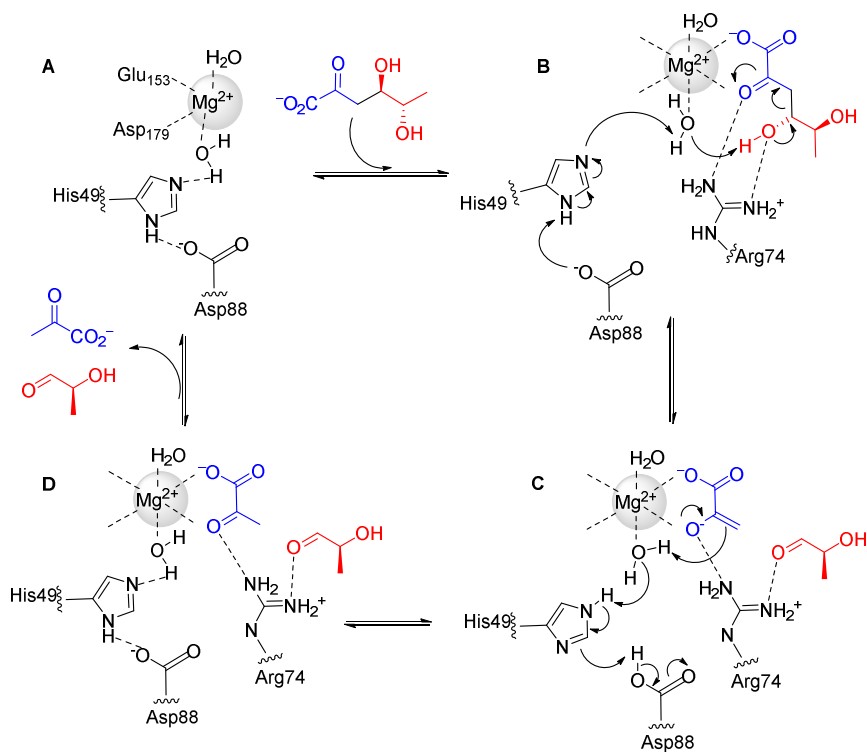


Figure 1.25 Suggested catalytic mechanism of YfaU: **A** Ground state of the active site of the enzyme, **B** His49 deprotonates the metal-bound water, the substrate binds to the metal ion and the hydroxide ion abstracts its β -proton, **C** the products are stabilized by the metal ion and Arg74, pyruvate is formed by protonation and **D** release of products and returning the enzyme to the ground state to complete the catalytic cycle. Adapted from literature.⁸⁵

The mechanism clearly shows the importance of Arg74 (that binds and activates the C2 keto group and stabilizes the enolate) and His49 (forms the Asp88-His49-W5 motif that act as a general base to abstract the proton from the hydroxyl group). The catalytic importance of these two residues was confirmed by site-directed mutagenesis; the Arg74Ala and His49Ala mutant were totally devoid of activity.⁸⁵

1.6.2 Biocatalytic applications of YfaU

When it comes to the study of YfaU in biocatalysis, our group was pioneer in its application. YfaU from *E. coli* K12 was cloned as a fusion protein with maltose binding protein (MBP-YfaU), since in our hands the wild-type protein was mainly expressed as inclusion bodies. YfaU catalyzed the enzymatic aldol addition of pyruvate to formaldehyde retaining the activity at substrate concentrations of >1 M. This was surprising as formaldehyde, which is a strongly electrophilic aldehyde, often denature proteins.⁸⁹ Different bivalent metal cofactors were tested, obtaining that the enzymatic activity was enhanced using Ni²⁺. Nevertheless, at high concentrations the metal itself catalyzed the reaction unespecifically rendering racemic mixtures. For this reason, Ni²⁺ was not used in this study. In our group, MBP-YfaU(Mg²⁺) was applied to the synthesis of L- and D-homoserine, combining it with a transaminase in a one-pot substrate cycling cascade (Figure 1.26).⁹⁰

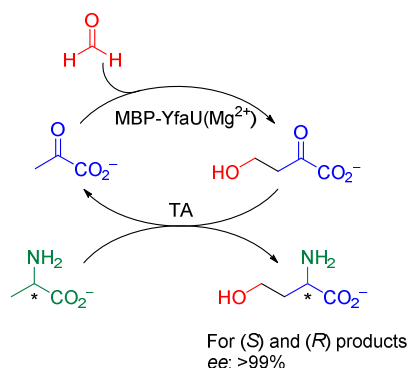


Figure 1.26 MBP-YfaU applied in the synthesis of L- and D-homoserine in a one-pot substrate cycling cascade with a transaminase (TA).

MBP-YfaU catalyzes the aldol addition of *N*-Cbz-aminoaldehydes to pyruvate. It was observed that (*S*) and (*R*)-aldehydes gave aldol adducts with preferentially (*R*) and (*S*)-configuration, respectively at the newly formed stereocenter (i.e., the one generated from the addition to the aldehyde) whereas achiral aldehydes rendered racemic aldol adducts. Then, catalytic reductive

Introduction

amination of the aldol adducts yielded 4-hydroxyproline and pyrrolizidine derivatives (Figure 1.27).⁹¹

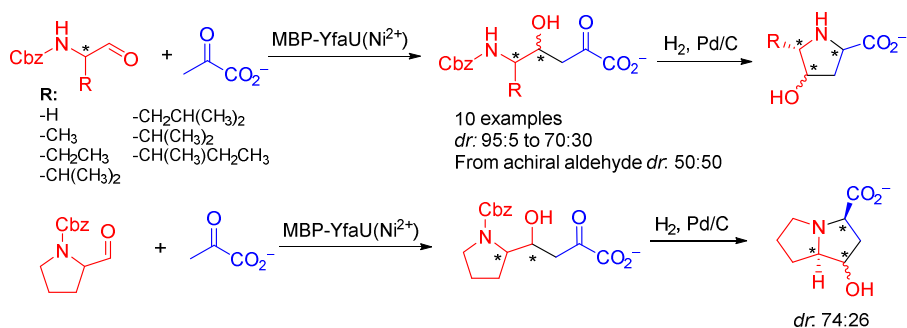


Figure 1.27 Chemoenzymatic synthesis of hydroxyprolines and pyrrolizidines derivatives. In the first step, MBP-YfaU(Ni²⁺) catalyzes the aldol addition of *N*-Cbz-aminoaldehydes to pyruvate.

The nucleophile promiscuity of the enzyme was also studied by using pyruvate analogues with linear and branched aliphatic chains. It was observed that 2-oxobutanoate was well accepted, but larger or branched oxoacids yielded poor conversions. Thus, five new variants of MBP-YfaU were created by structure-guided protein engineering. The best catalyst resulted to be the double variant W23V/L216A which generates enough space to accommodate large and branched substituents (Figure 1.28).⁹²

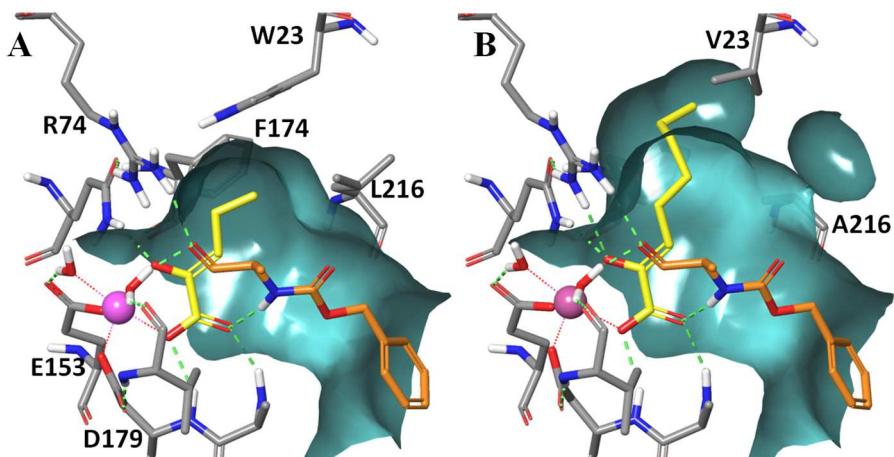


Figure 1.28 Models of **A** wild-type YfaU and **B** YfaU W23V/L216A complexed with different pyruvate analogues (yellow C atoms) and a *N*-Cbz-aminoaldehyde (orange C atoms). The metal cofactor (magenta) and the surface of the residues near to the substrates (cyan) are shown.

Using the MBP-YfaU single variant W23V and double variant W23V/L216A, a collection of 4-hydroxyproline and pyrrolizidine derivatives substituted at C3 were obtained (Figure 1.29).⁹²

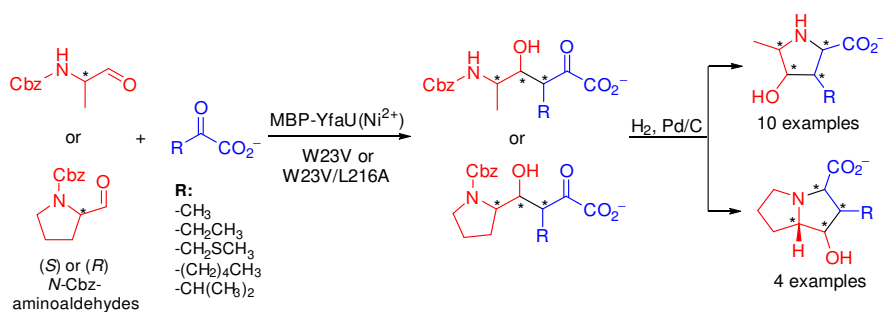


Figure 1.29 MBP-YfaU(Ni^{2+}) W23V and W23V/L216A variants catalyze the aldol addition of pyruvate analogues to *N*-Cbz-aminoaldehydes.

1.7 Synthesis and applications of relevant chiral building blocks

1.7.1 Synthesis and applications of Roche ester derivatives

3-Hydroxy-2-methylpropanoate (i.e., *Roche ester*) is an important chiral building block used in organic synthesis. Since its full development by Roush *et al.* 30 years ago⁹³ the “Roche ester” approach to the construction of building blocks for bioactive natural products synthesis has emerged as, and remains, one of the most widely employed. Among others, total synthesis of discodermolide (antimitotic activity),^{94, 95} carolacton (biofilm growth inhibitor),⁹⁶ sagopilone (epothilone analogue ZK-Epo),⁹⁷ callyspongiolides (cytotoxic marine natural products),^{98, 99} and zincophorin and soraphen A (antibiotics and antifungals)^{100, 101} have been successfully achieved (Figure 1.30).

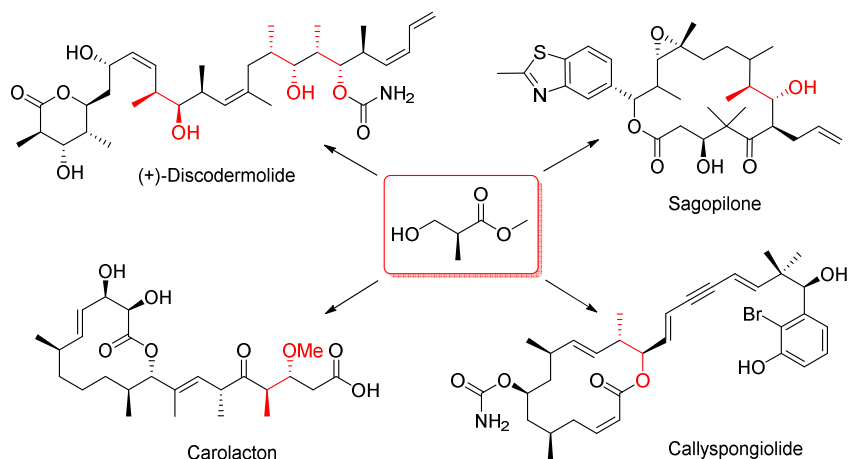


Figure 1.30 Examples of bioactive compounds synthesized from Roche ester.

Other chiral 2-substituted 3-hydroxy esters (Roche ester analogues), are also useful chiral building blocks widely used in complex molecule synthesis.¹⁰² For example, they can be found in the preparation of important antibacterial agents such as peptide deformylase (PDF) inhibitor among others (Figure 1.31).¹⁰³⁻¹⁰⁶

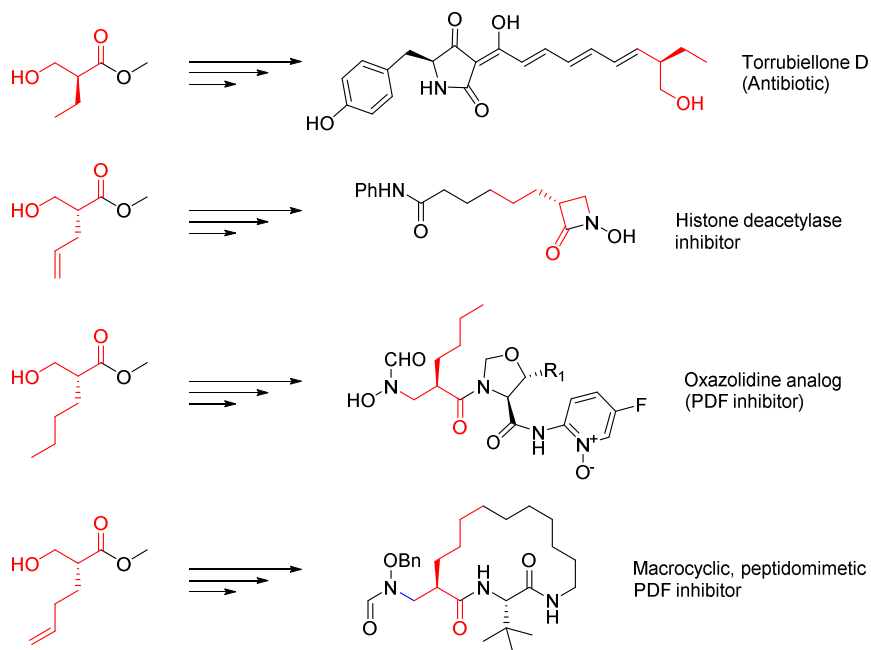


Figure 1.31 Examples of bioactive compounds synthesized from different chiral 2-substituted 3-hydroxycarboxylic esters.

There are a huge number of papers demonstrating the wide potential synthetic value of Roche esters or other synthetic equivalents such as chiral 2-hydroxymethyl aldehydes or carboxylic acids. Despite that, there are few reports on the synthesis of these compounds.

A straightforward access would imply the asymmetric α -hydroxymethylation of carboxylate esters using formaldehyde via aldol addition reaction. Among the methods developed to induce stereoselectivity in the reaction, chiral auxiliaries are widely used.⁵⁵ The Evans' chiral 2-oxazolidinones applied in α -alkylation and *syn*-aldol reactions auxiliary intermediate is an available stoichiometric strategy (Figure 1.32).^{53, 56, 107} This noncatalyzed strategy has limited possibilities of scale up since they require multiple operations and recycling of the auxiliaries.

Introduction

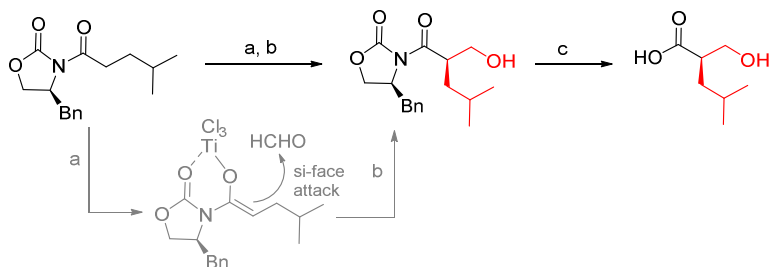


Figure 1.32 Evans' 2-oxazolidinones applied in the synthesis of (*R*)-2-(hydroxymethyl)-4-methylpentanoic acid. Reagents and conditions: a) TiCl₄, DIPEA, DCM, 0 °C; b) 1,3,5-trioxolane; c) H₂O₂, LiOH, THF:H₂O; ee not reported. Adapted from literature.¹⁰⁷

Catalytic stereoselective repertoire reported in the literature is the following. For example, asymmetric alkene hydroformylation was used to convert terminal alkenes directly into optically active α -substituted aldehydes.¹⁰⁸ These are useful Roche ester synthetic equivalents that can be used directly in the next synthetic step. Zhiyong Yu *et al.* used the commercially available Ph-BPE ligand to catalyze this reaction employing very low catalyst loadings (0.02 mol%). Nonetheless, the regioselectivity achieved was moderate (Figure 1.33).¹⁰⁹

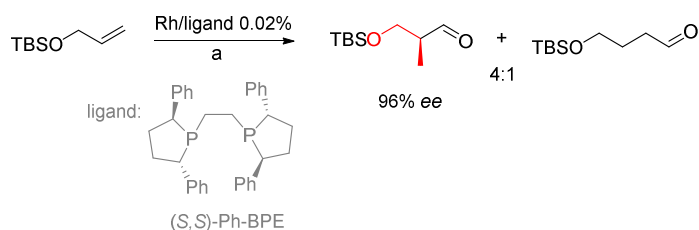


Figure 1.33 Synthesis of optically active aldehydes achieved by Hydroformylation of alkenes. Reagents and conditions: a) Rhodium acetylacetonate dicarbonyl complex, 150 psi CO/H₂, toluene, 80 °C. Adapted from literature.¹⁰⁹

Another strategy to prepare Roche esters is via stereoselective reduction of products from a Morita–Baylis–Hillman (MBH) reaction. α -Methylene- β -hydroxycarbonyl compounds can be formed by the addition of α,β -unsaturated carbonyl compounds to formaldehyde catalyzed by tertiary amine or phosphine.¹¹⁰ Hydrogenation using Rh or Ru complexes^{111, 112} or by enzymatic catalysis using ene-reductases (OYE, EC 1.6.99.1)¹¹³⁻¹¹⁶ rendered the Roche esters (Figure 1.34). The main drawback of this strategy is that is limited to the synthesis of 3-hydroxy-2-methylpropanoate.

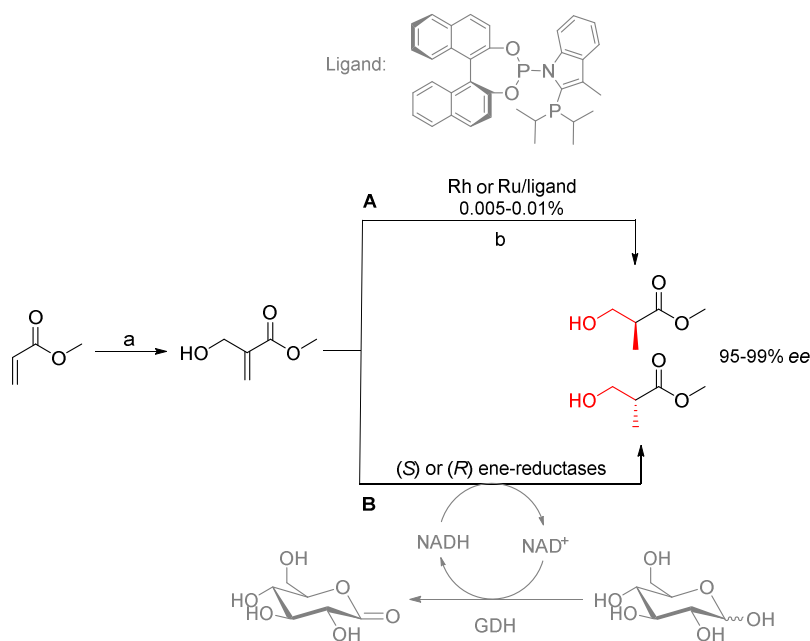


Figure 1.34 Synthesis of Roche ester by hydrogenation of α -hydroxymethyl-acrylate derivatives obtained by Morita-Baylis-Hillman reaction. Enantioselective reduction by **A** rhodium or ruthenium complex/H₂ and **B** Old Yellow Enzyme family. GDH = glucose dehydrogenase (EC 1.1.99.10). Reagents and conditions: a) HCHO, DABCO, 1,4-dioxane:H₂O 1:1 (v/v), rt; b) H₂, DCM, 10 bar, 20 °C.

Organocatalytic asymmetric addition of an aldehyde to formaldehyde has also been used to furnish 2-substituted 3-hydroxyaldehydes. For example, different α,α -substituted prolinol derivatives have been employed in amounts between 5

Introduction

to 30 mol %. Products required to be further transformed into readily isolable derivatives through chemical transformation due to the delicate nature of these compound (Figure 1.35).^{102, 117, 118}

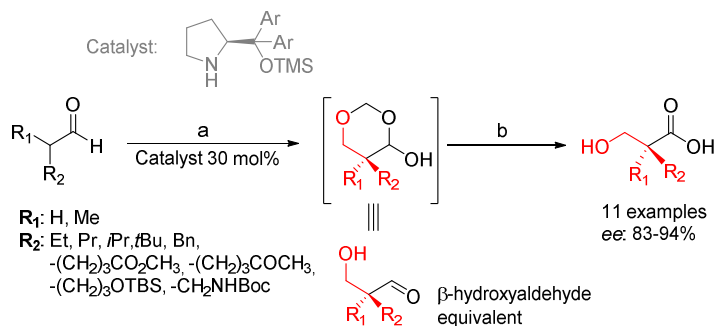


Figure 1.35 Organocatalytic methodology used to obtain Roche ester derivatives by an ensuing chemical transformation. Reagents and conditions: a) HCHO (aq), catalyst, buffer pH 7.0, toluene, rt; b) NaClO₂, NaH₂PO₄, 2-methyl-2-butene, *t*BuOH:H₂O (2:1). Adapted from literature.¹¹⁷

Access to (*S*)-3-hydroxy-2-methylpropionic acid by conversion of isobutyric acid or directly from glucose was achieved utilizing *Pseudomonas taiwanensis* VLB120 B83 T7 cells as catalyst. This strain carries a mutation in the gene encoding 3-hydroxyisobutyrate dehydrogenase (EC 1.1.1.30), leading to its inactivation and accumulation of the desired product (Figure 1.36).¹¹⁹ This strategy has limited range to structures with natural constitution.

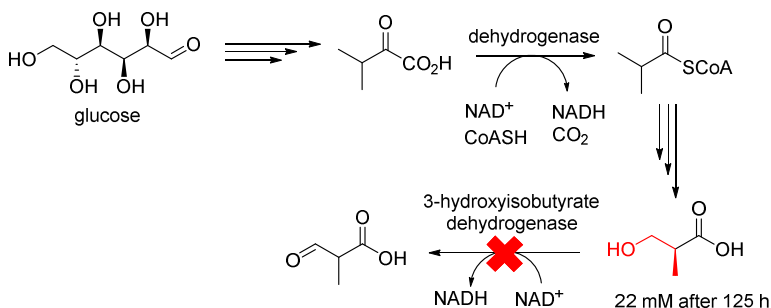


Figure 1.36 Biosynthesis of (*S*)-3-hydroxyisobutyric acid from glucose using *P. taiwanensis* VLB120 B83 T7. Adapted from literature.¹¹⁹

1.7.2 Synthesis and applications of compounds bearing quaternary centers

Quaternary centers (carbons with four different carbon substituents) are important structural units that can be found in naturally occurring, biologically active compounds and pharmaceutical ingredients. Among other examples, terpene derivatives and opioids possess unique polycyclic architectures and are relatively rich in all-carbon quaternary centers (Figure 1.37).¹²⁰⁻¹²³

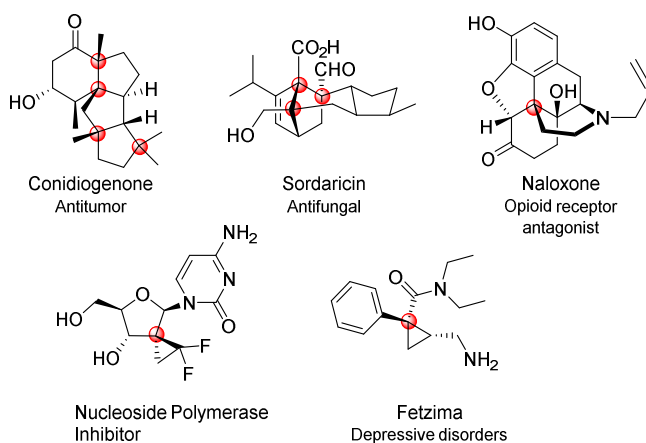


Figure 1.37 Examples of bioactive molecules and pharmaceuticals bearing quaternary centers.

Bioactive molecules and drugs bearing quaternary centers are becoming more appreciated in medicinal chemistry in recent years. These compounds have better efficacy and fewer side effects than the heteroaromatic and achiral “flat” molecules that were the focus of attention for medicinal chemists during many years. The presence of the congested feature of a quaternary carbon atom expands the chemical diversity of the compound and this would enhance the binding selectivity with target proteins avoiding unspecific interactions. Moreover, it improves very important properties such as drug solubility and bioavailability.^{124, 125}

Introduction

Synthetic access to quaternary stereocenters is a significant and challenging task for organic chemists as it implies overcome the steric hindrance between the carbon substituents. Considerable efforts have been dedicated to implement chemical methodologies for this purpose.^{126, 127}

An important and powerful method for the construction of quaternary carbons is the Michael addition using disubstituted donors or acceptors in the α or β carbon respectively.¹²⁸⁻¹³⁰ For example, the total synthesis of three monoterpenoid indole alkaloids, (-)-dehydrotubifoline, (-)-tubifoline and (-)-tubifolidine, was achieved through enantioselective tandem Michael addition obtaining a 3,3-disubstituted oxindole (Figure 1.38).¹³⁰

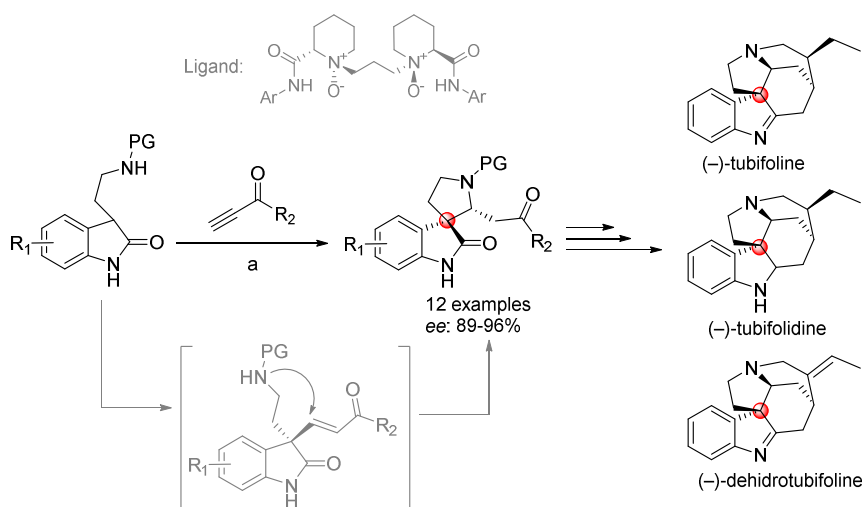


Figure 1.38 Synthesis of three monoterpenoids bearing a quaternary center by enantioselective Michael addition. Reagents and conditions: a) Sc(OTf)₃ (4 mol%), ligand (5 mol%), NaHCO₃, EDC, 50 °C. Adapted from literature.¹³⁰

There are many methodologies reported in the literature to access 3,3-disubstituted oxindoles as they are widely encountered in numerous biologically active natural products and pharmaceuticals.¹³¹⁻¹³³ For example, the dearomative alkylation of 3-halooxindoles with 3-substituted indoles lead to the formation of an interesting product containing two vicinal quaternary

centers used as precursor for the total synthesis of (+)-perphoramidine (Figure 1.39).¹³¹

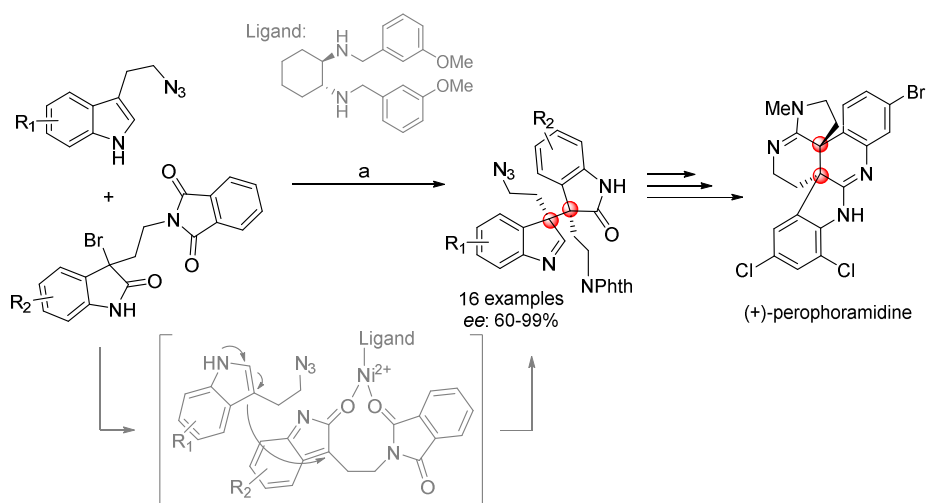


Figure 1.39 Synthesis of (+)-perphoramidine bearing two vicinal quaternary centers by dearomative alkylation of 3-haloindoles. Reagents and conditions: a) Ni(OAc)_2 (20 mol%), ligand (20 mol%), K_3PO_4 , THF, rt. Adapted from literature.¹³¹

The synthesis of two adjacent stereocenters and, in particular, two vicinal quaternary carbon stereocenters constitutes a daunting challenge in organic chemistry as the steric hindrance increases the difficulty on their synthesis. Among others, cycloaddition reaction, Claisen rearrangement and cyclopropanation are probably the most investigated processes for the construction of this structural feature.¹³⁴ For example, cyclopropanation involving oxindoles and styrenes mediated by a chiral catalyst was recently reported in the literature (Figure 1.40).¹³⁵

Introduction

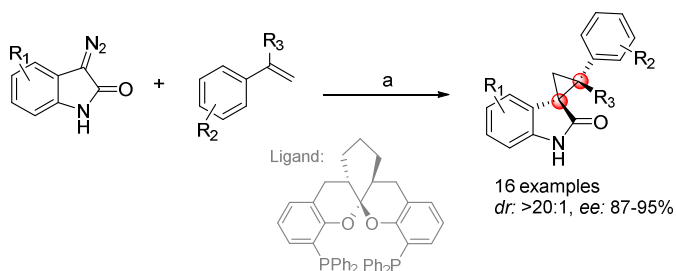


Figure 1.40 Synthesis of two adjacent quaternary centers by cyclopropanation. Reagents and conditions: a) AgOTf (4 mol%), ligand (AuCl)₂ (4.4 mol%), 1,4-F₂C₆H₄, 0 °C. Adapted from literature.¹³⁵

The synthesis of terpenes and steroids by polyene cyclization is also fundamental transformation in synthetic chemistry. These molecules contain multiple contiguous chiral and quaternary centers. Usually, chemically catalyzed polyene cyclizations are initiated with protonation or halogenation of the terminal isoprene. A recent reported example is the total synthesis of (+)-ferruginol and (+)-hinokiol initiated by a sulfenylating agent with the presence of a Lewis basic catalyst (Figure 1.41).¹³⁶

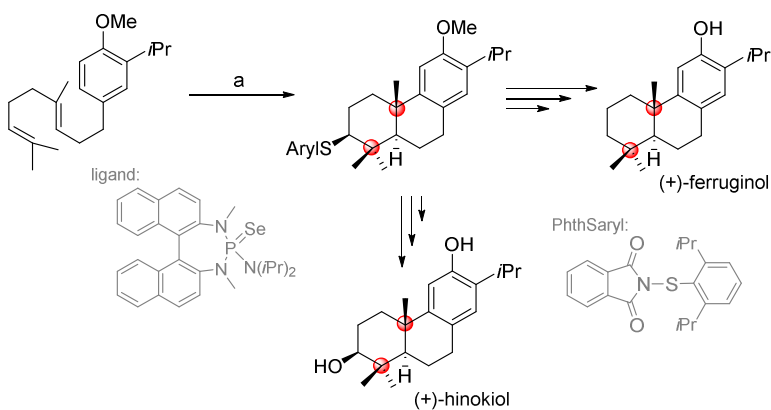


Figure 1.41 Synthesis of terpenes by polyene cyclization. Reagents and conditions: a) PhthSaryl (1 eq), ligand (0.05 eq), HFIP, 22 °C. Adapted from literature.¹³⁶

Quaternary centers are also found in non-natural pentose analogues present in nucleosides and nucleotides used as antiviral or anticancer drugs. Access to these compounds has been accomplished through enolate alkylation mediated by a Lewis acid, in a Mukaiyama aldol type reaction.¹³⁷ Following this strategy, the total synthesis of PSI-6130 that contains a tetrasubstituted chiral carbon and is an intermediate for the synthesis of Sofosbuvir, was achieved (Figure 1.42). This shows the potential of this methodology to create analogues of this prodrug.

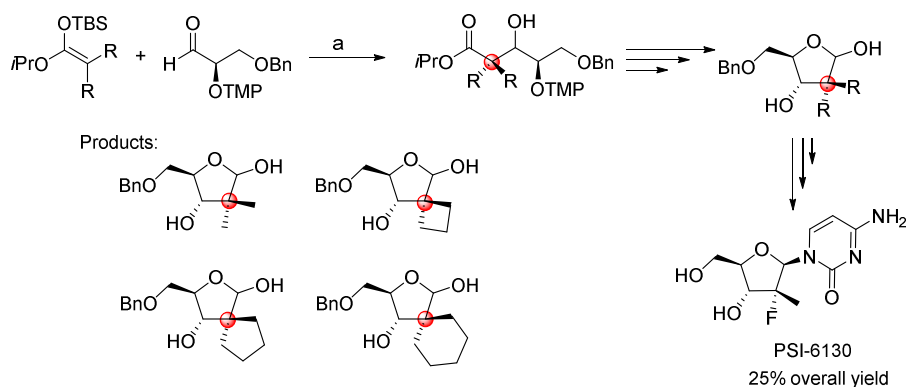


Figure 1.42 Synthesis of nucleoside derivatives by aldol reaction. Reagents and conditions: a) $\text{TiCl}_2(\text{O}i\text{Pr})_2$, DCM, $-20\text{ }^\circ\text{C}$. Adapted from literature.¹³⁷

Even though enzymatic methods to forge quaternary carbon stereocenters are scarce, biocatalysis has also been exploited recently as a tool to obtain these compounds with remarkable results. For instance, 3-substituted oxindoles and L-serine were used as substrates to enzymatically obtain the 3,3-disubstituted oxindoles.²⁴ In this case, six generations of directed evolution were needed to obtain the proper variant of the β -subunit of tryptophan synthase from *Pyrococcus furiosus* (TrpB $P_{f\text{quat}}$, EC 4.2.1.20) used as catalyst (Figure 1.43A).

Cyclopropanation of styrenes forming a quaternary center was also achieved using variants of cytochrome P450 from *Bacillus megaterium* (P450_{BM3}, EC 1.14.14.1).¹³⁸ More than 90 variants of this enzyme were tested to finally select 10 hits that gave the products with high diastereo- and enantioselectivity

Introduction

(Figure 1.43B). These two works highlight the power of protein engineering to modify existing enzymes for the catalysis of synthetically important reactions not previously observed in nature.

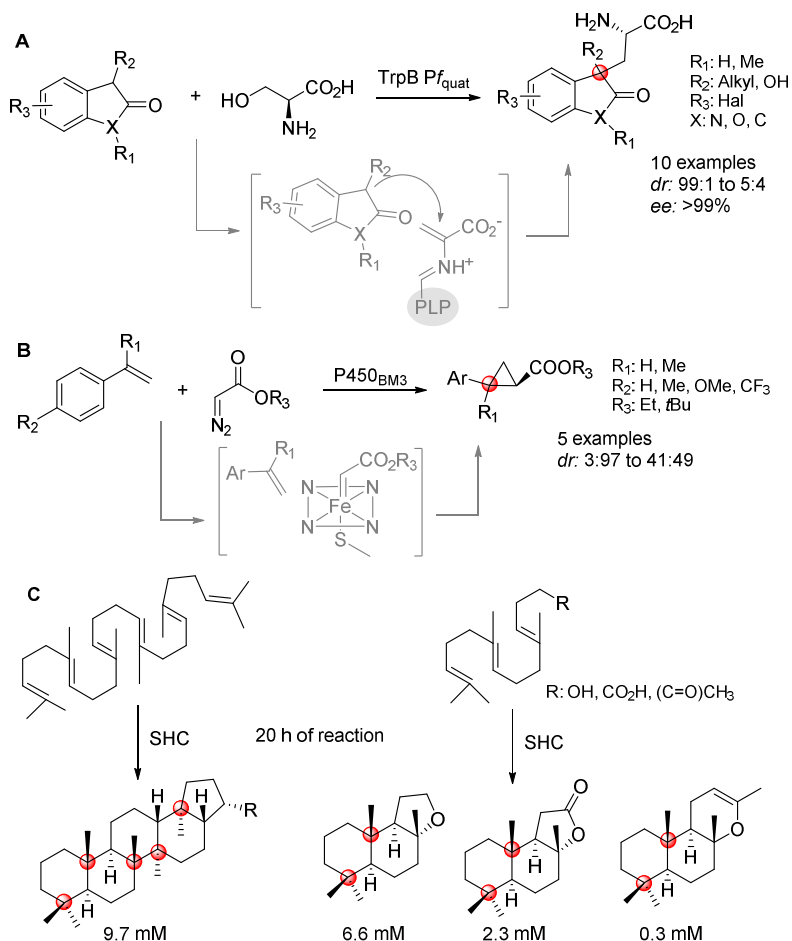


Figure 1.43 Biocatalysis applied in the formation of quaternary centers. **A** Synthesis of 3,3-disubstituted oxindoles catalyzed by the β -subunit of tryptophan synthase ($\text{Trp Pf}_{\text{quat}}$). **B** Cyclopropanation of styrenes obtaining two vicinal quaternary centers catalyzed by cytochrome (P450). **C** Cyclization of poly-isoprene backbones catalyzed by squalene-hopene cyclases (SHC).

Squalene–hopene cyclases (SHC, EC 5.4.99.17) have been used for the cyclization of poly-isoprene backbones obtaining natural and unnatural

terpenoids bearing quaternary centers. In particular, the substrate promiscuity of AacSHC from *Alicyclobacillus acidocaldarius* and ZmoSHC1 from *Zymomonas mobilis* catalyzed stereospecific cyclizations of poly-isoprene backbones without the need of initial activation and varying chain length and terminal nucleophile (Figure 1.43C).^{139, 140}

1.7.3 Synthesis and applications of nucleoside analogues

Nucleotides (and nucleosides) are essential biomolecules for life as they serve as monomeric units of DNA and RNA, and they play a central role in metabolism forming molecules such as ATP. For these reasons, these molecules are in the spotlight of drug design and more than 30 analogues have been approved for use in treating cancers, viruses, bacterial and fungal infections (Figure 1.44).¹⁴¹⁻¹⁴³

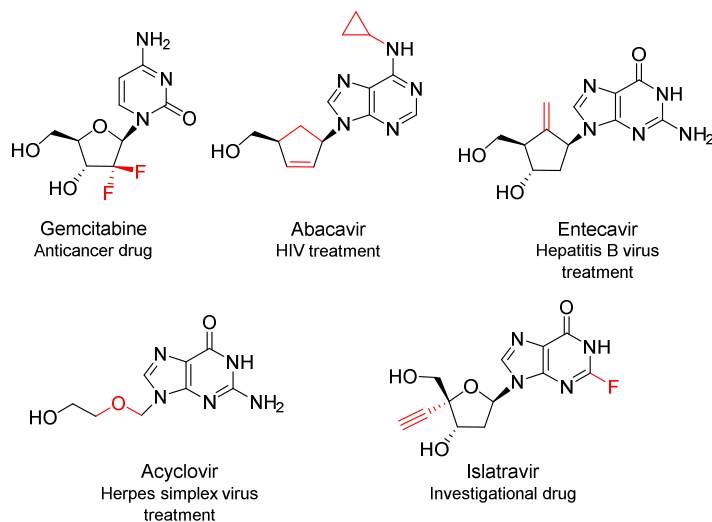


Figure 1.44 Examples of nucleoside analogues.

Several different sites can be considered for modifications to the natural nucleotide scaffold: the sugar moiety, the aromatic heterocyclic base, the glycosidic bond that connects the sugar to the heterocyclic base, and/or the phosphate group of the nucleotide.¹⁴⁴ Regarding the modifications of the

Introduction

furanose sugar component they include ring opening or ring size modification, halogenation, methylation, and hydroxylation or dehydroxylation (Figure 1.45).¹⁴⁵

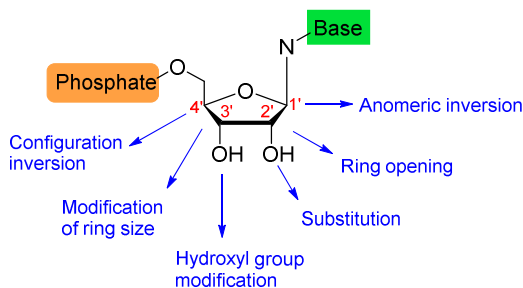


Figure 1.45 Different strategies for the modification of the furanose sugar moiety of a nucleotide. Adapted from literature.^{144, 146}

The earliest developed were the 2'-OH modifications and constitute the first medically relevant nucleoside analogues, which greatly impacted the field of drug design. They include Cytarabine, that is an arabinose analogue first synthesized during the 60s in which the configuration of the 2'-OH is inverted.¹⁴⁷ Some years later, the effect of a fluorine atom in this position was also explored and in the 90s the synthesis of Gemcitabine with geminal difluorine substituent was accomplished (Figure 1.46).^{148, 149}

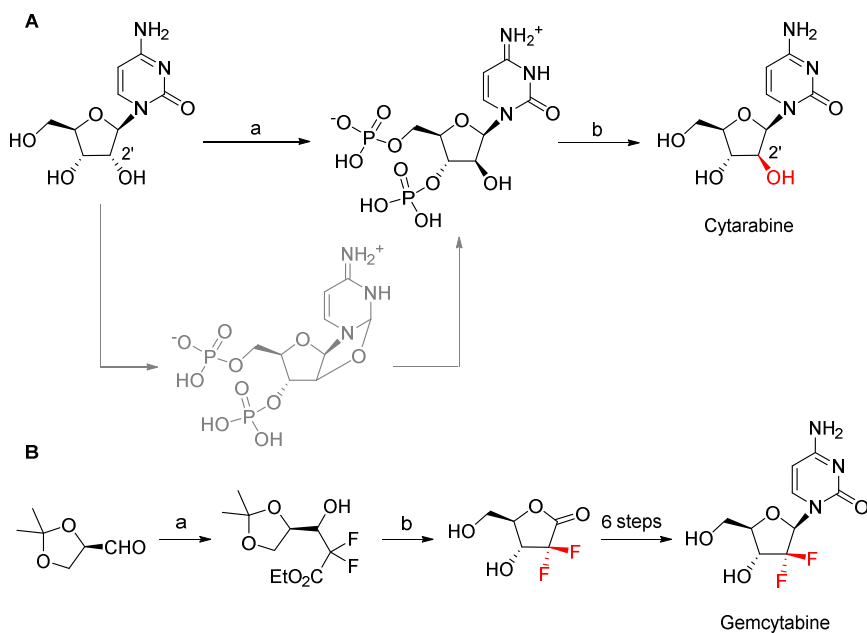


Figure 1.46 Synthesis of nucleosides with 2'-position modifications. **A** Cytarabine: a) $H_{n+2}P_nO_{3n+1}$ (polyphosphoric acid) and b) prostatic acid phosphatase (EC 3.1.3.5). **B** Gemcitabine: a) $BrCF_2CO_2Et$, Zn, THF, Et_2O and b) Dowex 50, MeOH, H_2O . Adapted from literature.¹⁵⁰

Numerous 2' modified nucleoside analogues have been developed since then. For example, methyl analogues or combinational approaches with fluorine replacement to yield 2'-deoxy-2'-fluoro-2'-methyl compounds have become common modifications for its effect on the overall conformation of the nucleoside.^{145, 151, 152} Moreover, modification of this position by cyano or ethynyl groups has been widely studied and were found to be important to enhance the stability of these analogues.^{153, 154} Modifications in the 4'-position of the furanose ring have been rather uncommon due to the synthetic challenges. Interestingly, 4'-fluoro and 4'-methyl modifications as well as the insertion of an azido and ciano groups have been also developed obtaining promising candidates for clinical trials.¹⁵⁵

Introduction

Islatravir (4'-ethynyl-2-fluoro-2'-deoxyadenosine, EFdA) is a paradigmatic example of antiviral drug with potent anti-HIV. Isaltavir was designed combining several strategic structural modifications. The fluorine at 2-position of the adenosine nucleobase and the 4'-ethynyl moiety work synergistically decreasing the susceptibility to adenosine deaminase while enhances the antiviral activity. The retention of the 3'-OH group also plays an important role blocking the incorporation of further nucleotides by the reverse transcriptase.¹⁵⁵⁻¹⁵⁷

Several approaches for the total synthesis of islatravir have been reported recently in the literature. The first one was described in 2004 and required a lengthy 18-step sequence from the expensive starting material 2-amino-2'-deoxyadenosine, which resulted in an overall yield of 2.5%.¹⁵⁸ Later on, several synthetic routes to islatravir have been reported reducing the number of steps and starting from different unexpensive materials such as diacetone-D-glucose, 1,3-diacetoxyacetone or 2-deoxy-D-ribose (Figure 1.47).¹⁵⁹⁻¹⁶²

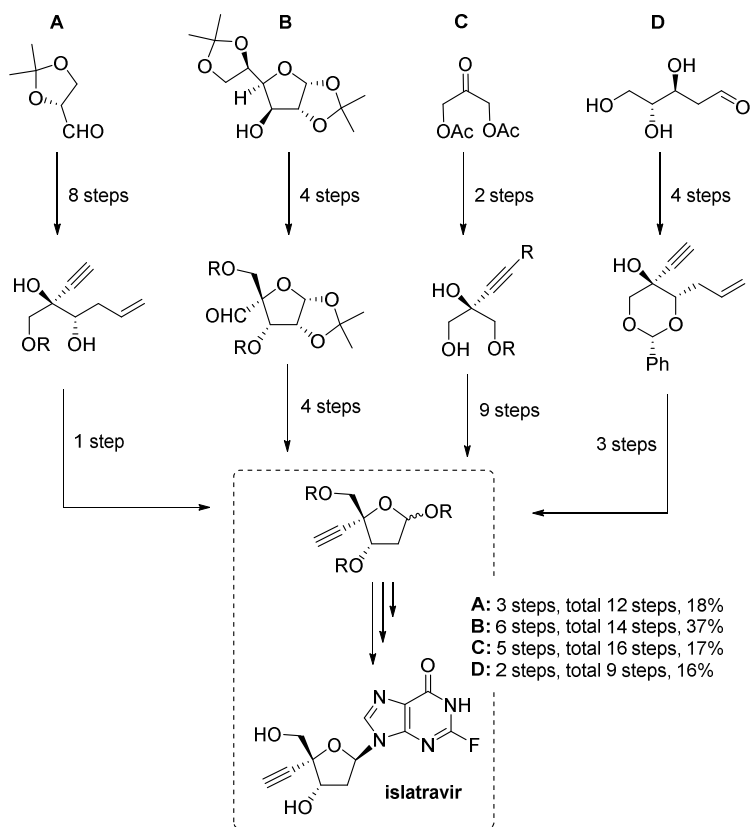


Figure 1.47 Comparison of different chemical approaches for the total synthesis of islatravir.

All these approaches require several protection and deprotection steps in addition to purification techniques for the separation of diastereomeric intermediates. To overcome these drawbacks, a biocatalytic cascade synthesis of islatravir achieving a 51% yield from the achiral building block 2-ethynylglycerol was reported in 2019. Five enzymes were engineered through directed evolution to accept non-natural substrates and four were used as auxiliary enzymes. It is important to notice that the synthesis of the starting material 2-ethynylglycerol was obtained following a 4-step synthesis with 10% yield (Figure 1.48A).¹⁶³

Introduction

Recently, a new and elegant route to the chiral precursor aldehyde was reported in order to improve the access to the intermediates. In this case, enantioselectivity was obtained using a chiral ligand for the alkylation of the ketone and followed by an ozonolysis step lead the final precursor in a 77% yield. This approach leverages the final enzymatic step of the previous synthesis (Figure 1.48B).¹⁶⁴

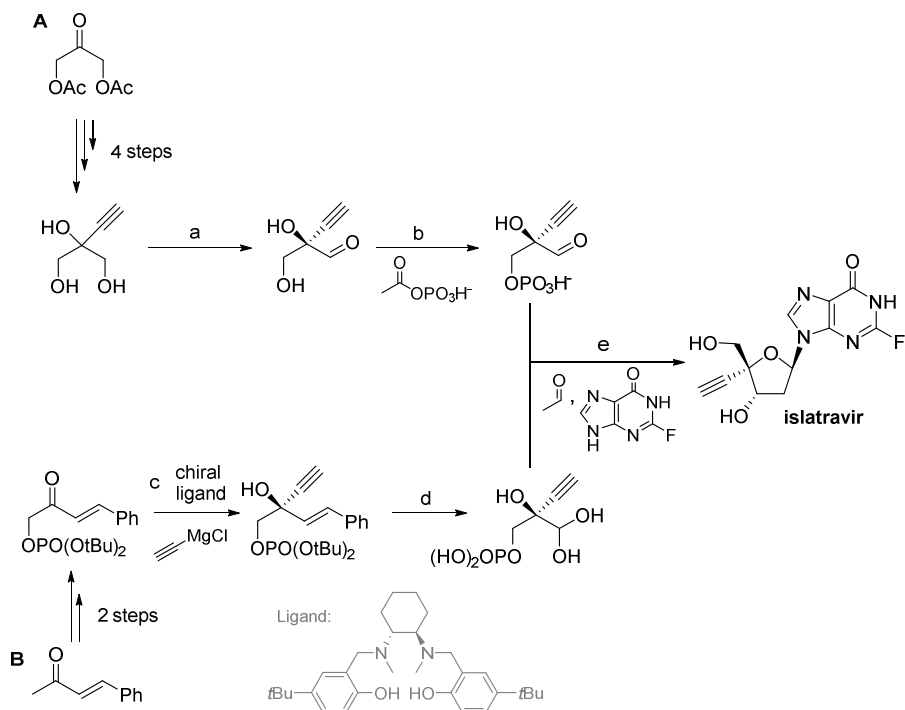


Figure 1.48 Two chemoenzymatic synthesis of islatravir with a final common enzymatic step. **A** Nine enzyme cascade synthesis: a) galactose oxidase Rd13BB, catalase, horseradish peroxidase; b) pantothenate kinase Rd4BB, acetate kinase. **B** Five-step synthesis: c) ligand (50 mol%), LiHMDS (25 mol%), THF, 0 °C; d) H₂O:acetone (1:9), O₃, Me₂S. Final common step: e) deoxyribose-5-phosphate aldolase (DERA) Rd3BB, phosphopentomutase Rd3BB, purine nucleoside phosphorylase Rd5BB, sucrose phosphorylase.

2 OBJECTIVES

General objective of the present doctoral thesis:

Development of biocatalytic applications of metal-dependent 2-oxoacid aldolases for the synthesis of chiral multifunctional compounds.

This objective involves:

2.1 Application of KPHMT and MBP-YfaU as biocatalysts for the chemoenzymatic synthesis of Roche esters derivatives.

- Cloning, expression, and characterization of the class II aldolase KPHMT from *E. coli*.
- Chemical synthesis of 2-oxoacids and evaluation as substrates in the aldol addition to formaldehyde catalyzed KPHMT and MBP-YfaU.
- Design and construction of variants of KPHMT by molecular biology techniques to enhance its nucleophile promiscuity.
- Chemoenzymatic synthesis, purification, and structural characterization (e.g., NMR, chiral HPLC and X-ray diffraction) of Roche ester derivatives (2-substituted 3-hydroxycarboxylate esters).

2.2 Usage of KPHMT as biocatalyst for the construction of molecules bearing quaternary carbon stereocenters

- Chemical synthesis and evaluation of 3,3-disubstituted-2-oxoacids and a panel of aldehydes as substrates for KPHMT.
- Design and construction of variants of KPHMT to increase its substrate scope.
- Preparative enzymatic synthesis, purification, and structural characterization (e.g., NMR, chiral HPLC and X-ray diffraction) of the aldol adducts bearing quaternary centers.

Objectives

2.3 Study the application of KPHMT and MBP-YfaU as biocatalysts for the synthesis of precursors of nucleoside analogues

- Chemical synthesis of aldehydes derived from D-glyceraldehyde including *O*-protected D-glyceraldehyde and α,α -disubstituted- α -hydroxyaldehydes.
- Screening of KPHMT and MBP-YfaU variants towards the aldol addition of selected 2-oxoacids and D-glyceraldehyde derivatives.
- Preparative enzymatic synthesis, purification, and structural characterization (e.g., NMR, chiral HPLC and X-ray diffraction) of the decarboxylated aldol adducts.

3 RESULTS AND DISCUSSION

3.1 Chemoenzymatic synthesis of Roche ester derivatives

3.1.1 Introduction

As mentioned in the introduction (section 1.7.1), Roche ester (i.e., 3-hydroxy-2-methylpropanoate) and its derivatives (2-substituted-3-hydroxycarboxylic esters) are an important class of chiral building blocks widely used in organic synthesis. They are largely employed in the synthesis of bioactive natural compounds and pharmaceuticals.¹¹⁶

Despite there are some catalytic and non-catalytic methodologies described in the literature to approach Roche ester derivatives, we envisaged a robust chemoenzymatic method for its enantiomerically pure synthesis. The first step consisted of an aldol addition of 2-oxoacids to formaldehyde catalyzed by an aldolase. Then, the corresponding aldol adducts were submitted to oxidative decarboxylation mediated by H₂O₂ and subsequently esterified to furnish 2-substituted-3-hydroxycarboxylic esters (**4**) (Figure 3.1.1).

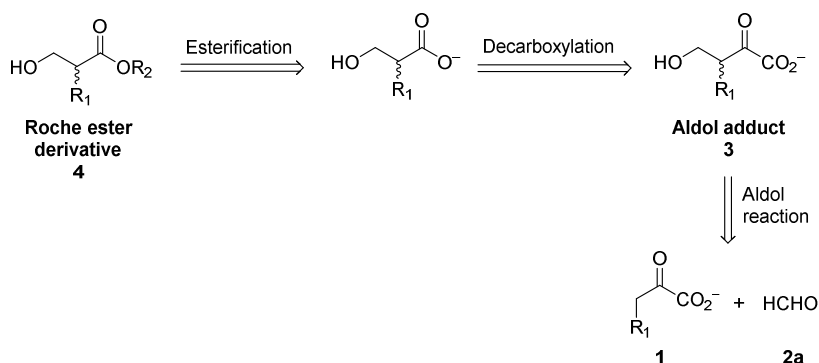


Figure 3.1.1 Retrosynthetic approach to Roche ester derivatives.

Hence, the initial enzymatic step features an aldolase that tolerates formaldehyde, a strong electrophile that inactivates enzymes and denatures proteins, and diverse 2-oxoacids. Class I aldolases are particularly sensitive to formaldehyde concentration, because the catalytic lysine residue reacts with formaldehyde, inhibiting or inactivating the enzyme.^{89, 165} For example, 2-deoxyribose-5-phosphate aldolase (DERA, EC 4.1.2.4) and D-fructose-6-

Results and discussion

phosphate aldolase (FSA, EC 4.1.2.-) are two well-known Class I aldolases that tolerate formaldehyde but in low concentrations (100 mM and 25 mM respectively).⁸⁹ In contrast, Class II aldolases utilize a metal ion as a cofactor to promote the enolization of the substrate, therefore they are less prone to be inactivated by strong electrophiles.⁷⁰ This makes Class II aldolases the biocatalysts of choice for the target reaction.

Herein, we exploited the potential capacities of two Class II aldolases that tolerate formaldehyde and utilize 2-oxoacids to furnish the synthesis of these important compounds. The first choice was YfaU (2-keto-3-deoxy-L-rhamnonate aldolase, EC 4.1.2.53) that catalyzes the reversible cleavage of 2-keto-3-deoxy-L-rhamnonate to furnish L-lactaldehyde and pyruvate.⁸⁵ In previous studies in our group, we reported YfaU aldolase from *E. Coli*, fused with the maltose binding protein (MBP) and variants thereof as a robust biocatalysts for aldol additions of 2-oxoacids to a variety of electrophiles.^{91, 92} Moreover, MBP-YfaU is unique among aldolases in that it retains activity at formaldehyde concentration >1 M and therefore is a highly qualified biocatalyst for the planned reactions.⁹⁰ Moreover, it was found that, even Mg²⁺ is the natural metal cofactor, MBP-YfaU with Ni²⁺ as non-natural metal cofactor displayed higher activity.^{85, 90}

The second choice was Class II KPHMT (ketopantoate hydroxymethyltransferase, EC 2.1.2.11) that catalyzes the transfer of an hydroxymethyl group from MTHF to α -KIV to furnish ketopantoate.⁷⁵ It was demonstrated that this enzyme utilizes formaldehyde as a source of the hydroxymethyl group operating as an aldolase under a tetrahydrofolate independent mechanism.⁷³ Due to this promiscuous activity, KPHMT was used with synthetic applications for the first time in this present work.

3.1.2 KPHMT as biocatalyst in aldol additions of 2-oxoacids to formaldehyde

KPHMT from *E. coli* K-12 was cloned in a pQE60 and obtained as glycerinated preparation in a concentration of 10 mg mL⁻¹ in high yields (170 mg protein L⁻¹ medium culture) after expression and purification (Figure 3.1.2). The use of glycerol as a cosolvent in aqueous solution is widely used in protein conservation because it is known to enhance the stability of proteins by inhibiting its aggregation. Moreover, the use of this polyol allows to have concentrated proteins samples after dialysis.¹⁶⁶ Analysis of the electrophoresis gel showed that the overexpressed KPHMT represented the 38% of the total amount of soluble protein (lane 1). Purification and dialysis yielded KPHMT in a 94% purity (lane 5). The electrospray mass spectrometry confirmed the molecular weight of the protein (Figure 3.1.3).

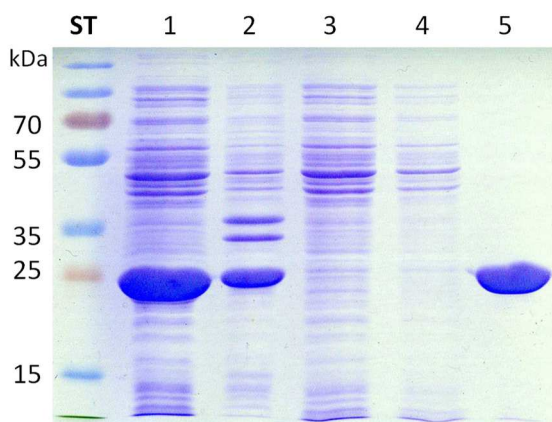


Figure 3.1.2 Coomassie Blue-stained SDS-PAGE analysis of wild-type KPHMT purification steps. The gel was loaded with samples from supernatant of lysis in which KPHMT represents the 34% of the soluble protein (**1**), pellet after lysis (**2**), flow-through fraction (**3**), wash fraction (**4**) and elution and dialyzed fraction with 94% purity of KPHMT (**5**). The molecular masses of the proteins in the Standard Molecular Weight Marker (ST) are as indicated. The predicted molecular mass of KPHMT is 29.5 kDa. Image analysis was performed using ImageJ.

Results and discussion

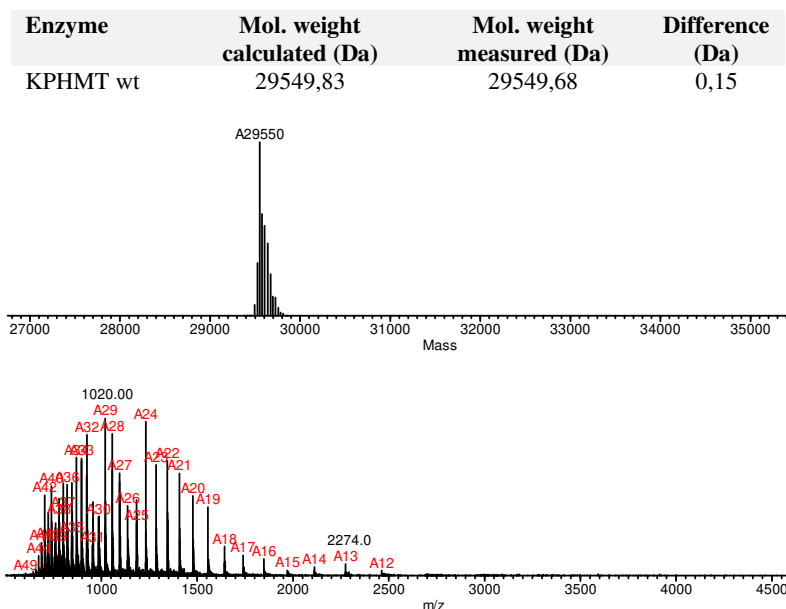


Figure 3.1.3 Molecular weight determination and MS ESI/TOF spectra and deconvolution spectra of the KPHMT wild-type. Molecular weight was calculated using ProtParam.

The activity of KPHMT as a function of metal cofactors was determined in the aldol addition of different nucleophiles to formaldehyde (Figure 3.1.4). The reactions were monitored after 30 min of reaction by HPLC after pre-column derivatization of the carbonyl group using *O*-benzylhydroxylamine. The results determined that the use of Co^{2+} enhanced the activity of the enzyme compared with the natural metal cofactor Mg^{2+} with the three nucleophiles tested. Particularly, the activity using Co^{2+} was almost two-fold higher than that with Mg^{2+} using 2-oxobutanoate (**1b**). Using Ni^{2+} the activity of KPHMT was the same as with Mg^{2+} for α -KIV (**1a**) or improved for 2-oxobutanoate (**1b**) and pyruvate (**1c**). Other bivalent metals have a deleterious effect on the activity of KPHMT.

Sugantino *et al.* showed that Mg^{2+} was the best bivalent metal cofactor for KPHMT.⁷³ However, this result is compatible with the ones obtained in this present work. The differences may be caused by the fact that they studied the

enolization rate of α -KIV and not the product formation after the aldol addition. These two processes may occur at different rates depending on the bivalent metal used. Moreover, it would be possible that using the natural substrate MTHF, the preferred metal cofactor would not be the same.

The use of non-physiological metals that can improve the activity of the enzymes, has been observed for other Class II aldolases such as L-rhamnulose-1-phosphate aldolase (RhuA, EC 4.1.2.19) or 4-hydroxy-2-oxoheptanedioate aldolase (HpaI, EC 4.1.2.52).¹⁶⁷⁻¹⁶⁹ In this thesis, MBP-YfaU with Ni²⁺ and KPHMT with Co²⁺ were used for the rest of the study.

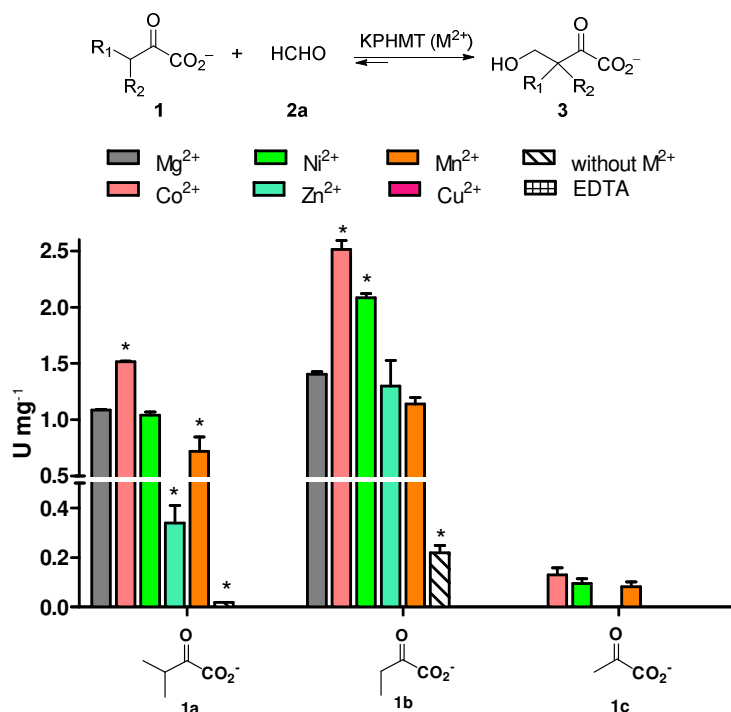


Figure 3.1.4 Activity of KPHMT-M²⁺ with different metal cofactors. One unit of activity was defined as the amount of KPHMT that catalyzes the formation of 1 μmol of aldol adduct per min. Activities were determined in duplicate and the standard error of the mean is shown. Comparisons were performed using one-way ANOVA and Bonferroni's post hoc test, * $P < 0.01$ vs Mg²⁺.

Results and discussion

Unexpected results were observed when comparing the activities between nucleophiles (Figure 3.1.4). Firstly, KPHMT was more active with 2-oxobutanoate (**1b**) than with its natural substrate α -KIV (**1a**). These results may indicate that the active site of KPHMT does not accommodate the two methyl groups of α -KIV with the same degree of affinity, one of the binding sides might stabilize much better than the other. Also, α -KIV is a more sterically hindered nucleophile and the formation of the active enolate and the approach to formaldehyde could be more hindered than with **1b**. Secondly, the activity of the catalyst was almost negligible with pyruvate (**1c**). In this case, the lack of an aliphatic chain at the β -carbon of pyruvate might preclude a good interaction with the enzyme active site becoming a poor substrate. This also could be related with the natural evolution of this enzyme, which was evolved to avoid consuming pyruvate, a central metabolite of paramount importance for the survival of the cell.

Another aspect in the catalytic mechanism of KPHMT is the role of the residue E181 that is proposed to be the acid-base residue in the literature.^{73, 79} To demonstrate this hypothesis, Glu 181 was substituted by Gln by site-directed mutagenesis. Once the variant E181Q was obtained, the enzymatic activity with the natural substrate α -KIV (**1a**) and formaldehyde (**2a**) using Mg^{2+} and Co^{2+} as cofactors was also determined (Figure 3.1.5).

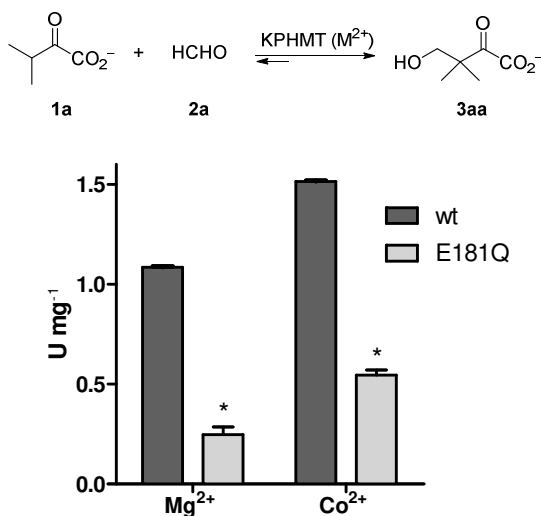


Figure 3.1.5 Comparison of the activity of KPHMT wt and E181Q with Mg²⁺ or Co²⁺ as cofactors. One unit of activity was defined as the amount of KPHMT that catalyzes the formation of 1 μ mol of aldol adduct per min. Activities were determined in duplicate and the standard error of the mean is shown. Student's t-test analysis was performed for comparison, * $P < 0.001$ vs wild-type enzyme.

The results showed that the enzymatic activity of the KPHMT variant E181Q decreased substantially compared with the wild-type with both metal cofactors. When using Mg²⁺, the activity decreased more than 4 times and in the case of Co²⁺ it decreased almost 3 times. The conversions after 24 h were also determined and in all cases, they were >95%. These results may indicate that the residue E181 plays an important role in the enzyme catalysis but that it might not be essential in the abstraction of the β -proton of the nucleophile. When E181 is missing, the proton abstraction may occur via an alternative mechanism through a catalytic water molecule which may act as an acid base (Figure 3.1.6). Furthermore, it must be considered that in this case one of the substrates employed was formaldehyde, which is a strong electrophile. It may be possible that in the natural reaction of KPHMT, where MTHF is used, the residue E181 was crucial for the catalysis. For these reasons, and for the

Results and discussion

observed activity, the molecular models and computational analysis of KPHMT were performed with E181 as the catalytic residue.

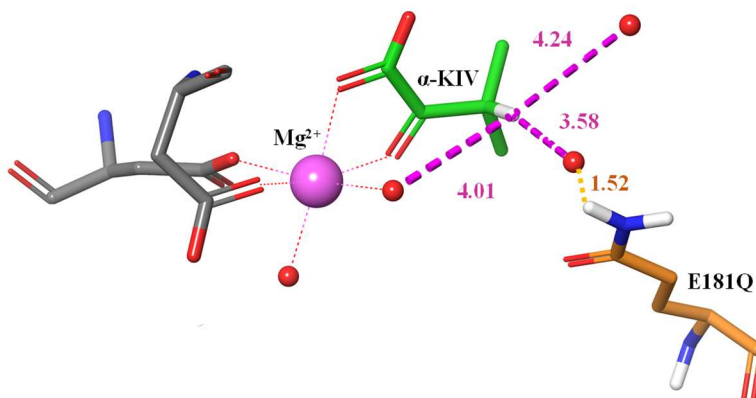


Figure 3.1.6 Model of the active site of KPHMT E181Q showing the distance of the closest water molecules to β -proton of substrate α -KIV.

3.1.3 Study of the aldol addition of 2-oxobutanoate to formaldehyde catalyzed by MBP-YfaU or KPHMT

To establish the reaction conditions between 2-oxobutanoate (**1b**) and formaldehyde (**2a**) catalyzed by MBP-YfaU and KPHMT we performed a discontinuous assay to determine the initial reaction rates and the conversions at 24 h. Conditions were: enzymes (4 mg mL⁻¹), metal cofactor (0.25 mM for Ni²⁺ and 0.6 mM for Co²⁺ in the reaction respectively, 4.5 eq respect to the biocatalyst) and two equimolar substrate concentrations (0.1 M and 1 M). Additionally, for both conditions, a control experiment without adding the enzyme was performed (Figure 3.1.7).

We detected complete conversions (>95%) of substrates to product after 24 h of reaction, for both aldolases at two concentration of substrates. Since strong electrophilic aldehydes such as formaldehyde often inactivate enzymes, the initial reaction rate is usually affected.⁸⁹ Concerning MBP-YfaU it was noticed that the initial reaction rates were not affected by high concentrations of formaldehyde, as it was also observed in previous studies in our laboratory

(Figure 3.1.7A).⁹⁰ Contrary, KPHMT became easily inactivated by this aldehyde and its initial reaction rate decreased notably at substrates concentration of 1 M. The fact that the conversion at 24 h was not reduced would mean that the enzyme retains its activity to transform completely the substrates before its complete deactivation (Figure 3.1.7B).

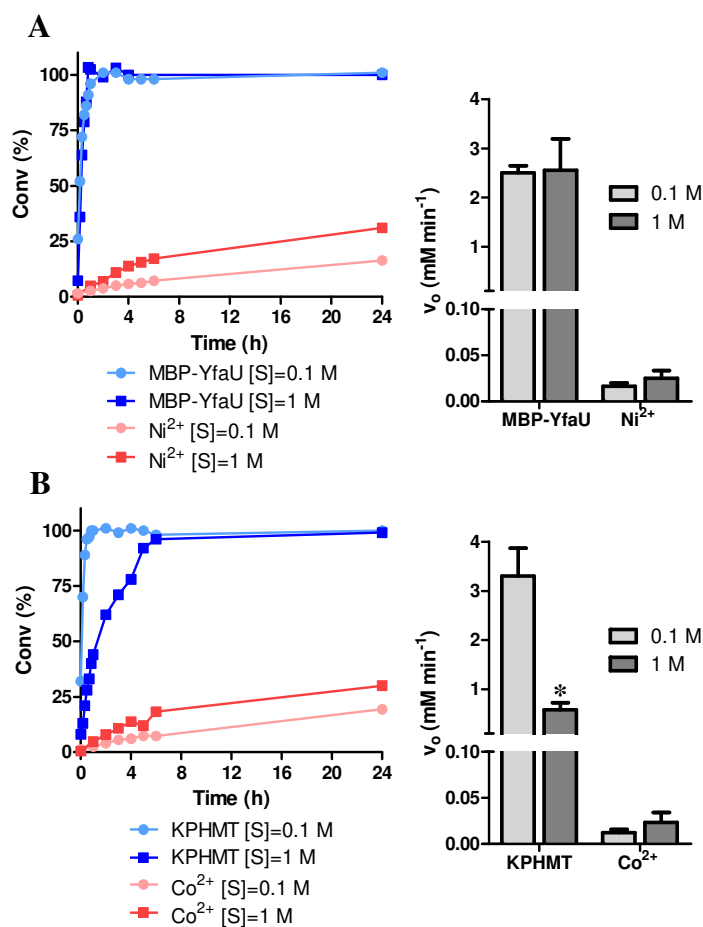


Figure 3.1.7 Conversion after 24 h and initial reaction rates for the aldol reactions between 2-oxobutanoate (**1b**) and formaldehyde (**2a**) catalyzed by **A** MBP-YfaU or **B** KPHMT. Conditions: [**1b**] = [**2a**] = 0.1 M or 1 M, 4 mg mL⁻¹ of enzyme, 4.5 eq M²⁺ respect to the catalyst. Student's t-test analysis was performed for comparison, **P* < 0.05 vs condition at 0.1 M.

Results and discussion

Moreover, in control experiments (without enzyme added) aldol product formation around 15–20% for substrates concentration of 0.1 M and 30% for 1 M concentration was observed. This background activity might be caused by the free metal cofactor Ni^{2+} and Co^{2+} in the reaction media, as well as due to the high reactivity of formaldehyde. It has to be taken into account that this could affect the enantiomeric excess of the biocatalytic products since the inactivation of the enzymes by formaldehyde would not stop the reaction course, which would continue in a non-enantioselective fashion. Therefore, the effect of the formaldehyde concentration on the stereochemistry of the products will have to be carefully observed.

In order to structurally characterize the aldol adduct **3ba**, we proceeded to scale up the aldol addition reaction of 2-oxobutanoate (**1b**) to formaldehyde (**2a**) catalyzed by MBP-YfaU or KPHMT. Different strategies to purify this type of aldol adducts are reported in the literature being the most common ones through ion exchange chromatography or purification after lactonization.¹⁷⁰⁻¹⁷² This last approach was attempted by incubating the aldol adduct with concentrated HCl overnight at 25°C. However, in our hands, under these conditions, the material was isolated as a complex mixture of products probably because of a combination of dehydration, lactonization and enolization reactions (Figure 3.1.8).

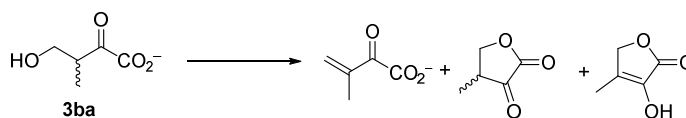


Figure 3.1.8 A complex mixture of products was obtained after the attempt to directly purify **3ba**.

Thus, to facilitate the product purification and characterization, the aldol adduct was transformed in an ester derivative (**4a**). The whole process resulted in a robust and effective three-step chemoenzymatic method for the synthesis of 2-methyl-3-hydroxycarboxylic esters (Figure 3.1.9).

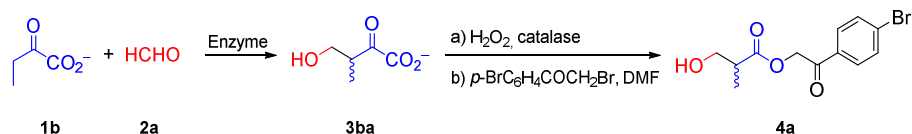


Figure 3.1.9 Chemoenzymatic synthesis of 2-methyl-3-hydroxycarboxylate esters.

In the first step, different equimolar concentrations of substrates (i.e., 0.1, 0.2, 0.4 and 1 M) were used to analyze the effect of formaldehyde concentration on the stereochemistry of the product. The reaction was followed by HPLC after precolumn derivatization using *O*-benzylhydroxylamine (Figure 3.1.10) and was processed when consumption of both substrates was observed (Figure 3.1.11).

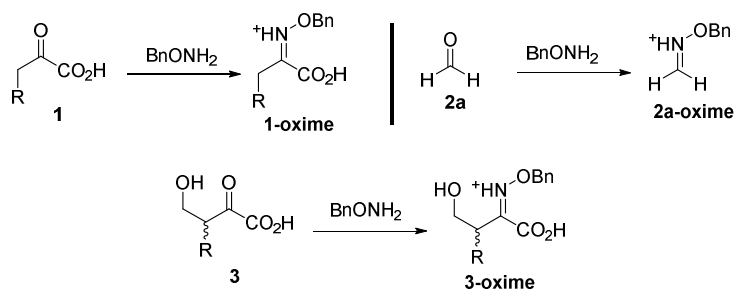


Figure 3.1.10 Pre-column derivatization reaction of carbonyl compounds with *O*-benzylhydroxylamine.

Results and discussion

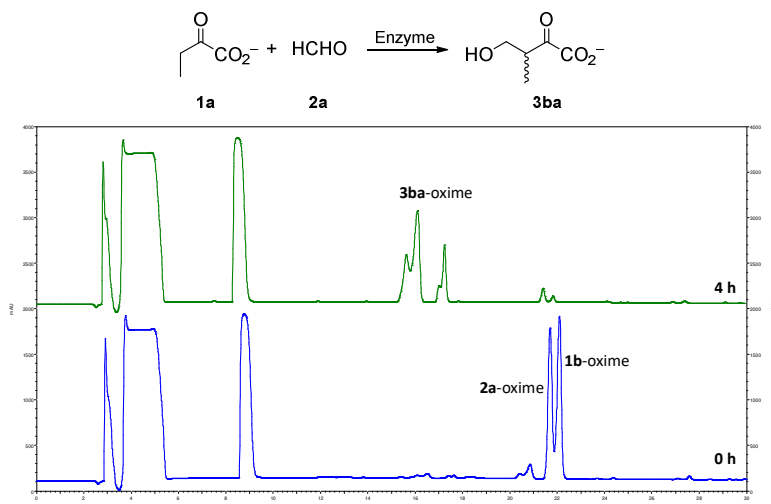


Figure 3.1.11 HPLC analysis of the aldol addition of 2-oxobutanoate (**1b**) to formaldehyde (**2a**) catalyzed by MBP-YfaU or KPHMT.

It is known that 2-oxoacids are rapidly and quantitatively decarboxylated by oxidizing reagents such as ceric sulfate, hydrogen peroxide or potassium permanganate.¹⁷³ Among them, the most common and well-studied is by using hydrogen peroxide, which can be performed in a wide pH range (between pH 4 to 9).¹⁷⁴ Moreover, the reaction produces only water and carbon dioxide as by-products and the unreacted hydrogen peroxide can be rapidly removed by the action of catalase (EC 1.11.1.6) that transform H₂O₂ into H₂O. Thus, once the aldol addition was complete (conversion > 95%, determined by HPLC) the aldol adduct (**3ba**) was submitted to an oxidative decarboxylation in situ obtaining the 2-methyl-3-hydroxycarboxylate (Figure 3.1.12A).

In the last step, the aldol adduct carboxylate was esterified with 2,4'-dibromoacetophenone furnishing 2-methyl-3-hydroxycarboxylate ester derivative (**4a**) (Figure 3.1.12B). While the use of this protecting group is not very common, in this case was convenient because of the mild conditions used for its introduction (i.e., in a polar aprotic solvent such as DMF without adding any base).¹⁷⁵ Furthermore, usually the products are solids and easy to purify,

and the presence of a Br atom facilitates its crystallization and characterization by X-ray diffraction if needed, simplifying the determination of the absolute stereochemistry.

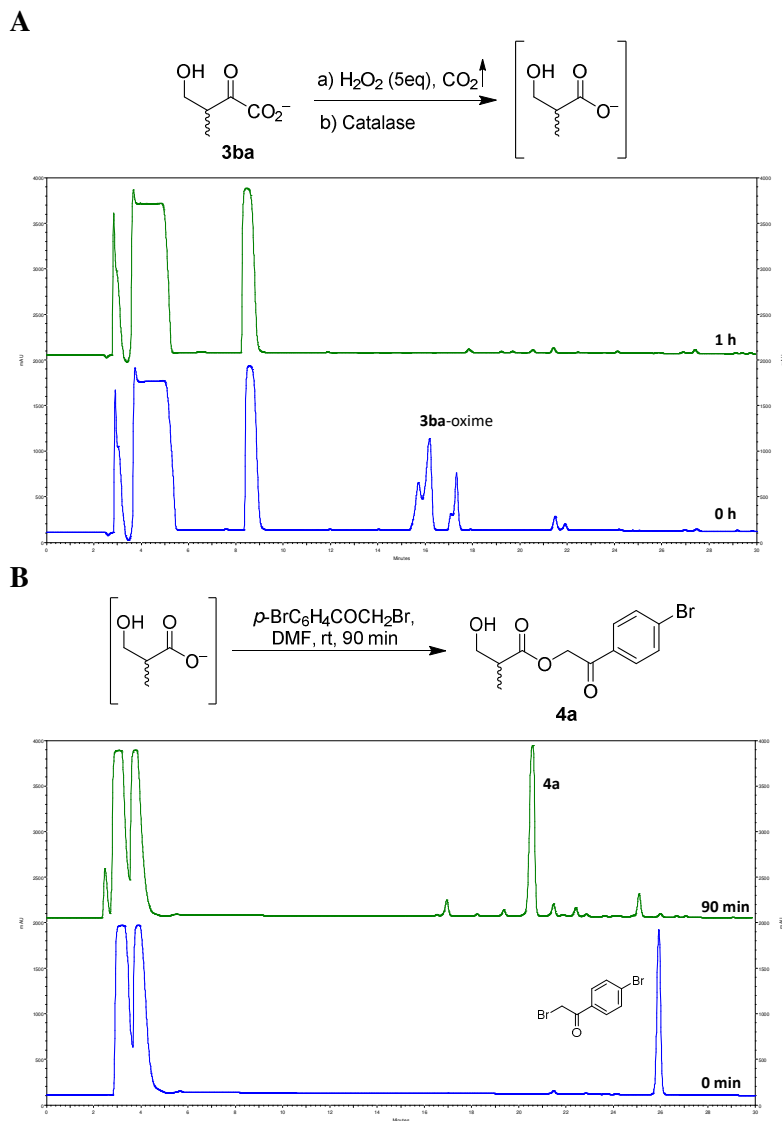


Figure 3.1.12 HPLC monitoring of A oxidative decarboxylation of aldol adduct (3ba) and B synthesis of 4-bromophenacyl ester (4a).

Results and discussion

The stereochemical characterization of products **4a** was performed by HPLC analysis on chiral stationary phases (Figure 3.1.13). Authentic samples of enantiomerically pure (*S*) and (*R*)-phenacyl ester derivatives were synthesized from commercially available (*S*) and (*R*)- β -hydroxyisobutyric acid sodium salts. Likewise, its equimolar mixture was used as a racemic sample mixture (*rac*-**4a**). The results showed that MBP-YfaU and KPHMT catalyzed the formation of enantiocomplementary products producing the (*S*) and the (*R*) enantiomer respectively.

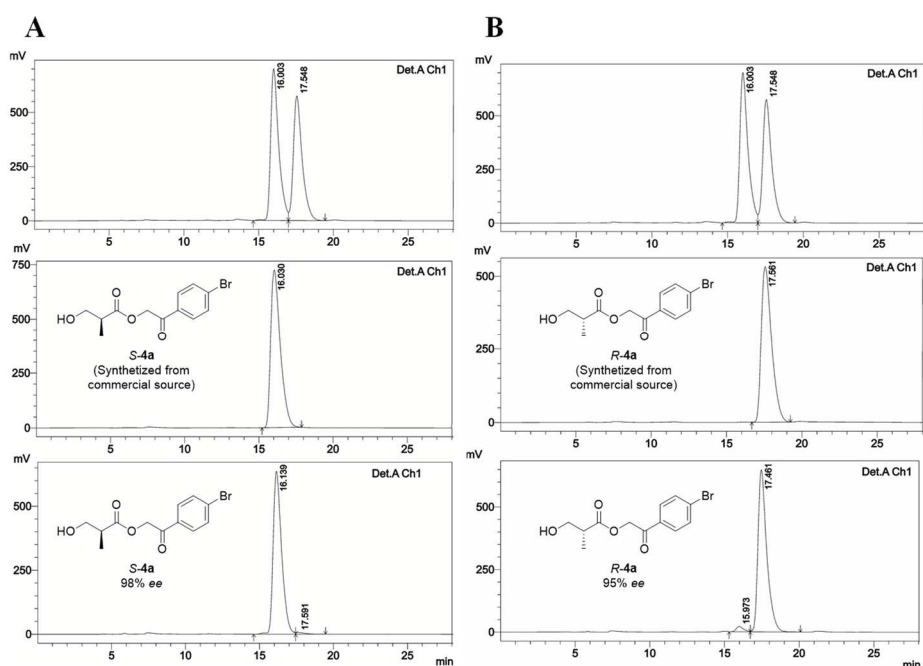


Figure 3.1.13 Chiral HPLC analysis chromatogram of **A** *S*-**4a** synthesized with MBP-YfaU and **B** *R*-**4a** synthesized with KPHMT. Conditions: CHIRALCELL® OD 46 x 250 mm column, 5 μ m, flow rate 0.7 mL min⁻¹ at 20 °C and UV detection (254 nm). Isocratic elution hexane:iPrOH 80:20.

Using the X-ray structures of MBP-YfaU and KPHMT available we could generate computational models of the enolate formation of **1b** in the active site of the enzymes. Both biocatalysts generated *Z*-enolates in their active sites and

the difference of enantioselectivities lies in the fact that the configuration of the pocket exposed different enantiotopic faces of the enolate to formaldehyde. In fact, the enzyme-enolate complex generated by both enzymes can be considered epimers. Thus, in MBP-YfaU, the exposed face of the enolate was the *re*-face whereas in the case of KPHMT the exposed face was the *si*-face giving (*S*) and (*R*) aldol adducts respectively (Figure 3.1.14).

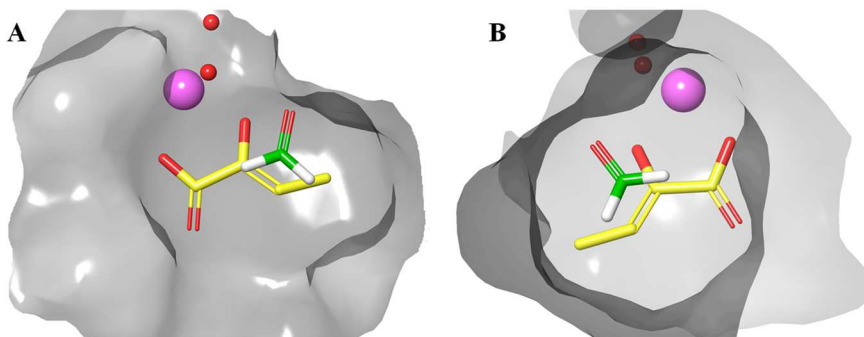


Figure 3.1.14 Z-enolate formation in the active sites of **A** MBP-YfaU, where the electrophile approaches to the *re*-face of the enolate and **B** KPHMT, where the electrophile approaches to the *si*-face.

Moreover, the effect of the formaldehyde concentration on the enantiomeric excess of the products was analyzed (Figure 3.1.15). According to previous results, KPHMT became more rapidly inactivated by high concentrations of formaldehyde than MBP-YfaU. Although the conversions at 24 h were not affected (>95%), the inactivation of KPHMT caused a decrease in the enantiomeric excess (from 98% ee at 0.1 M of formaldehyde to 80% ee at 1 M). MBP-YfaU tolerated high concentrations of formaldehyde and the ee was not altered by this parameter.

Results and discussion

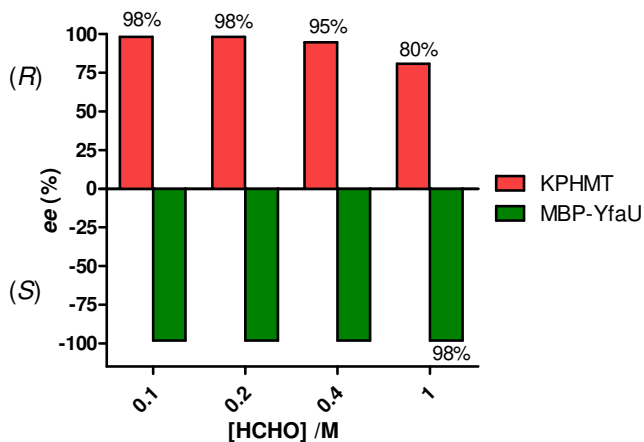


Figure 3.1.15 Enantiomeric excess of the enzymatic products *S* and *R*-**4a** at different concentrations of formaldehyde. [**1b**] = [**2a**], 4 mg mL⁻¹ of enzyme, 4.5 eq M²⁺.

3.1.4 Synthesis and screening of a panel of 2-oxoacids

In order to generate enantiomerically pure Roche ester derivatives we expanded the approach to a variety of 2-oxoacids as nucleophile components in the aldol addition to formaldehyde (**2a**) catalyzed by MBP-YfaU and KPHMT (Figure 3.1.16).

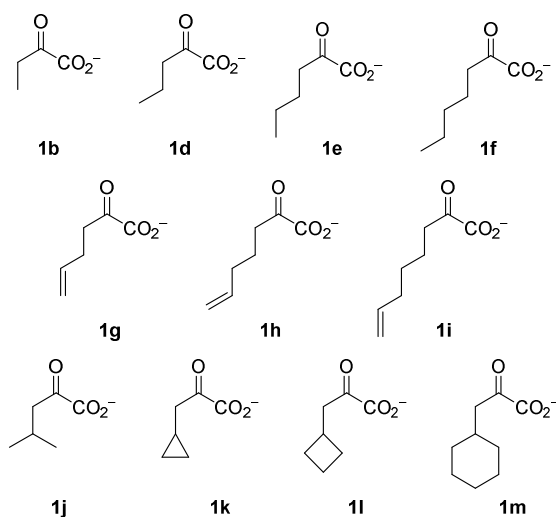
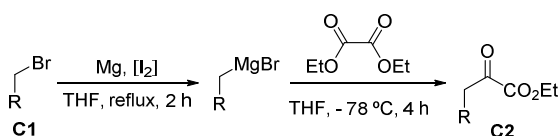


Figure 3.1.16 Panel of selected nucleophiles for the synthesis of Roche ester derivatives.

2-Oxoacids **1b**, **1d** and **1j** were commercially available while the others were synthesized in our lab. There are different methodologies reported in the literature for the synthesis of 2-oxoacids and we envisaged its preparation through the synthesis of ethyl ester intermediates obtained through a Grignard reaction.^{173, 176} Thus, the preparation of 2-oxoesters **C2e-i** and **m** was accomplished by the addition alkyl-magnesium bromides to diethyloxalate. Alkyl-magnesium bromides were obtained from the corresponding bromoalkanes (**C1e-i,m**), using standard Grignard methodology (Table 3.1.1).

Table 3.1.1 Isolated yields (%) of the synthesis of 2-oxoesters (**C2e-i** and **m**) from its corresponding bromoalkanes (**C1**) through Grignard reaction.



R	Yield (%)
e	89
f	93
g	92
h	84
i	79
m	91

There are several chemical methods for ester hydrolysis such as the acid catalyzed or the basic catalyzed (i.e., saponification) hydrolysis. Nevertheless, these usually require extreme pHs and high temperatures. This is not usually compatible with the stability of 2-oxoesters because the inherent acidity of the α -proton of the carbonyl group and the vicinal carbonyl and carboxyl groups. For this reason, we envisaged the application of lipases for the hydrolysis of the precursors **C2**. Enzymatic methods employing lipases, which catalyze this hydrolysis at neutral pH and room temperatures, have been widely used to this aim, also in large scale synthesis.^{173, 177, 178}

Results and discussion

Thus, a screening of different commercially available lipases was realized. The reference substrate was **C2e**, and reactions were performed in a biphasic system composed by 2-MeTHF/ sodium phosphate buffer (1 M, pH 7.0), 1:1 (v/v). Reactions were analyzed after 24 h by TLC (Figure 3.1.17).

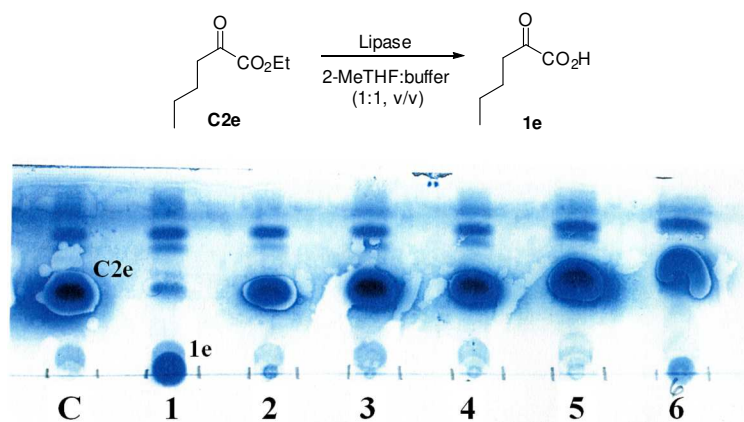
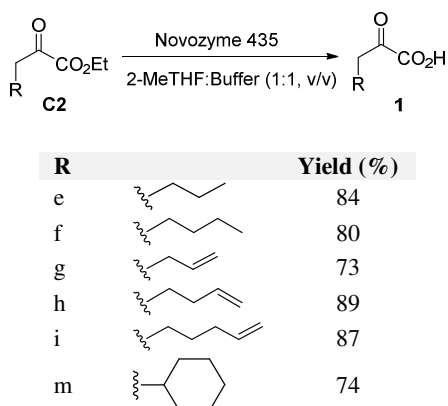


Figure 3.1.17 Screening experiment using different lipases for the hydrolysis of **C2e**. TLC eluted with hexane:AcOEt, 1:1 (v/v), stained with cerium ammonium molybdate stain. Control experiment without lipase (C), Novozyme 435 (1), Lipozyme TL IM (2), Lipozyme RM IM (3), Lipozyme immobilized from *Mucor miehei* (4), Lipozyme TL 100L (5) and Lipase from porcine pancreas type II (6) are shown.

The results showed that the Novozyme 435 was the best for the hydrolysis of **C2e**, obtaining almost complete transformation of the substrate. Once complete conversions were detected by visual inspection of the TLC plates, the 2-oxoacids (**C1**) were easily extracted from reaction media under mild acidic conditions, yielding pure compounds without the need of any further purification step (Table 3.1.2).

Table 3.1.2 Isolated yields (%) of the synthesis of 2-oxoacids (**1e–i** and **m**) from its corresponding 2-oxoesters (**C2e–i** and **m**) using the Novozyme 435 lipase.



The synthesis of **C2k** was attempted using the same methodology but rendered the **C2g**. This transformation was also previously observed in the literature.¹⁷⁹ It was reasoned that the intermediate cyclopropylmethyl magnesium bromide behaved as a carbanion that through a push-pull mechanism underwent ring opening isomerization generating 3-butenyl substituent, which was added to diethyl oxalate (Figure 3.1.18).^{180, 181}

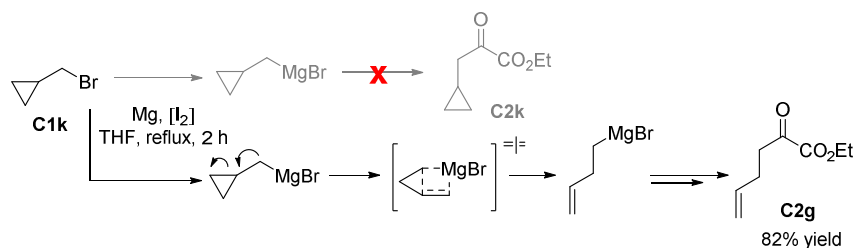


Figure 3.1.18 Proposed mechanism of the ring opening isomerization of cyclopropylmethyl Grignard reagent.

Hence, the synthesis of **1k** and **1l** was achieved by another strategy previously reported in the literature that resulted to be effective for the synthesis of 2-oxoesters.^{182, 183} It consisted on the alkylation of ethyl 1,3-dithiane-2-carboxylate with the corresponding bromocycloalkane (**C1k–l**), followed by

Results and discussion

oxidative removal of the dithiane group using *N*-bromosuccinimide. None of the intermediates of this synthesis needed to be isolated. Finally, ethyl esters (**C2k–l**) were enzymatically hydrolyzed using Novozyme 435 (Figure 3.1.19).

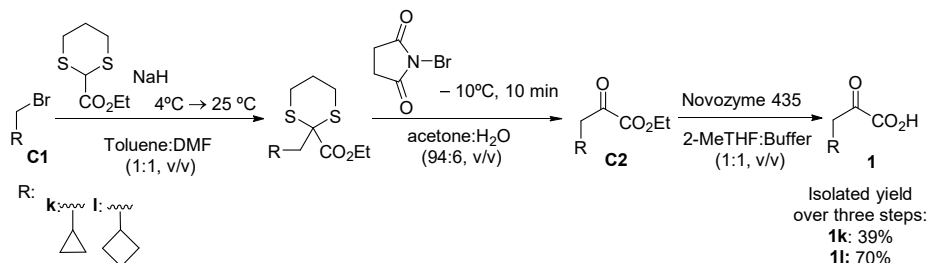


Figure 3.1.19 Chemoenzymatic synthesis of 2-oxoacids (**1k–l**) from its corresponding bromoalkanes (**C1**) through ethyl 1,3-dithiane-2-carboxylate alkylation.

Using the first methodology, the products **1e–i** and **m** were achieved in 67–75% isolated yields over three steps. The procedure followed for the synthesis of **1k** and **1l** rendered the 2-oxoacids in 39 and 70% isolated yields, respectively.

The panel of 2-oxoacids was screened with formaldehyde (**2a**) as electrophile, using the stereocomplementary aldolases MBP-YfaU and KPHMT (Figure 3.1.20). Both enzymes accepted a wide variety of nucleophiles. Analogues with the shortest aliphatic chains (i.e., **1b,d** and **1k**) rendered the highest conversions at 24 h. Lower conversions were achieved for 2-oxoacid homologues with larger substituents than ethyl or cyclopropyl. An exception was the allyl homologue (**1g**) using KPHMT catalyst.

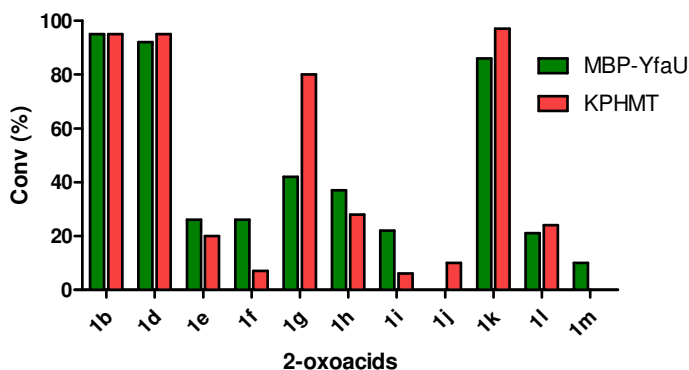
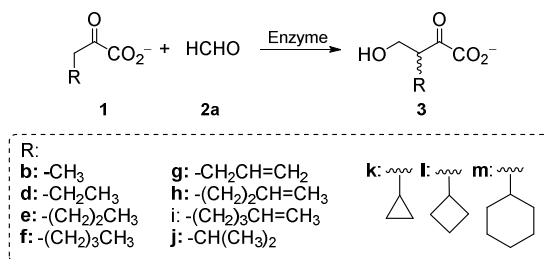


Figure 3.1.20 Conversion (%) after 24 h of the aldol addition of 2-oxoacids (**1**) to formaldehyde (**2a**) catalyzed by MBP-YfaU and KPHMT. [**1**] = [**2a**] = 0.1 M, 4 mg mL⁻¹ of enzyme, 4.5 eq M²⁺ respect to the catalyst.

The difficulty of both aldolases to accept 2-oxoacids with large hydrocarbon chains can be attributed to size limitations of the nucleophile binding site. Regarding MBP-YfaU, similar observations had already been reported in previous studies in our group.⁹²

3.1.5 Construction of enzyme variants and screening with different nucleophiles

In previous works in our group, it was observed that wild-type MBP-YfaU has limitations on accepting nucleophiles with long or branched alkyl chains. To alleviate the steric hindrance in the active site and accommodate larger groups, variants of this enzyme were designed for this purpose. Thus, examining the X-ray structure, it was noticed that the alkyl chain of the nucleophiles was oriented

Results and discussion

towards the residues W23 and L216, which form a small hydrophobic pocket in the active site of YfaU.⁹² Thus, two variants of MBP-YfaU (W23V and W23V/L216A) that were available in our laboratory were used in this thesis to be screened with the panel of different nucleophiles.

Regarding KPHMT, molecular models in complex with the **1k**-enolate and **2a** were constructed. This showed a relatively tight packing of the nucleophile cyclopropyl substituent against the hydrophobic cavity where the distances are less than 4 Å. The residues delimiting this cavity in the active site were the L42, H136, V179, E181, I202 and I212. To increase the size of the cavity, residues L42, I202 and I212 were selected to be mutated by a smaller residue such as Ala (Figure 3.1.21).

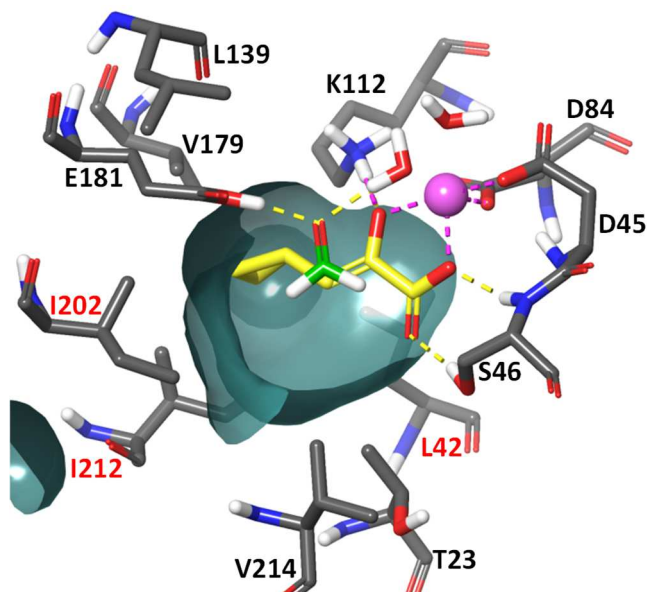


Figure 3.1.21 Model of wild-type KPHMT complexed with nucleophile (**1k**, yellow C atoms) and formaldehyde (**2a**, green C atoms). The metal cofactor (magenta), water molecules (red) and surface of the active site cavity (cyan) are shown. Selected residues to be mutated are highlighted in red. The model is built starting from the crystal structure of KPHMT in complex with ketopantoate (PDB 1M3U).

Usually Ala is selected (e.g., in the alanine scanning approach) because is a chemically inert, non-bulky residue that maintains the methyl functional group important for the folding of the protein in its native tridimensional structure.¹⁸⁴ Other residues could have been good candidates for Leu or Ile substitution. For example, Val, which is a smaller branched amino acid, could be a good option but we considered that the change would be too conservative. Contrary, mutation to Gly or Pro was discarded in the first place as it could imply a critical change in the structure of the enzyme leading to inclusion bodies formation.

Thus, variants L42A, I212A, L42A/I212A and I202A were generated by site-directed mutagenesis through two different strategies. Mutation at the L42 position was achieved by QuickChange® methodology. Mutation at the position I212 was also attempted by this strategy but was not possible. Thus, the megaprimer methodology, which resulted to be highly reproducible, was used to construct all the other variants that were obtained in high yields (102–170 mg protein L⁻¹ medium culture) (Figure 3.1.22).

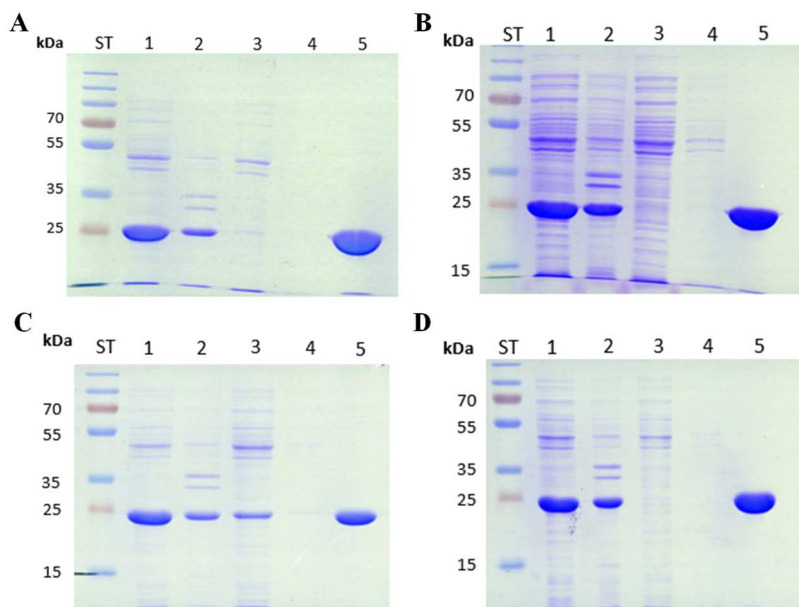


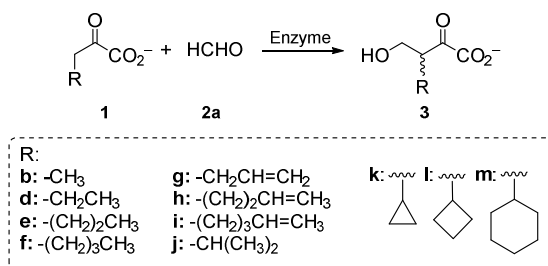
Figure 3.1.22 Analysis of KPHMT purification steps by Coomassie Blue-stained SDS-PAGE. Wild-type (A), L42A variant (B), I212A variant (C), L42A/I212A variant (D)

Results and discussion

and I202A variant (**E**). The gel was loaded with samples from supernatant of lysis (lane 1), pellet after lysis (lane 2), flow-through fraction (lane 3), wash fraction (lane 4) and elution and dialyzed fraction (lane 5). The molecular masses of the proteins in the Standard Molecular Weight Marker (ST) are as indicated. The predicted molecular mass of KPHMT is 29.5 kDa.

The variants of both aldolases were able to catalyze most of all aldol addition of 2-oxoacids to formaldehyde with good to excellent conversions (Table 3.1.3). In particular, for MBP-YfaU the single mutation W23V was sufficient to accommodate all the nucleophiles with excellent conversions after 24 h of reaction (85–97%), even for the largest one with the cyclohexyl substituent (**1m**). The double variant W23V/L216A showed similar product conversions than the single mutant.

Regarding KPHMT, one unique variant was not enough for efficiently accept all the different nucleophiles. Thus, KPHMT I212A variant accepted nucleophiles with long chain substituents (**1e–i**), furnishing high conversions (88–94%) but it was not competent with branched (**1j**) or larger cyclic (**1l–m**) derivatives. Fortunately, the I202A variant displayed some activity with these later types of nucleophiles, which resulted in reasonable conversions for **1j** (57%) and **1l** (79%). Nevertheless, the I202A variant was still inefficient with the largest cyclic substitution (**1m**). The L42A mutation alone displayed a deleterious effect relative to the wild-type enzyme and when combined with the I212A did not appear to improve the effect of the single mutation.

Table 3.1.3 Conversion after 24 h (%) of the aldol addition of 2-oxoacids (**1**) to formaldehyde (**2a**) catalyzed by MBP-YfaU and KPHMT and variants.

	2-oxoacid (1)										
	1b	1d	1e	1f	1g	1h	1i	1j	1k	1l	1m
	Aldol adduct (3)										
	3ba	3da	3ea	3fa	3ga	3ha	3ia	3ja	3ka	3la	3ma
MBP-YfaU											
wt	95	92	26	26	42	37	22	- ^a	86	21	10
W23V		95	95	95	95	95	90	93	97	95	85
W23V/L216A		95	88	78	95	95	84	90	97	92	74
KPHMT											
wt	95	95	20	7	80	28	6	10	97	24	- ^a
L42A			- ^a	- ^a	26	- ^a	5	- ^a	29	14	- ^a
I212A			88	88	92	93	88	12	94	22	- ^a
L42A/I212A			87	87	95	86	90	19	88	20	- ^a
I202A								57	94	79	- ^a

[**1**] = [**2a**] = 0.1 M, 4 mg mL⁻¹ of enzyme, 4.5 eq M²⁺ respect to the catalyst. ^aProduct not detected.

The results of the screening were coincident with the analysis done *in silico* for both enzymes. For example, a molecular model of the ternary complex between wild-type YfaU, the **1k**-enolate and the electrophile **2a**, showed a good accommodation of the substrates in the active site (Figure 3.1.23A). Fitting larger nucleophiles would imply strained conformations. We observed that the single W23V mutant could nicely accommodate the largest cyclic nucleophile (**1m**) in the cavity without perturbing the approach of the formaldehyde molecule (Figure 3.1.23B).

Results and discussion

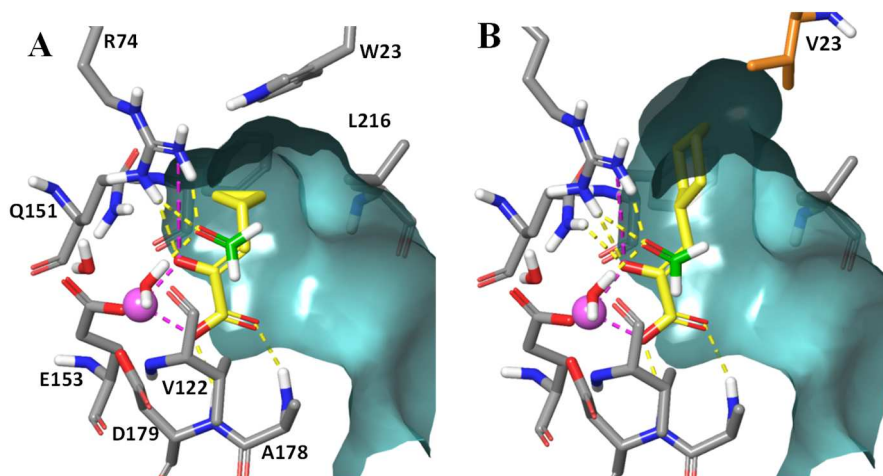


Figure 3.1.23 Models of **A** wild-type YfaU and **B** YfaU W23V complexed with formaldehyde (**2a**, green C atoms) and nucleophiles (**1k** and **1m** respectively, yellow C atoms). The metal cofactor (magenta), water molecules (red) and surface of the active site cavity (cyan) are shown. Models are built starting from the crystal structure of YfaU in complex with pyruvate (PDB 2VWT).

Concerning KPHMT, molecular models of the variants showed that the I212A generated a deeper cavity at one site and therefore accepted nucleophiles with long chain substituents such as **1i** (Figure 3.1.24A). I202A mutation extended and increased the volume of the other site of the cavity, allowing an adequate placement of branched substrates such as **1j** (Figure 3.1.24B). These observations were coincident with the results of the screening.

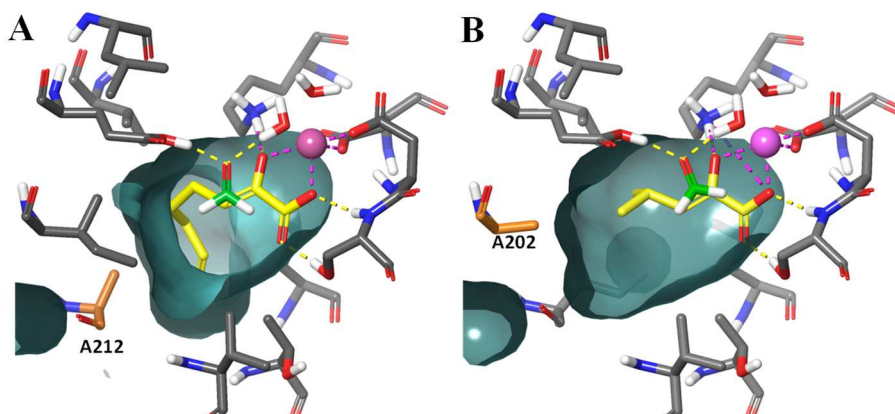


Figure 3.1.24 Models of **A** KPHMT I212A and **B** KPHMT I202A complexed with formaldehyde (**2a**, green C atoms) and nucleophiles (**1i** and **1j** respectively, yellow C atoms). The metal cofactor (magenta), water molecules (red) and surface of the active site cavity (cyan) are shown. Models are built starting from the crystal structure of KPHMT in complex with pyruvate (PDB 1M3U).

The initial rates of the aldol addition reactions were determined to choose the best biocatalyst for each case and run the preparative scale experiments. Wild-type MBP-YfaU displayed a significant activity (v_0) for **1b** but considerably lower for **1d** and **1k**, and much lower for the other nucleophiles (Figure 3.1.25A). MBP-YfaU variants were able to increase these activities considerably. In general, W23V showed moderately higher reaction rates than the double mutant and this, together with the similar tendency obtained in the conversions after 24 h, were determinant to choose the enzyme MBP-YfaU W23V to perform the scale up reactions.

Wild-type KPHMT showed substantial activities for nucleophiles with small substituents such as methyl (**1b**), ethyl (**1d**) and cyclopropyl (**1k**), and some activity for allyl (**1g**). However, it exhibited low efficiency with long alkyl or alkenyl and branched substituents. The results of the reaction rates were consistent with the ones of the conversion after 24 h. KPHMT I212A variant highly improved reaction rates relative to wild-type for the nucleophiles with

Results and discussion

long chain substituents (**1e–i**) and I202A mutation moderately improved this activity with the branched and larger cyclic derivatives (**1j–l**) (Figure 3.1.25B).

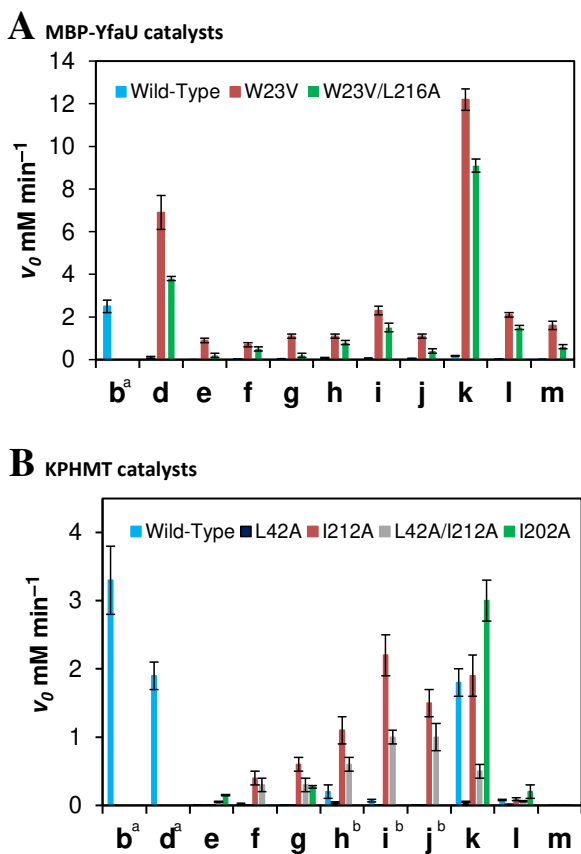


Figure 3.1.25 Initial reaction rates determined for the aldol addition of 2-oxoacids (**1**) to formaldehyde (**2a**) catalyzed by **A** MBP-YfaU(Ni²⁺) wild-type and variants and **B** KPHMT(Co²⁺) wild-type and variants. ^aOnly determined for the wild-type enzyme. ^bNot determined for the I202A variant. [1] = [2a] = 0.1 M, 4 mg mL⁻¹ of enzyme, 4.5 eq M²⁺ respect to the catalyst.

Prior to perform the preparative scale synthesis of the products (**4**), the substrate concentration of the reactions was adjusted to achieve the maximum yield and enantiomeric excess. By measuring the conversions after 24 h of reaction at different concentrations of formaldehyde, the maximum concentration tolerated for each aldol addition reaction was determined. MBP-YfaU catalyst

accepted a formaldehyde concentration range between 0.6–1.0 M and KPHMT wild-type and its variants a range between 0.1–0.6 M (see Supplementary Material, section 6.2.2).

3.1.6 Preparative synthesis of Roche ester derivatives

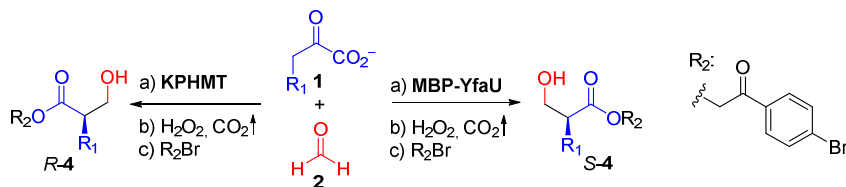
The best biocatalyst for each case was selected to run preparative scale experiments and evaluate the isolated yields, enantiomeric excesses, and absolute stereochemistry of products (*S*) and (*R*)-**4a–k** (Table 3.1.4). Enantiomeric excesses values were determined by HPLC analysis on chiral stationary phases against authentic racemic samples obtained by chemical synthesis (cHPLC analysis in Supplementary Material, section 6.2.6).

MBP-YfaU gave very good enantioselectivities (94–96% ee) for **1h–i**, and **1l–m** and excellent values (98–99%) for **1b,d–g** and **1k** at 0.6–1.0 M equimolar substrate concentration. It was also observed that on increasing the length of the alkenyl substituent from butenyl (**1h**) to pentenyl (**1i**) the ee decreased from 95% to 78%. Since the background reaction was negligible (<5% for **1i**), this phenomenon can not be explained by the non-enantioselective reaction catalyzed by the free metal. Alternatively, this was likely due to an increased occurrence of the inverted orientation of the R1 substituent (giving rise to a *E*-enolate) owing to the steric interactions with the protein.

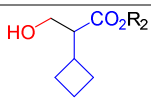
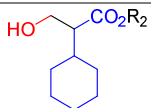
The best KPHMT catalysts exhibited very good enantiomeric excesses (92–98%) for nucleophiles **1b,d–i**. An equimolar substrate concentration at 0.1 or 0.2 M was best to achieve the maximum product formation under the selected reaction conditions. More specifically, for **1b,d–e** and **g–h**, wild-type KPHMT and the I212A variant gave ee values between 95% and 98%. For **1f** and **1i** the ee values were better for L42A/I212A than those with I212A. For branched **1j** and cyclic **1l** nucleophile substituents, the I202A variant gave 92% and 75% ee, respectively. Cyclopropyl (**1k**) was a particular case since it was tolerated for the wild-type and I202A, but both with moderate ee (83–87%) as compared with the rest of the selected nucleophiles.

Results and discussion

Table 3.1.4 Preparative scale synthesis of products (*S*) and (*R*)-**4a–k** after MBP-YfaU and KPHMT wild-type and variants catalyzed aldol addition of 2-oxoacids (**1b,d–m**) to formaldehyde (**2a**).



2-Oxoacid	Biocatalyst	[S] ^a	Product (4)	Yield ^b	ee ^c	
1b	MBP-YfaU ^{wt}	1.0		S-4a	80	98
	KPHMT ^{wt}	0.4		R-4a	88	95
1d	MBP-YfaU ^{W23V}	1.0		S-4b	81	99
	KPHMT ^{wt}	0.2		R-4b	63	95
1e	MBP-YfaU ^{W23V}	1.0		S-4c	68	99
	KPHMT ^{I212A}	0.1		R-4c	60	95
1f	MBP-YfaU ^{W23V}	0.6		S-4d	65	99
	KPHMT ^{I212A}	0.1		R-4d	55	86
	KPHMT ^{L42A/I212A}	0.1		R-4d	57	93
1g	MBP-YfaU ^{W23V}	1.0		S-4e	73	98
	KPHMT ^{I212A}	0.2		R-4e	68	96
1h	MBP-YfaU ^{W23V}	0.8		S-4f	69	95
	KPHMT ^{I212A}	0.2		R-4f	68	97
1i	MBP-YfaU ^{W23V}	0.6		S-4g	68	78
	KPHMT ^{I212A}	0.2		R-4g	72	88
	KPHMT ^{L42A/I212A}	0.2		R-4g	64	93
1j	MBP-YfaU ^{W23V}	1.0		S-4h	75	99
	KPHMT ^{I202A}	0.1		R-4h	49	92
1k	MBP-YfaU ^{W23V}	1.0		S-4i	73	98
	KPHMT ^{I202A}	0.6		R-4i	63	83
	KPHMT ^{wt}	0.4		R-4i	68	87

1l	MBP-YfaU ^{W23V}	0.8		<i>S</i> - 4j	80	94
	KPHMT ^{I202A}	0.2		<i>R</i> - 4j	48	75
1m	MBP-YfaU ^{W23V}	0.3		<i>S</i> - 4k	73	96

^aEquimolar concentration (M) of substrates **1b,d-m** and **2a**. ^bIsolated yield (%) of products **4**. ^cEnantiomeric excess (%) determined by chPLC against racemic mixtures.

Besides 2-(4'-bromophenyl)-2-oxoethyl esters (**4**), benzyl and 4-nitrobenzyl esters (**5**) were produced to demonstrate that products with higher synthetic value can be obtained without eroding the enantiomeric purity. Nucleophiles **1a** and **1h** were selected for the aldol addition to formaldehyde catalyzed by MBP-YfaU or KPHMT. The aldol adducts were decarboxylated and esterified using the corresponding benzyl bromide or 4-nitrobenzyl bromide in the presence of CsCl (Figure 3.1.26).

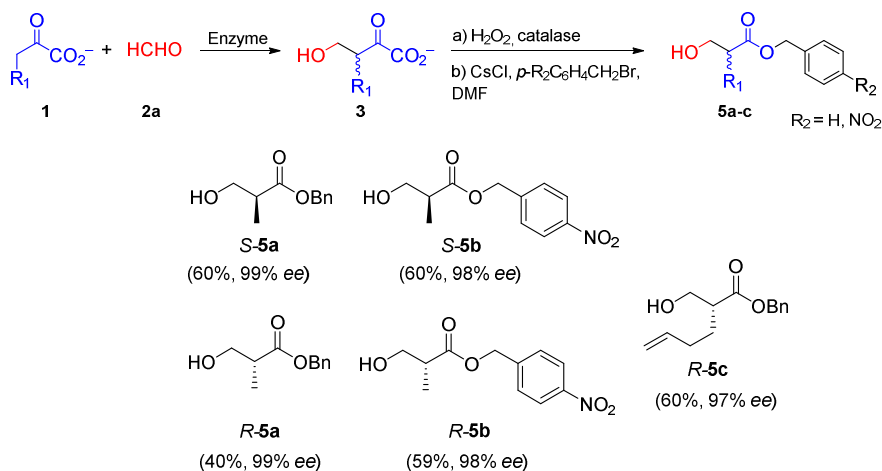


Figure 3.1.26 Synthesis of benzyl and 4-nitrobenzyl esters (**5a-c**) obtained from *R*-**3** and *S*-**3** aldol adduct precursors.

To synthesize the racemic mixtures of the products, the non-enzymatic aldol reaction catalyzed by the free metal cofactor was exploited. Thus, the effect of

Results and discussion

adding more equivalents of the cofactor (i.e., Ni^{2+} was used as a reference cofactor) or adding buffer (sodium phosphate buffer, 50 mM, pH 7.0) in the reaction was tested taking as a reference the nucleophile **1b** (Figure 3.1.27). Results showed that increasing the concentration of the bivalent metal also increased the conversion of the non-enzymatic reaction from 25% to 38% after 24 h. Moreover, when adding sodium phosphate buffer, the conversion rose up to 83%. It is known that phosphate buffers form complexes with metal ions such as Co^{2+} , Ni^{2+} and Mg^{2+} and this might enhance the acid/base role of the metal.¹⁸⁵

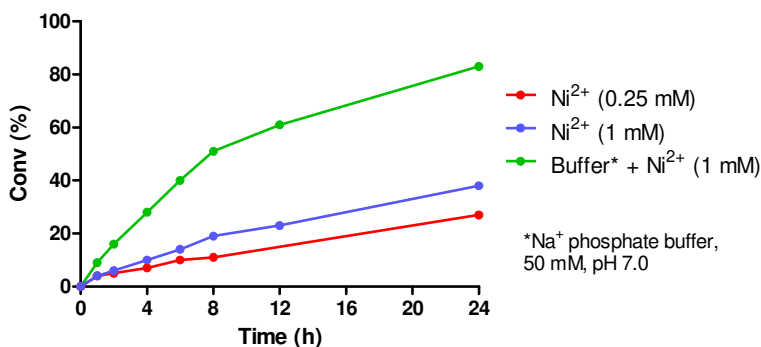


Figure 3.1.27 Reaction time course of aldol addition of 2-oxobutanoate (**1b**) to formaldehyde (**2a**) catalyzed by the free metal cofactor.

This non-enantioselective reaction was leveraged to synthesize the racemic mixtures of the products. The aldol reactions were monitored by HPLC until no evolution of substrates and products were detected (times between 24 h for **1d** and 10 days for **1e**, reaction time course in the Supplementary Material, section 6.2.5). Then, the aldol adduct was treated as the enzymatic products to obtain *rac*-**4a-k** and *rac*-**5a-c**.

3.1.7 Absolute stereochemistry determination

The absolute stereochemistry of products **4a-k** was determined using three different strategies. As explained in the section 3.1.3, the absolute

stereochemistry of the enzymatic products *S* and *R*-**4a** was unequivocally determined using chiral HPLC by the synthesis of authentic samples of *S* and *R*-**4a** from commercially available (*S*)- and (*R*)- β -hydroxyisobutyric acid sodium salts.

Secondly, regarding products **4b–f** and **4h**, absolute stereochemistry was assigned by transforming the aldol adducts in compounds already reported in the literature. Concretely, the aldol adduct *S*-**3da** was converted to the corresponding carboxylic acid and esterified using MeOH and SOCl₂ obtaining a β -hydroxy carboxylic methyl ester (*S*-**6a**). Concerning aldol adducts *S*-**3ea–ga** and **3ja**, they were transformed into β -hydroxy carboxylic acids (*S*-**6b–e**) and isolated by direct acidic aqueous–organic solvent extraction. Finally, product *S*-**6d** and aldol adduct *R*-**3ha** were transformed into products *S*-**6b** and *R*-**6c** respectively by hydrogenation (Figure 3.1.28).

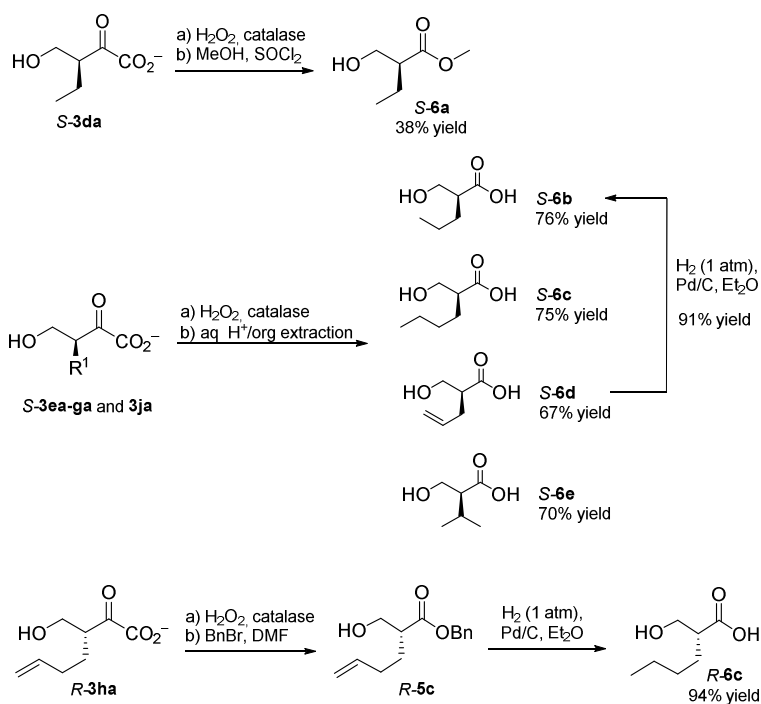


Figure 3.1.28 Scheme of aldol adducts derivatives synthesized to determine absolute stereochemistry of products **4b–f,h**.

Results and discussion

Once these products were obtained, the sign of the specific rotation values could be compared with the ones reported in the literature (Table 3.1.5).

Table 3.1.5 Sign of specific rotation of compounds **6a–e** compared with the corresponding literature values.

Aldol adduct	This work $[\alpha]^{20}_{\text{D}}$	Reported $[\alpha]^{20}_{\text{D}}$
<i>S</i> -3da → <i>S</i> -6a	– 3.8 (<i>S</i>)	– 5.9 (<i>S</i>) (> 95% ee) ¹⁸⁶
<i>S</i> -3ea → <i>S</i> -6b	+ 2.8 (<i>S</i>)	– 3.0 (<i>R</i>) (92% ee) ¹⁸⁷
<i>S</i> -3ga → <i>S</i> -6b	+ 1.8 (<i>S</i>)	
<i>S</i> -3fa → <i>S</i> -6c	– 5.9 (<i>S</i>)	+ 6.5 (<i>R</i>) (99% ee) ¹⁰²
<i>R</i> -3ha → <i>R</i> -6c	+ 6.0 (<i>R</i>)	
<i>S</i> -3ja → <i>S</i> -6e	+ 4.1 (<i>S</i>)	– 5.4 (<i>R</i>) (98% ee) ¹⁸⁷

In the case of compounds **4i–k**, the absolute stereochemistry was determined by X-ray diffraction (Figure 3.1.29). These compounds were crystallized by evaporation after dissolving them into isopropyl alcohol (*S*-**4i**) or diethyl ether (*S*-**4j,k**). Based on the high stereopreference observed for the enzymes MBP-YfaU and KPHMT, the absolute configuration of products *S*-**4g** and *R*-**4g** respectively was inferred.

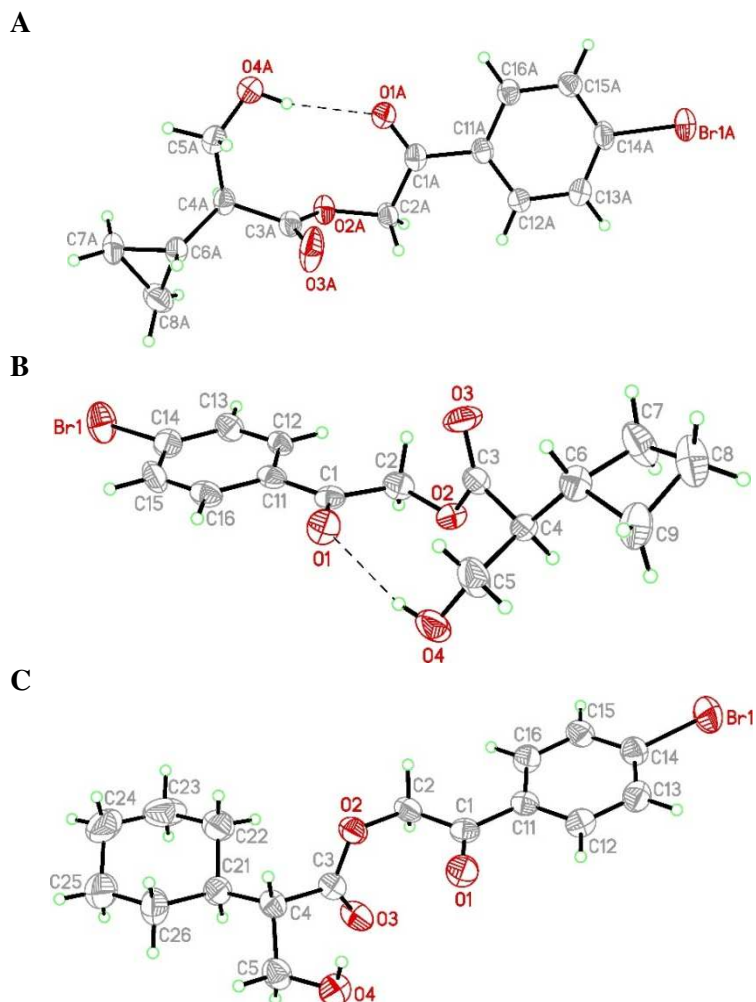


Figure 3.1.29 X-ray diffraction analysis for the determination of the absolute configuration of **A** product *S*-**4i**, **B** product *S*-**4j** and **C** product *S*-**4k**. ORTEP-type plot displaying ellipsoids at the 50 % probability level. The dashed line indicates a hydrogen bond.

3.1.8 Summary

We presented herein two enantioselective aldolases, MPB-YfaU and KPHMT, useful to catalyze the aldol addition of 2-oxoacids (**1**) to formaldehyde (**2a**) to furnish (*S*) and (*R*)-3-substituted 4-hydroxy-2-oxoacid precursors respectively. These precursors were transformed by oxidative

Results and discussion

decarboxylation and esterification into enantiomerically pure 2-substituted 3-hydroxycarboxylate esters (**4** and **5**) (i.e. Roche ester derivatives) useful chiral building blocks for the synthesis of more complex molecules. This novel chemoenzymatic methodology provided high isolated yields and enantiomeric excesses through simple reactions and workup procedures.

The synthesis of the racemic mixtures of the products was also easily performed thanks to the non-enzymatic reaction catalyzed by the free metal (Ni^{2+}) and the presence of sodium phosphate buffer (50 mM, pH 7.0) in the reaction media. The racemic products (*rac*-**4a-k**) were used as a reference for chiral HPLC analysis.

A wide panel of structurally diverse nucleophiles was used to enzymatically generate different 3-substituted aldol adducts. To overcome the difficulty of both aldolases to accept larger 2-oxoacids than the 2-oxobutanoate, new variants designed in our lab were used. For MBP-YfaU a single W23V mutation was sufficient to accommodate even the largest cyclohexane substitution (**1m**), without perturbing the approach of the electrophile. For KPHMT three variants, I202A, I212A and L42A/I212A, were constructed to accomplish the required nucleophile tolerance. More specifically, mutation I212A was critical to adequately fit longer hydrophobic chains (**1e-i**), L42A/I212A was needed to improve the enantiomeric excesses in some cases (**1f** and **1i**) and I202A was useful for the branched and cyclic 2-oxoacids (**1j-l**). None of these variants were sufficient to fit the largest cyclic nucleophile (**1m**).

For both aldolases, excellent (94–99% ee) to very good (88–93% ee) stereoselectivities and isolated yields (57–88%) were achieved at substrate concentrations in a range between 0.1 and 1.0 M.

3.2 Biocatalytic construction of quaternary centers

3.2.1 Introduction

Quaternary centers are important structural units that can be found in naturally occurring, biologically active compounds and pharmaceutical ingredients. In recent years, considerable efforts have been dedicated to implement chemical methodologies to the synthesis of these congested structures. These usually involve enantioselective Michael addition, cycloaddition and dearomative cyclization among others.^{126, 127}

Some biocatalytic methodologies have also been developed recently to forge quaternary carbon stereocenters but these approaches are still scarce. For example, natural squalene–hopene cyclases (SHC, EC 5.4.99.17) for the preparation of isoprene backbones and the use of engineered β -subunit of tryptophan synthase (TrpB Pf_{quat} , EC 4.2.1.20) and cytochrome P450 (P450_{BM3}, EC 1.14.14.1) have been applied for its synthesis.^{24, 138, 139}

In this work, we explored the capabilities of the Class II aldolase KPHMT to accomplish the synthesis of quaternary centers as it does in its natural reaction (Figure 3.2.1). As described in the previous chapter, KPHMT(Co^{2+}) catalyzes the aldol addition of α -KIV to formaldehyde to produce ketopantoate, bearing a *gem*-dimethyl quaternary center, and tetrahydrofolate. Thus, we planned to generate ketopantoate analogues by expanding the diversity of 3,3-disubstituted 2-oxoacids nucleophiles and aldehyde electrophiles.

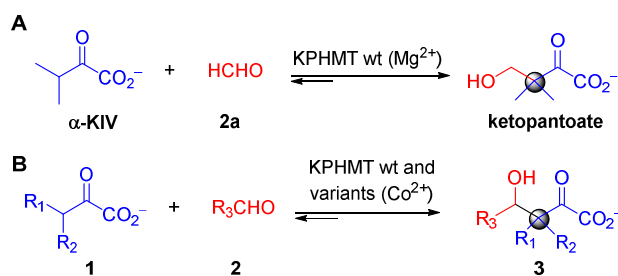


Figure 3.2.1 A Aldol addition of α -KIV to formaldehyde catalyzed by KPHMT *in vitro*.

B Approach to the synthesis of ketopantoate analogues bearing quaternary centers.

3.2.2 Synthesis of 3,3-disubstituted 2-oxoacids

Different 3,3-disubstituted 2-oxoacids were selected to be used as nucleophiles in the aldol addition to different electrophiles catalyzed by KPHMT (Figure 3.2.2). The 2-oxoacid **1a** was commercially available, while the others (**1n–x**) were synthesized in our laboratory.

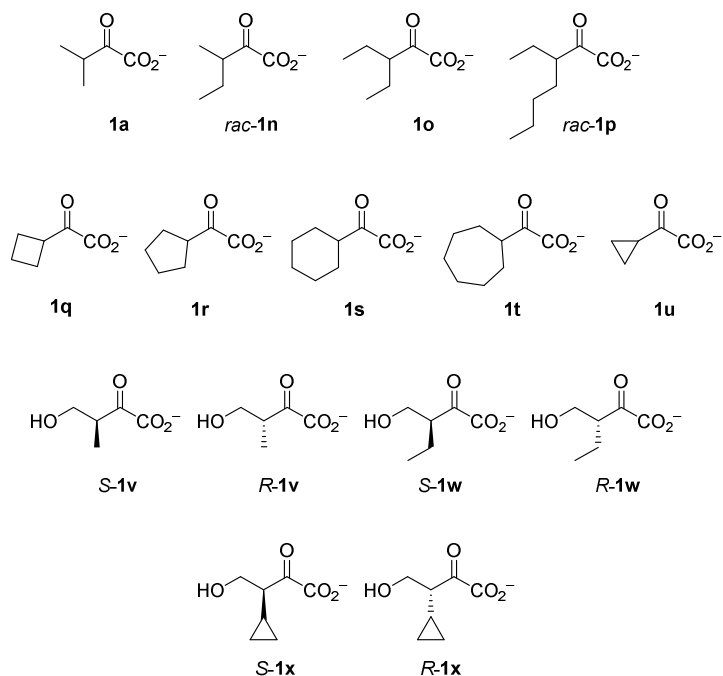


Figure 3.2.2 Panel of selected 3,3-disubstituted 2-oxoacids used as nucleophiles for the synthesis of quaternary centers.

Compounds **1n–u** were synthesized using the methodology described in the previous chapter (Section 3.1.4) in moderate yields (26–65 % over three steps) (Figure 3.2.3). The fact that the Grignard reaction was also useful for the synthesis 3,3-disubstituted 2-oxoesters, demonstrated that it is an efficient and reproducible methodology to furnish a great variety of compounds. Likewise, 16 different 2-oxoesters (**C2e–i,k–u**) could be hydrolyzed using Novozyme 435, confirming the huge potential of this readily available immobilized lipase for application in organic synthesis.¹⁸⁸

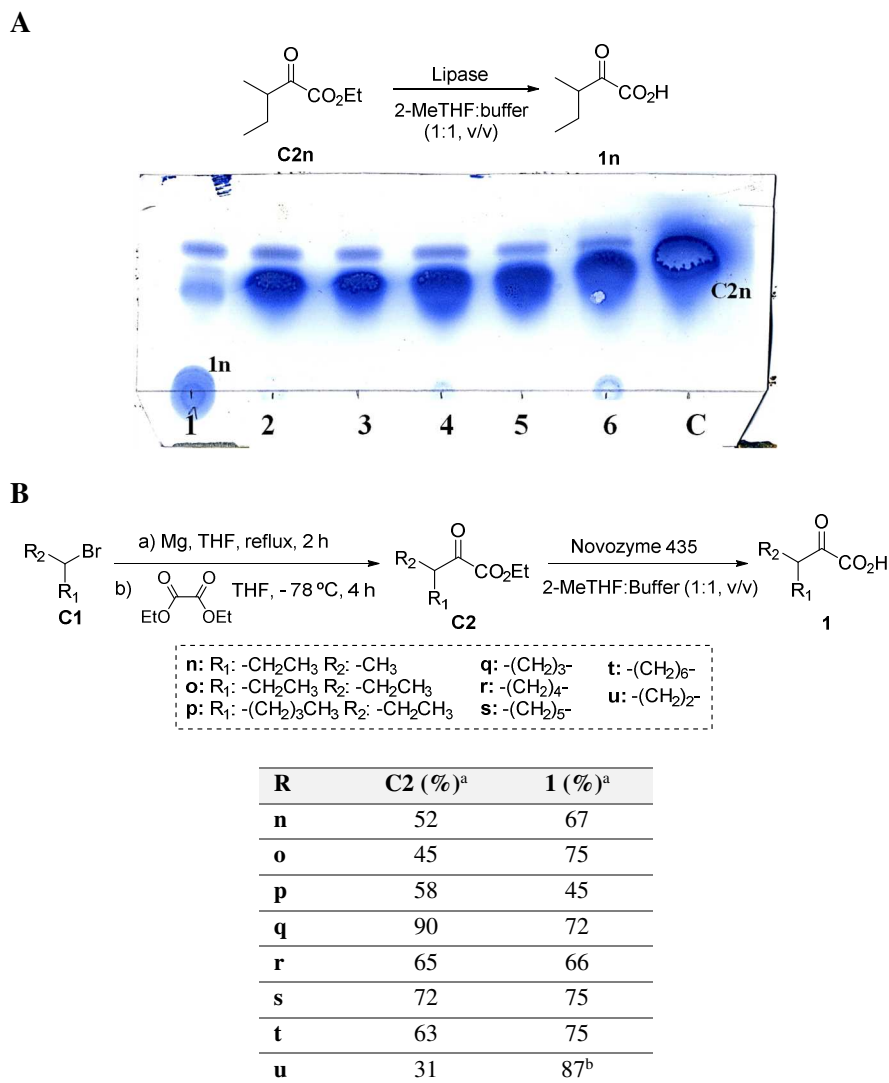


Figure 3.2.3 A Screening experiment using different lipases for the hydrolysis of **C2n**. TLC eluted with hexane:AcOEt, 9:1 (v/v), stained with cerium ammonium molybdate stain. Novozyme™ 435 (**1**), Lipozyme™ TL IM (**2**), Lipozyme™ RM IM (**3**), Lipozyme™ immobilized from *Mucor miehei* (**4**), Lipozyme™ TL 100L (**5**) and lipase from porcine pancreas type II (**6**) and control experiment without lipase (**C**) are shown. **B** Isolated yields (%) for the synthesis of 2-oxoesters **C2n-u** and 2-oxoacids **1n-u**. ^aIsolated yield of products (%). ^bObtained using a different workup procedure and estimated from the final aqueous solution (10 mL, 1 M).

Results and discussion

The synthesis of **1u** by the same approach used for the other 2-oxoacids was not possible because of two main drawbacks. First, the purification of the intermediate ethyl ester (**C2u**) resulted in an inseparable mixture of the desired compound and the unreacted diethyl oxalate. Second, the ester hydrolysis rendered **1u** in low isolated yields (21%) due to the low efficiency of the extraction from the aqueous phase of the reaction that caused large loss of material.

In view of these issues we decided to vary the reaction conditions. First, the synthesis of **C2u** was performed by adding 0.7 eq of the diethyl oxalate, which was consumed completely at the end of the reaction. Second, **1u** was used directly from the ester hydrolysis reaction solution. To do so, the lipase was dissolved in TEA buffer instead of phosphate buffer to prevent inactivation of KPHMT during the aldol addition by the metal chelating properties of phosphate.¹⁸⁵ When the hydrolysis was complete, the workup procedure consisted of adjusting the reaction aqueous phase to pH 8.0 and washing it with organic solvent. Then, the pH of the aqueous phase was neutralized and the resulting solution containing **1u** (10 mL, 1 M) was used without any further purification.

In order to furnish chiral 3,3-disubstituted 2-oxoacids (*S* and *R*-**1v-x**) we exploited the results from the previous chapter, in which the aldol addition of 2-oxoacids to formaldehyde catalyzed by KPHMT or MBP-YfaU gave enantiocomplementary aldol adducts with high ee (Figure 3.2.4).

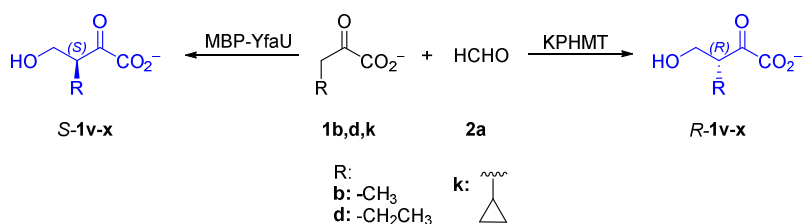


Figure 3.2.4 Strategy to generate chiral 2-oxoacids (i.e., *S* or *R*-**1v-x**). The aldol adducts were characterized in the previous chapter of this thesis.

These aldol adducts can be used as substrates for a second aldol addition to an electrophile, in a one-pot two-step process, generating a quaternary center.

The synthesis of 2-oxoacids **1y** and **1z** was attempted through the Grignard reaction but resulted to be unsuccessful. Unfortunately, the reaction rendered the homocoupling adducts **C3** and **C4** (Figure 3.2.5A and 3.2.6). It is likely that the aromatic ring or the double bond of organomagnesium compounds promote the homocoupling reaction by an S_N1 mechanism with a carbocation intermediate or through a single electron transfer process with radical intermediates (Figure 3.2.5B).¹⁸⁹ This has been reported in the literature and, in fact, is a widely used methodology for the synthesis of biaryl compounds, which can be catalyzed by several kinds of promoters such as cobalt, titanium or iodine.¹⁹⁰⁻¹⁹²

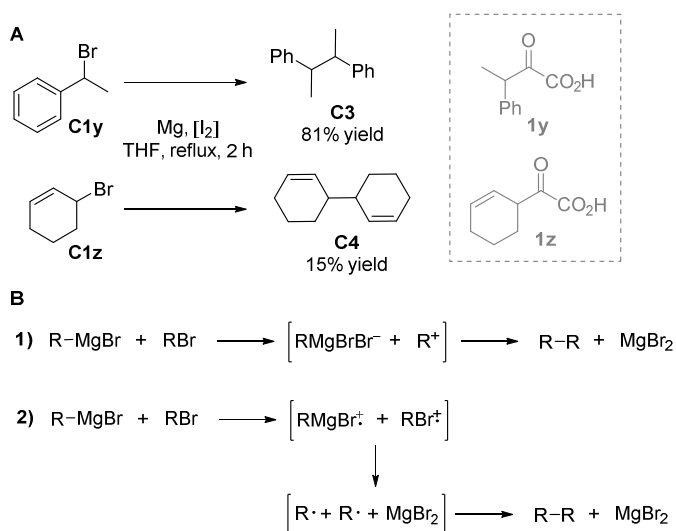


Figure 3.2.5 A Attempted synthesis of 2-oxoacids **1y** and **1z**, which resulted with the obtention of homocoupling products **C3** and **C4**. **B** Proposed mechanisms for the homocoupling reaction through S_N1 mechanism with a carbocation intermediate (1) or through a single electron transfer process with radical intermediates (2).

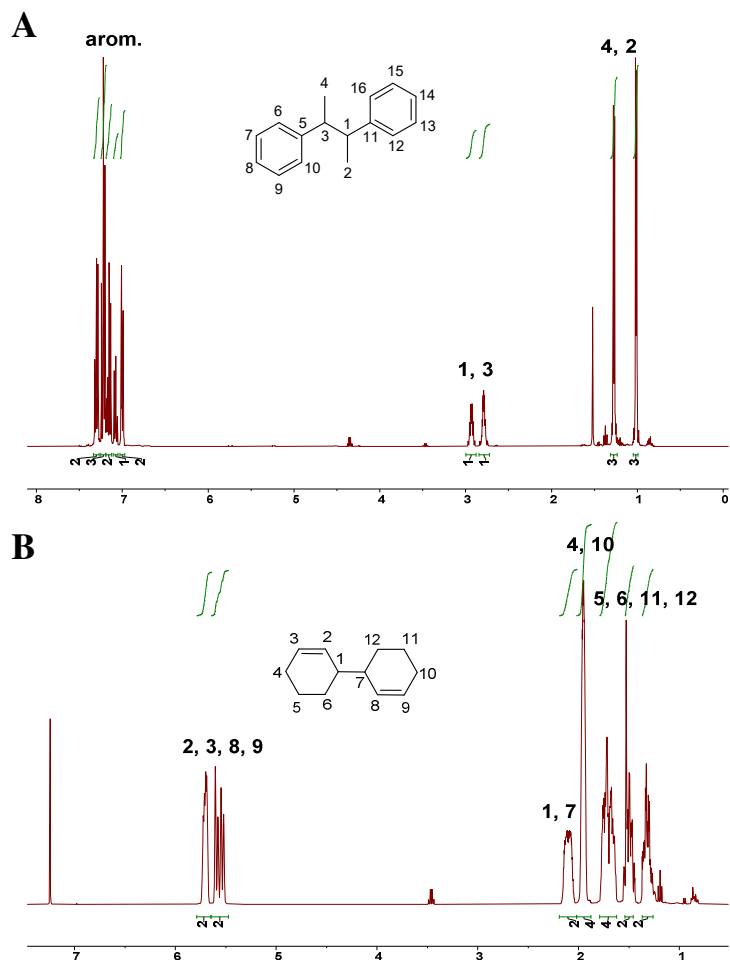


Figure 3.2.6 NMR ^1H spectra (CDCl_3) of **A** compound **C3** and **B** compound **C4**.

3.2.3 Construction of new variants of KPHMT

From the previous chapter of this thesis, we know that the KPHMT variants I212A and I202A tolerate 3-monosubstituted 2-oxoacids with linear, branched or cyclic substituents. To establish the residues of the KPHMT active site that have to be engineered for optimal activity toward 3,3-disubstituted 2-oxoacids, molecular models were constructed and analyzed. We envisaged that KPHMT I212A and I202A variants could be useful to accommodate one of the substituents of the nucleophiles. In addition, we envisaged that V214 could also

play an important role to alleviate steric hindrance of the other substituent (Figure 3.2.7). In particular, mutation of Gly for Val could expand the active site steric volume in the appropriate direction.

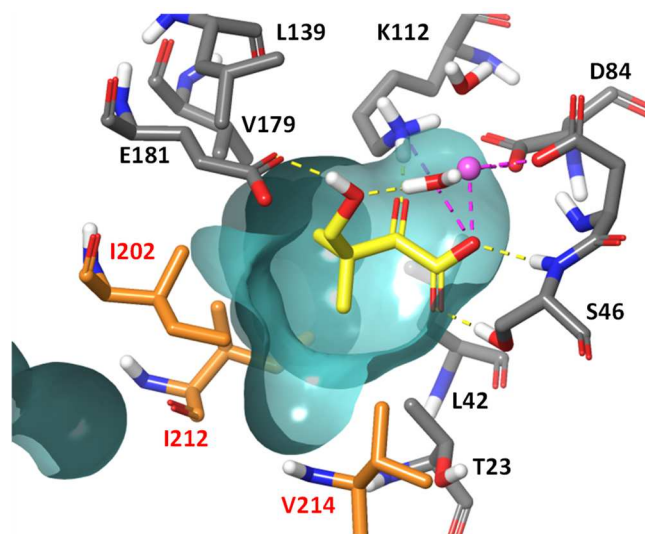


Figure 3.2.7 Model of wild-type KPHMT (PDB 1M3U) complexed with its natural product ketopantoate (yellow C atoms). The metal cofactor (magenta), water molecules (red) and surface of the active site cavity (cyan) are shown. Selected residues to be mutated (orange) are highlighted in red.

Molecular models of variants at these positions showed larger active sites that could accommodate the selected nucleophiles. Thus, seven KPHMT variants, i.e., I212A, I202A, V214G, I202A/I212A, I202A/V214G, I212A/V214G, and I202A/I212A/V214G, were constructed and tested as biocatalysts. The enzymes were obtained in high yields after expression and purification (88–205 mg of protein L⁻¹ medium culture). Purified KPHMT catalysts were stored and used in the reactions as glycerinate preparations.

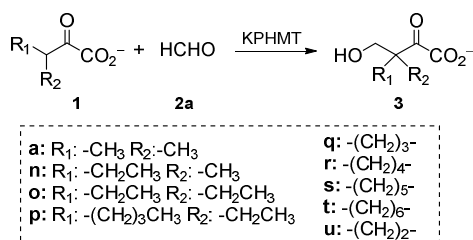
3.2.4 Screening with formaldehyde

The new variants of KPHMT were screened for the aldol addition of nucleophiles (**1a** and **1n–u**) to formaldehyde (**2a**). The conversion after 24 h of

Results and discussion

reaction (Table 3.2.1) and the initial reaction rates were measured (Supplementary Material, section 6.3.3). KPHMT wild-type accepted efficiently the smaller nucleophile **1a** (95%), less efficiently nucleophiles with larger or cyclic aliphatic chains such as **1n** and **1q,r** (41-53%) and the more sterically demanding nucleophiles (**1o,p** and **1s-u**) were not well accepted (<8%). Some of the variants enhanced the activity compared to the wild-type. For example, I202A and the double variant I202A/I212A were the most efficient catalysts for **1q,r** achieving around 90% of conversion. As well, these improved the conversion of **1o** and **1t** up to 40% respectively. Nucleophile **1s** was only accepted by I212A (20%) and **1p** by I202A/V214G (23%). For nucleophiles *rac*-**1n** and *rac*-**1p** the variants that gave conversions $\leq 50\%$ were selected. We hypothesized that these enzymes would tolerate only one enantiomer of the nucleophiles indicating its stereoselectivity.

Table 3.2.1 Conversion after 24 h (%) of the aldol addition of 2-oxoacids (**1**) to formaldehyde (**2a**) catalyzed by KPHMT wild-type and variants.



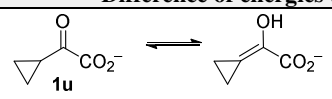
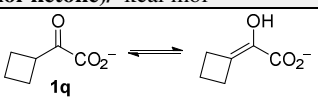
KPHMT	E Nu	2a								
		1a	1n	1o	1p	1q	1r	1s	1t	1u
wild-type		95	41	8	- ^a	53	49	- ^a	5	- ^a
I212A		71	47	- ^a	- ^a	63	67	20	12	- ^a
I202A		91	67	37	13	82	87	- ^a	10	- ^a
V214G		90	41	10	8	47	16	- ^a	10	- ^a
I202A/V214G		75	46	15	23	43	49	- ^a	5	- ^a
I212A/V214G		25	16	5	- ^a	30	22	- ^a	- ^a	- ^a
I202A/I212A/V214G		18	14	- ^a	10	31	54	- ^a	5	- ^a
I202A/I212A		63	35	10	7	72	90	8	40	- ^a

[**1**] = [**2a**] = 0.1 M, 2 mg mL⁻¹ of enzyme, 4.5 eq M²⁺ respect to the catalyst.

^aProduct not detected.

Unexpectedly, substrate **1u** was not converted by any of the catalysts assayed. We hypothesized that the energy for the enolate formation would be higher than that of the other 2-oxoacids with cyclic substituents (**1q–t**) due to the ring strain energy and this would preclude the progress of the reaction. This hypothesis was corroborated by comparing the energies of enolate formation of **1u** and **1q** (Table 3.2.2). The results showed that the enol is less stable than the ketone in both cases. The difference of energies for **1q** is about 12 kcal mol⁻¹ lower than for **1u**, indicating that the enolate formation of the first is easier than the later one (that is, making the reasonable assumption that these differences are maintained for the corresponding transition states).

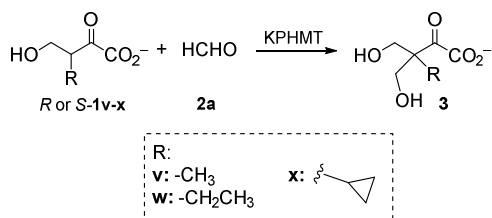
Table 3.2.2 DFT calculations for tautomerization equilibrium: enols vs. ketones for compounds **1u** and **1q**. The difference of energies for cyclobutyl is about 12 kcal mol⁻¹ lower than for cyclopropyl, indicating that **1u** enol formation is more restrained. DFT calculations @ B3LYP-D3/6-31G** level with software Jaguar 2021-1.

	Difference of energies (enol-ketone)/ kcal mol ⁻¹	
		
Gas phase	14.9	2.6
Implicit Water Solvation (PBF)	17.6	4.8

The variants of KPHMT were also tested with nucleophiles *R*- and *S*-**1v–x** (Table 3.2.3). The results showed that, with **1v**, the *S* enantiomer was better accepted (95%) than the *R* enantiomer (55%) by KPHMT I202A catalyst. The aldol addition of *S*- or *R*-**1v** to **2a** gave the same achiral aldol adduct, so the preparative synthesis of the product was performed using the best substrate (*S*-**1v**) as nucleophile. KPHMT catalysts hardly accepted *S*- or *R*-**1w**, the best variant I202A/I212A reached a 26% of conversion with the *S*-enantiomer, and did not accept either *S*- or *R*-**1x** as substrates.

Results and discussion

Table 3.2.3 Conversion after 24 h (%) of the aldol addition of 2-oxoacids (*R*- and *S*-**1v-x**) to formaldehyde (**2a**) catalyzed by KPHMT wild-type and variants.



KPHMT	E Nu	2a					
		<i>S</i> -1v	<i>R</i> -1v	<i>S</i> -1w	<i>R</i> -1w	<i>S</i> -1x	<i>R</i> -1x
wild-type		84	29	10	15	- ^a	- ^a
I212A		15	14	12	7	- ^a	- ^a
I202A		95	55	25	20	- ^a	- ^a
V214G		80	14	11	6	- ^a	- ^a
I202A/V214G		68	15	14	7	- ^a	- ^a
I212A/V214G		22	6	12	8	- ^a	- ^a
I202A/I212A/V214G		18	7	12	5	- ^a	- ^a
I202A/I212A		50	18	26	16	- ^a	- ^a

[**1**] = [**2a**] = 0.1 M, 2 mg mL⁻¹ of enzyme, 4.5 eq M²⁺ respect to the catalyst.

^aProduct not detected.

Molecular models of the active site of KPHMT were analyzed to explain the differences on the conversions in the aldol addition of *S* and *R*-**1v** to formaldehyde (95% and 55% respectively). The *S* configured nucleophile **1v** disposes the larger substituent oriented towards the cavity produced by the I202A mutation, generating the *E*-enolate (Figure 3.2.8A). Contrary, the C3-hydroxymethyl substituent of *R*-**1v** is oriented to the inner part of the active site, generating a *Z*-enolate with more steric repulsion (Figure 3.2.8B). These results explain why *S*-**1v** is better accepted for KPHMT.

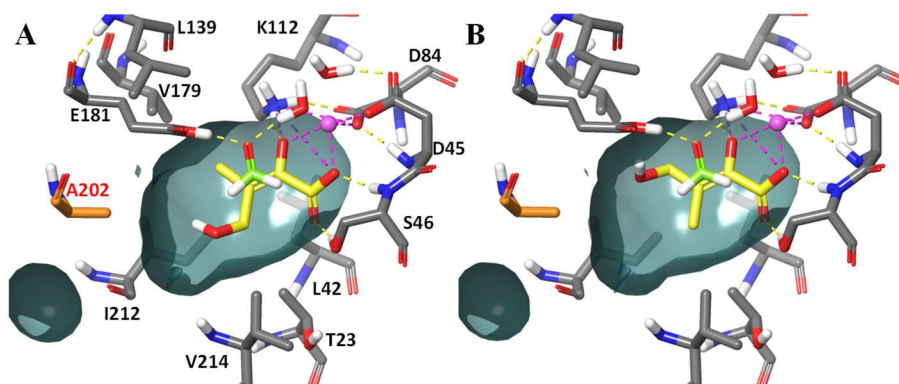


Figure 3.2.8 Model of the prereactive complex of KPHMT I202A with **A** *S*-**1v** or **B** *R*-**1v** (yellow) and **2a** (green). Mutated residues (orange C atoms), metal cofactor (purple) and surface of the active site (cyan) are shown.

3.2.5 Study of KPHMT catalyzed aldol addition of 2-oxoacids to other aldehydes

Diverse aldehydes were selected to test the electrophile promiscuity of KPHMT (Figure 3.2.9). Among them, those commercially available were acetaldehyde (**2b**), glycolaldehyde (**2c**), benziloxymethylaldehyde (**2d**), D-erythrose (**2h**), D-ribose (**2i**), D-arabinose (**2j**) and D-lyxose (**2k**). D- And L-lactaldehyde (**2e** and **2f**, respectively) and D-threose (**2g**), were synthesized in our lab.

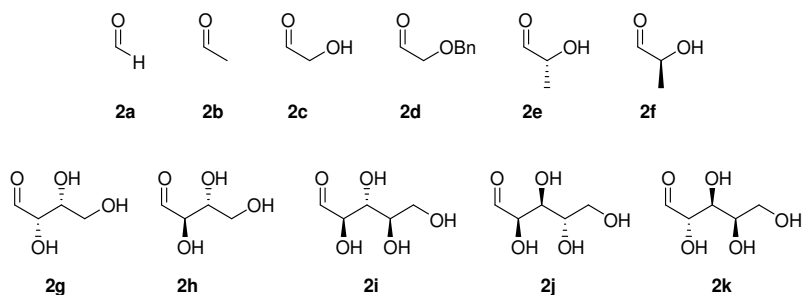


Figure 3.2.9 Panel of selected aldehydes used as electrophiles for the synthesis of quaternary centers.

Results and discussion

D- And L-lactaldehyde (**2e** and **2f**) were prepared from L- and D-threonine respectively, following a published procedure with some modifications.¹⁹³ For instance, the purification process used an anion exchange resin to remove the citrate buffer from the reaction. This process was not efficient enough and part of buffer remained on the product. Citrate has the capacity to chelate metals and this affects the KPHMT activity. To overcome this problem acetate buffer instead of citrate was used. Thus, D- or L-threonine, ninhydrin, and sodium acetate buffer were combined and boiled for 15 min under vigorous stirring to furnish L- and D-lactaldehyde, respectively (Figure 3.2.10).

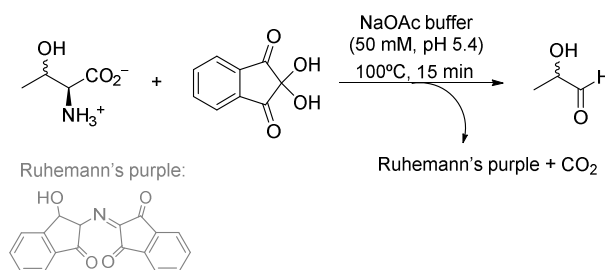
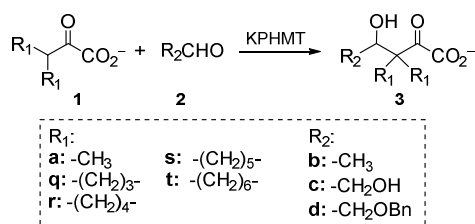


Figure 3.2.10 Synthesis of D- and L-lactaldehyde from L- and D-threonine respectively.

KPHMT wild-type and variants thereof were screened with the panel of different aldehydes as electrophiles. The nucleophiles used in this screening were the most efficient found with formaldehyde (i.e., **1a**, **1q** and **1r**), including **1s** and **1t**. We began to screen the selected nucleophiles with the achiral aldehydes (**2b–d**) (Table 3.2.4).

Table 3.2.4 Conversion after 24 h (%) of the aldol addition of selected 2-oxoacids (**1**) to aldehydes (**2b–d**) catalyzed by KPHMT wild-type and variants.



KPHMT	E Nu	2b ^a			2c					2d ^b		
		1a	1q	1r	1a	1q	1r	1s	1t	1a	1q	1r
wild-type		87	90	41	80	95	60	- ^c	- ^c	44	42	10
I212A		70	90	50	82	91	93	50	42	37	60	20
I202A		79	91	41	88	96	93	- ^c	- ^c	43	46	25
V214G		78	86	30	80	60	20	- ^c	- ^c	42	29	- ^c
I202A/V214G		73	83	35	77	43	40	- ^c	14	35	30	5
I212A/V214G		53	71	38	18	90	38	- ^c	14	5	41	5
I202A/I212A/V214G		22	54	48	12	40	70	- ^c	21	- ^c	21	5
I202A/I212A		48	90	40	68	93	85	- ^c	- ^c	12	54	28

[**1**] = [**2**] = 0.1 M, 2 mg mL⁻¹ of enzyme, 4.5 eq M²⁺ respect to the catalyst. ^a200 mM (2 eq) of **2b**. ^b20% of DMF in the reaction. ^cProduct not detected.

The equimolar aldol addition of **1a** to **2b** gave conversions around 50% with all the KPHMT variants. This equilibrium limitation was avoided by using 2 eq of the electrophile **2b**. Under this condition, the conversion was improved up to 87% with the wild-type. Thus, an excess of electrophile was used for the rest of reactions achieving almost complete conversions with **1q** and around 50% of conversions with **1r**.

The results of the screening using **2d** showed the same trends. In this case, increasing the electrophile concentration was not possible as DMF, which may have a deleterious effect on the enzyme activity, had to be used in large amounts to solubilize this highly hydrophobic aldehyde. Thus, increasing the nucleophile concentration up to 200 mM was attempted but resulted inefficient to enhance the conversions.

The HPLC chromatogram analysis of the aldol addition of 2-oxoacids to glycolaldehyde (**2c**) showed disappearance of the substrates without formation

Results and discussion

of any new peak. This may indicate that spontaneous formation of a cyclic hemiketal may occur due to the presence of an internal α -hydroxy electrophilic group in the molecule (Figure 3.2.11). The putative cyclic hemiketal was not prone to be derivatized under our conditions and hence was not detectable by HPLC. Interestingly, this spontaneous cyclic hemiketal formation shifted the reaction equilibrium to the aldol product and explained the high conversions achieved (i.e. around 90% for nucleophiles **1a,q-r** and 42% and 50% for **1s** and **1t**, respectively).

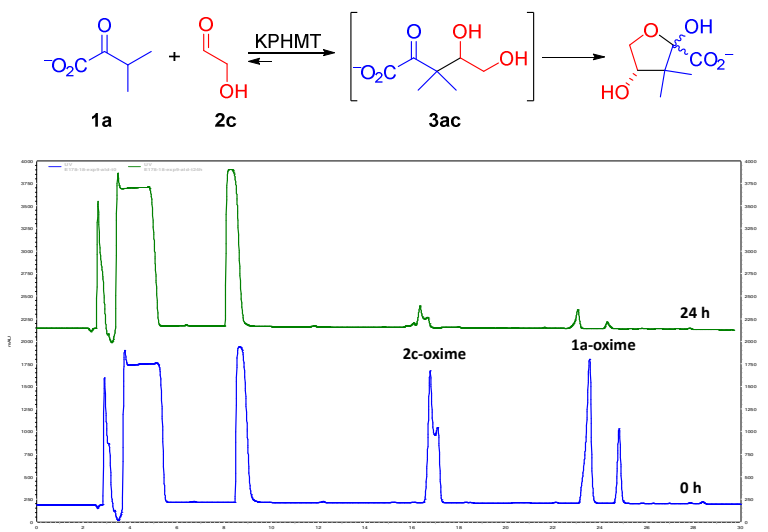
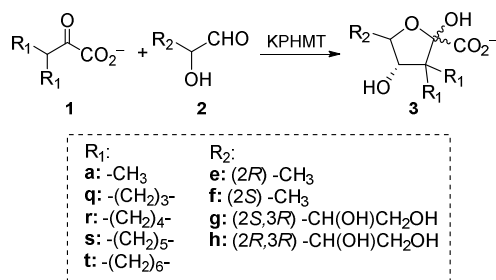


Figure 3.2.11 Example of HPLC chromatogram of the aldol addition of **1a** to **2c** showing the reduction of substrates peaks and no formation of aldol product (**3ac**).

The screening of KPHMT wild-type and variants with α -hydroxy aldehydes **2e-k**, showed a similar behavior (Table 3.2.5).

Table 3.2.5 Conversion after 24 h (%) of the aldol addition of selected 2-oxoacids (**1**) to aldehydes (**2e–h**) catalyzed by KPHMT wild-type and variants.



KPHMT	E Nu	2e					2f		
		1a	1q	1r	1s	1t	1a	1q	1r
wild-type		84	86	32	- ^a	- ^a	87	80	26
I212A		85	97	75	- ^a	- ^a	73	95	82
I202A		85	95	49	- ^a	- ^a	90	95	65
V214G		80	61	20	- ^a	- ^a	67	63	12
I202A/V214G		62	44	27	- ^a	- ^a	43	40	20
I212A/V214G		33	72	33	- ^a	- ^a	32	83	20
I202A/I212A/V214G		5	38	30	- ^a	- ^a	27	39	27
I202A/I212A		82	95	75	- ^a	- ^a	67	96	80
KPHMT	E Nu	2g ^b					2h ^b		
		1a	1q	1r	1s	1t	1a	1q	1r
wild-type		82	98	63	- ^a	- ^a	60	97	- ^a
I212A		79	98	91	- ^a	- ^a	42	98	64
I202A		80	98	67	- ^a	- ^a	73	61	- ^a
V214G		81	97	31	- ^a	- ^a	90	91	- ^a
I202A/V214G		74	53	40	- ^a	- ^a	33	27	- ^a
I212A/V214G		47	93	80	- ^a	- ^a	15	98	39
I202A/I212A/V214G		30	91	67	- ^a	- ^a	26	53	- ^a
I202A/I212A		79	98	90	- ^a	- ^a	26	98	30

[**1**] = [**2**] = 0.1 M, 2 mg mL⁻¹ of enzyme, 4.5 eq M²⁺ respect to the catalyst. ^aNo product formation was detected. ^b0.2 M (2 eq) of **2g,h**.

Indeed, the HPLC chromatograms and the high conversions achieved (between 82–98% of conversion with nucleophiles **1a** and **1q**, and 64–91% with **1r**) indicated that these aldol adducts existed as hemiketals in solution. The first screening of the reaction **1a+2g** gave maximum conversions around 60% probably caused by the fact that only around 5% of D-threose is present as acyclic specie.¹⁹⁴ The addition of 2 eq of **2g** and **2h** accomplished higher

Results and discussion

conversions. The aldehydes **2i-k** were not substrates of any KPHMT catalyst probably by the high K_M value and/or the even lower proportion (<1%) of its free aldehyde form.¹⁹⁵ Nucleophiles **1s** and **1t** were not converted by any of KPHMT variants with any of the electrophiles tested.

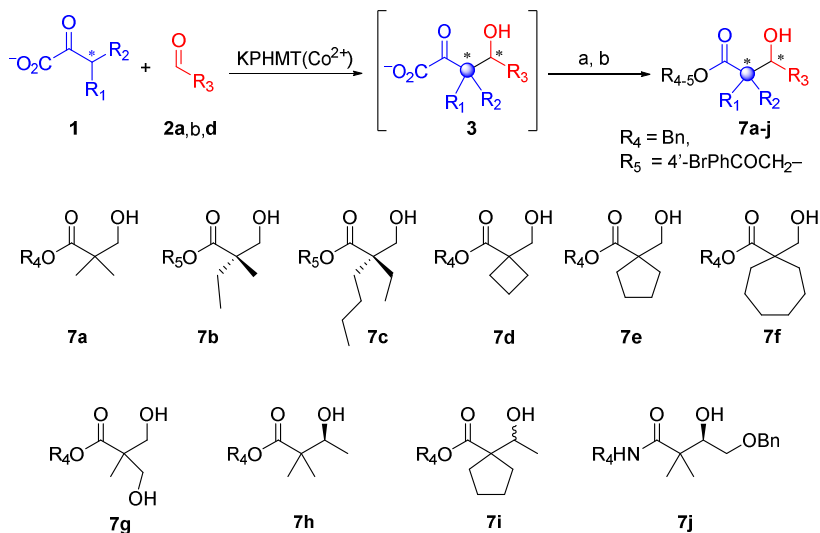
Prior to run the preparative scale synthesis of products, the initial reaction rates (v_0), akin with the enzymatic activity, were determined with the aim to choose the most suitable one for each reaction (Supplementary Material, sections 6.3.2 and 6.3.3). The results confirmed the catalytic efficiency of the variants at 0.068 mol% and were consistent with the conversions achieved.

3.2.6 Preparative synthesis and characterization of products obtained with aldehydes **2a,b,d**

The positive reactions from the previous screenings with the panel of nucleophiles (**1a** and **1n-x**) and electrophiles **2a,b** and **2d** were run at a preparative scale synthesis. These provided, after the adequate treatment, 3-hydroxy acid derivatives (**7a-j**) and 2-oxolactones (**8a-g**), all of them bearing a quaternary center.

The first strategy consisted of an oxidative decarboxylation of aldol adducts (**3**) followed by carboxylic group modification, leading to different 2,2-disubstituted 3-hydroxyesters (**7a-i**) and an amide (**7j**). These products, which were similar to the ones in the section 3.1, were synthesized with moderate to low isolated yields (Table 3.2.6). Attempts to obtain the corresponding phenacyl esters of chiral compounds **7h-j**, as in previous chapter, failed. Alternatively, synthesis of the benzyl esters (**7h,i**) and the amide **7j** was achieved in low yields (16–24%).

Table 3.2.6 KPHMT wild-type and variants catalyzed aldol addition of **1** to **2a–b** and **2d** obtaining products **7a–j**. Reagents and conditions: a) H₂O₂, catalase, 1 h, rt; b) For **7a,d–i**: BnBr, CsCl, DMF, 2 h, 60 °C; for **7b,c**: 4'-BrPhCOCH₂Br, DMF, 90 min, rt; for **7j**: BnBr, HOBT, EDAC, Et₃N, DMF, 4 °C, overnight.



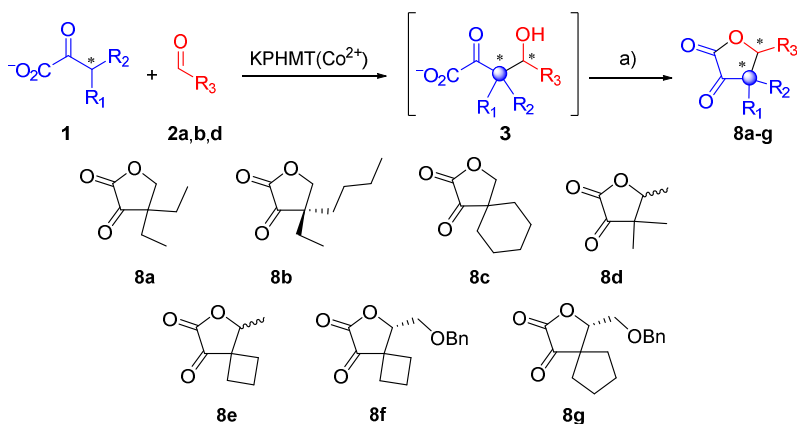
Nu	E	Catalyst ^a	Product	Conv ^b	Yield ^c	er ^d
1a	2a	wild-type	7a	94	53	-
		wild-type		43	36	90:10 ^e
<i>rac</i> - 1n	2a	I212A	7b	42	35	81:19 ^e
		V214G		44	28	91:9 ^e
<i>rac</i> - 1p	2a	I202A/V214G	7c	32	25	>90:10 ^f
1q	2a	I202A	7d	82	36	-
1r	2a	I202A	7e	>95	54	-
1t	2a	I202A/I212A	7f	30	13	-
<i>S</i> - 1v	2a	I202A	7g	>95	48	-
1a	2b	I202A	7h	86	16	66:34 ^g
1r	2b	wild-type	7i	50	24	50:50 ^e
1a	2d	wild-type	7j	42	20	77:33 ^g

^a2 mg mL⁻¹ of enzyme, 0.068 mol%. ^bConversion (%) after 24 h of reaction. ^cIsolated Yield (%) of products. ^dEnantiomeric ratio. ^eEnantiomeric ratio determined by HPLC on the chiral stationary phase. ^fThe absolute stereochemistry was determined by single-crystal X-ray diffraction. ^gEnantiomeric ratio determined by NMR using *R*-configured Pirkle's alcohol.

Results and discussion

2-Oxolactones (**8a–g**) were straightforwardly synthesized by KPHMT catalysis. After the reaction, **8a–g** were formed during the acidic aqueous–organic solvent workup and, when quantitative conversions were achieved, this methodology was enough to afford pure material. Otherwise, an additional extraction with aqueous buffer at neutral pH removed the remaining starting 2-oxoacid (**1**), which was the main impurity present (Table 3.2.7). Almost all the products were obtained in good yields except for the product **8d** (75% conversion, 10% yield). Owing to its low hydrophobicity, the extraction from the reaction media was inefficient and caused a major loss of material.

Table 3.2.7 KPHMT wild-type and variants catalyzed aldol addition of **1** to **2a–b** and **2d** obtaining products **7a–j**. a) aq H⁺/organic extraction.



Nu	E	Catalyst ^a	Product	Conv ^b	Yield ^c	er ^d
1o	2a	I202A	8a	37	26	-
<i>rac</i> - 1p	2a	I202A/V214G	8b	32	27	>90:10 ^e
1s	2a	I212A	8c	20	19	-
1a	2b	wild-type	8d	75	10	50:50 ^f
1q	2b	I212A	8e	95	76	50:50 ^g
1q	2d	I212A	8f	57	32	53:47 ^g
1r	2d	I202A	8g	28	21	93:7 ^g

^a2 mg mL⁻¹ of enzyme, 0.068 mol%. ^bConversion (%) after 24 h of reaction. ^cIsolated Yield (%) of products. ^dEnantiomeric ratio. ^eAbsolute stereochemistry assigned based on crystal X-ray diffraction of compound **7c**. ^fInferred from the value of optical rotation. ^gEnantiomeric ratio determined by NMR using *R*-configured Pirkle's alcohol.

These products were of interest as they are used as precursors or as building blocks in the synthesis of naturally occurring and synthetic biologically active compounds. For example, 2,2-disubstituted 3-hydroxyesters (**7a–j**) were used in the synthesis of different drugs such as Avibactam (β -lactamase inhibitor) or 2,2-bis(hydroxymethyl) propionate derivatives (curcuminoids with anticancer activity).^{196, 197} On the other hand, the 2-oxo group of the 2-oxolactones (**8a–g**) can be reduced affording α -hydroxy- γ -butyrolactones. For instance, (*R*) and (*S*)-pantolactone and analogues have been used in the synthesis of drugs such as Cyanolide A (potent mollusk pesticide), Empagliflozin (treatment of type II diabetes) and Amprenavir (treatment for HIV infection) (Figure 3.2.12).^{198, 199}

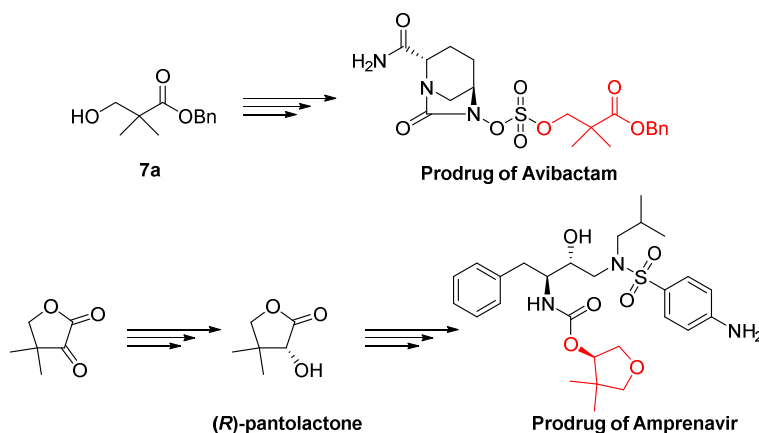


Figure 3.2.12 Examples of drugs synthesized using as building blocks 2,2-disubstituted 3-hydroxyesters or (*R*)-pantolactone.

3.2.6.1 Stereochemistry of products **7b** and **7c**

Products **7b** and **7c** were particular cases as they were obtained from racemic mixture of substrates *rac*-**1n** and *rac*-**1p** respectively. Conversions below 50 % indicated that the catalyst may be stereoselective accepting only one of the two enantiomers. For this reason, in the case of the aldol addition of *rac*-**1n** to **2a**, KPHMT wild-type and variants I212A and V214G were selected, because they gave conversions around 40%.

Results and discussion

The absolute stereochemistry **7b** was first determined indirectly by analyzing the outcome of the unreacted substrate **1n**. Thus, after the aldol addition, the unreacted substrate **1n** and the aldol adduct **3na** were oxidatively decarboxylated and esterified as phenacyl esters (**7b** and **C5**) (Figure 3.2.13).

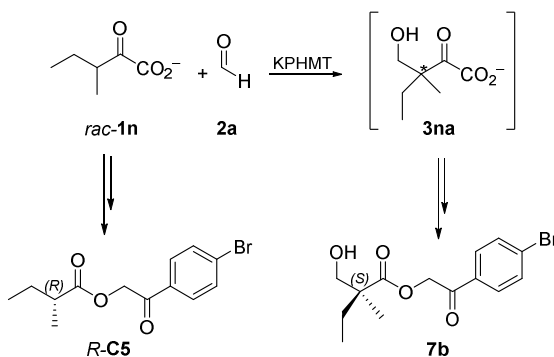


Figure 3.2.13 Synthesis **7b** and the phenacyl ester from the unreacted substrate **rac-1n** (**R-C5**).

Following the same approach used in the previous chapter of this thesis, the racemic mixtures of both products (**rac-7b** and **rac-C5**) were also synthesized. Moreover, the enantiopure sample **S-C5** was obtained from commercial (*S*)-2-methylbutanoic acid that was esterified with 2,4'-dibromoacetophenone with the presence of the weak base KF. The stereochemistry of product **C5** was assessed by chiral HPLC against the standards (Figure 3.2.14A). This was determined to be *R* configured indicating that mainly the (*S*)-enantiomer of **1n** was converted giving to **S-7b** (Figure 3.2.14B).

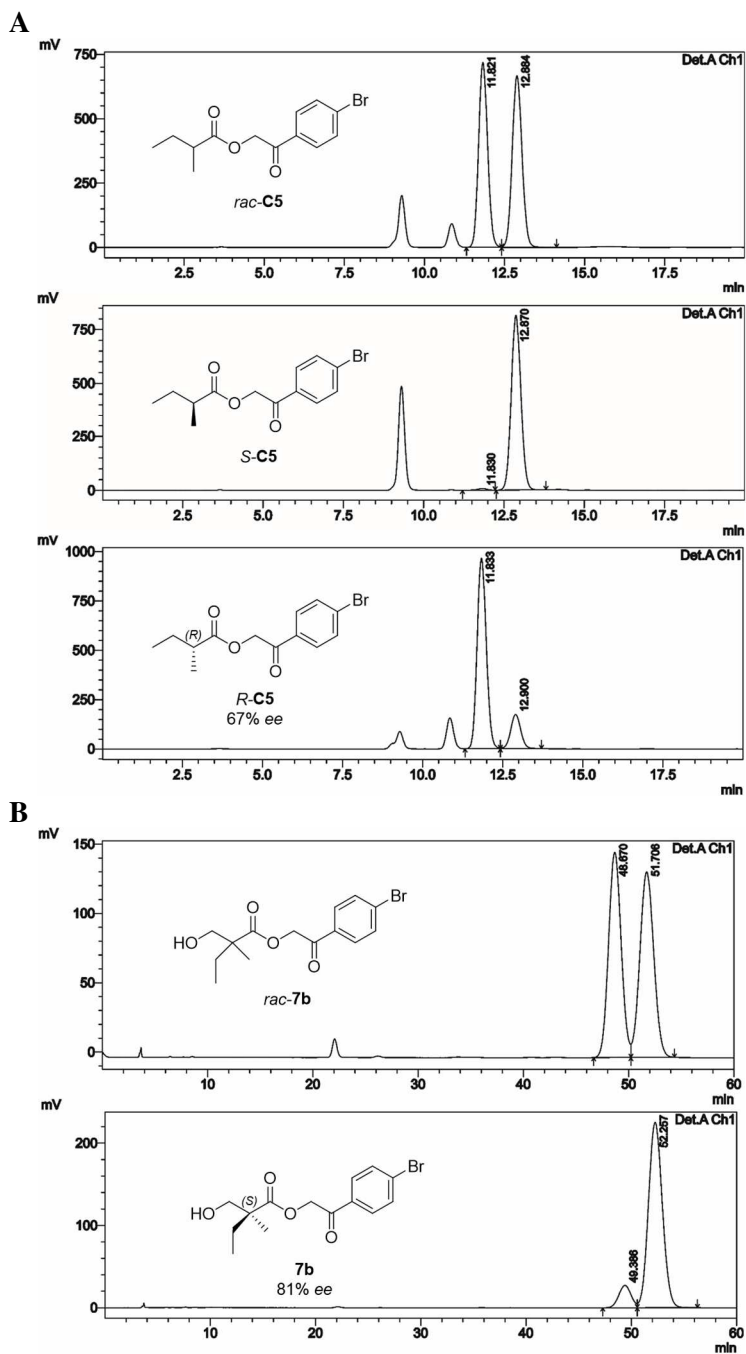


Figure 3.2.14 Chiral HPLC analysis chromatogram of **A** compound **C5**, isocratic elution hexane:iPrOH 98:2 and **B** compound **7b**, isocratic elution hexane:iPrOH 95:5; synthesized with KPHMT wild-type. Conditions: CHIRALPACK® IC 46 x 250 mm column, 5 μm , flow rate 1 mL min^{-1} at 20 °C and UV detection (254 nm).

Results and discussion

Indeed, from mechanistic considerations of KPHMT catalysis, and based on molecular models, it may be inferred that the *S*-**1n** furnished *S*-**7b**. Formation of the corresponding enolates, nucleophiles **1** should adopt a bound orientation in the catalytic site with their H atom at C3 oriented toward the proposed catalytic residue (E181). Therefore, the (*S*)-enantiomer of **1n** can adopt an appropriate conformation with minimal steric repulsion in its C3-ethyl substituent. Having this configuration, the corresponding *E*-enolate would then expose its *re*-face to the electrophile, providing the *S*-**3na** aldol adduct, a precursor of *S*-**7b** (Figure 3.2.15).

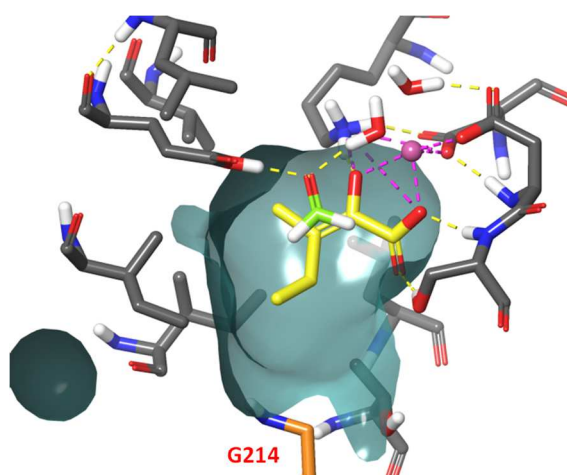


Figure 3.2.15 Model of the prereactive complex of KPHMT V214G with *S*-**1n** (yellow) and **2a** (green) which shows the *E*-enolate formation exposing its *re*-face to the electrophile. Mutated residues (orange C atoms), metal cofactor (purple) and surface of the active site (cyan) are shown.

In contrast, *R*-**1n** has to adopt a different bound conformation, with its C3-ethyl substituent pointing toward residue V179, in order to place its α -proton within reach of the catalytic residue. This conformation, which is less favored because of the proximity of the ethyl moiety to the side chains of V179 and E181, would generate a *Z*-enolate that would expose its *si*-face to the electrophile, providing the alternative *R*-**3na** aldol adduct (Figure 3.2.16). In fact, this less favored

orientation of the nucleophile would be also occurring and might be the responsible of the moderate ee obtained (82% with KPHMT V214G).

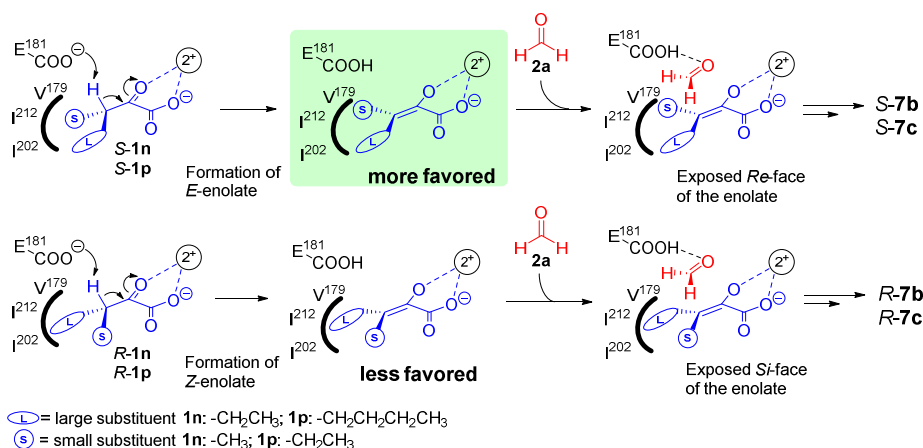


Figure 3.2.16 Enolization mechanism of nucleophiles **1n** and **1p** showing that the formation of *E*-enolates, which gives to *S*-**7b,c**, is the most favored conformation.

Similarly, each enantiomer of nucleophile **1p** can only adopt one reactive conformation that would generate the corresponding *E*- and *Z*-enolates, from *S*- and *R*-**1p**, respectively. Due to the larger size of the *n*-butyl C3-substituent, formation of the *E*-enolate would be faster, and consequently, the *S*-**3pa** aldol adduct is formed preferentially (Figure 3.2.17). As in the previous case, part of the *R*-**1p** would be also accepted as a substrate generating the *R*-**3pa** aldol adduct. This gave a final ee of the product **7c** of 80%.

Results and discussion

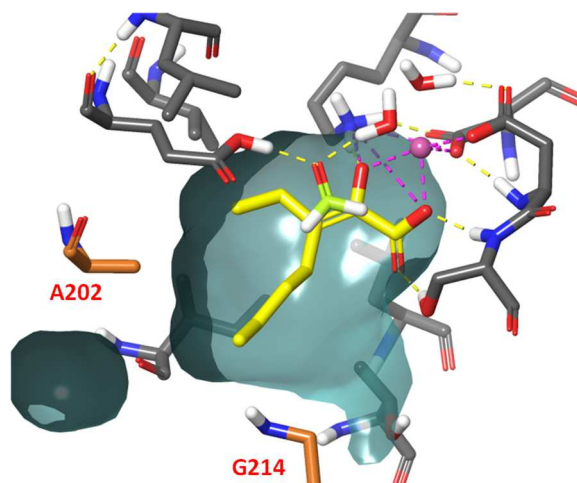
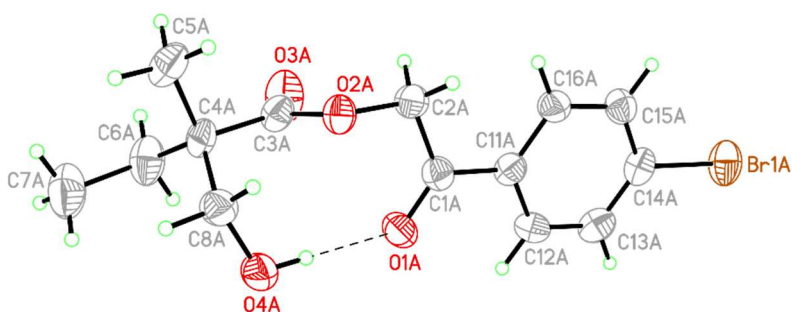


Figure 3.2.17 Model of the prereactive complex of KPHMT I202A/V214G with *S*-1p (yellow) and 2a (green) which shows the *E*-enolate formation exposing its *re*-face to the electrophile. Mutated residues (orange C atoms), metal cofactor (purple) and surface of the active site (cyan) are shown.

The above computational mechanistic analysis of the products 7b and 7c was confirmed by X-ray diffraction, which established the absolute (*S*)-configuration of both products (Figure 3.2.18).

A



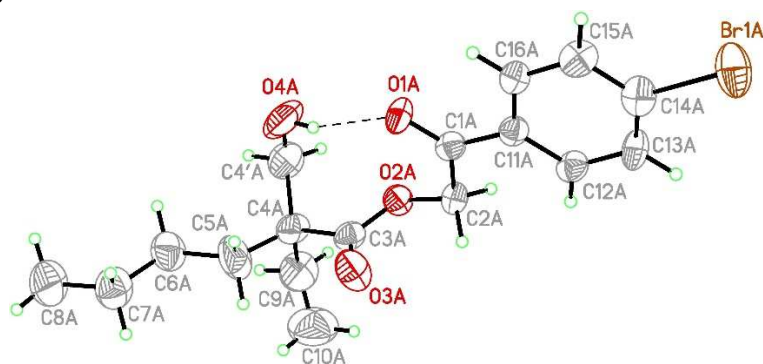
B

Figure 3.2.18 Crystal structures of **A** product *S*-**7b** and **B** product *S*-**7c**. Displacement ellipsoids are drawn at the 50 % probability level. The dashed line indicates a hydrogen bond.

3.2.6.2 Stereochemistry determination of products **7h–j** and **8e–g**

Several attempts were carried out to synthesize the racemic mixtures of the products **7h–j** as standards. These were based on the alkylation of acetoacetate ester derivatives **C6** followed by the subsequent reduction of the carbonyl group rendering racemic mixtures of **7h–j** (Figure 3.2.19). Initially, the alkylation of **C6a** was performed with 1,4-dibromobutane using potassium carbonate as a base following a previously reported procedure.²⁰⁰ However, this strategy failed in our hands. Alternatively, alkylation of **C6a** and **C6c** with 1,4-dibromobutane or iodomethane respectively and using sodium hydride as a base was also tried but again was unsuccessful.

Results and discussion

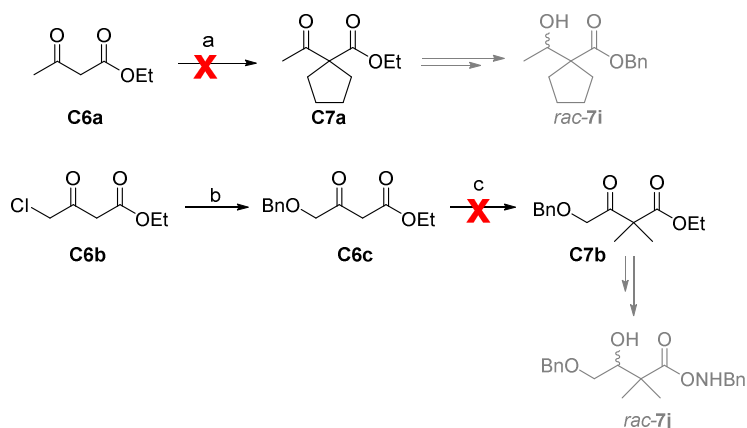


Figure 3.2.19 Approaches for the synthesis of the racemic mixtures of the products **7h–j**. Reagents and conditions: a) 1,4-dibromobutane, 1-butyl-3-methylimidazolium bromide, K_2CO_3 , DMF, rt, 24 h or 1,4-dibromobutane, NaH, DMF, rt, overnight; b) BnOH, NaH, DMF, rt, overnight, 76%; c) MeI, NaH, THF, rt, overnight.

The second strategy used was to oxidize the hydroxyl group of the enzymatic products **7h–j** to a ketone that was symmetrically reduced again to obtain *rac-7h–j*. This approach was only useful for the compound *rac-7i* (Figure 3.2.20A). The chiral HPLC analysis of **7i** enzymatically prepared revealed that it had the same profile than *rac-7i*, and thus KPHMT was not stereoselective (Figure 3.2.20B).

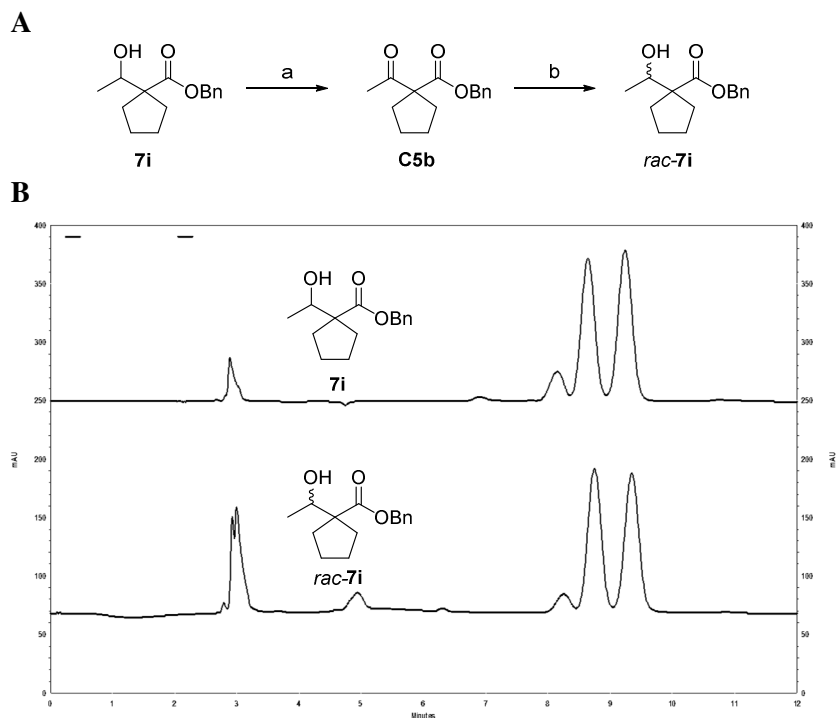


Figure 3.2.20 **A** Synthesis of *rac-7i* through the stepwise oxidation and reduction of the enzymatic product **7i**. Reagents and conditions: a) H_5IO_6 , CrO_3 , ACN, 0 °C, 1 h, 83%; b) NaBH_4 , THF, 0 °C, 1 h, 68 %. **B** Chiral HPLC analysis chromatogram of **7i** synthesized with KPHMT wild-type. Conditions: CHIRALPACK® IC 46 x 250 mm column, 5 μm , flow rate 1 mL min^{-1} at 20 °C and UV detection (254 nm). Isocratic elution hexane:iPrOH 95:5.

Owing to the difficulty of synthesizing the racemic mixtures of products **7h** and **7j**, its enantiomeric purity was determined by NMR by complex formation using *R*-configured Pirkle's alcohol, which gives enantiomeric ratios of 66:34 and 77:23, respectively. Likewise, the stereochemistry of 2-oxolactones **8e–g** was also determined using the same NMR methodology. Products **8e** and **8f** were obtained as racemic mixtures whereas **8g** was obtained with an enantiomeric ratio of 93:7 (spectra in Supplementary Material, section 6.3.4).

The enantiomeric excesses of these products could be explained based on the orientation of the aldehyde in the active site of the enzyme. Firstly, all the

Results and discussion

aldehydes should adopt a bound conformation where the carbonyl oxygen atom can interact with the acid-base catalytic residue. Thus, **2b** and **2d** can approach the enolate either from their *re*- or *si*-face, generating two possible configurations at C4 of the corresponding aldol adducts **3**.

These non-hydroxylated electrophiles provided, in most cases, products with low or null enantiomeric excess indicating that they could fit almost equally well with either orientation into the KPHMT active site cavity (figures in Supplementary Material, section 6.3.5). Only the product from the aldol addition of **1r** to **2d** exhibited a good ee value (85%), which could be explained on the basis of the steric repulsion caused by the cyclopentylidenyl moiety of the nucleophile enolate, which favors the approach of the electrophile from its *si*-face (Figure 3.2.21).

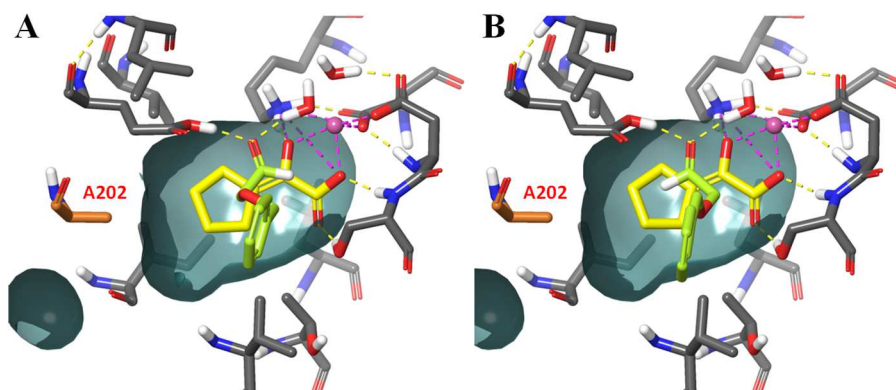
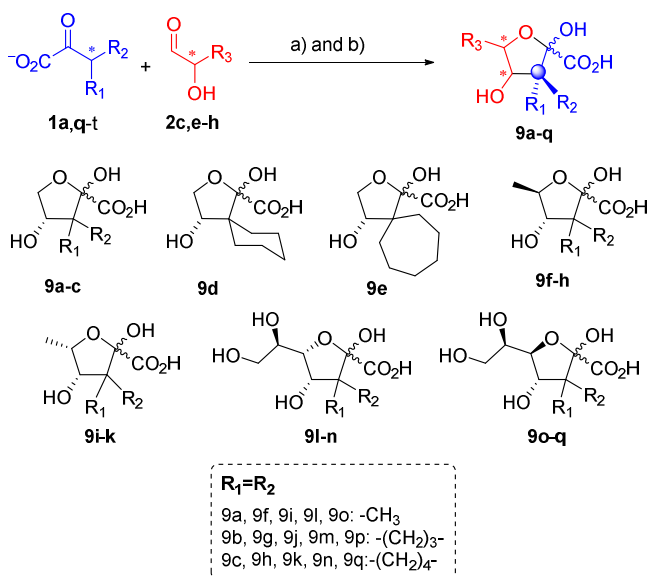


Figure 3.2.21 Model of the prereactive complex of KPHMT I202A with **1r** (yellow) and **2d** (green). The electrophile **2d** is shown approaching the enolate from **A** its *re*-face which is less favored or from **B** its *si*-face which is more favored. Mutated residues (orange C atoms), metal cofactor (purple) and surface of the active site (cyan) are shown.

3.2.7 Preparative synthesis and characterization of products obtained with α -hydroxy aldehydes

The previous reactions using the panel of nucleophiles (**1a** and **1q–t**) and the hydroxy aldehydes **2c** and **2e–h** were run at a preparative scale. The use of these aldehydes effectively shifted the reaction equilibrium owing to the formation of cyclic hemiketal species reaching high conversions after 24 h (>90% for nucleophiles **1a** and **1q** with the best biocatalyst). The resulting hemiketals (**9a–q**) were easily purified by anion exchange chromatography (Table 3.2.8). The products, which could be classified as ulosonic acid type products, bore a new formed stereocenter at C4 and *gem*-dialkyl, and spirocyclic quaternary centers at C3.

Table 3.2.8 KPHMT wild-type and variants catalyzed aldol addition of **1a** and **1q–t** to **2c** and **2e–h** obtaining products **9a–q**. a) KPHMT(Co²⁺) wild-type and variants. b) Anion exchange chromatography HCO₂⁻/HCO₂H.



Nu	E	Catalyst ^a	Product	Yield ^b	$\alpha:\beta^c$
1a	2c	I202A	9a	87	60:40
1q	2c	wild-type	9b	90	60:40

Results and discussion

1r	2c	I202A	9c	76	77:23
1s	2c	I212A	9d	47	97:3
1t	2c	I212A	9e	30	80:20
1a	2e	wild-type	9f	61	23:74
1q	2e	I212A	9g	72	42:58
1r	2e	I212A	9h	50	37:63
1a	2f	wild-type	9i	72	21:79
1q	2f	I212A	9j	77	45:55
1r	2f	I212A	9k	65	10:90
1a	2g	wild-type	9l	81	76:24
1q	2g	I212A	9m	91	56:44
1r	2g	I212A	9n	73	76:24
1a	2h	V214G	9o	80	24:76
1q	2h	I212A	9p	88	50:50
1r	2h	I212A	9q	48	50:50

^a2 mg mL⁻¹ of enzyme, 0.068 mol%. ^bIsolated Yield (%) of products. ^c α : β anomeric ratio.

In some cases, minor cyclic structures such as 2-oxolactones (**C8**) and the corresponding hydrated form (**C9**) were identified by NMR. It is likely that the purification process under acid conditions and freeze drying favored their formation (Figure 3.2.22).

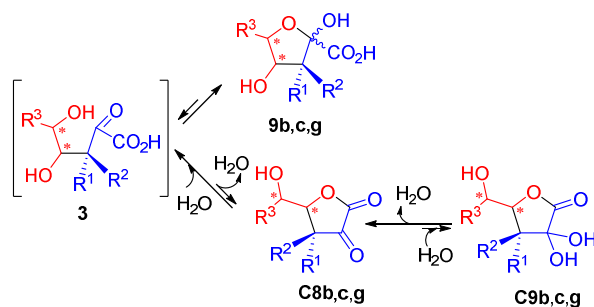


Figure 3.2.22 Equilibrium between lactones **C8** and **C9** and hemiketal **9** in acidic aqueous medium.

The absolute stereochemistry of products **9f–q** was determined by NMR, taking as a reference one or two chiral centers of defined absolute configuration that act as a reference in the determination of their overall relative configuration. It

was found that, the absolute stereochemistry of the chiral center coming from the electrophile was invariably *S* regardless of the aldehyde substrate used. By extension, the stereochemical outcome of products **9a–e** together with **8f,g** and **7h,j** from the previous section, was also assigned to be *S* configured.

Molecular models showed that the hydroxylated electrophiles exhibited different options of establishing hydrogen-bonds with residues of the active site or with the bound nucleophile enolates. For the monohydroxylated electrophiles **2c**, **2e** and **2f** the models suggested that the hydroxyl group could mainly interact with the carboxylates of residue E181 or that of the enolate (Figure 3.2.23). The fact that all the isolated products from **2e** and **2f**, exhibited a high ee indicated that the approach of the electrophile from its *si*-face was preferred over that from its *re*-face. This suggested that the interaction of the 2-hydroxyl group of the electrophile with the enolate carboxylate was more favorable than that with E181. This could also be extended to the polyhydroxylated electrophiles **2g** and **2h**, although in these cases the interactions of the other hydroxyl groups could also play a role on the stereoselectivities observed.

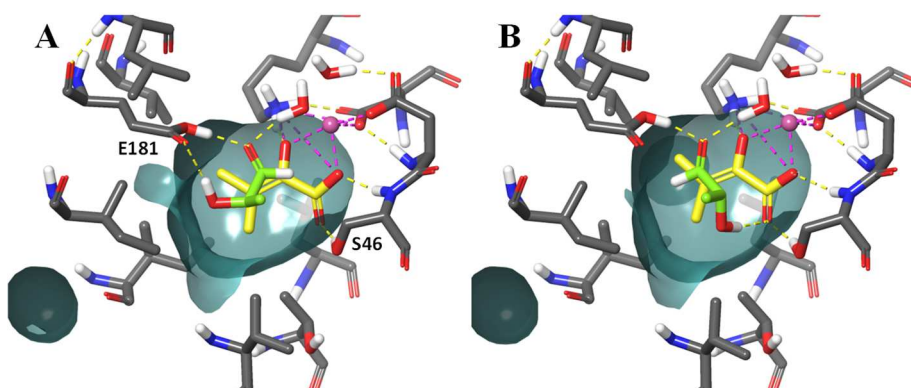


Figure 3.2.23 Model of the prereactive complex of KPHMT wild-type with **1a** (yellow) and **2e** (green). The electrophile **2e** is shown approaching the enolate from **A** its *re*-face which interacts with the carboxylate of E181 or from **B** its *si*-face which is more favored interacting with the carboxylate of the enolate. Metal cofactor (purple) and surface of the active site (cyan) are shown.

Results and discussion

The products **9a–q** could be classified as ulosonic acid type products, bearing a quaternary center at C3 (Figure 3.2.24). These have not been hitherto reported, and their preparation using conventional chemical procedures may be anticipated to be elusive because of the number of functional groups and the intrinsic reactivity of the 2-oxoacid moiety.²⁰¹ This type of products constitutes an important biologically active compounds involved in cellular recognition and communication.^{202, 203}

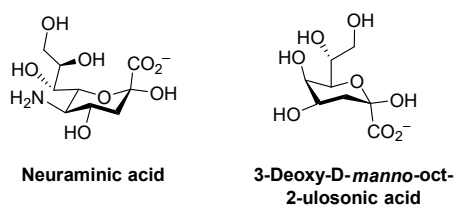


Figure 3.2.24 Examples of important ulosonic acid type products.

3.2.8 Enzymatic cascade reactions

The development of one-pot tandem biocatalytic reactions *in vitro* has gained interest in recent years because they mimic the synergistic effects of cascade reactions catalyzed by multiple enzymes in nature. This presents extraordinary advantages from the synthetic point of view, since it allows a reversible process to become irreversible, to shift the equilibrium reaction towards the formation of enantiopure compounds from racemic substrates and reduce or eliminate tedious purification procedures of intermediates among others.^{204, 205}

For instance, compound **7g** from the Section 3.2.6 was prepared through a biocatalytic cascade reaction, in a one-pot two-step process. MBP-YfaU was used in the first place to furnish the aldol adduct *S*-**1v**, studied in the Section 3.1.3. Then, KHPMT catalyzed the formation of a quaternary center through a second aldol addition to formaldehyde (conversion 95%) (Figure 3.2.25).

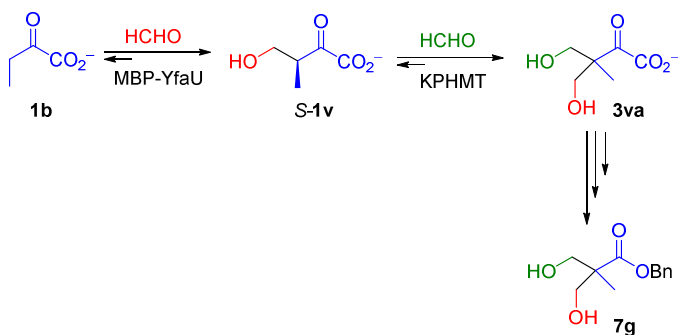


Figure 3.2.25 One-pot two-step reactions to catalyze the formation of the aldol adduct **3va** using MBP-YfaU and KPHMT.

Following the same approach, the addition of **1a**, **1q**, and **1r**, to D-threose was planned as a simultaneous biocatalytic one-pot two-step cascade reaction. To this end, D-threose (**2g**) was first produced by enzymatic homoaldol addition of glycolaldehyde (**2c**) catalyzed by D-fructose-6-phosphate aldolase variant A129G (FSA A129G) (Figure 3.2.26).²⁰⁶ Once **2g** was produced, **1a** and KPHMT were added to the reaction mixture yielding **9l**. When the second step was carried out without removal of FSA A129G a significant amount of **9a** (~27%), from the addition of **1a** and **2c**, was detected by NMR. This side reaction was minimized (~5%) by removing FSA A129G from the medium by simply centrifuging and filtering the reaction (Figure 3.2.27). This result suggested that **2c** was better substrate than **2g** for KPHMT, and that it was transformed into **9a** by this catalyst, via FSA-catalyzed retro-aldol reaction of **2g**. This observation was also made in other investigations in our group, where HBPA (i.e., hydroxybenzylidene pyruvate hydratase-aldolase, EC 4.1.2.45) was removed from the reaction media before a second enzymatic reaction to avoid retroaldolysis, in a one-pot two-step approach.²⁰⁷

Results and discussion

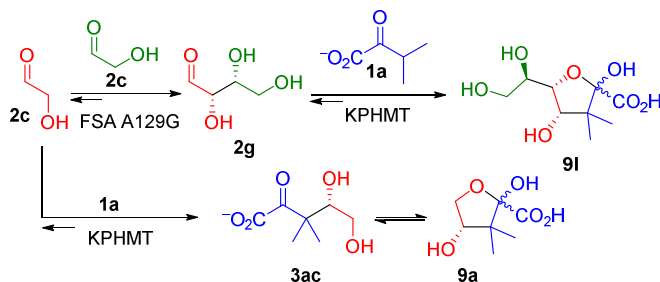


Figure 3.2.26 Attempted one-pot two-step enzymatic synthesis of product **9I**.

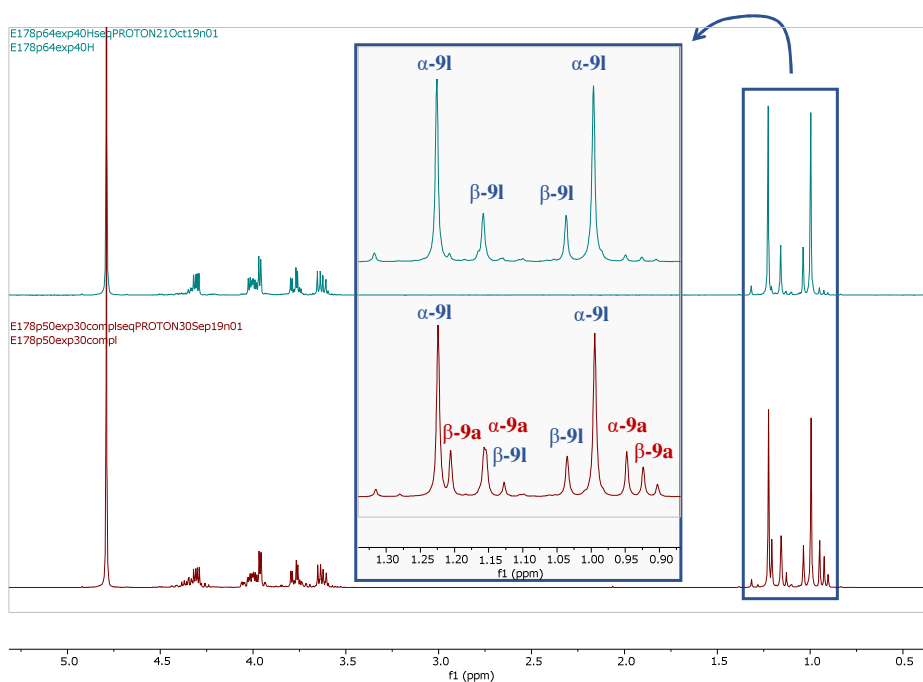


Figure 3.2.27 NMR ¹H spectra (D₂O) of **9I** obtained without removal of FSA A129G (bottom, red line) or removing FSA A129G (top, blue line) from the reaction media before the second aldol addition with KPHMT catalyst.

In order to generate diverse products bearing chiral quaternary carbons, we envisaged the aldol addition of 3-substituted 2-oxoacids to two different aldehydes catalyzed by aldolases. The first aldol addition would generate an

aldol adduct disubstituted at C3 that would be used as nucleophile for the second aldol addition to another aldehyde.

We started our investigation by the stepwise aldol addition of 2-oxobutanoate (**1b**) to acetaldehyde (**2b**) catalyzed by MBP-YfaU, which formed the aldol adduct **3bb** in high conversion (81%). Moreover, from the previous chapter of this thesis, we know that the aldol adduct formed by MBP-YfaU (**3bb**) would have an *S*-stereochemistry at C3.⁹²

Thus, the aldol adduct **3bb** was used without any further purification for the aldol addition to formaldehyde (**2a**) catalyzed by KPHMT. These reactions were planned as a one-pot two-step since **3bb** was not substrate for MBP-YfaU and there was no need to remove it from the reaction medium before the second aldol addition. Unexpectedly, after the second aldol addition, the main product detected by HPLC resulted to be the previously characterized **3ua**. This, comes from the aldol addition of **3bb** to formaldehyde (Figure 3.2.28). This result might be caused by the fact that the reaction catalyzed by MBP-YfaU (**1b**+**2a**) was almost irreversible and this shifted the equilibrium towards the retro-aldol reaction of **3bb** to form the more kinetically stable aldol adduct *S*-**1v**. Then, as studied previously, *S*-**1v** was a good substrate for KPHMT, which catalyzes an aldol addition to the formaldehyde that remained in the reaction media.

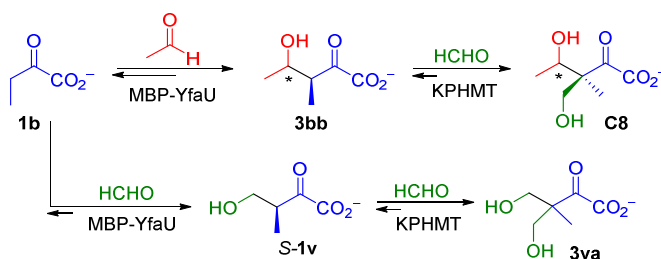


Figure 3.2.28 Attempted one-pot two-step reaction for the aldol addition of **1b** to acetaldehyde and formaldehyde catalyzed by MBP-YfaU and KPHMT.

In a second approach, MBP-YfaU was used to catalyze the aldol addition of **1b** to **2a** in the first place. In this way, formaldehyde was consumed, and the

Results and discussion

reaction generated *S*-**1v**. Then, KPHMT and glycolaldehyde (**2c**) were added. The main advantages of this approach were: *i*) *S*-**1v** was a good substrate for KPHMT as we know from previous results, and *ii*) the use of α -hydroxy aldehydes promoted spontaneous cyclization of products shifting the equilibrium towards the formation of the aldol adduct **3vc**. After the purification of this aldol adduct by anion exchange chromatography, a mixture of two diastereomeric lactones (dr 91:9) were identified by NMR. The acidic elution conditions (i.e., HCOH, 1 M) and the lyophilization of the fraction pool promoted the lactonization of the hemiketal intermediate (Figure 3.2.29).

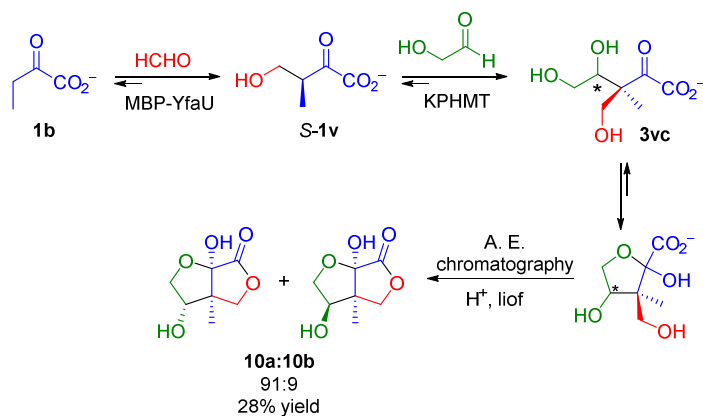


Figure 3.2.29 Synthesis of the bicyclic lactones **10a** and **10b** by combining the aldol addition of **1b** to formaldehyde and glycolaldehyde in a one-pot two-step cascade.

The high stereopreference observed could also be explained through molecular models that suggested that the approach of the electrophile **2c** to the enolate from its *si*-face was preferred over that from its *re*-face. In this case, the hydroxyl group of **2c** is interacting by hydrogen bonding with the hydroxyl and the carbonyl groups of *S*-**1v** enolate (Figure 3.2.30).

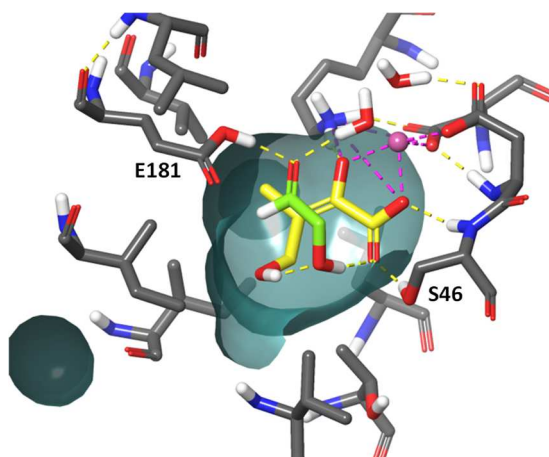


Figure 3.2.30 Model of the prereactive complex of KPHMT wild-type with *S*-1v (yellow) and **2c** (green). The aldehyde approaches the enolate from its *si*-face, which is more favored due to the hydrogen bonds with the hydroxyl and carbonyl groups of the enolate. Metal cofactor (purple) and surface of the active site (cyan) are also shown.

3.2.9 Summary

In summary, we demonstrated the utility of the promiscuous aldolase KPHMT for the creation of quaternary carbon centers using a structurally diverse array of 3,3-disubstituted 2-oxoacid nucleophiles and aldehyde substrates. Besides the variants obtained in the previous chapter of this thesis, we envisaged the residue V214 as crucial for KPHMT to accept this type of nucleophiles. Thus, seven variants were generated by site directed mutagenesis and tested as catalysts. The positive reactions in the screening were run at preparative scale synthesis.

The reported biocatalytic approach resulted a straightforward process that allowed access, using different methodologies, to 2-oxolactones, 3-hydroxy acid derivatives, and ulosonic acid type products, all of them bearing gem-dialkyl, gemcycloalkyl, and spirocyclic quaternary centers. 3-Hydroxy esters were elaborated by oxidative decarboxylation of the carbonyl group followed by esterification. The 2-oxolactones were produced during workup and were

Results and discussion

obtained when quantitative conversions of the aldol addition were achieved. The determination of the enantiomeric excess and the absolute configuration of these compounds was challenging due to the difficulty for obtaining the racemic mixtures of the products.

When 2-hydroxyaldehydes were used as electrophiles, it leads to the spontaneous formation of cyclic hemiketals, which were easily purified by anion exchange chromatography obtaining high isolated yields (48–91%). Also, a bicyclic lactone was obtained by lactonization of the hemiketal intermediate. The relative configuration of these compounds was mainly determined by NMR and resulted that the chiral center coming for the electrophile was invariably *S*.

The present study expands the portfolio of biocatalytic aldol reactions leading to unprecedented structures and offering new synthetic opportunities for pharmaceutically relevant compounds and chiral precursors. We anticipate a range of new applications by performing further engineering of the KPHMT variants to render new biocatalysts, efficient toward new substrate classes.

3.3 Preliminary studies of the application of KPHMT and MBP-YfaU on the synthesis of nucleoside analogues

3.3.1 Introduction

Nucleotides are organic molecules consisting of a nucleoside, formed by a deoxyribose, a nucleobase (e.g., adenine (A); cytosine (C); guanine (G); thymine (T), and uracil (U)), and a phosphate group. These are essential building blocks for the construction of nucleic acids (DNA and RNA) and for the replication and transcription of genetic information within all life-forms on Earth. For this reason, they are in the spotlight of drug design and several important analogues such as Gemcitabine (anticancer), Abacavir, Entecavir and Acyclovir (antivirals) have been approved among others.¹⁴¹⁻¹⁴³ Different sites can be considered for modifications of the natural nucleotide scaffold: the sugar moiety, the nucleobase, the glycosidic bond and/or the phosphate group.¹⁴⁴ Modifications of this scaffold have been applied successfully in recent years giving rise to several approved drugs.¹⁴⁵

From the previous results of this thesis, we envisaged the use of aldolases to construct the furanose moiety of nucleosides. The enzymatic synthesis would consist of two steps. The first comprises the aldol addition of 2-oxoacids (**1**) to aldehydes (**2**) catalyzed by KPHMT or MBP-YfaU. Then, in the second step, the corresponding aldol adduct (**3**) is oxidatively decarboxylated and cyclized to obtain a lactone that can be used as a precursor for the synthesis of nucleosides (Figure 3.3.1).

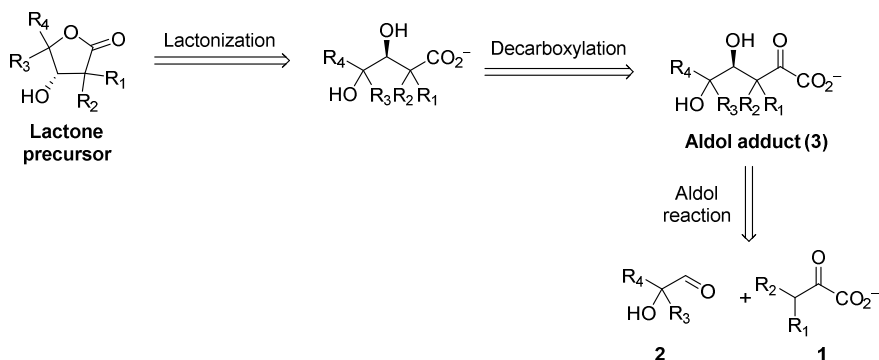


Figure 3.3.1 Retrosynthetic approach for the synthesis of lactone precursor analogues for the synthesis of nucleosides through aldol addition using aldolases.

Results and discussion

For the first step, we selected the 2-oxoacids (**1**) nucleophiles that allowed to install modifications at the C2' position of the lactone precursor. As electrophiles, D-glyceraldehyde (**2l**) and analogues such as *O*-protected D-glyceraldehyde (**2m**) or α,α -disubstituted- α -hydroxy aldehydes (**2n-q**) were chosen to insert modifications at C4' position (Figure 3.3.2).

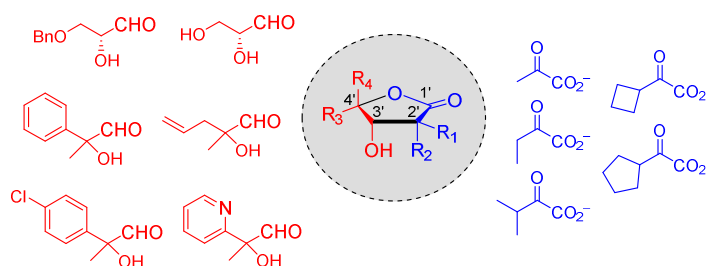


Figure 3.3.2 Modifications at C2' and C4' positions in the lactone precursor for the synthesis of nucleosides by using a panel of 2-oxoacids and aldehydes developed in this thesis.

Then, a nucleobase can be added to the lactones to furnish the final nucleoside derivative. The most used approach consists on the protection of the 3'-OH group of the lactone followed by the reduction of the carbonyl group and acetylation of the hemiketal. Then, the nucleobase is added forming the *N*-glycosidic bond and the 3'-OH group deprotected to achieve the final nucleoside (Figure 3.3.3A).¹⁵⁰

Other interesting nucleoside analogues are the C-nucleosides that can be achieved straight forward from lactone precursors. These bear a more metabolically stable C-C bond instead of the naturally occurring anomeric C-N union between the saccharide and the base units.²⁰⁸ Their synthesis can be achieved by a two-step sequence consisting of a nucleophilic addition of an aryllithium to the lactone and subsequent silicon based reduction of the lactol intermediate (Figure 3.3.3B).¹³⁷

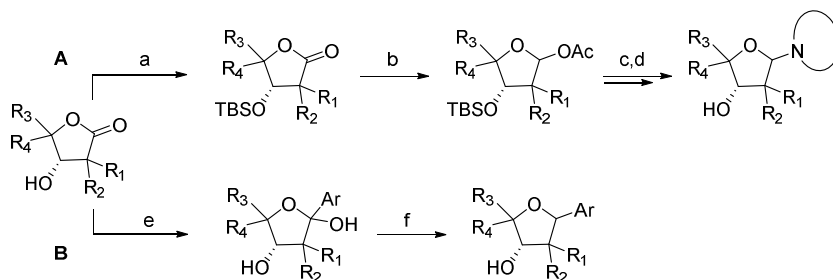


Figure 3.3.3 Synthesis of nucleosides analogues from lactone precursors. **A** Synthesis of nucleosides by the addition of a nucleobase in C1' position of the furanose scaffold and **B** synthesis of C-nucleosides by the addition of an aryl group on the carbonyl group of the lactone through lactol intermediate. Reagents and conditions: a) 2,6-lutidine, TBDMSOTf, DCM, 0 °C to rt, 1 h; b) DIBAL-H, pyridine, DMAP, Ac₂O, DCM, -78 °C to rt, overnight; c) nucleobase, SnCl₄, PhCl, 70 °C, 15 h; d) HCl, dioxane, MeOH, rt, overnight; e) ArLi, THF, -78 °C, 2 h; f) Et₃SiH, BF₃·OEt₂, DCM, -40 °C, 2 h.

3.3.2 Enzymatic synthesis of lactone precursors using (*R*)-3-(benzyloxy)-2-hydroxypropanal as an electrophile in aldol reactions

To start our investigations, we synthesized (*R*)-3-(benzyloxy)-2-hydroxypropanal (**2m**) as the electrophile component for the enzymatic aldol addition, using the commercially available (*R*)-1,3-dioxolane-4-methanol (**C11a**) as starting material. The hydroxyl group was first protected as benzyl ether furnishing a benzyloxymethyl isopropylidene acetal (**C11b**) that was hydrolyzed obtaining a diol (**C11c**) following a previously reported procedure.²⁰⁹ Finally, the oxidation of the primary alcohol of **C11c** furnished the corresponding aldehyde **2m** under mild conditions using trichloroisocyanuric acid (TCC) in the presence of catalytic TEMPO (Figure 3.3.4). TCC is a safe, stable, and easily handled solid that was used as a substitute of sodium hypochlorite to perform this reaction in a greener manner. Moreover, this approach was reported to be efficient for the oxidation of

Results and discussion

primary alcohols to aldehydes, in the presence of secondary alcohols, without overoxidation to carboxylic acids.²¹⁰

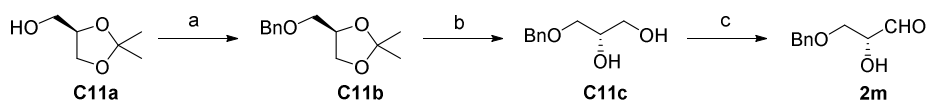
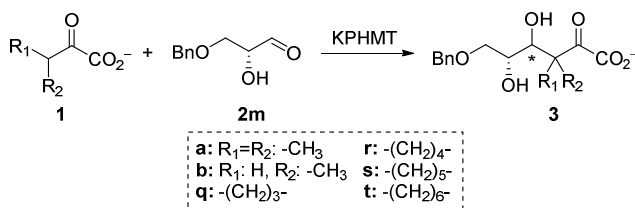


Figure 3.3.4 General approach for the synthesis of (*R*)-3-(benzyloxy)-2-hydroxypropanal (**2m**). Reagents and conditions: a) BnBr, NaH, DMF, rt, overnight, quantitative yield; b) MeOH:HCl 1 M (1:1, v/v), rt, overnight, quantitative yield; c) NaHCO₃, TEMPO, TCC, DCM, 4 °C, 1 h, 73%.

In general, the synthesis of (*R*)-3-(benzyloxy)-2-hydroxypropanal (**2m**) resulted in an efficient methodology (73% yield over three steps) in which the intermediates were isolated by simple workup procedures avoiding tedious purification processes. However, in our hands, it was not possible to purify the aldehyde because it polymerizes during isolation. Therefore, **2m** was used as a DMF solution, and quantified by HPLC with a reference compound.

Aldehyde **2m** was used without any further purification as electrophile in aldol addition with diverse nucleophiles catalyzed by KPHMT wild-type and variants. Conversions after 24 h were measured following the reactions by HPLC (Table 3.3.1).

Table 3.3.1 Conversion after 24 h (%) of the aldol addition of 2-oxoacids (**1**) to (*R*)-3-(benzyloxy)-2-hydroxypropanal (**2m**) catalyzed by KPHMT wild-type and variants.



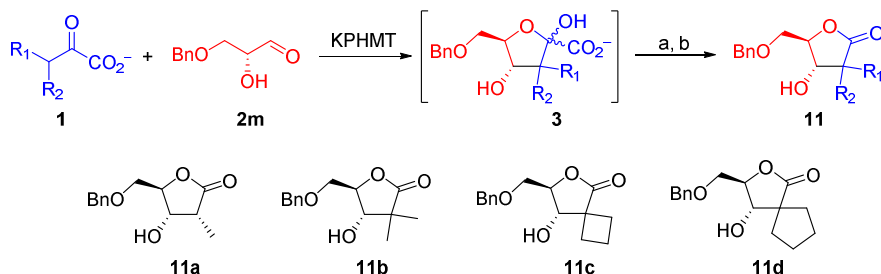
KPHMT	E Nu	2m					
		1a	1b	1q	1r	1s	1t
wild-type		77	75	87	13	- ^a	- ^a
I212A		45	72	90	67	- ^a	- ^a
I202A		76	60	86	51	- ^a	- ^a
V214G		73	53	35	46	- ^a	- ^a
I202A/V214G		9	43	49	11	- ^a	- ^a
I212A/V214G		7	45	40	7	- ^a	- ^a
I202A/I212A/V214G		14	30	27	19	- ^a	- ^a
I202A/I212A		46	65	83	69	- ^a	- ^a

[**1**] = [**2m**] = 0.1 M, 2 mg mL⁻¹ of enzyme, 4.5 eq M²⁺ respect to the catalyst. ^aProduct not detected.

The results showed that KPHMT wild-type and variants thereof accepted **2m** as an electrophile. For nucleophiles **1a** and **1b** the best conversions were achieved with wild-type catalyst (75%). For nucleophiles **1q** and **1r** the best variants were I212A (87%) and the double variant I202A/I212A (69%) respectively. Nucleophiles **1s** and **1t** were not converted by any biocatalysts. The results of the substrate tolerance of KPHMT variants were consistent with the ones reported in the chapter 3.2 of this thesis. The positive hits in the screening were run at preparative scale providing, after oxidative decarboxylation step, lactones with different substituents at C2 (Table 3.3.2).

Results and discussion

Table 3.3.2 KPHMT wild-type and variants catalyzed aldol addition of 2-oxoacids (**1**) to (*R*)-3-(benzyloxy)-2-hydroxypropanal (**2m**) obtaining products **11a–d**. Reagents and conditions: a) H₂O₂ (10 eq), 100 °C, 5 h; b) catalase.



Nu	Catalyst ^a	Product	Conv ^b	Yield ^c
1b	wild-type	11a	68	40
1a	wild-type	11b	80	52
1q	I212A	11c	85	65
1r	I202A/I212A	11d	50	43

^a2 mg mL⁻¹ of enzyme, 0.068 mol%, 4.5 eq M²⁺ respect to the catalyst. ^bConversion (%) after 24 h of reaction. ^cIsolated Yield (%) of products.

The conditions of the aldol adduct decarboxylation used in previous experiments (i.e., 1 h of reaction with 5 eq of H₂O₂ at room temperature) resulted to be inefficient. We hypothesized that the aldol adducts underwent spontaneous cyclization forming hemiketal products (**3**), complicating its decarboxylation. Thus, strongest conditions were required: reflux at 100 °C, and using 10 eq of hydrogen peroxide. The reaction was followed by HPLC until the complete consumption of the aldol adducts (1 h to 5 h).

The aqueous reaction media containing the carboxylic acids was adjusted to pH 8 with bicarbonate and washed with EtOAc. Unexpectedly, the products were found in the organic phase and were purified by silica gel chromatography (40–56% of isolated yields). The products **11a–d** were characterized by NMR as lactones, as assessed by HMBC experiments. The relative stereochemistry of the products was also evaluated by NMR. The absolute configuration was determined considering the internal reference chiral center of defined absolute

configuration from the electrophile **2m** component. The analysis showed that the stereochemistry of the new chiral center coming from the electrophile was invariably *S*. These results were consistent with the ones reported in the Section 3.2.7.

The great advantage of using **2m** as electrophile, was that lactones **11a–d** were already protected at the primary hydroxyl group. This, together with the protection of the remaining hydroxyl group in C3, allow to prepare the final nucleoside with the addition of the nucleobase.

Compounds **11a–d** were already reported by Peifer *et. al.*. They used a Lewis acid mediated diastereoselective Mukaiyama aldol addition of silyl ketene acetal to a fully protected D-glyceraldehyde derivative.¹³⁷ The lactonization of the adducts rendered compounds **11** in 93–94% yields and dr (>95:5). This chemical synthesis involved the use of a copper catalyst and organocatalyst for the synthesis of the chiral aldehyde (Figure 3.3.5A), requiring fully protection of reactants and stoichiometric amounts of titanium salts as Lewis acid for the aldol addition. Moreover, all the intermediates needed to be purified using different techniques such as crystallization, distillation, silica gel or flash chromatography (Figure 3.3.5). Even though we obtained lower isolated yields, the diastereomeric ratios achieved were excellent and the synthesis of substrates and the enzymatic catalyzed aldol addition resulted to be simpler, avoiding tedious purification steps and the use of multiple orthogonal protective groups.

Results and discussion

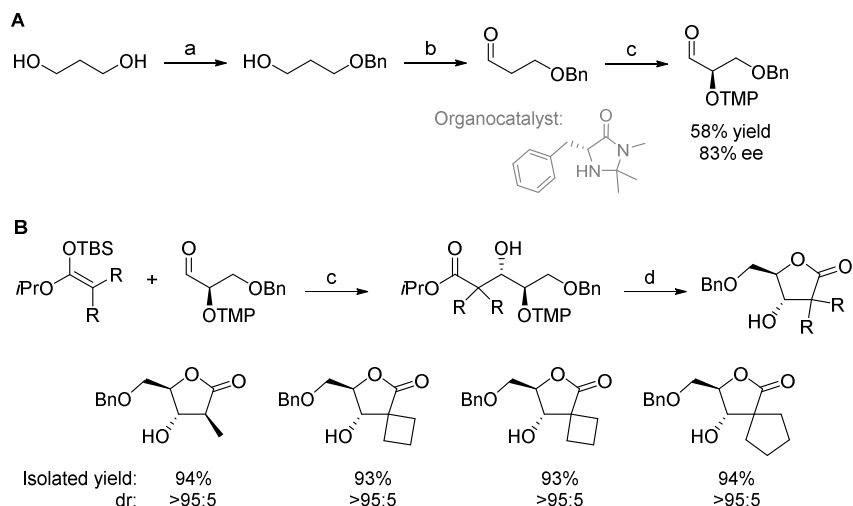


Figure 3.3.5 Synthetic approach used by Peifer *et. al.* rendering the lactones **11a–d**. **A** Synthesis of the chiral aldehyde by the synergistic action of a copper catalyst and organocatalyst and **B** Mukaiyama aldol reaction of a preformed enolate to the chiral aldehyde and subsequent lactonization of the product. Reagents and conditions: a) NaH, BnBr, 0 °C to rt, overnight, 87%; b) TEMPO, PIDA, DCM, rt, overnight, 89%; c) organocatalyst·HBF₄, 4 Å molec sieves, CuCl₂, TEMPO, EtOAc, –30 °C to rt, 24 h, 58%; d) TiCl₂(OiPr)₂, DCM, –20 °C; d) Zn, TFA, toluene:H₂O, 1:1 (v/v).

3.3.3 Use of D-glyceraldehyde as electrophile in aldol reactions

The use of fully unprotected D-glyceraldehyde (**2l**) as electrophile in aldol additions was also considered. Although it is commercially available, different approaches for its preparation were planned as it is expensive (1 g costs 259 € in Sigma-Aldrich). At the beginning, we explored the chemical synthesis but most of the routes reported in the literature use chiral precursors that need multiple cumbersome protection steps. Moreover, due to the high hydrophilic nature, it was usually obtained fully protected or, alternatively, used directly in solution without isolation in the follow up chemistry (Figure 3.3.6A).^{211, 212} Likewise, chemoenzymatic and direct enzymatic routes, including the racemic resolution of the achiral aldehyde, have been developed but expensive substrates with cofactor regeneration systems are needed (Figure 3.3.6B).²¹³

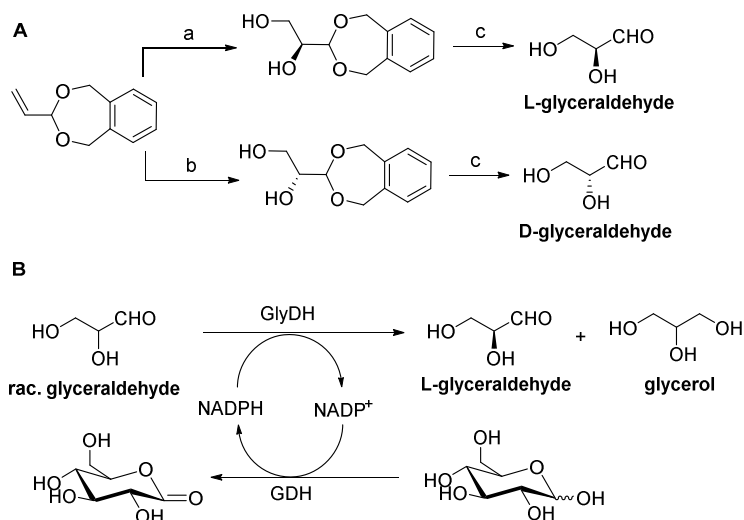


Figure 3.3.6 **A** Chemical synthesis of D- and L-glyceraldehyde. Reagents and conditions: a) AD-mix- β , *t*BuOH:H₂O, 1:1, rt, 48 h; b) AD-mix- α , *t*BuOH:H₂O, 1:1, 25 °C, 48 h; c) Pd(OH)₂, H₂ (50psi), MeOH, rt, 48 h. **B** Enzymatic synthesis of L-glyceraldehyde by kinetic resolution of *rac*-glyceraldehyde catalyzed by glycerol dehydrogenase (GlyDH, EC 1.1.1.72) and glucose 1-dehydrogenase (GDH, EC 1.1.1.119) to regenerate the cofactor.

From previous investigations in our group, we envisaged the generation of D-glyceraldehyde (**2l**) by the retro aldol reaction of D-fructose catalyzed by FSA. Then, the aldehyde could be used *in situ* in the aldol addition with α -KIV (**1a**) catalyzed by KPHMT (Figure 3.3.7). To this end, FSA wild-type and the variant A129S, which was reported to have higher specific activity, were used as catalysts for the retro-aldol reaction of D-fructose.²¹⁴ The reactions were followed by HPLC.

Results and discussion

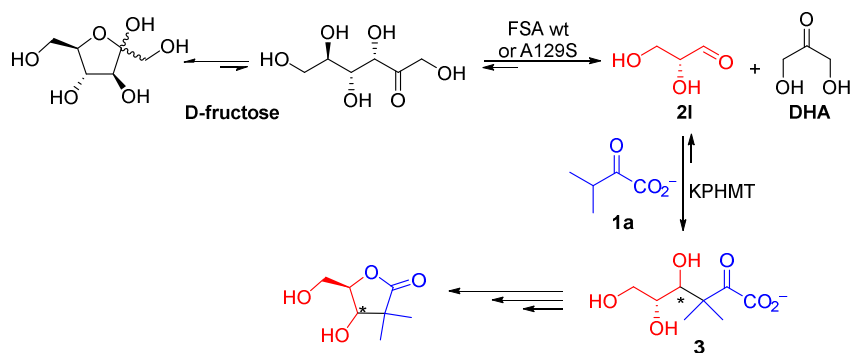


Figure 3.3.7 Generation of D-glyceraldehyde *in situ* by using FSA wild-type or A129S.

The initial conditions (50 mM of α -KIV and 2 eq of D-fructose) fail to give positive results. Thus, these were modified with the aim to increase the concentration of D-glyceraldehyde in the reaction. For example, we tried to heat the D-fructose at 80 °C for 10 minutes to enhance the proportion of its opened form, which is actually the substrate for FSA. We also increased the excess of D-fructose (10 to 50 eq) to shift the equilibrium towards the retroaldolysis reaction. Finally, we repeated the previous experiments using D-fructose-6-phosphate, which would generate D-glyceraldehyde-3-phosphate. These modifications did not give positive results either indicating that the concentration of the aldehyde released by FSA catalysis might be insufficient to allow KPHMT catalysis.

As this coupled enzymatic approach was unfruitful, we envisaged the synthesis of α,α -disubstituted- α -hydroxy aldehydes as D-glyceraldehyde analogues, thus bearing tetrasubstituted carbon atom at C2.

3.3.4 Synthesis of α,α -disubstituted- α -hydroxy aldehydes

One paradigmatic example of nucleoside that can be obtained using α,α -disubstituted- α -hydroxy aldehydes is Islatravir. As explained in the introduction (Section 1.7.3), several chemical and enzymatic approaches have been reported in recent years to achieve its total synthesis.^{158, 159, 163} We

envisaged the use of aldolases to furnish the furanose scaffold of Islatravir and other analogues using aldehydes with a tetrasubstituted α -carbon.

One strategy to prepare D-glyceraldehyde analogues was using dihydroxyacetone (DHA) as starting material. Its carbonyl group was directly transformed into a tertiary alcohol through a Grignard reaction and the corresponding product oxidized rendering the desired aldehyde (Figure 3.3.8). Deceivingly, after the Grignard reaction, the putative **C12a**, a new spot detected by TLC, was not possible to be extracted from the aqueous phase probably due to its high hydrophilicity. Different strategies such as continuous flow extraction or crystallization were attempted but resulted to be unfruitful. On the other hand, **C12b**, which was presumed to be more hydrophobic, was obtained but in unpractical low yields (5%).

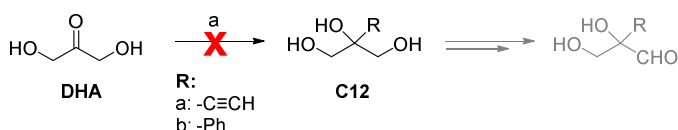


Figure 3.3.8 General approach for the synthesis of α,α -disubstituted- α -hydroxy aldehydes using DHA as starting material. Reagents and conditions: a) RMgBr (3.5 eq), THF, $-78\text{ }^\circ\text{C}$ to rt, overnight.

Examination of the literature reports revealed that alkylation on the carbonyl group of DHA was more feasible when one or both hydroxyl groups of the ketone are protected.^{215, 216} Therefore, we envisaged the synthesis of a *O*-protected DHA following an approach previously reported in the literature (Figure 3.3.9).²¹⁷ We used DHA dimer (**C13a**) as starting material that was protected at the acetal position with triethyl orthoformate in ethanol rendering **C13b** as a pure white solid by crystallization in hexane.

The primary hydroxyl groups of **C13b** were protected as benzyl ethers following a previously reported procedure.²¹⁸ The product **C13c** was crystallized in EtOH and was obtained as a stereoisomeric mixture (90% yield,

Results and discussion

58:49 *cis:trans*). Finally, dioxane **C13c** was deprotected under acidic conditions giving the benzyloxy hydroxypropanone **C13d**. Crystallization of the product was attempted but this was not successful in our hands.²¹⁸ Alternatively, **C13d** was purified by silica gel chromatography in good yields (60%, 52% isolated yield over three steps).

The ketone **C13d** was subjected to alkylation with two different commercial Grignard reagents (PhMgBr, MeMgBr), but the reactions failed rendering a complex mixture of products that were not identified.

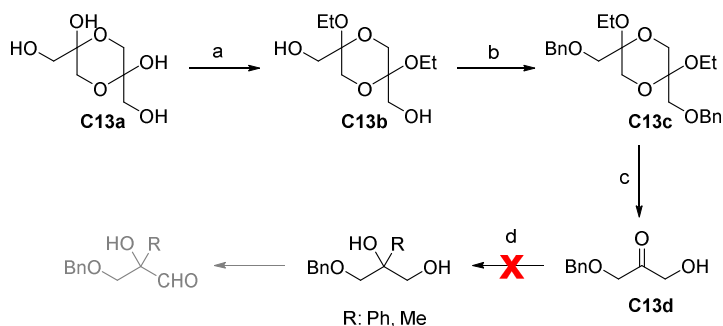


Figure 3.3.9 General approach for the synthesis of O-protected DHA, precursor of α,α -disubstituted- α -hydroxy aldehydes. Reagents and conditions: a) triethyl orthoformate, EtOH, H₂SO₄, 4 °C, 96 h (DHA dimer added every 12 h over 3 days), 97% ; b) NaH, BnBr, DMF, rt, overnight, 90%; c) H₂SO₄/THF 8 M (1:1, v/v), 4 °C, 1 h, 60%; d) RMgBr (3 eq), THF, -78 °C, 2 h.

Hence, inspired in reports found in the literature, we envision the synthesis of a DHA equivalent obtained as a cyclic ketal (Figure 3.3.10).^{219, 220} Benzaldehyde dimethyl acetal (**C14a**) and Tris-HCl were used as starting materials, which were readily converted to **C14b** by transketalization. Then, periodate oxidation of **C14b** rendered the corresponding 1,3-dioxane-5-one (**C14c**) which can undergo alkylation. Unfortunately, the Grignard reaction did not give good results obtaining a complex mixture of products.

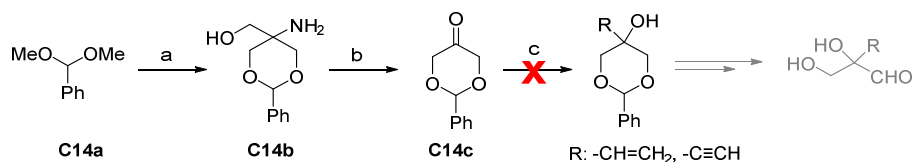
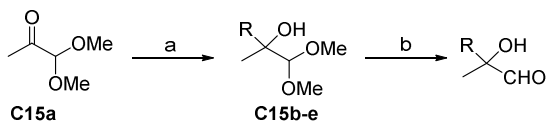


Figure 3.3.10 Second general approach for the synthesis of deprotected DHA, precursor of α,α -disubstituted- α -hydroxy aldehydes. Reagents and conditions: a) Tris-HCl, TsOH, DMF, rt, overnight, 61%; b) KH_2PO_4 , NaIO_4 , H_2O , 5 °C, 5 h, 97%; c) RMgBr (1.5 eq), THF, -78 °C to rt, overnight.

Given the difficulty of performing the Grignard reaction over DHA derivatives, the alkylation of pyruvic aldehyde dimethylacetal (**C15a**) followed by deprotection of the acetal was planned as an alternative. Through this methodology, the synthesis of four different acetal intermediates (**C15b–e**) was accomplished but its deprotection resulted to be challenging. For each compound, several settings such as different solvent systems ($\text{Et}_2\text{O}/\text{H}_2\text{O}$ or $\text{THF}/\text{H}_2\text{O}$, 1:1, v/v) and various acid conditions (HCl and H_2SO_4 , from 1 to 6 M) were tested. Finally, solvent system composed by $\text{Et}_2\text{O}/\text{HCl}$ 1 M, 1:1 was useful to render the aldehyde **2n** with an overall yield of 63% (Table 3.3.3).

Results and discussion

Table 3.3.3 Synthesis of α,α -disubstituted- α -hydroxy aldehydes using pyruvic aldehyde dimethyl acetal as starting material. Reagents and conditions: a) RMgBr (1.5 eq) or ArBr (1.5 eq) and *n*BuLi, THF, -78 °C to rt, overnight; b) For **2n**: Et₂O/HCl 1 M, 1:1 (v/v), rt, overnight.

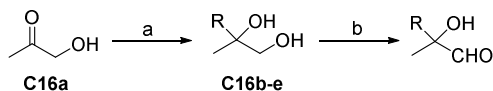


R	Reaction a ^a	Reaction b ^a	Aldehyde
	79	80	2n
	63	- ^b	
	96	- ^b	
	26	- ^b	
	- ^b		

^aIsolated yields (%). ^bNo reaction.

With the aim to avoid the acetal deprotection step, we planned the synthesis of analogues of **2n** using hydroxyacetone (HA) as starting material. The fact that direct nucleophile addition to the carbonyl group of HA was reported in the literature²²¹ and that the oxidation of the primary hydroxyl group was achieved for the aldehyde **2m** encouraged us to follow this approach. Thus, the synthesis of aldehydes **2o–q** was accomplished with good to moderate isolated yields (11–56% overall yields) (Table 3.3.4).

Table 3.3.4 Synthesis of α,α -disubstituted- α -hydroxy aldehydes using HA as starting material. Reagents and conditions: a) RMgBr (2.5 eq) or ArBr (2.5 eq) and *n*BuLi, THF, -78 °C to rt, overnight; b) NaHCO₃, TEMPO, TCC, DCM, 4 °C, 1 h.



R	Reaction a ^a	Reaction b ^a	Aldehyde
	86	65	2o
	49	22	2p
	71	75	2q
	63	- ^b	
	- ^b		
	- ^b		

^aIsolated yields (%). ^bNo reaction.

Aldehydes **2n–q** were used in DMF solution after quantification by NMR using maleic acid as internal standard. These solutions were used directly without any further purification in the enzymatic aldol reactions.

3.3.5 Enzymatic synthesis using aldehydes **2n–q** as electrophiles in aldol reactions

KPHMT wild-type and variants developed in previous chapter were screened in the aldol addition of α -KIV (**1a**) to aldehydes **2n–q**. No product formation was detected indicating that these aldehydes, were not tolerated as substrates for any KPHMT catalysts (results not shown).

Then, we screened the aldol addition of 2-oxobutanoate (**1b**) and pyruvate (**1c**) as nucleophiles to **2n–q** using MBP-YfaU wild-type and variant W23V as catalysts (Table 3.3.5). The results showed that MBP-YfaU wild-type using pyruvate (**1c**) was efficient for aldehydes **2o** and **2q** (80 and 64% of conversion respectively) but moderate for **2n** and **2p** (around 30% of conversions). Instead,

Results and discussion

when **1b** was used the only positive reaction was with **2o** (52%). The conversions achieved with MBP-YfaU W23V variant were identical.

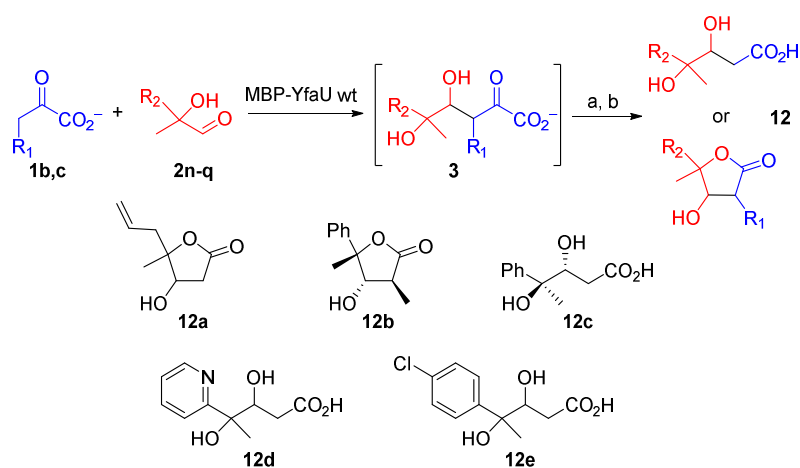
Table 3.3.5 Conversion after 24 h (%) of the aldol addition of 2-oxoacids (**1**) to aldehydes (**2n–q**) catalyzed by MBP-YfaU wild-type and W23V variant.

Nu	E			
	2n	2o	2p	2q
1b	- ^a	52	- ^a	- ^a
1c	36	80	31	64

^aProduct not detected.

The positive reactions were conducted at preparative scale. The aldol adducts were oxidatively decarboxylated and purified. This methodology rendered products **12a,c–e** in moderate isolated yields (35-62%) , whereas **12b** in 18% isolated yield (Table 3.3.6).

Table 3.3.6 MBP-YfaU wild-type catalyzed aldol addition of 2-oxoacids (**1b** and **c**) to aldehydes **2n–q**. Reagents and conditions: a) H₂O₂ (10 eq), 100 °C, 5 h, b) catalase.



Nu	E	Product	Conv ^a	Yield ^b	dr ^c
1c	2n	12a	47	35	57:43
1b	2o	12b	50	18	>95:5
1c	2o	12c	75	50	80:20
1c	2p	12d	54	46	95:5
1c	2q	12e	73	62	75:25

^aConversion (%) after 24 h of reaction. ^bIsolated Yield (%) of products. ^cDiastereomeric ratio.

Product **12b** was lactonized spontaneously after the oxidative decarboxylation and purified by silica gel chromatography. Alternatively, **12a,c–e** were purified through anion exchange chromatography. Product, **12a** was initially afforded as carboxylate, but a minor cyclic lactone was detected by NMR. The total lactonization of the product was achieved by dissolving the product in HCO₂H (1 M) and lyophilizing (this process was repeated three times). These lactone structures were not detected for products **12c–e** but their lactonization can be probably achieved repeating the same procedure several times.

The stereochemistry of **12b** was determined by NMR taking as a reference the chiral methyl group at C2, which can be safely assume that is *S* configured as it was assessed in Section 3.1.3. The analysis showed that the two other

Results and discussion

stereocenters at C3 and at C4 (i.e., the tetrasubstituted carbon atom) are also *S* configured. No other diastereomers were detected by NMR. The diastereomeric ratios of compounds **12a–e** were assessed by NMR.

3.3.6 Determination of the stereochemistry of **12c**

The experiments conducted to establish the stereochemistry of **12c** began with the synthesis of its racemic mixture. The first strategy was to prepare the aldehyde **2o** with the hydroxyl group protected in order to perform a Claisen reaction with ethyl acetate. This would be then hydrolyzed to obtain the racemic mixture of **12c** (Figure 3.3.11).

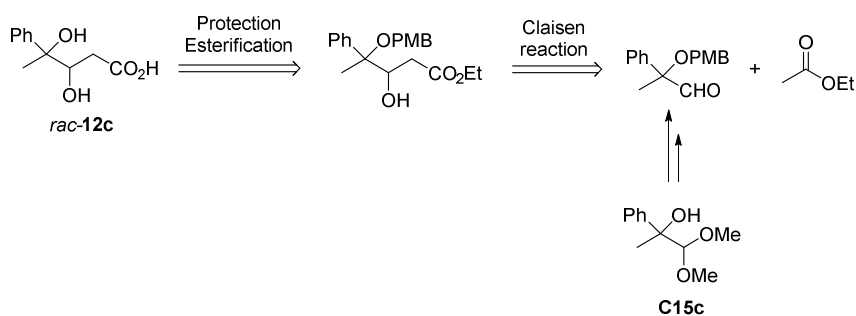


Figure 3.3.11 Retrosynthetic approach for the synthesis of the racemic mixture of **12c**.

Initially, protecting the hydroxyl group of **C15c** as benzyl ether was considered but in previous experiments the deprotection of similar compounds by hydrogenation gave undesired products. We hypothesized that molecules bearing a tertiary alcohol suffered dehydration under hydrogenation conditions (Figure 3.3.12).

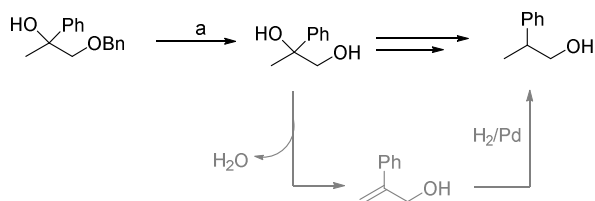


Figure 3.3.12 Proposed mechanism for the dehydration of a tertiary alcohol during hydrogenation. Reagents and conditions: a) MeOH, Pd/C, H₂, 1 atm, 1h.

For this reason, we chose *p*-methoxybenzyl (PMB) protecting group as it is useful under mild conditions and its deprotection could be easily achieved by oxidation.²²² The product **C15f** was achieved in good yields (81%) following a procedure described in the literature.^{223, 224} Then, we planned to perform a iodine-catalyzed deprotection of the acetal group of **C15f**, which was reported to be an efficient method in the presence of other sensitive protecting groups (i.e., PMB).²²⁵ After some attempts, this step was unsuccessful in our hands obtaining a complex mixture of compounds as detected by TLC (Figure 3.3.13A).

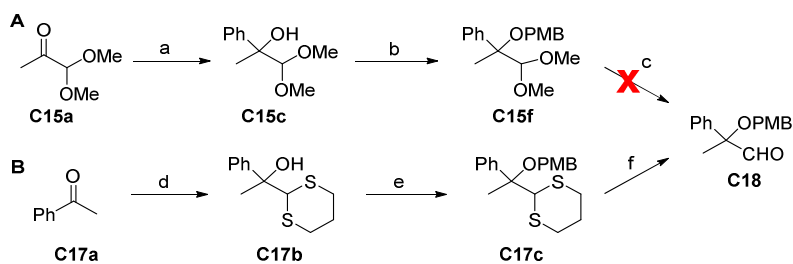


Figure 3.3.13 Approaches for the synthesis of the aldehyde **C18** through **A** the deprotection of the dimethyl acetal or **B** the deprotection of a dithiane. Reagents and conditions: a) PhMgBr, THF, -78 °C to rt, overnight, 79%; b) PMBCl, NaH, NBu₄Br, DMF, 4 °C to rt, overnight, 81%; c) I₂, ACN, 3 h; d) 1,3-dithiane, *n*-BuLi, THF, 0 °C, 5 h, 91%; e) PMBCl, NaH, Bu₄NBr, DMF, 4 °C to rt, overnight, 73%; f) NBS, ACN:H₂O (96:4, v/v), -5 °C, 1 h, 63%.

Results and discussion

As an alternative, we envisaged the synthesis of a dithiane carbonyl adduct (**C17b**), which was protected with *p*-methoxybenzyl chloride (PMBCl) (Figure 3.3.13B).^{226, 227} The dithiane deprotection step of **C17c** was accomplished by using *N*-bromosuccinimide in acetone and rendered the aldehyde **C18** in an overall isolated yield of 42%.

The aldehyde **C18** was used in a Claisen reaction with ethyl acetate, which is reported to be a good method for the synthesis of β -hydroxyesters, and **C19a** was obtained in excellent yields (96%) (Figure 3.3.14).²²⁸ The deprotection of the PMB group of **C19a** was planned by using 2,3-dichloro-5,6-dicyano-*p*-benzoquinone (DDQ), that a mildly removes the PMB group.²²² It was found that DDQ is also used for protecting diols departing from the monoprotected compound.^{229, 230} Thus, monoprotected **C19a** rendered **C19b** after treatment with DDQ. Then, **C19b** was subjected to deprotection under acidic conditions previously reported in the literature.²³¹ This procedure, however, rendered a complex mixture of products that could not be identified.

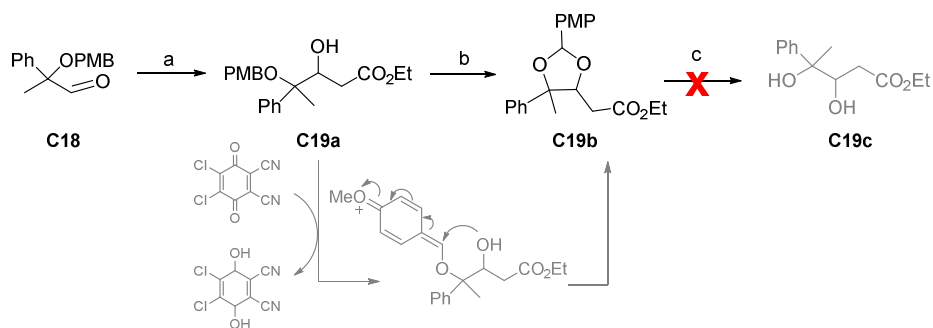


Figure 3.3.14 Attempted strategy for the obtention of **C19c** through the formation of the protected diol **C19b**. Reagents and conditions: a) EtOAc, LDA, THF, -78 °C, 3 h, 96%; b) DDQ, DCM:H₂O (9:1, v/v), rt, 1 h 30%; c) AcOH:THF:H₂O, 3:1:1 (v/v/v), rt, overnight.

Therefore, we envision another strategy that allowed us to furnish the two diastereomers of **12b** separately in order to facilitate its stereochemical characterization by NMR and chiral HPLC (Figure 3.3.15).

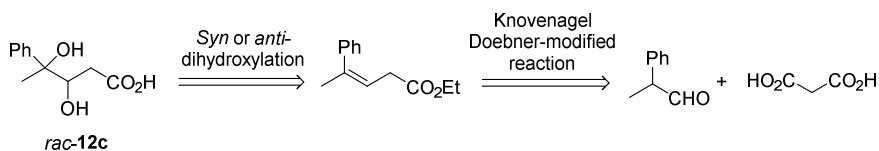


Figure 3.3.15 Retrosynthetic approach for the synthesis of the racemic mixture of **12c**.

The approach started with the synthesis of the alkene **C20b** through a Knoevenagel Doebner-modified reaction between malonic acid and 2-phenylpropanal (**C20a**), which gave the *E* isomer of the alkene.²³² Then, the product **C20b** was transformed into a methyl ester **C20c** (Figure 3.3.16).

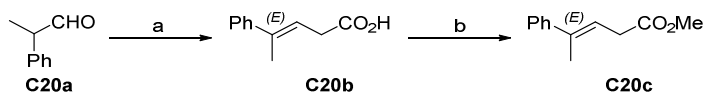


Figure 3.3.16 Synthesis of **C20c** through methylation of Knoevenagel-Doebner-adduct (**C20b**). Reagents and conditions: a) Malonic acid, Et₃N, reflux, 2 h, 87%; b) MeI, K₂CO₃, ACN, reflux, overnight, 65%.

In order to perform either *syn*- or *anti*-dihydroxylation of the *E*-alkene, compound **C20c** was subjected to two different procedures (Figure 3.3.17). For the *syn*-dihydroxylation, an approach using catalytic K₂OsO₄ and *n*-methylmorpholine *N*-oxide (NMO) as reoxidant was used.²³³ Then, the ester **C20d** was hydrolyzed under mild conditions, using LiOH as a base and a solvent system consisting in MeOH:H₂O.²³⁴ This procedure rendered the **C21a** as a racemate (3*R*,4*R* and 3*S*,4*S*) (Figure 3.3.17A).

Results and discussion

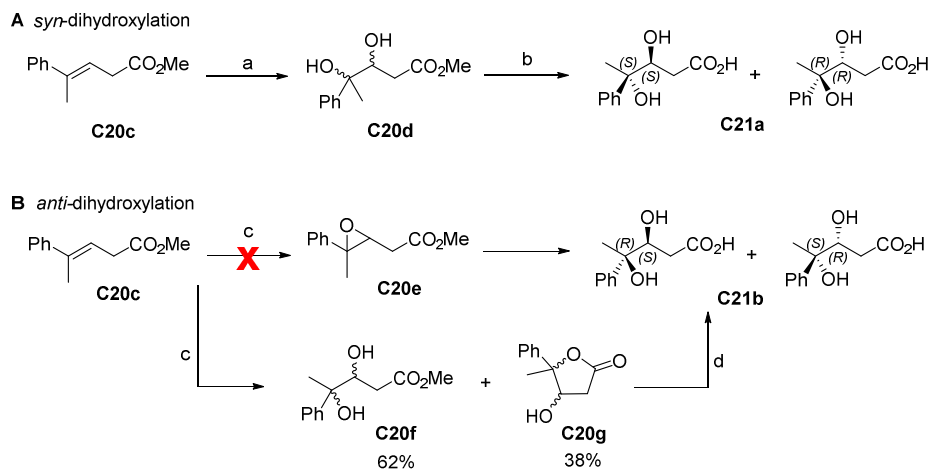


Figure 3.3.17 **A** Synthesis of **C21a** through osmium-catalyzed *syn*-dihydroxylation of the alkene **C20c** and **B** synthesis of **C21b** by *anti*-dihydroxylation of the alkene **C20c**. Reagents and conditions: a) K_2OsO_4 , NMO, citric acid, *t*BuOH:H₂O, 1:1 (v/v), rt, 3 h, 67%; b) LiOH, MeOH:H₂O, 3:1 (v/v), 5 °C, overnight, 63%; c) MCPBA, DCM, 4 °C to rt, 3 h, 53%; d) LiOH, MeOH:H₂O, 3:1 (v/v), 5 °C, overnight, 79%.

For the *anti*-dihydroxylation, we started with the formation of the epoxy **C20e** from **C20c** using 4-chloroperoxybenzoic acid (MCPBA) following a published procedure with some modifications (Figure 3.3.17B).²³⁵ Unexpectedly, the resulting main product was a mixture of the dihydroxylated compound (**C20f**, 62%) and the lactone (**C20g**, 38%). The isolation of the epoxy compound was in principle feasible on the light of some reported examples in which similar products are purified.^{235, 236} We reasoned that compound **C20e** was formed but underwent an epoxide-opening reaction during workup. Intramolecular transesterification through the nucleophilic attack of the alkoxide to the carbonyl group resulted in the formation of the lactone **C20g** during this reaction (Figure 3.3.18). Then, the mixture of **C20f** and **C20g** was submitted to basic hydrolysis to furnish the desired carboxylic acid **C21b** as racemate (3*R*,4*S* and 3*S*,4*R*).

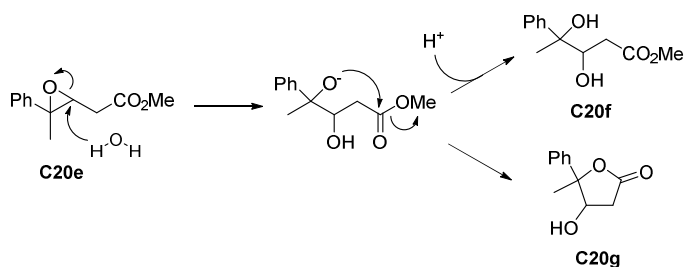


Figure 3.3.18 Proposed mechanism for the epoxide ring opening during workup.

The racemates **C21a** and **C21b** and the enzymatic product **12b** were analyzed by NMR and HPLC on chiral stationary phase. The analysis of the diastereotopic proton signals of C2 in NMR spectra determined the relative stereochemistry of **12b** (Figure 3.3.19). The major diastereomer corresponded with **C21b** and the peak integration indicated a diastereomeric ratio of 76:24.

Results and discussion

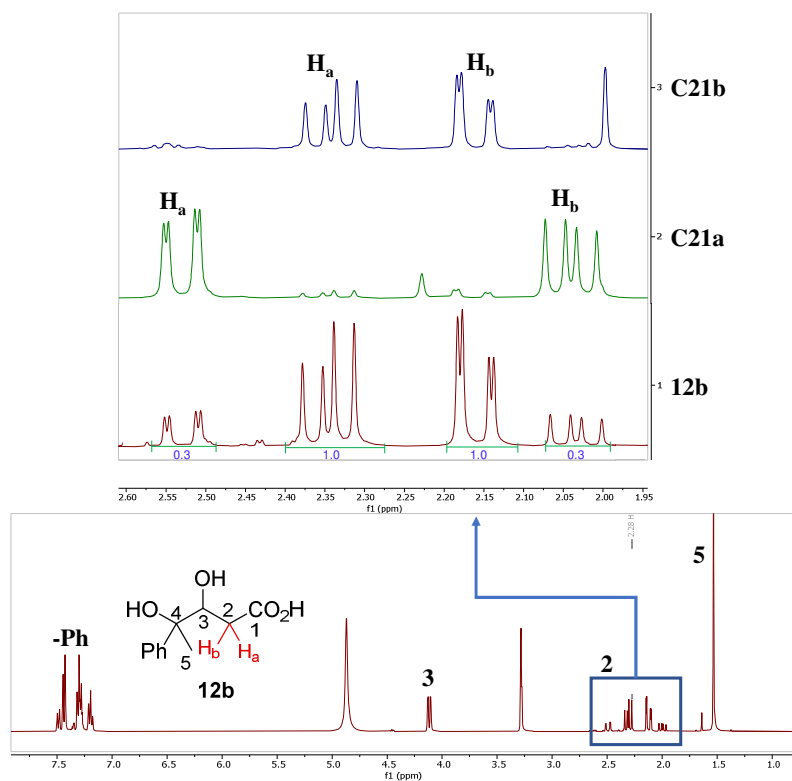


Figure 3.3.19 Determination of relative stereochemistry of compound **12b**. ¹H NMR spectra (MeOD) of **12b** and detailed comparison of the C2 proton signals with compounds **C21a** and **C21b**.

Complementary, analysis by HPLC on chiral stationary phase confirmed the results obtained by ¹H NMR and allowed the determination of the enantiomeric ratios of each diastereomer that were 70:30 and 91:9 for the major and minor ones respectively (Figure 3.3.20).

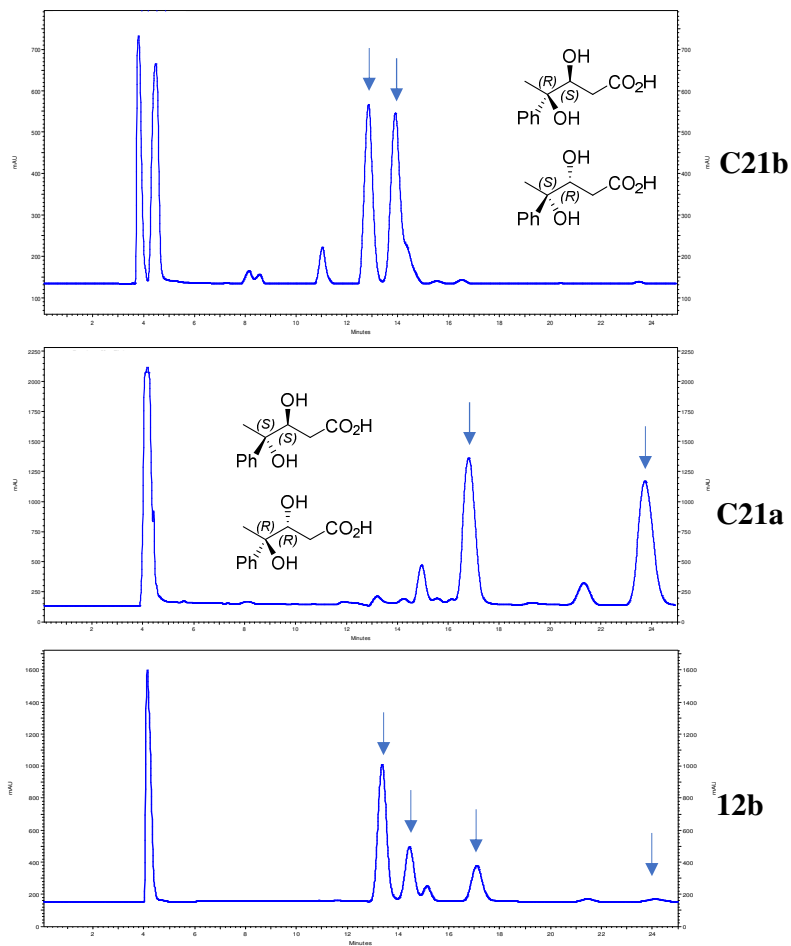


Figure 3.3.20 Chiral HPLC analysis chromatogram of compound **12b**. Isocratic elution hexane:*i*PrOH 90:10, CHIRALPACK® IC 46 x 250 mm column, 5 μm , flow rate 0.8 mL min^{-1} at 20°C and UV detection (254 nm).

The absolute stereochemistry of **12b** was determined by X-ray diffraction of the carboxylate cesium salt, which showed that the main crystals formed were 3*R*,4*S* (Figure 3.3.21).

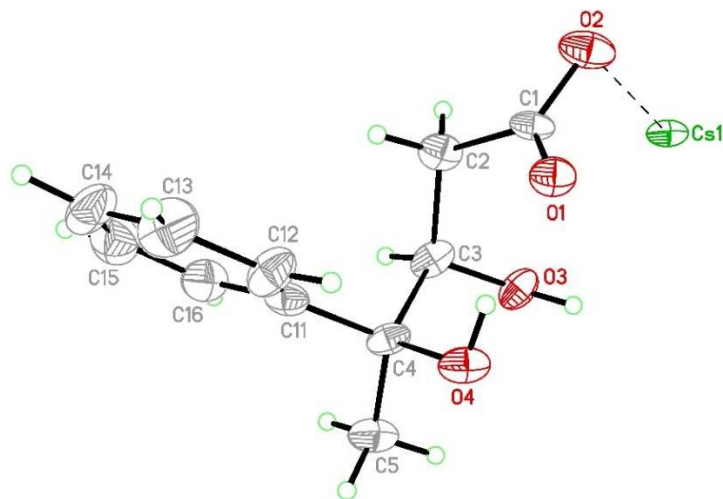


Figure 3.3.21 X-ray diffraction analysis for the determination of the absolute configuration of **12b**. ORTEP-type plot displaying ellipsoids at the 50 % probability level. The dashed line indicates a hydrogen bond.

3.3.7 Future perspectives

The future works in this topic should be focused in two aspects: biocatalyst optimization by protein engineering and the chemical substrates synthesis. From the protein engineering point of view, further variants of KPHMT or MBP-YfaU must be designed either to accept a wider variety of substrates or to enhance the stereochemistry of the aldol adducts. In fact, computational models of KPHMT complexed with substrates **1a** and *R*- and *S*-**2o** were analyzed and showed that some residues sterically hinder the access of the electrophile to the active site (Figure 3.3.22). The responsible residues are Phe229 and Ser46, which can be substituted for smaller residues such as Val, Ala or Gly respectively. Moreover, it might be considered that the Ph and Me group at the α -carbon of the aldehyde may interact with α -KIV enolate nucleophile precluding the adequate accommodation of nucleophile and electrophile for the reaction.

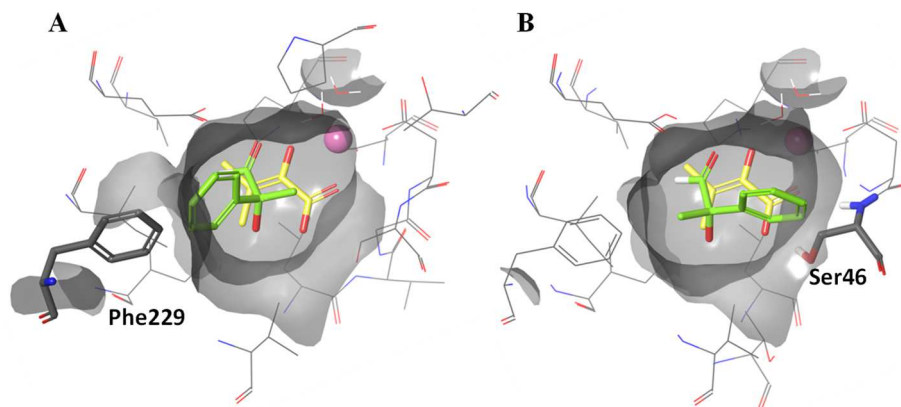


Figure 3.3.22 Model of the prereactive complex of KPHMT wild-type with **1a** (yellow) and **A R-2o** or **B S-2o** (green). The proposed residues to be mutated are highlighted. Metal cofactor (purple) and surface of the active site (grey) are shown.

Furthermore, homologous enzymes of KPHMT or YfaU from other microorganisms can be cloned and expressed to find novel activities.

From the chemistry point of view, diverse 2-oxoacids and aldehydes for the modification in C2' and C4' position respectively, would be essential to generate furanose derivatives with different functional substituents necessary for drug discovery. For instance, fluorine, cyano or ethynyl replacement at these positions have been developed obtaining promising candidates for clinical trials.^{145, 155}

Regarding the synthesis of 2-oxoacids, the methodology employed for **1k,l** in the chapter 3.1, through alkylation of a dithiane carboxylate analogue, was further exploited without obtaining positive results (Figure 3.3.23). Hence, new strategies for the synthesis of these compounds must be developed.

Results and discussion

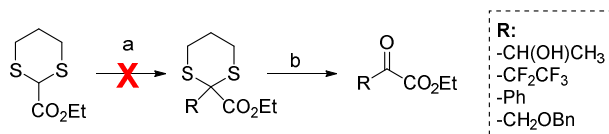


Figure 3.3.23 Attempted synthesis of 2-oxoesters through alkylation of dithiane carboxylate analogue. Reagents and conditions: a) RBr (or (CF₃CF₂CO)₂O), NaH, DMF, 4 °C to rt; b) NBS, acetone: H₂O, 94:6 (v/v), -10 °C.

In this chapter, it was demonstrated that the synthesis of aldehydes derived from D-glyceraldehyde is not trivial. The presence of multiple hydroxyl groups makes the molecule prone to suffer polymerization and requires the use of protecting groups for its manipulation. Alternatively, KPHMT or MBP-YfaU with more affinity for D-glyceraldehyde may be useful to exploit cascade reactions. Thus, FSA-catalyzed retroaldolysis of D-fructose can be effectively coupled with KPHMT or MBP-YfaU aldol addition of 2-oxoacids to D-glyceraldehyde. Another possibility will be to use D-fructose-1,6-bisphosphate aldolase (FruA, EC 4.1.2.13) catalyzed retroaldolysis of D-fructose-1,6-bisphosphate, which has been successfully used in the past to generate DHAP and D-glyceraldehyde-3P.⁶⁶

For the synthesis of α,α -disubstituted- α -hydroxy aldehydes we were inspired by the procedure developed by Huffman *et. al.*, in which alkylation with acetylide at the carbonyl group of diacetoxyacetone is performed.¹⁶³ Initially, we avoided the use of this protecting group as is incompatible with the presence of strong bases and nucleophiles²³⁷ but further research can be done with ethynyl derivatives (Figure 3.3.24). As an alternative to chemical oxidation for the primary hydroxyl group to reach the aldehyde, which gave some troubles during our investigations, biocatalytic oxidation can be done using alcohol dehydrogenases (ADH, EC 1.1.1.1). These can be evolved by directed evolution to accept bulky substrates, and the positive variants can be selected by fluorescence based high-throughput screening methods. In the example, a

cascade reaction using diaphorase (EC 1.8.1.4), leads to the formation of the red fluorescent molecule resofurin.²³⁸

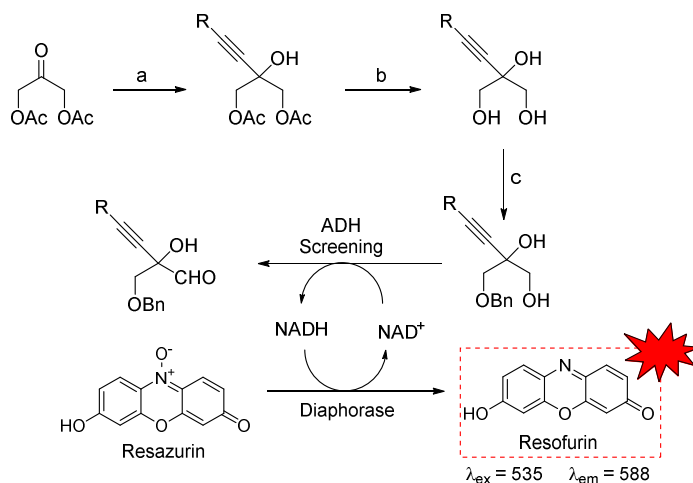


Figure 3.3.24 Proposed approach for the synthesis of α,α -disubstituted- α -hydroxy aldehydes bearing an ethynyl substituent catalyzing the final oxidation step by an ADH. Reagents and conditions: a) RMgBr or terminal alkyne and $n\text{BuLi}$, THF, $-78\text{ }^\circ\text{C}$; b) LiOH , $\text{MeOH:H}_2\text{O}$, 3:1 (v/v); c) BnBr , Bu_2SnO , Et_3N , toluene:ACN, reflux.

Another strategy that can be exploited is the one used by Guinan *et. al.*, through alkylation at the carbonyl group of an α,β -unsaturated ketone and subsequent ozonolysis (Figure 3.3.25).¹⁴¹ The main drawback of this approach is that R group containing an alkene would not resist ozonolysis. As an advantage, this would avoid the need of oxidation or deprotection steps to reach the aldehyde, which have caused troubles in previous experiments in this chapter.

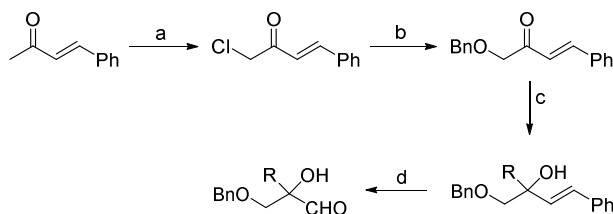


Figure 3.3.25 Synthesis of aldehydes with a tertiary alcohol through alkylation of α,β -unsaturated ketone and further ozonolysis. Reagents and conditions: a) BTMAICl_2 ,

Results and discussion

THF, rt; b) BnOH, NaH, DMF, rt; c) RMgBr, THF, $-78\text{ }^{\circ}\text{C}$; d) O_3 , DCM, Me_2S , $-78\text{ }^{\circ}\text{C}$.

Moreover, the stereochemical outcome of the enzymatic products needs to be determined. In this chapter, many efforts have been done for the synthesis of the authentic samples of compound **12c**, which demonstrate that the chemical synthesis of furanose analogues is an arduous process. We envisage that the strategy used can be adapted and optimized for the rest of the compounds **12a,d,e**. Finally, the addition of the nucleobase in the C1' position of the furanose scaffold would lead to the nucleoside. There are several reports that accomplish this synthesis departing from a fully protected lactone precursor.¹⁵⁰

3.3.8 Summary

In the last chapter of this thesis, the capacity of KPHMT and MBP-YfaU to catalyze the synthesis of derivatives of the furanose moiety of nucleosides was exploited. By using these two aldolases, the synthesis of nine precursors of the furanose scaffold (**11a–d** and **12a–e**) with different substituents at C2 and C4 positions were achieved.

Compounds **11a–d** were obtained by the aldol addition of different 2-oxoacids (**1**) to (*R*)-3-(benzyloxy)-2-hydroxypropanal (**2m**) catalyzed by KPHMT wild-type and variants (best conversions between 50–85%). The decarboxylation of the aldol adducts, which were in the hemiketal form, was performed under tough conditions at reflux and adding 10 eq of hydrogen peroxide. This reaction led to the spontaneous lactonization of the products yielding **11a–d** (40–56% isolated yields).

The use of α,α -disubstituted- α -hydroxy aldehydes, which were only accepted by MBP-YfaU catalyst, yielded compounds **12a–e**. In particular, the aldol addition of pyruvate (**1c**) to these aldehydes followed by decarboxylation and purification by anion exchange chromatography yielded **12a,c–e** as carboxylic acids (35–62% of isolated yield). Only compound **12a** showed a partially lactonized minor product detected by NMR. Thus, the compound was

redissolved in formic acid and lyophilized repeatedly to completely achieve the lactonized product. Product **12b** lactonized spontaneously after the decarboxylation and was purified by silica gel chromatography (18% of isolated yield).

The determination of the stereochemistry of products **11a–d** and **12b** was performed by NMR taking as a reference the chiral center of defined absolute configuration. The stereochemical characterization of **12c** was achieved by synthesizing the racemic mixture of both diastereomers, which were analyzed by NMR and chiral HPLC, and by X-ray diffraction on the crystalized product.

The chemical synthesis of the authentic samples of **12c** resulted in a laborious process that needed multiple steps and the optimization of different purification techniques. This demonstrated the efficacy of our enzymatic methodology to furnish the desired compounds.

4 CONCLUSIONS

In this thesis, the metal-dependent 2-oxoacid aldolases KPHMT and MBP-YfaU were applied as biocatalysts for the synthesis of chiral building blocks. The most remarkable conclusions for each objective previously described in chapter 2 are highlighted in this section:

4.1 KPHMT and MBP-YfaU were efficient enantiocomplementary biocatalysts for the chemoenzymatic synthesis of Roche ester derivatives.

- The procedure for cloning, expression, and purification of KPHMT from *E. coli* resulted efficient for its obtention in excellent yields (170 mg protein L⁻¹ medium culture) as soluble glycerinated protein. Its characterization determined that Co²⁺ was the best divalent metal cofactor, that residue E181 plays an important role in the catalysis and that formaldehyde was accepted as substrate even at high concentrations (0.1–1 M).
- Two different procedures were developed for the synthesis of 2-oxoacids in good yields (39–75%). The screening of the aldol addition to formaldehyde determined that wild-type MBP-YfaU and KPHMT accepted 2-oxoacids with short aliphatic chains as substrates.
- Structure-guided site directed mutagenesis was useful to furnish variants of KPHMT (the bests were I202A and I212A) with higher substrate tolerance towards larger nucleophiles. Variants of MBP-YfaU that were available in our laboratory (the most efficient one was W23V) permitted the accommodation of the largest 2-oxoacids.
- The aldol addition of 2-oxoacids to formaldehyde catalyzed by the developed variants of both catalysts furnished aldol adducts that were oxidative decarboxylated and esterified. This approach rendered (*S*) and (*R*)-Roche ester derivatives in good yields (57–88%) and ee (88–99%).

4.2 KPHMT wild-type and variants were useful biocatalysts for the construction of molecules bearing quaternary carbon stereocenters

- The approach developed in the previous chapter was also useful for the synthesis of 3,3-disubstituted-2-oxoacids (26–65 % isolated yields).

Conclusions

- The design of new variants of KPHMT based on molecular models was effective for the accommodation of tertiary carbon nucleophiles and the selected aldehydes in the active site.
- Different methodologies on the aldol adducts rendered 3-hydroxy acid derivatives, 2-oxolactones and ulosonic acid type products. The enantiomeric excesses of the products were dependent on the nature of the electrophiles: chiral α -hydroxyaldehydes yielded enantiopure products while achiral aldehydes gave racemic products or with moderate ee.

4.3 KPHMT and MBP-YfaU were suitable biocatalysts for the synthesis of lactones and carboxylic acids, which can be used as precursors of nucleoside analogues.

- The synthesis of (*R*)-3-(benzyloxy)-2-hydroxypropanal was achieved in good yields (73% over three steps). α,α -Disubstituted- α -hydroxyaldehydes were synthesized transforming the carbonyl group of hydroxyacetone and pyruvic aldehyde dimethylacetal into a tertiary alcohol through Grignard reaction, and rendered the aldehydes in lower yields (11–63%).
- KPHMT accepted (*R*)-3-(benzyloxy)-2-hydroxypropanal as electrophile. Contrary, α,α -disubstituted- α -hydroxyaldehydes, with a congested tetrasubstituted carbon atom, were not used as substrates by this biocatalyst. As an alternative, MBP-YfaU wild-type efficiently catalyzed the aldol addition using these aldehydes.
- Decarboxylation of the aldol adducts rendered six lactones (18–56% isolated yields) and three carboxylic acids (46–62% isolated yields). Diastereomeric ratios were determined by NMR. The synthesis of authentic samples of **12c** (dr 80:20) allowed the determination of enantiomeric ratios of each diastereomer (70:30 and 91:9 for the major and minor ones respectively).

5 EXPERIMENTAL SECTION

5.1 Biological materials

Synthetic oligonucleotides were purchased from Eurofins Genomics. Antibiotics, isopropyl- β -D-1-thiogalactoside (IPTG) and 3-morpholinopropane-1-sulfonic acid (MOPS) were from Carl Roth. Culture media components for *E. coli* were from Pronadisa (Madrid, Spain). Molecular biology reagents were from Thermo Scientific. High-density IDA-Agarose 6BCL nickel charged was from GE Healthcare Life Science.

5.1.1 Microorganisms

Two types of bacterial strains were used in this work for the molecular biology experiments: *E. coli* Nova Blue and *E. coli* M15. Their most relevant characteristics are shown in Table 5.1.

Table 5.1 Bacterial strains and their most relevant characteristics used in this study.

Strains	Relevant genotype	Ref./Origin
<i>E. coli</i> Nova Blue (used for plasmid preparation)	<i>endA1</i> , <i>hsdR17</i> (rB ⁺ , mB ⁺), <i>supE44</i> , <i>thi1</i> , <i>recA1</i> , <i>gyrA96</i> , <i>relA1</i> , <i>lac</i> F' [proA ⁺ B ⁺ , <i>lacI</i> ^q Z Δ M15::Tn10] (<i>Tet</i> ^R).	Qiagen
<i>E. coli</i> M15 [pREP4] (used for protein expression)	<i>nal</i> ^s , <i>str</i> ^s , <i>rif</i> ^s , <i>thi</i> ⁻ , <i>lac</i> ⁻ , <i>ara</i> ⁺ , <i>gal</i> ⁺ , <i>mtl</i> ⁻ , F ⁻ , <i>recA</i> ⁺ , <i>uvr</i> ⁺ , <i>lon</i> ⁺ .	Novagen

5.1.2 Vectors

The plasmids vectors used in this study and their construction and most important characteristics are listed in Table 5.2. The plasmid pQE60*panB* containing the gene for expression of KPHMT was constructed in our lab using routine procedures of molecular biology.

Experimental section

Table 5.2 Plasmid vectors used in this study and their construction.

Plasmids	Relevant genetic characteristics	Ref./Origin
pQE60	Bacterial vector for high-level expression and purification of C-terminally 6xHis-tagged proteins	Qiagen
pQE60 <i>panB</i> ^a	<i>panB</i> gene (795 bp) from <i>E. coli</i> K-12 (NCBI data base accession number NC_000913.3) cloned in pQE60 (NcoI and BglII)	This thesis
pQE60 <i>panB</i> E181Q	Plasmid pQE60 <i>panB</i> as template (Gibson assembly)	This thesis
pQE60 <i>panB</i> L42A	Plasmid pQE60 <i>panB</i> as template (QuickChange site-directed mutagenesis)	This thesis
pQE60 <i>panB</i> I212A	<i>panB</i> gene as template (megaprimer site-directed mutagenesis)	This thesis
pQE60 <i>panB</i> L42A/ I212A	<i>panB</i> L42A gene as template (megaprimer site-directed mutagenesis)	This thesis
pQE60 <i>panB</i> I202A	<i>panB</i> gene as template (megaprimer site-directed mutagenesis)	This thesis
pQE60 <i>panB</i> V214G	<i>panB</i> gene as template (megaprimer site-directed mutagenesis)	This thesis
pQE60 <i>panB</i> I202A/ V214G	<i>panB</i> I202A gene as template (megaprimer site-directed mutagenesis)	This thesis
pQE60 <i>panB</i> I212A/ V214G	<i>panB</i> gene as template (megaprimer site-directed mutagenesis)	This thesis
pQE60 <i>panB</i> I202A/ I212A/ V214G	<i>panB</i> I202A gene as template (megaprimer site-directed mutagenesis)	This thesis
pQE60 <i>panB</i> I202A/ I212A	<i>panB</i> I212A gene as template (megaprimer site-directed mutagenesis)	This thesis
pQE40 <i>malE</i> ^b - <i>rmhA</i> ^c		91
pQE40 <i>malE</i> - <i>rmhA</i> W23V		92
pQE40 <i>malE</i> - <i>rmhA</i> W23V/ L216A		92
pQE40 <i>fsa</i> ^d A129G		239

^a*panB* gene codes for 3-methyl-2-oxobutanoate hydroxymethyltransferase (KPHMT, EC 2.1.2.11). ^b*malE* gene codes for maltose binding protein (MBP). This version of the gene does not encode a signal sequence, so fusion protein remains in the cytosol. ^c*rmhA*

gene codes for 2-keto-3-deoxy-L-rhamnonate aldolase (YfaU, EC 4.1.2.53). *4fsaA* gene codes for fructose-6-phosphate aldolase 1 (FSA A EC 4.1.2.13).

5.1.3 Oligonucleotides

The oligonucleotides specifically designed for this study are listed in Table 5.3, with the mutated codons highlighted in bold and italics.

Table 5.3 Sequences of oligonucleotides used in this study in site-directed mutagenesis.

Oligonucleotides	Sequences (5'→3')
E181Q	GAA(E) →CAR(Q) Forward: GCCTTAGAAGCTGCTGGGGCACAGCTGCTGGTGCTG <i>CA</i> <i>RT</i> GC GTGCCGTTGAACTGG Reverse: GTGCCCCAGCAGCTTCTAAGGC
A1	Forward: GAATTCATTAAGAGGAGAAATTAACCATGGACATGAA ACCGACCACC
A2	Reverse: GGTTAATTTCTCCTCTTTAATGAATTCTGTGTG
B1	Forward: GCTTAATTAGCTGAGCTTGGACTCC
B2	Reverse: GGAGTCCAAGCTCAGCTAATTAAGCTTAGTGATGGTGA TGGTGATGAGATCTATGG
L42A	CGT(L)→GCG(A) Forward: ACGTCATG <i>GCG</i> GTGGGCGATTTCGCTGGG Reverse: ATCGCCAC <i>CGC</i> CATGACGTTAAGCCCTTC
I212A	ATC(I)→GCG(A) Forward: CTGACGGGCAG <i>GCG</i> CTCGTGATGCAC
I202A	ATT(I)→GCG(A) Forward: ATCCCGTTATTGG <i>CGC</i> GGGCGCAGGCA
V214G	GTG(V)→GGC(G) Forward: GGGCAGATCCT <i>CGC</i> CATGCACGACGCCTTT
I212A/V214G	ATC(I)→GCG(A) and GTG(V)→GGC(G) Forward: GACGGGCAG <i>GCG</i> CT <i>CGC</i> CATGCACGACGCCTTT
F1	Forward: ATGAAACCGACCACC
F2	Forward: ATCGATTAACCATGGACATGAAACCGACCACC
R	Forward: GCAGGTACAAGATCTATGGAAACTGTGTTC

5.1.4 Culture media and solutions

The culture media and solutions used in this work were prepared with ultrapure distilled water and were sterilized by autoclaving during 30 minutes at 121 °C. The thermolabile components (e.g. antibiotics), and concentrated microelement solutions were sterilized by filtration with 0.22 µm filters.

Luria-Bertani (LB) medium: LB medium is a rich medium that is used extensively in recombinant DNA work to culture *E. coli*. Its composition: Tryptone (10 g L⁻¹), yeast extract (5 g L⁻¹) and NaCl (10 g L⁻¹). To use this medium in solid form (in plates), 1.5% agar was added. In most cases LB medium was complemented with antibiotics necessary for maintaining the plasmid selection. Antibiotics added to LB were ampicillin (100 µg mL⁻¹) and kanamycin (25 µg mL⁻¹).

5.2 Molecular biology techniques

5.2.1 Isolation and purification of plasmid DNA (Miniprep)

A plasmid preparation is a method used to extract and purify plasmid DNA on a small scale from *E. coli* cultures. All methods are based on three steps: growth of the bacterial culture, harvesting and lysis of the bacteria and purification of the plasmid DNA. In this study a commercial kit from Roche – Applied Sciences was used, following the protocol provided by the manufacturer.

The kit relies on alkaline lysis to release plasmid DNA from bacteria. RNase removes all RNA in the lysate. Then, cellular debris and genomic DNA are removed by centrifugation. Under the buffer conditions used in the procedure, the plasmid binds to the glass fiber fleece, while contaminating substances (salts, proteins, and other cellular contaminants) do not. Brief wash-and-spin steps readily remove these contaminants. Once purified, the plasmid can be easily eluted in a small volume of water.

5.2.2 Agarose gel electrophoresis of DNA

Agarose gel electrophoresis was used for the separation and visualization of the plasmids or PCR products. The electrophoresis takes place on a horizontally submerged agarose gel (analytical grade, Roche – Applied sciences) with the adequate concentration for the DNA size. The gels were run using the Wide Mini-Sub Cell GT System from Bio-Rad. The gel was prepared with dissolving agarose (1%) in TAE 1X buffer (Tris-base 40 mM, acetic acid 20 mM, EDTA 1 mM, pH 8.1), and 5 μ L SYBR-Safe DNA stain (Invitrogen) was added before casting. The samples were prepared with 1:5 volume equivalent of DNA loading dye 6X (Fermentas) and were loaded into the gel. To facilitate the identification of DNA by the size a DNA ladder (GeneRuler DNA ladder mix, Fermentas) was also applied. For the separation a constant 5-10 V cm^{-1} voltage is applied, and the gel is run until the front reaches until approx. 50% of the gel. When the electrophoresis is finished, the DNA is visualized by fluorescence under ultraviolet light (302 nm) in a transilluminator (TFX-20.M, Ecogen).

5.2.3 Quantification of nucleic acids

The measurements to determine the DNA concentration were realized with a SpectroStar Nano, BMG Labtech. The absorbance values are converted to concentration, with respect to a standard value of $A_{260}=1$ what is generally accepted as 50 $\mu\text{g mL}^{-1}$ double-stranded DNA. With each measurement the absorbance at 260 nm is compared to other absorbance at 280 nm and 230 nm to establish the purity of each sample. When the ratio A_{260}/A_{280} is lower than 1.8, indicates contamination of protein in the sample, and if the ratio A_{260}/A_{230} is higher than 2, the sample is contaminated with RNA.

5.2.4 Mutagenesis techniques

5.2.4.1 QuickChange

The *panB* gene mutation L42A was introduced with the QuickChange site-directed mutagenesis strategy using the plasmid pQE60 *panB* as template and performed according to the manufacturer's protocols (QuickChange®,

Experimental section

Stratagene; QuikChange® Site-Directed Mutagenesis Kit. Instruction manual Catalog #200518 and #200519 Revision A. *Stratagene. p 1-20*), with some modifications in PCR procedure (Table 5.4). Chemically competent *E. coli* Nova Blue strain cells (Merckmillipore) were transformed with DNA preparation (without any purification step). The plasmid DNA was isolated with the GeneJET Plasmid Miniprep Kit (Thermo Scientific) and the expected mutations were confirmed by DNA sequencing.

Table 5.4 QuickChange site-directed mutagenesis PCR protocol.

Components	V/ μ L	Final concentration (50 μ L volume)	PCR cycles		
			Step	Temp / $^{\circ}$ C	Time/ min
Water, nuclease free	35.5		Initial denaturation	98	3
5X Green Buffer ^a	10			35 PCR cycles	98
dNTP mix (10 mM each)	1	0.2 mM each	55		1
Forward primer (125 ng μ L ⁻¹)	1	2.5 ng μ L ⁻¹	72		12
Reverse primer (125 ng μ L ⁻¹)	1	2.5 ng μ L ⁻¹	Final extension		72
Template DNA (10 ng μ L ⁻¹)	1	0.2 ng μ L ⁻¹		4	hold
DNA Polymerase (2 U μ L ⁻¹) ^b	0.5	0.02 U μ L ⁻¹			

^a5X Phusion Green HF Buffer (Thermo Scientific). ^bPhusion Green High-Fidelity DNA Polymerase (Thermo Scientific).

5.2.4.2 Megaprimer site-directed mutagenesis

The *panB* gene mutations I212A, I202A, V214G and double and triple variants were introduced with the Megaprimer site-directed mutagenesis strategies with PCR procedure described in (Table 5.5).

Table 5.5 Megaprimer site-directed mutagenesis PCR protocol.**a) PCR 1**

Components	V/ μ L	Final concentration (50 μ L volume)	PCR cycles		
			Step	Temp/ $^{\circ}$ C	Time/sec
Water, nuclease free	35.5				
5X Green Buffer ^a	10		Initial denaturation	98	30
dNTP mix (10 mM each)	1	0.2 mM each	35 PCR cycles	98	10
F1, forward primer (25 μ M)	1	0.5 μ M		55	10
R, reverse primer (25 μ M)	1	0.5 μ M		72	16
Template DNA (1 ng μ L ⁻¹)	1	0.02 ng μ L ⁻¹	Final extension	72	5 min
DNA Polymerase (2 U μ L ⁻¹) ^b	0.5	0.02 U μ L ⁻¹		4	hold

b) PCR 2

Components	V/ μ L	Final concentration (50 μ L volume)	PCR cycles		
			Step	Temp/ $^{\circ}$ C	Time/sec
Water, nuclease free	35.5				
5X Green Buffer ^a	10		Initial denaturation	98	30
dNTP mix (10 mM each)	1	0.2 mM each	35 PCR cycles	98	10
M, mutagenic primer (25 μ M)	1	0.5 μ M		55	10
R, reverse primer (25 μ M)	1	0.5 μ M		72	16
Template DNA (1 ng μ L ⁻¹)	1	0.02 ng μ L ⁻¹	Final extension	72	5 min
DNA Polymerase (2 U μ L ⁻¹) ^b	0.5	0.02 U μ L ⁻¹		4	hold

Experimental section

c) PCR 3

Components	V/ μ L	Final concentration (50 μ L volume)	PCR cycles		
			Step	Temp / $^{\circ}$ C	Time/ sec
Water, nuclease free	Up to 50		Initial denaturation	98	30
5X Green Buffer ^a	10			35 PCR cycles	98
dNTP mix (10 mM each)	1	0.2 mM each	55		10
F2, forward primer (25 μ M)	1	0.5 μ M	72		16
Megaprimer (product of PCR2)	- ^b	Up to 0.5 μ M	Final extension	72	5 min
Template DNA (18 pg μ L ⁻¹)	1	0.36 pg μ L ⁻¹		4	hold
DNA Polymerase (2 U μ L ⁻¹) ^c	0.5	0.02 U μ L ⁻¹			

^a5X Phusion Green HF Buffer (Thermo Scientific). ^bThe concentration of Megaprimer depends on the efficiency of the PCR2. Megaprimer size: 173 bp (I212A) and 207 bp (I202A). ^cPhusion Green High-Fidelity DNA Polymerase (Thermo Scientific).

Product of PCR3 and pQE60 were digested with FastDigest NcoI and BglII (Thermo Scientific) and fragments were purified from agarose gel according to the manufacturer's protocol (Thermo Scientific, GeneJET Gel Extraction and DNA Cleanup Micro Kit, instruction manual Catalog #K0831 and #K0832). Ligation of DNA fragments was performed using T4 DNA Ligase (Thermo Scientific) according to the manufacturer's protocol. Chemically competent *E. coli* Nova Blue (Merckmillipore) strain cells were transformed with ligation reaction. The plasmid DNA was isolated with the GeneJET Plasmid Miniprep Kit (Thermo Scientific) and the expected mutations in the gene sequence were confirmed by DNA sequencing.

5.2.4.3 Gibson assembly

The *panB* gene mutation E181Q was introduced by site-directed mutagenesis. Six different primers were used to generate three overlapping fragments that were assembled using NEBuilder® HiFi DNA Assembly Master Mix (New England Biolabs). The PCR procedures are described in Table 5.6.

Table 5.6 DNA assembly-based mutagenesis PCR protocol.**a) PCR 1:** Amplification of fragment 1

Components	V/ μ L	Final concentration (50 μ L volume)	PCR cycles			
			Step	Temp/ $^{\circ}$ C	Time/sec	
Water, nuclease free	36.5		Initial denaturation	98	3 min	
5X Green Buffer ^a	10			35 PCR cycles	98	10
dNTP mix (10 mM each)	1	0.2 mM each			70	15
A1, forward primer (25 μ M)	0.5	0.5 μ M	72		16	
Mutagenic reverse primer (25 μ M)	0.5	0.5 μ M	Final extension	72	10 min	
Template DNA (1 ng μ L ⁻¹)	1	0.02 ng μ L ⁻¹		4	hold	
DNA Polymerase (2 U μ L ⁻¹) ^b	0.5	0.02 U μ L ⁻¹				

b) PCR 2: Amplification of fragment 2

Components	V/ μ L	Final concentration (50 μ L volume)	PCR cycles			
			Step	Temp/ $^{\circ}$ C	Time/sec	
Water, nuclease free	36.5		Initial denaturation	98	3 min	
5X Green Buffer ^a	10			35 PCR cycles	98	10
dNTP mix (10 mM each)	1	0.2 mM each			70	15
Mutagenic forward primer (25 μ M)	0.5	0.5 μ M	72		16	
B2 reverse primer (25 μ M)	0.5	0.5 μ M	Final extension	72	10 min	
Template DNA (1 ng μ L ⁻¹)	1	0.02 ng μ L ⁻¹		4	hold	
DNA Polymerase (2 U μ L ⁻¹) ^b	0.5	0.02 U μ L ⁻¹				

Experimental section

c) *PCR 3*: Amplification of plasmid

Components	V/ μ L	Final concentration (50 μ L volume)	PCR cycles		
			Step	Temp/ $^{\circ}$ C	Time/sec
Water, nuclease free	36.5		Initial denaturation	98	3 min
5X Green Buffer ^a	10				
dNTP mix (10 mM each)	1	0.2 mM each	35 PCR cycles	98	10
B1 forward primer (25 μ M)	0.5	0.5 μ M		64	15
A2 reverse primer (25 μ M)	0.5	0.5 μ M		72	2 min
Template DNA (1 ng μ L ⁻¹)	1	0.02 ng μ L ⁻¹	Final extension	72	10 min
DNA Polymerase (2 U μ L ⁻¹) ^b	0.5	0.02 U μ L ⁻¹		4	hold

^a5X Phusion Green HF Buffer (Thermo Scientific). ^bPhusion Green High-Fidelity DNA Polymerase (Thermo Scientific).

PCR products were digested DpnI (Thermo Scientific) (see procedure below) and fragments were purified from agarose gel according to the manufacturer's protocol (Thermo Scientific, GeneJET Gel Extraction and DNA Cleanup Micro Kit, instruction manual Catalog #K0831 and #K0832). Overlapping fragments were assembled using NEBuilder® HiFi DNA Assembly Master Mix (New England Biolabs). Chemically competent *E. coli* Nova Blue (Merckmillipore) strain cells were transformed with assembling reaction. The plasmid DNA was isolated with the GeneJET Plasmid Miniprep Kit (Thermo Scientific) and the expected mutations in the gene sequence were confirmed by DNA sequencing.

5.2.4.4 DpnI digestion of the amplification product

To eliminate the parental plasmids (non-mutated plasmid) 1 μ L of *DpnI* restriction enzyme (10 U μ L⁻¹, Fermentas) was added to the reaction mixture, and was incubated at 37 $^{\circ}$ C for 4 hours.

5.2.5 Heat shock transformation of the competent cells

For plasmid transformation 10-50 ng DNA was added to 100 μL of competent cells, mixing it gently with circular motion and then incubated on ice for 5 minutes. Then the heat shock was applied for 30 seconds at 42 $^{\circ}\text{C}$ followed by incubation of 2 minutes on ice again. Finally, 800 μL LB was added and incubated at 37 $^{\circ}\text{C}$, 250 rpm for 45 minutes, and plated on LB agar plate, and finally incubated overnight at 37 $^{\circ}\text{C}$. In all cases at least 20 colonies/plate grew. From these, 3-10 colonies were selected, and their plasmid was extracted. To verify the presence of the mutations the DNA was analyzed by DNA sequencing by the DNA Sequencing Service of CRAG.

5.2.6 Analysis of the DNA sequences

The analyses of the DNA sequences were performed using various computer programs. To visualize and analyze the obtained chromatograms the software Chromas (Technelysium Pty Ltd) was used. The sequences with high homology were identified using the Basic Local Alignment Search Tool (BLAST).²⁴⁰ To translate the DNA sequence, and find the open reading frames SnapGene®Viewer was used. The protein sequence BLAST searches were realized on line using the database and web page of the SIB Bioinformatics Resource Portal (Swiss Institute of Bioinformatics), from the Proteomic Service ExPASy (<http://www.expasy.org/>). The alignment of the protein sequences was carried out using the program ClustalW, offered online also by the ExPASy service.

5.3 KPHMT expression and purification

Competent *E. coli* M-15[pREP-4] strain cells from QIAGEN, were transformed with plasmid pQE60 *panB* and grown in LB medium with ampicillin (100 $\mu\text{g mL}^{-1}$) and kanamycin (25 $\mu\text{g mL}^{-1}$) at 37 $^{\circ}\text{C}$, on a rotary shaker at 200 rpm. A final optical density at 600 nm (OD600) of 3–4 was usually achieved. An aliquot of the pre-culture (20 mL) was transferred into a baffled shaker flask (2 L) containing LB medium (1000 mL) plus ampicillin (100 $\mu\text{g mL}^{-1}$), kanamycin

Experimental section

(25 $\mu\text{g mL}^{-1}$) and antifoam SE-15 (0.02% v/v), and incubated at 37 °C with shaking at 200 rpm. During the middle exponential phase growth ($\text{DO}_{600} \approx 0.5\text{-}0.8$), the temperature was decreased to 30 °C to minimize inclusion bodies formation and then, isopropyl- β -D-1-thiogalactopyranoside (IPTG; 1 mM final concentration) was added. After 12-16 h, cells from the induced-culture broths (5 L, 20-25 g of cells) were centrifuged (2500 g for 45 min at 4 °C). The pellet was re-suspended in starting buffer (400 mL) consisting of 50 mM sodium phosphate buffer pH 8.0, containing NaCl (300 mM), imidazole (10 mM) and glycerol (10%). Cells were lysed using a cell disrupter (Constant Systems) and cellular debris were removed by centrifugation at 35 000 g for 45 min at 4 °C. The clear supernatant was applied to a cooled HR 16/40 column (GE Healthcare) packed with Ni SepharoseTM High Performance (50 mL bed volume, GE Healthcare) and washed with starting buffer (400 mL) at 3 mL min^{-1} . The protein was eluted with gradient from 10 mM to 500 mM of imidazole at 5 mL min^{-1} . Fractions containing the recombinant protein were pooled and dialyzed against 20 mM MOPS buffer pH 7.0 containing NaCl (50 mM) and glycerol (50%) at 4 °C (3x1 L 24 h each). The dialyzed solution obtained (60-100 mL) was stored at - 20 °C. Protein concentration was determined using Pierce® 660 nm Protein Assay Reagent (Thermo Scientific) in 96 wells plate according to the manufacturer's protocols. The glycerol in dialysis buffer minimizes protein precipitation after purification.

5.3.1 Protein electrophoresis (SDS-PAGE)

The protein electrophoresis (SDS-PAGE) was carried out with denatured proteins in the presence of sodium dodecyl sulphate (SDS) according to the method described by Laemmli.²⁴¹ During this study 12% acrylamide/bis-acrylamide separator gel conditions were used.

For staining the SDS-PAGE and the visualization of the proteins Coomassie brilliant blue dye was used, which binds to the aromatic and basic residues of the protein, permitting the visualization and coloration of the protein with a detection limit of 30-100 ng, depending on the protocol.²⁴² The staining took

place in 3 steps i) Fixation: once the electrophoresis is finished, the gel was removed from the cast and incubated during 2 minutes in a solution of 45% methanol and 9% acetic acid, ii) Staining: The prestaining solution was discarded and the gel was submerged in dying solution (40% methanol, 7% acetic acid and 0.25% Coomassie Brilliant Blue (Bio-Rad)) and warmed in a microwave oven for 30 seconds, iii) Destaining: the staining solution was removed and the gel was left in the destaining solution (5% MeOH, 7.5% acetic acid) and warmed in the microwave oven for 30 seconds, and left for a couple of hours with slight mixing. The solution was changed until the coloration was saturated. Finally, the gels were scanned and analyzed.

5.3.2 Electrospray mass spectrometry of proteins

Glycerinated proteins were diluted in water/formic acid (0.1% v/v) (1 mg protein mL⁻¹, final concentration in the solution) and glycerol and salts were removed with PD MiniTrap G-10 of (GE Healthcare). The samples were eluted in water/formic acid (0.1% v/v, 0.5 mL) and injected (5 µL) to an Acquity UPLC BEH C4, 1.7 µm, 2.1 x 50 mm column connected to a mass spectrometer ESI-TOF instrument (LCT PremierWaters, Milford, MA, USA), equipped with a 4 GHz time-to-digital converter (TDC) with a dual ESI source (LockSpray). The second sprayer provided the lock mass calibration with leucine enkephalin (m/z 556.2771). The ESI-TOF was operated in the W-optics mode, thus providing a mass resolution of at least 10 000 full width at half maximum (FWHM). The acquisition time per spectrum was set to 0.2 s, and the mass range was from 500 to 1800 Da. Data were acquired using a cone voltage of 50 V, capillary voltage of 3000 V, desolvation temperature of 35 °C, and source temperature of 100 °C. The desolvation gas flow was set at 400 L h⁻¹ and the cone gas flow was set at 30 L h⁻¹. The solvent system used for the elution was: solvent (A): 0.1% formic acid in CH₃CN/H₂O (70/30, v/v) and solvent (B): 0,1% (v/v) formic acid in H₂O, gradient elution from 28% A to 100% A in 25 min, 100% A for 2 min and 28% A for 18 min, flow rate 0.2 mL min⁻¹. MassLynx 4.1 software (Waters. Milford, MA, USA) was used for data

Experimental section

acquisition and processing. Magtran software²⁴³, kindly provided by Dr. Zhongqi Zhang (Amgen, Inc.; Thousand Oaks, CA), was used for molecular weight deconvolution from ESI-MS spectra of proteins.

5.4 Chemical and analytical materials

Formaldehyde, dimethylformamide (DMF), 2,4'-dibromoacetophenone, benzyl bromide, 4-nitrobenzyl bromide, commercial 2-oxoacids were from Sigma-Aldrich. Other reagents were from Sigma-Aldrich. Water for analytical HPLC and for the preparation of buffers and other assay solutions was obtained from an Arium pro ultrapure water purification system (SartoriusStedim Biotech). All other solvents used were of analytical grade.

5.5 Chemical and analytical general methods

Chromatography: Thin layer chromatography was performed using precoated silica gel plates with or without fluorescent indicator UV₂₅₄ (Macherey-Nagel GmbH & Co. KG, Kieselgel 60). Column chromatography was performed in a glass column (AFORA, 5880/2, 47x4.5) packed with silica gel (100 g, 35-70 μm , 200-500 mesh, Merck). Stains were detected on TLC plates using UV₂₅₄ fluorescence or developed with ceric ammonium molybdate (CAM) stain ($\text{Ce}(\text{SO}_4)_2$ (10 g L⁻¹) and $(\text{NH}_4)_6\text{Mo}_7\text{O}_{24}\cdot 4\text{H}_2\text{O}$ (50 g L⁻¹) in H₂SO₄ 2 M).

Specific rotation: Specific rotation values were measured with a Perkin Elmer Model 341 (Überlingen, Germany).

Melting points. Melting points were determined using a BUCHI fully automatic melting point B-545, heating rate: 0.5 °C/min between 30 °C to 150 °C.

NMR analysis. Routine, ¹H (400 MHz) and ¹³C (101 MHz) NMR spectra of compounds were recorded with a Varian Mercury-400 spectrometer. Full characterization of the described compounds was performed using typical gradient-enhanced 2D experiments: COSY and HSQC recorded under routine conditions.

HPLC analysis. HPLC analyses were performed on a RP-HPLC XBridge C18, 5 μm , 4.6 \times 250 mm column (Waters). The solvent system used was: solvent (A): 0.1% (v/v) trifluoroacetic acid (TFA) in H_2O and solvent (B): 0.095% (v/v) TFA in $\text{CH}_3\text{CN}/\text{H}_2\text{O}$ 4:1, flow rate 1 mL min^{-1} , detection at 215 nm and column temperature at 30 $^\circ\text{C}$. The amount of products and substrates were quantified from the peak areas using an external standard methodology.

HPLC monitoring of carbonyl group of compounds: Samples from the reaction mixture (10 μL) were withdrawn and diluted with plain water to adjust the concentration between the limits of linearity (i.e., from 3 to 100 mM). Then, an aliquot sample (10 μL) of the diluted solution was mixed with a solution of *O*-benzylhydroxylamine hydrochloride (50 μL of a 0.13 mM stock solution in pyridine:methanol:water 33:15:2). After incubation at 25 $^\circ\text{C}$ for 5 min, samples were diluted with methanol (500 μL), centrifuged (20 000 g, 5 min) and analyzed by HPLC.

The HPLC reaction monitoring for the synthesis of 4'-phenacylestere was carried out as follows: samples (10 μL) were withdrawn from the reaction mixture, diluted with methanol (500 μL) and after centrifugation (20 000 g, 5 min) analyzed by HPLC. Other samples were directly analyzed with HPLC. In general, samples were taken (50 μL) and diluted in methanol (450 μL). After centrifugation they were directly injected to the HPLC.

Chiral HPLC analysis. Enantiomeric excesses (ee) were determined using chiral HPLC analysis on 46 x 250 mm columns, 5 μm particle size and 254 nm or 209 nm UV detection. Column type, specific elution conditions and flow rates are described for each compound.

5.5.1 Activity assay of KPHMT

The activity of KPHMT was determined by a discontinuous assay. One unit of activity was defined as the amount of KPHMT, which catalyzes the formation of 1 μmol of aldol adduct per min at 25 $^\circ\text{C}$ in 20 mM MOPS buffer pH 7.0, containing 1 mM of the bivalent metal cofactor. The assay procedure was as follows: To an equimolar solution mixture of 2-oxoacids and formaldehyde

Experimental section

(150 μL of a 133 mM solution in 20 mM MOPS pH 7.0 containing MCl_2 (1.3 mM)), a solution of the enzyme (50 μL , of stock solution between 10.7–0.17 mg protein mL^{-1} in 20 mM MOPS buffer pH 7.0) was added. The total reaction volume was 0.2 mL. Reaction monitoring was as follows: at 30 min, samples (10 μL) were analyzed by HPLC as described above.

5.5.2 Determination of the initial reaction rates

Reaction time course of aldol addition of 2-oxoacids to aldehydes catalyzed by wild-type MBP-YfaU or KPHMT and variants thereof was determined as follows: To a solution of enzyme (4 mg protein mL^{-1} in the reaction), plain water and the oxoacid (0.05 mmol, 1 eq, 0.1 M in the reaction) were added. NiCl_2 (1.3 μL of a 0.1 M stock solution, 0.25 mM in the reaction) or CoCl_2 (3 μL of a 0.1 M stock solution, 0.6 mM in the reaction) were added. The reaction was started by adding the aldehyde (0.05 mmol, 1 eq, 0.1 M in the reaction). The total reaction volume was 0.5 mL. The reaction was monitored by HPLC as described above every 10 min during the first hour, then every hour during 6 h and finally at 24 h.

The initial reaction rates were calculated at the beginning of the reaction (i.e. samples taken every 10 min during the first hour keeping reaction conversions <10%) to ensure a linear dependence of the product formation versus time. The product formed for the screening was calculated at 24 h. Concentrations of the aldol products were calculated with an external standard method from peak areas.

5.5.3 Determination of the effect of formaldehyde on the conversion of the aldol addition.

The effect of the concentration of formaldehyde in the aldol addition catalyzed by KPHMT or by MBP-YfaU was determined by measuring the conversion of the aldol addition at 24 h with different concentration of substrates (0.1, 0.2, 0.4, 0.8 and 1 M). The reaction conditions were the same as the ones explained for the activity assay.

5.5.4 2-Oxoacid stock solution preparation

Aqueous stock solutions of 2-oxoacids (1 M) at pH 7 were prepared adjusting the pH to 7.0 with NaOH (1 M) and stored at 4 °C. Under these conditions some of the compounds precipitated as sodium salts. Prior to utilization in aldol additions, they were carefully re-dissolved by gently warming up with a heat gun until a clear solution was achieved.

5.5.5 Crystallization for X-ray structure determination

In some cases, the absolute stereochemistry was determined by X-ray diffraction. Compound **S-4i** (100 mg) was dissolved in (iPr)₂O (3 mL) and **S-4j,k** (100 mg) were dissolved in Et₂O (2 mL and 3 mL respectively). Crystals were obtained by evaporation in glass vials (6 mL, 4.5 cm, Ø 1.3 cm) after 24 h at 25 °C. Compounds **7b** and **7c** (100 mg) were dissolved in hexane:Et₂O 3:2 (v/v) (5mL). Crystals were obtained by evaporation in glass vials (6 mL, 3.5 cm, Ø 1.4 cm) after 72 h at 25 °C. Product **12b** (50 mg) was dissolved in H₂O (0.5 mL) and CsCO₃ (1 eq) was added to form the cesium salt. Water was removed by evaporation and the residue was dissolved in MeOH (12 mL). Crystals were obtained by evaporation in glass vials (20 mL, 5.7 cm, Ø 2.7 cm) after 7 days at 25 °C.

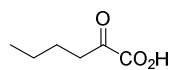
Crystals were analyzed in collaboration with Dr. Michael Bolte from Institut fuer Anorganische Chemie, Frankfurt.

5.6 Synthesis and characterization of products from section 3.1

5.6.1 Synthesis of substrates

5.6.1.1 Method A

2-oxohexanoic acid (**1e**)



Typical procedure: A dried three-necked round bottomed flask equipped with a reflux condenser was charged with magnesium (2.13 g, 87.58 mmol, 1.2 eq) under N₂ atmosphere. A small crystal of iodine was added and heated until the iodine was sublimated. After cooling down at

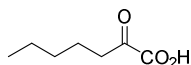
Experimental section

room temperature, a solution of 1-bromobutane (**C1e**, 10.0 g, 72.98 mmol, 1.0 eq) in THF (100 mL) was added drop-wise over the course of 30 minutes, so that the mixture was continuously boiling. The reaction was refluxed for 2 h, cooled down to room temperature and added drop-wise to a solution of diethyl oxalate (9.06 g, 62.01 mmol, 0.85 eq) in THF (50 mL) at $-78\text{ }^{\circ}\text{C}$. After 4 h, the reaction was quenched by the addition in a saturated ammonium chloride solution (400 mL) and extracted with Et₂O (3 x 200 mL). The organic phases were combined, washed with brine (100 ml) dried over anhydrous magnesium sulfate, filtered and the solvent removed in vacuo. The product was loaded onto a silica column chromatography and was eluted with a step gradient of hexane:Et₂O: 100:0, 200 mL, 98:2, 400 mL, 95:5, 500 mL and 90:10, 500 mL. Pure fractions were pooled and the solvent removed in vacuo affording the 2-oxoester intermediate (**C2e**) as a yellow oil (8.75 g, 89%). The spectral properties of this product agreed with those reported in the literature.²⁴⁴ ¹H NMR (400 MHz, CDCl₃) δ 4.29 (q, J = 2x7.2, 7.1 Hz, 2H), 2.80 (t, J = 2x7.3 Hz, 2H), 1.59 (p, J = 2x7.6, 2x7.5 Hz, 2H), 1.41 – 1.26 (m, 5H), 0.90 (t, J = 2x7.4 Hz, 3H). ¹³C NMR (101 MHz, CDCl₃) δ 194.8, 161.3, 62.3, 38.9, 25.0, 22.1, 14.0, 13.7.

The 2-oxoester intermediate (**C2e**, 8.75 g, 55.31 mmol) was dissolved in 2-methyltetrahydrofuran (2-MeTHF, 55 mL). Then, 1.0 M sodium phosphate buffer pH 7.0 (32 mL) and Novozym 435 (0.64 g, 20 mg mL⁻¹ final concentration in aqueous phase) were added. The reaction, in a closed vessel (250 mL), was conducted at 25 °C and orbital shaker. After 24 h, the starting material was not detected on TLC. The reaction was then filtered and NaHCO₃ 5% (300 mL) was added. The mixture was washed with Et₂O (3 x 100 mL). Then, the aqueous solution was acidified at pH = 1.0 (HCl 37%) and the product was extracted with Et₂O (3 x 100 ml). The organic phases were combined, dried over anhydrous magnesium sulfate, filtered and the solvent removed *in vacuo* affording the titled compound (**1d**) as a colorless oil that crystallized as a yellow solid after overnight storage at $-20\text{ }^{\circ}\text{C}$ (6.04 g, 84%, isolated yield over two

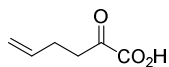
steps: 75%). This material was used without any further purification. The spectral properties of this product agreed with those reported in the literature.²⁴⁵ ¹H NMR (400 MHz, CDCl₃) δ 2.93 (t, *J* = 2x7.3 Hz, 2H), 1.63 (p, *J* = 2x7.5, 2x7.4 Hz, 2H), 1.36 (dq, *J* = 14.6, 2x7.4, 7.2 Hz, 2H), 0.92 (t, *J* = 2x7.4 Hz, 3H). ¹³C NMR (101 MHz, CDCl₃) δ 196.0, 159.3, 36.9, 25.1, 22.0, 13.7.

2-oxoheptanoic acid (**1f**)



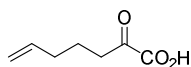
The titled compound (**1f**) was obtained as a colorless oil that crystallized as a yellow solid after overnight storage at – 20 °C (8.45 g, 80%, isolated yield over two steps: 74%) was prepared following the procedure described for (**1d**). The spectral properties of this product agreed with those reported in the literature.²⁴⁶ ¹H NMR (400 MHz, CDCl₃) δ 2.90 (t, *J* = 2x7.3 Hz, 2H), 1.64 (p, *J* = 2x7.2, 2x7.1 Hz, 2H), 1.37 – 1.24 (m, 4H), 0.88 (t, *J* = 2x6.8 Hz, 3H). ¹³C NMR (101 MHz, CDCl₃) δ 195.9, 159.9, 37.4, 31.0, 22.7, 22.2, 13.8.

2-oxohex-5-enoic acid (**1g**)



The titled compound (**1g**) was obtained as a colorless oil that crystallized as a yellow solid after overnight storage at – 20 °C (5.37 g, 73%, isolated yield over two steps: 67%) was prepared following the procedure described for (**1e**). The spectral properties of this product agreed with those reported in the literature.²⁴⁷ ¹H NMR (400 MHz, CDCl₃) δ 5.79 (ddt, *J* = 16.8, 10.2, 2x6.5 Hz, 1H), 5.13 – 4.96 (m, 2H), 3.04 (t, *J* = 2x7.2 Hz, 2H), 2.4 (qt, *J* = 3x7.2, 2x1.4 Hz, 2H). ¹³C NMR (101 MHz, CDCl₃) δ 195.1, 159.4, 135.5, 116.3, 36.5, 26.9.

2-oxohept-6-enoic acid (**1h**)

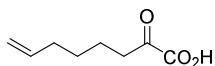


The titled compound (**1h**) was obtained as a colorless oil that crystallized as yellow solid after overnight storage at – 20 °C (6.06 g, 89%, isolated yield over two steps: 75%) was prepared following the procedure described for (**1e**). ¹H NMR (400 MHz, CDCl₃) δ 5.73 (ddt, *J* = 16.9, 10.2, 2x6.7 Hz, 1H), 5.07 – 4.95 (m, 2H), 2.94 (t, *J* = 2x7.2 Hz, 2H), 2.10 (q, *J*

Experimental section

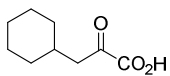
= 3x7.1 Hz, 2H), 1.76 (p, $J = 2 \times 7.3$, 2×7.2 Hz, 2H). ^{13}C NMR (101 MHz, CDCl_3) δ 195.8, 159.3, 137.1, 116.0, 36.4, 32.7, 22.2.

2-oxooct-7-enoic acid (**1i**)



The titled compound (**1i**) was obtained as a colorless oil that crystallized as a yellow solid after overnight storage at $-20\text{ }^\circ\text{C}$ (5.58 g, 87%, isolated yield over two steps: 69%) was prepared following the procedure described for (**1e**). ^1H NMR (400 MHz, CDCl_3) δ 5.76 (ddt, $J = 16.9$, 10.2 , 2×6.7 Hz, 1H), 5.05 – 4.89 (m, 2H), 2.93 (t, $J = 2 \times 7.2$ Hz, 2H), 2.06 (q, $J = 2 \times 7.1$, 6.9 Hz, 2H), 1.66 (p, $J = 4 \times 7.3$ Hz, 2H), 1.43 (p, $J = 2 \times 7.5$, 2×7.3 Hz, 2H). ^{13}C NMR (101 MHz, CDCl_3) δ 195.6, 159.8, 138.0, 115.0, 37.2, 33.2, 28.0, 22.4.

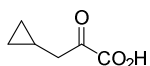
3-cyclohexyl-2-oxopropanoic acid (**1m**)



The titled compound (**1m**) was obtained as a white solid (8.80 g, 74%, isolated yield over two steps: 67%) was prepared following the procedure described for (**1e**). The spectral properties of this product agreed with those reported in the literature.²⁴⁸ ^1H NMR (400 MHz, CDCl_3) δ 2.80 (d, $J = 6.8$ Hz, 2H), 1.90 (dtt, $J = 14.8$, 2×7.0 , 3.4 , 3.4 Hz, 1H), 1.74 – 1.59 (m, 5H), 1.38 – 1.21 (m, 2H), 1.20 – 1.07 (m, 1H), 1.06 – 0.92 (m, 2H). ^{13}C NMR (101 MHz, CDCl_3) δ 195.7, 159.3, 44.3, 33.7, 33.0, 25.9, 25.9.

5.6.1.2 Method B

3-cyclopropyl-2-oxopropanoic acid (**1k**)

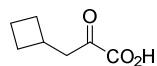


Typical procedure: A three-necked round bottomed flask was charged with toluene (100 mL) and NaH (1.54 g, 38.58 mmol, 1.2 eq, 60% dispersion in mineral oil) was added under N_2 atmosphere. A solution of (bromomethyl)cyclopropane (**C1k**, 4.34 g, 32.15 mmol, 1.0 eq) and ethyl 1,3-dithiane-2-carboxylate (6.18 g, 32.15 mmol, 1.0 eq) in DMF (100 mL) was added drop-wise over the course of 30 min at $4\text{ }^\circ\text{C}$. The mixture was stirred 1h and at room temperature overnight. The reaction was quenched by the

addition of NaH_2PO_4 5% solution (100 mL) and the organic phase was separated, washed with water (3 x 100 mL), NaHCO_3 5% (3 x 100 mL) and brine (3 x 100 mL). Finally, the organic phase was dried over anhydrous magnesium sulfate and filtered. The filtrate was concentrated *in vacuo* to give colorless viscous oil, which was not characterized. In the next reaction step, the crude product was dissolved in acetone (50 ml) and was added dropwise to a solution of *N*-bromosuccinimide (45.77 g, 257.16 mmol, 8 eq) in acetone:water 94:6 v/v (100 mL) mixture and stirred at -10 °C. The solution quickly turned red (bromine) but soon faded to yellow-orange. The reaction was stirred for 10 min and quenched with a saturated sodium sulfite solution (200 mL). The mixture was extracted with Et_2O (3 x 100 mL), then the organic phases were combined, washed with NaHCO_3 5% (3 x 100 mL), brine (3 x 100 mL), dried over anhydrous magnesium sulfate, filtered and the solvent removed *in vacuo* to give a colorless viscous oil that was not characterized. In the last reaction step, the crude material was dissolved in 2-methyltetrahydrofuran (2-MeTHF, 32 mL). Then, 1.0 M sodium phosphate buffer pH 7.0 (32 mL) and, Novozym 435 (0.64 g, 20 mg mL^{-1} final concentration in aqueous phase) were added. The reaction, in a closed vessel (250 mL), was conducted at 25 °C and orbital shaker. After 24 h, the starting material was not detected on TLC and the reaction was filtered and NaHCO_3 5% (300 mL) was added. The mixture was washed with Et_2O (3x100 mL). Then, the aqueous solution was acidified at pH = 1.0 (HCl 37%) and the product was extracted with Et_2O (3x100 mL). The organic phases were combined, dried over anhydrous magnesium sulfate, filtered and the solvent removed *in vacuo* affording the titled compound (**1k**) as a yellow oil that crystallized as a yellow solid after overnight storage at -20 °C (1.59 g, isolated yield over three steps: 39%). This material was used without any further purification. ^1H NMR (400 MHz, CDCl_3) δ 2.82 (d, $J = 6.9$ Hz, 2H), 1.13 – 0.97 (m, 1H), 0.60 (dt, $J = 8.0, 2 \times 6.0$ Hz, 2H), 0.18 (dt, $J = 6.2, 2 \times 4.8$ Hz, 2H). ^{13}C NMR (101 MHz, CDCl_3) δ 195.3, 159.6, 42.1, 5.3, 4.4.

Experimental section

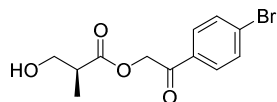
3-cyclobutyl-2-oxopropanoic acid (**1l**)



The titled compound (**1l**) was obtained as a colorless oil that crystallized as a yellow solid after overnight storage at $-20\text{ }^{\circ}\text{C}$ (2.50 g, isolated yield over three steps: 70%) was prepared following the procedure described for (**1k**). ^1H NMR (400 MHz, CDCl_3) δ 3.04 (d, $J = 7.2$ Hz, 2H), 2.73 (hept, $J = 6 \times 7.7$ Hz, 1H), 2.21 – 2.09 (m, 2H), 1.88 (tddd, $J = 2 \times 14.7, 11.7, 9.2, 6.4$ Hz, 2H), 1.69 (pd, $J = 9.2, 3 \times 9.0, 2.4$ Hz, 2H). ^{13}C NMR (101 MHz, CDCl_3) δ 195.1, 159.2, 43.8, 30.8, 28.3, 18.8.

5.6.2 Enzymatic synthesis of phenacyl ester derivatives

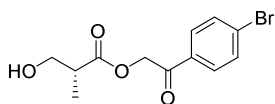
2-(4-bromophenyl)-2-oxoethyl (S)-3-hydroxy-2-methylpropanoate (**S-4a**)



Typical procedure: Reaction (2 mL total volume) was conducted at room temperature in a round-bottom flask (100 mL) with magnetic stirring (250 rpm). MBP-YfaU wild-type (16 mg of lyophilized powder, 4 mg protein mL^{-1} in the reaction, 0.005 mol%) was dissolved in a solution of sodium 2-oxobutanoate (**1a**, 1 mL of a 2 M stock solution pH 7.0, 2 mmol, 1 eq, 1 M in the reaction). Plain water (0.85 mL) and NiCl_2 (5 μL of a 0.1 M stock solution, 0.25 mM in the reaction) were added. The reaction was started by adding formaldehyde (**2**, 0.15 mL of a 13.3 M commercial solution, 2 mmol, 1 eq, 1 M in the reaction). The reaction was monitored by HPLC and after 4 h hydrogen peroxide (1.14 mL of a 8.8 M commercial solution, 10 mmol, 5 eq) was added. When the 2-oxoacid (**S-3a**) was not detected by HPLC, catalase from bovine liver (50 mg) dissolved in 1 mL of 10 mM sodium phosphate buffer, pH 7.0 was added. The reaction mixture was diluted with methanol (20 mL), filtered through Celite[®] and the pellet was washed with methanol (3x50 mL). Glycerol (2-3 mL) was added to solubilize the sodium salt residue once the solvent was removed under vacuum. Then, the mixture was diluted with DMF (10 mL) and 2,4'-dibromoacetophenone (556 mg, 2 mmol, 1 eq) was added. EtOAc (200 mL) was added to the reaction mixture and washed with H_2O (3x50 mL). The

combined organic phases were dried over anhyd MgSO_4 , absorbed onto silica gel (100 mL) and loaded onto a silica gel column. Product was eluted with a step gradient of hexane:EtOAc: 100:0, 200 mL, 90:10, 200 mL, 80:20, 200 mL, 70:30, 200 mL, 60:40, 200mL and 50:50, 600 mL. Pure fractions were pooled and the solvent removed in vacuo affording *S*-**4a** as a white solid (482 mg, 80%). $[\alpha]_D^{20} = +19.0$ ($c = 1$ in MeOH). Chiral HPLC analysis: CHIRALCELL[®] OD, isocratic elution hexane/isopropanol 80/20 (v/v), flow rate 0.7 mL min⁻¹, t_r (*S*) = 16.0, t_r (*R*) = 17.55, 98% *ee*.

2-(4-bromophenyl)-2-oxoethyl (*R*)-3-hydroxy-2-methylpropanoate (*R*-**4a**)

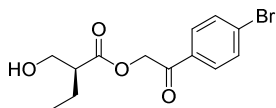


Typical procedure: Reaction (2 mL total volume) was conducted at room temperature in a round-bottom flask (100 mL) with magnetic stirring (250 rpm). To a solution of KPHMT wild-type (0.75 mL of a 10 mg mL⁻¹ stock glycerinated protein solution, 4 mg mL⁻¹ in the reaction, 0.005 mol%), sodium 2-oxobutanoate (**1a**, 0.8 mL of a 1 M stock solution pH 7.0, 0.8 mmol, 1 eq, 0.4 M in the reaction) was added. Plain water (0.37 mL) and CoCl_2 (12 μL of a 0.1 M stock solution, 0.6 mM in the reaction) were added. The reaction was started by adding formaldehyde (**2a**, 60 μL of a 13.3 M commercial solution, 0.8 mmol, 1 eq, 0.4 M in the reaction). The reaction was monitored by HPLC and after 6 h hydrogen peroxide (0.5 mL of a 8.8 M commercial solution, 4 mmol, 5 eq) was added. When the 2-oxo acid (*R*-**3a**) was not detected by HPLC, catalase from bovine liver (50 mg) dissolved in 1 mL of 10 mM sodium phosphate buffer, pH 7.0 was added. The reaction mixture was diluted with methanol (20 mL), filtered through Celite[®] and the pellet was washed with methanol (3x50 mL). The solvent was removed under vacuum. Synthesis of 4'-phenacyl ester was performed as described for *S*-**4a**. The product was obtained as a white solid (214 mg, 88%). $[\alpha]_D^{20} = -18.5$ ($c = 1$ in MeOH). Chiral HPLC analysis: CHIRALCELL[®] OD, isocratic elution hexane/isopropanol 80/20 (v/v), flow rate 0.7 mL min⁻¹, t_r (*S*) = 16.0, t_r (*R*) = 17.55, 95% *ee*. NMR of *S* and *R*-**4a**: ¹H NMR (400 MHz, CDCl_3) δ 7.77 (d, $J = 8.8$ Hz, 2H), 7.64 (d, $J = 8.7$ Hz, 2H),

Experimental section

5.46 (d, $J = 16.5$ Hz, 1H), 5.30 (d, $J = 16.5$ Hz, 1H), 3.86 (dd, $J = 11.4, 4.3$ Hz, 1H), 3.77 (dd, $J = 11.4, 7.4$ Hz, 1H), 2.86 (pd, $J = 7.2, 3 \times 7.1, 4.3$ Hz, 1H), 1.23 (d, $J = 7.1$ Hz, 3H). ^{13}C NMR (101 MHz, CDCl_3) δ 192.1, 174.7, 132.4, 132.3, 129.6, 129.3, 65.7, 65.3, 42.3, 13.0. ESI-TOF m/z for *S* and *R*-**4a**: Calcd for $[\text{M}+\text{Na}^+]$ $\text{C}_{12}\text{H}_{13}\text{O}_4\text{NaBr}$: 322.9895, found $[\text{M}+\text{Na}^+]$: 322.9889. Melting point: 67.3-67.9 °C.

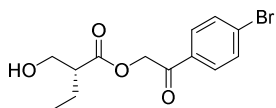
2-(4-bromophenyl)-2-oxoethyl (*S*)-2-(hydroxymethyl)butanoate (*S*-**4b**)



The title compound was prepared using MBP-YfaU W23V variant and the procedure described for *S*-**4a**.

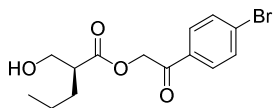
The product was obtained as a white solid (512 mg, 81%). $[\alpha]_{\text{D}}^{20} = +4.3$ ($c = 1$ in MeOH). Chiral HPLC analysis: CHIRALPAK[®] IC, isocratic elution hexane/isopropanol 80/20 (v/v), flow rate 0.7 mL min⁻¹, t_{r} (*S*) = 19.85, t_{r} (*R*) = 22.47, 99% *ee*.

2-(4-bromophenyl)-2-oxoethyl (*R*)-2-(hydroxymethyl)butanoate (*R*-**4b**)



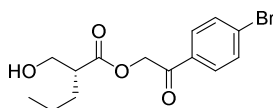
The title compound was prepared using KPHMT wild-type and the procedure described for *R*-**4a**. The product was obtained as a white solid (157 mg, 63%).

$[\alpha]_{\text{D}}^{20} = -5.2$ ($c = 1$ in MeOH). Chiral HPLC analysis isocratic elution: CHIRALPAK[®] IC, hexane/isopropanol 80/20 (v/v), flow rate 0.7 mL min⁻¹, t_{r} (*S*) = 19.85, t_{r} (*R*) = 22.47, 95% *ee*. NMR of *S* and *R*-**4b**: ^1H NMR (400 MHz, CDCl_3) δ 7.77 (d, $J = 8.7$ Hz, 2H), 7.63 (d, $J = 8.7$ Hz, 2H), 5.43 (d, $J = 16.5$ Hz, 1H), 5.34 (d, $J = 16.5$ Hz, 1H), 3.89 – 3.78 (m, 2H), 2.69 (dtd, $J = 8.0, 6.7, 6.5, 5.1$ Hz, 1H), 1.84 – 1.68 (m, 1H), 1.66 – 1.51 (m, 1H), 0.99 (t, $J = 2 \times 7.5$ Hz, 3H). ^{13}C NMR (101 MHz, CDCl_3) δ 192.1, 174.2, 132.4, 132.3, 129.6, 129.3, 65.7, 63.7, 50.0, 21.2, 11.8. ESI-TOF m/z for *S* and *R*-**4b**: Calcd for $[\text{2M}+\text{Na}^+]$ $\text{C}_{26}\text{H}_{30}\text{O}_8\text{NaBr}_2$: 651.0205, found $[\text{2M}+\text{Na}^+]$: 651.0229. Melting point: 51.3-51.7 °C.

2-(4-bromophenyl)-2-oxoethyl (S)-2-(hydroxymethyl)pentanoate (S-4c)

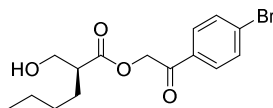
The title compound was prepared using MBP-YfaU W23V variant and the procedure described for *S*-4a.

The product was obtained as a white solid (669 mg, 68%). $[\alpha]_D^{20} = +2.8$ ($c = 2$ in MeOH). Chiral HPLC analysis: CHIRALPAK[®] IC, isocratic elution hexane/isopropanol 75/25 (v/v), flow rate 0.7 mL min⁻¹, t_r (*S*) = 16.13, t_r (*R*) = 18.81, 99% *ee*.

2-(4-bromophenyl)-2-oxoethyl (R)-2-(hydroxymethyl)pentanoate (R-4c)

The title compound was prepared using KPHMT I212A variant and the procedure described for *R*-4a.

The product was obtained as a white solid (291 mg, 60%). $[\alpha]_D^{20} = -2.9$ ($c = 2$ in MeOH). Chiral HPLC analysis: CHIRALPAK[®] IC, isocratic elution hexane/isopropanol 75/25 (v/v), flow rate 0.7 mL min⁻¹, t_r (*S*) = 16.13, t_r (*R*) = 18.81, 95% *ee*. NMR of *S* and *R*-4c: ¹H NMR (400 MHz, CDCl₃) δ 7.77 (d, $J = 8.5$ Hz, 2H), 7.63 (d, $J = 8.4$ Hz, 2H), 5.42 (d, $J = 16.5$ Hz, 1H), 5.34 (d, $J = 16.5$ Hz, 1H), 3.86 – 3.80 (m, 2H), 2.77 (dq, $J = 8.3, 6.4, 2 \times 6.1$ Hz, 1H), 1.71 (dq, $J = 13.2, 7.6, 2 \times 7.3$ Hz, 1H), 1.49 (ddt, $J = 12.9, 9.6, 2 \times 6.3$ Hz, 1H), 1.44 – 1.34 (m, 2H), 0.93 (t, $J = 2 \times 7.2$ Hz, 3H). ¹³C NMR (101 MHz, CDCl₃) δ 192.2, 174.4, 132.4, 132.3, 129.6, 129.3, 65.7, 64.0, 48.2, 30.0, 20.5, 13.9. ESI-TOF m/z for *S* and *R*-4c: Calcd for $[M+Na^+]$ C₁₄H₁₇O₄NaBr: 351.0208, found $[M+Na^+]$: 351.0159. Melting point: 38.1-38.2 °C.

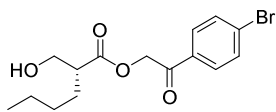
2-(4-bromophenyl)-2-oxoethyl (S)-2-(hydroxymethyl)hexanoate (S-4d)

The title compound was prepared using MBP-YfaU W23V variant and the procedure described for *S*-4a.

The product was obtained as a white solid (650 mg, 65%). $[\alpha]_D^{20} = -1.9$ ($c = 4$ in iPrOH). Chiral HPLC analysis: CHIRALPAK[®] IC, isocratic elution hexane/isopropanol 75/25 (v/v), flow rate 0.7 mL min⁻¹, t_r (*S*) = 15.93, t_r (*R*) = 19.09, 99% *ee*.

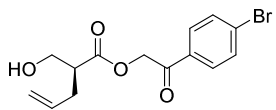
Experimental section

2-(4-bromophenyl)-2-oxoethyl (*R*)-2-(hydroxymethyl)hexanoate (*R*-4d)



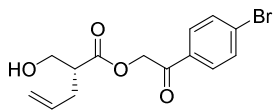
The title compound was prepared using the enzyme variant KPHMT L42A/I212A and the procedure described for *R*-4a. The product was obtained as a white solid (291 mg, 57%). $[\alpha]^{20}_{\text{D}} = +2.2$ ($c = 4$ in *i*PrOH). Chiral HPLC analysis: CHIRALPAK[®] IC, isocratic elution hexane/isopropanol 75/25 (v/v), flow rate 0.7 mL min⁻¹, t_{r} (*S*) = 15.93, t_{r} (*R*) = 19.09, 93% *ee*. NMR of *S* and *R*-4d: ¹H NMR (400 MHz, CDCl₃) δ 7.77 (d, $J = 8.7$ Hz, 2H), 7.63 (d, $J = 8.7$ Hz, 2H), 5.43 (d, $J = 16.5$ Hz, 1H), 5.34 (d, $J = 16.5$ Hz, 1H), 3.90 – 3.76 (m, 2H), 2.75 (dtd, $J = 7.9, 2 \times 6.6, 5.3$ Hz, 1H), 1.72 (dtd, $J = 15.4, 8.2, 7.9, 4.2$ Hz, 1H), 1.59 – 1.43 (m, 1H), 1.4 – 1.3 (m, 4H), 0.89 (t, $J = 2 \times 6.9$ Hz, 3H). ¹³C NMR (101 MHz, CDCl₃) δ 192.2, 174.4, 132.4, 132.3, 129.6, 129.3, 65.7, 64.0, 48.5, 29.4, 27.6, 22.6, 13.9. ESI-TOF *m/z* for *S* and *R*-4d: Calcd for [M+Na⁺] C₁₅H₁₉O₄NaBr: 365.0379, found [M+Na⁺]: 365.0364. Melting point: 72.1-73.5 °C.

2-(4-bromophenyl)-2-oxoethyl (*S*)-2-(hydroxymethyl)pent-4-enoate (*S*-4e)



The title compound was prepared using MBP-YfaU W23V variant and the procedure described for *S*-4a. The product was obtained as a white solid (719 mg, 73%). $[\alpha]^{20}_{\text{D}} = -2.8$ ($c = 2$ in *i*PrOH). Chiral HPLC analysis: CHIRALPAK[®] IC, isocratic elution hexane/isopropanol 80/20 (v/v), flow rate 0.7 mL min⁻¹, t_{r} (*S*) = 22.28, t_{r} (*R*) = 24.55, 98% *ee*.

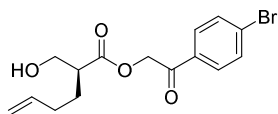
2-(4-bromophenyl)-2-oxoethyl (*R*)-2-(hydroxymethyl)pent-4-enoate (*R*-4e)



The title compound was prepared using KPHMT I212A variant and the procedure described for *R*-4a. The product was obtained as a white solid (445 mg, 68%). $[\alpha]^{20}_{\text{D}} = +2.8$ ($c = 2$ in *i*PrOH). Chiral HPLC analysis: CHIRALPAK[®] IC, isocratic elution hexane/isopropanol 80/20 (v/v), flow rate 0.7 mL min⁻¹, t_{r} (*S*) = 22.28, t_{r} (*R*) = 24.55, 96% *ee*. NMR of *S* and *R*-4e: ¹H NMR (400 MHz,

CDCl₃) δ 7.77 (d, J = 8.3 Hz, 2H), 7.63 (d, J = 8.3 Hz, 2H), 5.80 (ddt, J = 17.2, 10.1, 2x6.9 Hz, 1H), 5.46 (d, J = 16.5 Hz, 1H), 5.31 (d, J = 16.5 Hz, 1H), 5.12 (dq, J = 17.0, 3x1.7 Hz, 1H), 5.06 (dq, J = 10.4, 1.4, 2x1.3 Hz, 1H), 3.90 (dd, J = 11.4, 4.2 Hz, 1H), 3.83 (dd, J = 11.5, 7.3 Hz, 1H), 2.84 (qd, J = 3x7.2, 4.3 Hz, 1H), 2.51 (dt, J = 14.3, 2x6.9 Hz, 1H), 2.32 (dt, J = 14.5, 2x7.0 Hz, 1H). ¹³C NMR (101 MHz, CDCl₃) δ 192.1, 173.6, 134.8, 132.4, 129.7, 129.3, 117.3, 65.8, 63.4, 47.8, 32.1. ESI-TOF m/z for *S* and *R*-**4e**: Calcd for [M+Na⁺] C₁₄H₁₅O₄NaBr: 349.0051, found [M+Na⁺]: 349.0070. Melting point: 50.4-50.6 °C.

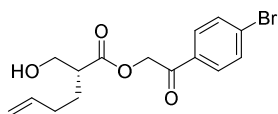
2-(4-bromophenyl)-2-oxoethyl (*S*)-2-(hydroxymethyl)hex-5-enoate (*S*-**4f**)



The title compound was prepared using MBP-YfaU W23V variant and the procedure described for *S*-**4a**.

The product was obtained as a white solid (563 mg, 69%). $[\alpha]_D^{20}$ = -8.4 (c = 4 in iPrOH). Chiral HPLC analysis: CHIRALPAK® IC, isocratic elution hexane/isopropanol 80/20 (v/v), flow rate 0.7 mL min⁻¹, t_r (*S*) = 18.68, t_r (*R*) = 22.56, 95% *ee*.

2-(4-bromophenyl)-2-oxoethyl (*R*)-2-(hydroxymethyl)hex-5-enoate (*R*-**4f**)



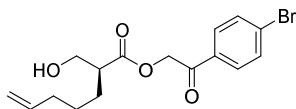
The title compound was prepared using KPHMT I212A variant and the procedure described for *R*-**4a**.

The product was obtained as a white solid (467 mg, 68%). $[\alpha]_D^{20}$ = +8.2 (c = 4 in iPrOH). Chiral HPLC analysis: CHIRALPAK® IC, isocratic elution hexane/isopropanol 80/20 (v/v), flow rate 0.7 mL min⁻¹, t_r (*S*) = 18.68, t_r (*R*) = 22.56, 97% *ee*. NMR of *S* and *R*-**4f**: ¹H NMR (400 MHz, CDCl₃) δ 7.77 (d, J = 8.4 Hz, 2H), 7.64 (d, J = 8.4 Hz, 2H), 5.78 (ddt, J = 16.9, 10.2, 2x6.7 Hz, 1H), 5.44 (d, J = 16.5 Hz, 1H), 5.33 (d, J = 16.5 Hz, 1H), 5.04 (dq, J = 17.2, 3x1.6 Hz, 1H), 4.99 (dtd, J = 10.1, 2x1.7, 0.9 Hz, 1H), 3.98 – 3.70 (m, 2H), 2.78 (tdd, J = 2x7.8, 6.1, 4.3 Hz, 1H), 2.15 (dt, J = 9.0, 2x6.6 Hz, 2H), 1.86 (dq, J = 13.5, 3x7.7 Hz, 1H), 1.62 (dtd, J = 13.9, 2x7.7, 6.0 Hz, 1H). ¹³C NMR (101 MHz, CDCl₃) δ 192.1, 174.1, 137.5, 132.4, 129.7, 129.3, 115.5, 65.7, 63.9, 47.6, 31.3, 27.0. ESI-TOF m/z for *S* and *R*-**4f**: Calcd for [M+Na⁺]

Experimental section

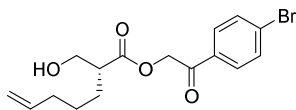
$C_{15}H_{17}O_4NaBr$: 363.0235, found $[M+Na^+]$: 363.0208. Melting point: 44.6-45.2 °C.

2-(4-bromophenyl)-2-oxoethyl (*S*)-2-(hydroxymethyl)hept-6-enoate (*S*-4g)



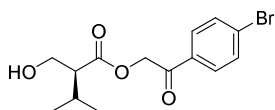
The title compound was prepared using MBP-YfaU W23V variant and the procedure described for *S*-4a. The product was obtained as a white solid (723 mg, 68%). $[\alpha]_D^{20} = -3.5$ ($c = 4$ in *i*PrOH). Chiral HPLC analysis: CHIRALPAK® IC, isocratic elution hexane/isopropanol 80/20 (v/v), flow rate 0.7 mL min⁻¹, t_r (*S*) = 17.91, t_r (*R*) = 21.79, 78% *ee*.

2-(4-bromophenyl)-2-oxoethyl (*R*)-2-(hydroxymethyl)hept-6-enoate (*R*-4g)



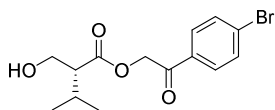
The title compound was prepared using KPHMT L42A/I212A variant and the procedure described for *R*-4a. The product was obtained as a white solid (454 mg, 64%). $[\alpha]_D^{20} = +4.1$ ($c = 4$ in *i*PrOH). Chiral HPLC analysis: CHIRALPAK® IC, isocratic elution hexane/isopropanol 80/20 (v/v), flow rate 0.7 mL min⁻¹, t_r (*S*) = 17.91, t_r (*R*) = 21.79, 93% *ee*. NMR of *S* and *R*-4g: ¹H NMR (400 MHz, CDCl₃) δ 7.77 (d, $J = 8.6$ Hz, 2H), 7.64 (d, $J = 8.6$ Hz, 2H), 5.78 (ddt, $J = 16.9, 10.2, 2 \times 6.7$ Hz, 1H), 5.43 (d, $J = 16.5$ Hz, 1H), 5.34 (d, $J = 16.5$ Hz, 1H), 5.00 (dq, $J = 17.1, 3 \times 1.6$ Hz, 1H), 4.95 (ddt, $J = 10.7, 2.3, 2 \times 1.1$ Hz, 1H), 3.90 – 3.77 (m, 2H), 2.76 (ddt, $J = 10.8, 7.3, 2 \times 3.8$ Hz, 1H), 2.07 (q, $J = 2 \times 6.9, 6.8$ Hz, 2H), 1.73 (ddd, $J = 15.0, 9.4, 5.8$ Hz, 1H), 1.55 (dt, $J = 8.9, 2 \times 6.4$ Hz, 1H), 1.53 – 1.40 (m, 2H). ¹³C NMR (101 MHz, CDCl₃) δ 192.1, 174.2, 138.2, 132.4, 132.3, 129.7, 129.3, 114.9, 65.7, 64.0, 48.3, 33.5, 27.4, 26.5. ESI-TOF m/z for *S* and *R*-4g: Calcd for $[M+Na^+]$ $C_{16}H_{19}O_4NaBr$: 377.0362, found $[M+Na^+]$: 377.0364. Melting point: 60.3-60.6 °C.

2-(4-bromophenyl)-2-oxoethyl (S)-2-(hydroxymethyl)-3-methylbutanoate (S-4h)



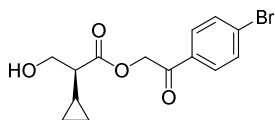
The title compound was prepared using MBP-YfaU W23V variant and the procedure described for *S-4a*. The product was obtained as a white solid (488 mg, 75%). $[\alpha]^{20}_{\text{D}} = -6.1$ ($c = 4$ in CHCl_3). Chiral HPLC analysis: CHIRALPAK® ID, isocratic elution hexane/isopropanol 75/25 (v/v), flow rate 0.7 mL min^{-1} , $t_{\text{r}}(R) = 19.51$, $t_{\text{r}}(S) = 22.33$, 99% *ee*.

2-(4-bromophenyl)-2-oxoethyl (R)-2-(hydroxymethyl)-3-methylbutanoate (R-4h)



The title compound was prepared using KPHMT I202A variant and the procedure described for *R-4a*. The product was obtained as a white solid (321 mg, 49%). $[\alpha]^{20}_{\text{D}} = +5.1$ ($c = 4$ in CHCl_3). Chiral HPLC analysis: CHIRALPAK® ID, isocratic elution hexane/isopropanol 75/25 (v/v), flow rate 0.7 mL min^{-1} , $t_{\text{r}}(R) = 19.51$, $t_{\text{r}}(S) = 22.33$, 92% *ee*. NMR of *S* and *R-4h*: $^1\text{H NMR}$ (400 MHz, CDCl_3) δ 7.77 (d, $J = 8.6 \text{ Hz}$, 2H), 7.63 (d, $J = 8.5 \text{ Hz}$, 2H), 5.46 (d, $J = 16.5 \text{ Hz}$, 1H), 5.32 (d, $J = 16.5 \text{ Hz}$, 1H), 4.06 – 3.69 (m, 2H), 2.54 (td, $J = 2 \times 8.4$, 4.2 Hz, 1H), 2.22 – 1.74 (m, 1H), 1.01 (d, $J = 2.2 \text{ Hz}$, 3H), 0.99 (d, $J = 2.2 \text{ Hz}$, 3H). $^{13}\text{C NMR}$ (101 MHz, CDCl_3) δ 192.1, 173.9, 132.5, 132.3, 129.6, 129.3, 65.6, 62.4, 55.6, 27.4, 21.0, 20.1. ESI-TOF m/z for *S* and *R-4h*: Calcd for $[\text{M}+\text{Na}^+]$ $\text{C}_{14}\text{H}_{17}\text{O}_4\text{NaBr}$: 351.0208, found $[\text{M}+\text{Na}^+]$: 351.0159. Melting point: 82.0-82.9 °C.

2-(4-bromophenyl)-2-oxoethyl (S)-2-cyclopropyl-3-hydroxypropanoate (S-4i)

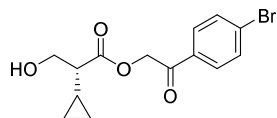


The title compound was prepared using MBP-YfaU W23V variant and the procedure described for *S-4a*. The product was obtained as a white solid (717 mg, 73%). $[\alpha]^{20}_{\text{D}} = -25.4$ ($c = 4$ in $i\text{PrOH}$). Chiral HPLC analysis: CHIRALPAK®

Experimental section

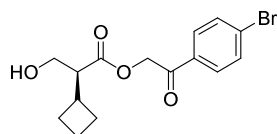
IC, isocratic elution hexane/isopropanol 80/20 (v/v), flow rate 1.0 mL min⁻¹, t_r (*S*) = 18.85, t_r (*R*) = 20.50, 98% *ee*.

2-(4-bromophenyl)-2-oxoethyl (R)-2-cyclopropyl-3-hydroxypropanoate (*R*-4i)



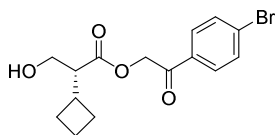
The title compound was prepared using the enzyme KPHMT wild-type and the procedure described for *R*-4a. The product was obtained as a white solid (444 mg, 68%). $[\alpha]_D^{20} = +23.2$ ($c = 4$ in iPrOH). Chiral HPLC analysis: CHIRALPAK[®] IC, isocratic elution hexane/isopropanol 80/20 (v/v), flow rate 1.0 mL min⁻¹, t_r (*S*) = 18.85, t_r (*R*) = 20.50, 87% *ee*. NMR of *S* and *R*-4i: ¹H NMR (400 MHz, CDCl₃) δ 7.78 (d, $J = 8.5$ Hz, 2H), 7.64 (d, $J = 8.5$ Hz, 2H), 5.43 (d, $J = 16.3$ Hz, 1H), 5.38 (d, $J = 16.3$ Hz, 1H), 4.06 – 3.84 (m, 2H), 2.00 (ddd, $J = 10.1, 7.6, 4.8$ Hz, 1H), 1.04 (dddd, $J = 13.0, 9.9, 8.1, 4.9$ Hz, 1H), 0.67 – 0.50 (m, 2H), 0.42 – 0.30 (m, 1H), 0.26 – 0.17 (m, 1H). ¹³C NMR (101 MHz, CDCl₃) δ 192.1, 173.8, 132.4, 132.3, 129.6, 129.3, 65.7, 64.3, 53.5, 9.6, 3.9, 3.6. ESI-TOF m/z for *S* and *R*-4i: Calcd for [M+Na⁺] C₁₄H₁₅O₄NaBr: 349.0048, found [M+Na⁺]: 349.0051. Melting point: 76.9-78.9 °C.

2-(4-bromophenyl)-2-oxoethyl (S)-2-cyclobutyl-3-hydroxypropanoate (*S*-4j)



The title compound was prepared using MBP-YfaU W23V variant and the procedure described for *S*-4a. The product was obtained as a white solid (814 mg, 80%). $[\alpha]_D^{20} = -12.1$ ($c = 3$ in iPrOH). Chiral HPLC analysis: CHIRALPAK[®] IC, isocratic elution hexane/isopropanol 95/5 (v/v), flow rate 1.0 mL min⁻¹, t_r (*S*) = 67.68, t_r (*R*) = 73.46, 98% *ee*.

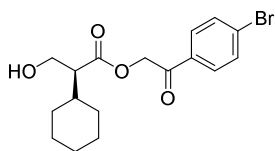
2-(4-bromophenyl)-2-oxoethyl (R)-2-cyclobutyl-3-hydroxypropanoate (R-4j)



The title compound was prepared using KPHMT I202A variant and the procedure described for *R*-4a.

The product was obtained as a white solid (328 mg, 48%). $[\alpha]_D^{20} = +7.2$ ($c = 3$ in *i*PrOH). Chiral HPLC analysis: CHIRALPAK® IC, isocratic elution hexane/isopropanol 95/5 (v/v), flow rate 1.0 mL min⁻¹, t_r (*S*) = 67.68, t_r (*R*) = 73.46, 75% *ee*. NMR of *S* and *R*-4j: ¹H NMR (400 MHz, CDCl₃) δ 7.76 (d, $J = 8.5$ Hz, 2H), 7.63 (d, $J = 8.4$ Hz, 2H), 5.40 (d, $J = 16.5$ Hz, 1H), 5.33 (d, $J = 16.5$ Hz, 1H), 3.79 (dd, $J = 11.4, 4.0$ Hz, 1H), 3.74 (dd, $J = 11.3, 7.5$ Hz, 1H), 2.76 (ddd, $J = 11.4, 7.5, 4.1$ Hz, 1H), 2.70 – 2.56 (m, 1H), 2.18 – 2.03 (m, 2H), 1.99 – 1.71 (m, 4H). ¹³C NMR (101 MHz, CDCl₃) δ 192.1, 173.3, 132.4, 132.3, 129.6, 129.3, 65.6, 62.0, 54.7, 33.9, 27.3, 26.9, 18.5. ESI-TOF *m/z* for *S* and *R*-4j: Calcd for [M+Na⁺] C₁₅H₁₇O₄NaBr: 363.0193, found [M+Na⁺]: 363.0208. Melting point: 98.0-99.0 °C.

2-(4-bromophenyl)-2-oxoethyl (S)-2-cyclohexyl-3-hydroxypropanoate (S-4k)



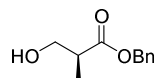
The title compound was prepared using MBP-YfaU W23V variant and the procedure described for *S*-4a.

The product was obtained as a white solid (542 mg, 73%). $[\alpha]_D^{20} = -1.8$ ($c = 2.4$ in *i*PrOH). Chiral HPLC analysis: CHIRALPAK® IC, isocratic elution hexane/isopropanol 95/5 (v/v), flow rate 1.0 mL min⁻¹, t_r (*S*) = 77.94, t_r (*R*) = 83.96, 96% *ee*. NMR of *S*-4k: ¹H NMR (400 MHz, CDCl₃) δ 7.77 (d, $J = 8.7$ Hz, 2H), 7.63 (d, $J = 8.7$ Hz, 2H), 5.46 (d, $J = 16.5$ Hz, 1H), 5.30 (d, $J = 16.5$ Hz, 1H), 3.93 (dd, $J = 11.3, 8.7$ Hz, 1H), 3.86 (dd, $J = 11.3, 4.2$ Hz, 1H), 2.59 (td, $J = 2 \times 8.4, 4.2$ Hz, 1H), 1.91 – 1.57 (m, 6H), 1.38 – 0.95 (m, 5H). ¹³C NMR (101 MHz, CDCl₃) δ 192.2, 173.9, 132.5, 132.3, 129.6, 129.3, 65.5, 62.1, 54.8, 36.8, 31.4, 30.4, 26.2. ESI-TOF *m/z* for *S*-4k: Calcd for [M+Na⁺] C₁₇H₂₁O₄NaBr: 391.0540, found [M+Na⁺]: 391.0521. Melting point: 118.9-119.1 °C.

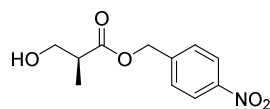
5.6.3 Enzymatic synthesis of benzyl and 4-nitrobenzyl ester derivatives

The aldol additions catalyzed by MBP-YfaU or KPHMT and the subsequent oxidative decarboxylation of **3** were performed as described for *S-4a*. Then, anhydrous DMF (50 mL) and CsCl (168 mg, 0.1 mmol, 0.2 eq) were added under N₂ atmosphere. The reactions were started by adding BnBr (654 mg, 5 mmol, 1 eq) or 4-NO₂C₆H₄CH₂Br (1.1 g, 5 mmol, 1 eq) and heated at 60 °C during 2 h. EtOAc (200 mL) was added to the reaction mixtures and washed with H₂O (3x50 mL). The organic phases were dried over anhydrous MgSO₄, absorbed onto silica gel (100 mL) and loaded onto a silica gel column. Products were eluted with a step gradient of hexane:AcOEt: 100:0, 200 mL, 90:10, 200 mL, 80:20, 200 mL, 70:30, 400 mL and 60:40, 800mL. Pure fractions were pooled, and the solvent removed in vacuo affording the title compounds.

Benzyl (*S*)-3-hydroxy-2-methylpropanoate (*S-5a*)

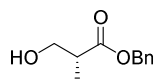
 The title compound was obtained as a yellow oil (852 mg, 60% over three steps). $[\alpha]^{20}_D = +18.6$ ($c = 0.85$ in MeOH) [lit: $[\alpha]^{20}_D = -24.2$, $c = 0.85$ in MeOH, 90% *ee*, *R*].²⁴⁹ Chiral HPLC analysis: CHIRALPACK® IB, isocratic elution hexane/isopropanol 98/2 (v/v), flow rate 1 mL min⁻¹, t_r (*S*) = 18.64, t_r (*R*) = 19.89, > 99% *ee*. ¹H NMR (400 MHz, CDCl₃) δ 7.42 – 7.27 (m, 5H), 5.14 (s, 2H), 3.88 – 3.59 (m, 2H), 2.71 (pd, $J = 4 \times 7.2$, 4.8 Hz, 1H), 1.19 (d, $J = 7.2$ Hz, 3H). ¹³C NMR (101 MHz, CDCl₃) δ 175.4, 135.8, 128.6, 128.3, 128.0, 66.4, 64.5, 41.8, 13.4. ESI-TOF *m/z*: Calcd for [M+H⁺] C₁₁H₁₅O₃: 195.1027, found [M+H⁺]:195.1021.

4-Nitrobenzyl (*S*)-3-hydroxy-2-methylpropanoate (*S-5b*)

 The title compound was obtained as a colorless oil which crystallized as white solid after overnight storage at -20 °C (1.15 g, 66% over three steps). $[\alpha]^{20}_D = +13.6$ ($c = 1$ in CHCl₃). Chiral HPLC analysis: CHIRALPACK® IB, isocratic elution hexane/isopropanol 95/5 (v/v), flow rate 1 mL min⁻¹, t_r (*S*) = 31.55, t_r

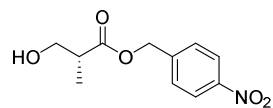
(*R*) = 32.97, 98% *ee*. ^1H NMR (400 MHz, CDCl_3) δ 7.78 (d, J = 8.5 Hz, 2H), 7.64 (d, J = 8.5 Hz, 2H), 5.43 (d, J = 16.3 Hz, 1H), 5.38 (d, J = 16.3 Hz, 1H), 4.06 – 3.84 (m, 2H), 2.00 (ddd, J = 10.1, 7.6, 4.8 Hz, 1H), 1.04 (dddd, J = 13.0, 9.9, 8.1, 4.9 Hz, 1H), 0.67 – 0.50 (m, 2H), 0.42 – 0.30 (m, 1H), 0.26 – 0.17 (m, 1H). ^{13}C NMR (101 MHz, CDCl_3) δ 192.1, 173.8, 132.4, 132.3, 129.6, 129.3, 65.7, 64.3, 53.5, 9.6, 3.9, 3.6. ESI-TOF m/z : Calcd for $[2\text{M}+\text{Na}^+]$ $\text{C}_{22}\text{H}_{26}\text{N}_2\text{O}_{10}\text{Na}$: 501.1508, found $[2\text{M}+\text{Na}^+]$: 501.1485. Melting point: 56.1–56.9 °C.

Benzyl (*R*)-3-hydroxy-2-methylpropanoate (*R*-5a)



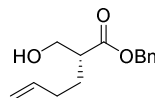
The title compound was obtained as a yellow oil (188 mg, 40% over three steps). $[\alpha]^{20}_{\text{D}} = -16.9$ ($c = 0.85$ in MeOH) [lit: $[\alpha]^{20}_{\text{D}} = -24.2$, $c = 0.85$ in MeOH, 90% *ee*, *R*].²⁴⁹ Chiral HPLC analysis: CHIRALPACK® IB, isocratic elution hexane/isopropanol 98/2 (v/v), flow rate 1 mL min^{-1} , t_{r} (*S*) = 18.64, t_{r} (*R*) = 19.89, > 99% *ee* (82% *ee* 2h at 60 °C). The spectral properties of this product coincided with *S*-5a.

4-Nitrobenzyl (*R*)-3-hydroxy-2-methylpropanoate (*R*-5b)



The title compound was obtained as a colorless oil which crystallized as white solid after overnight storage at –20 °C (355 mg, 59% over three steps). $[\alpha]^{20}_{\text{D}} = -13.4$ ($c = 1$ in MeOH). Chiral HPLC analysis: CHIRALPACK® IB, isocratic elution hexane/isopropanol 95/5 (v/v), flow rate 1 mL min^{-1} , t_{r} (*S*) = 31.55, t_{r} (*R*) = 32.97, > 98% *ee*. The spectral properties of this product coincided with *S*-5b.

Benzyl (*R*)-2-(hydroxymethyl)hex-5-enoate (*R*-5c)



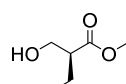
The title compound was obtained as a colorless oil (559 mg, 60% over three steps). $[\alpha]^{20}_{\text{D}} = +17.5$ ($c = 3$ in *i*PrOH). Chiral HPLC analysis: CHIRALPACK® ID, isocratic elution hexane/isopropanol 90/10 (v/v), flow rate 1 mL min^{-1} , t_{r} (*S*) = 8.15, t_{r} (*R*) = 8.94, 97% *ee*. ^1H NMR (400 MHz, CDCl_3) δ 7.42 – 7.29 (m, 5H), 5.74 (ddt, J = 16.9, 10.2, 2x6.7 Hz,

Experimental section

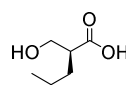
1H), 5.17 (d, $J = 12.3$ Hz, 1H), 5.13 (d, $J = 12.3$ Hz, 1H), 5.05 – 4.89 (m, 2H), 3.81 – 3.72 (m, 2H), 2.64 (qd, $J = 2 \times 6.7, 6.6, 4.9$ Hz, 1H), 2.07 (q, $J = 7.7, 2 \times 7.6$ Hz, 2H), 1.78 (dq, $J = 15.3, 7.6, 2 \times 7.5$ Hz, 1H), 1.63 (dq, $J = 14.1, 2 \times 7.6, 7.5$ Hz, 1H). ^{13}C NMR (101 MHz, CDCl_3) δ 175.0, 137.4, 128.6, 128.3, 128.1, 115.5, 66.4, 62.9, 46.7, 31.2, 27.5. ESI-TOF m/z : Calcd for $[\text{2M}+\text{Na}^+]$ $\text{C}_{28}\text{H}_{36}\text{O}_6\text{Na}$: 491.2435, found $[\text{2M}+\text{Na}^+]$: 491.2410.

5.6.4 Synthesis of derivatives for absolute stereochemistry determination

Methyl (*S*)-2-(hydroxymethyl)butanoate (*S*-6a)

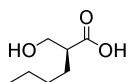
 Typical procedure: The aldol addition catalyzed by MBP-YfaU W23V and the subsequent oxidative decarboxylation of *S*-3da was performed as described for *S*-4a (without adding glycerol for salt solubilization). The sodium salt of carboxylic acid was resuspended in MeOH (200 mL), the mixture was cooled down to -80 °C and SOCl_2 (1.46 mL, 20 mmol, 5eq) was added dropwise. After stirring for 12 h at rt, sodium bicarbonate (200 mL, 5%) was added and the MeOH was removed under vacuum. The aqueous solution was extracted with AcOEt (3x100 mL), the combined organic phases were dried over anhydrous MgSO_4 , filtered and the solvent was removed in vacuo. The product (yellow oil, 203 mg, 38%) was used without any further purification. $[\alpha]_{\text{D}}^{20} = -3.8$ ($c = 1$ in CHCl_3) [lit: $[\alpha]_{\text{D}}^{20} = -5.9$, $c = 1$ in CHCl_3 , >95% *ee*, *S*].¹⁸⁶ The spectral properties of this product agreed with those reported in the literature.¹⁸⁷ ^1H NMR (400 MHz, CDCl_3) δ 3.81 – 3.71 (m, 2H), 3.70 (s, 3H), 2.50 (qd, $J = 3 \times 7.2, 4.5$ Hz, 1H), 1.75 – 1.49 (m, 2H), 0.92 (t, $J = 2 \times 7.5$ Hz, 3H). ^{13}C NMR (101 MHz, CDCl_3) δ 175.74, 62.76, 51.68, 48.86, 21.62, 11.65.

(*S*)-2-(Hydroxymethyl)pentanoic acid (*S*-6b)

 Typical procedure: The aldol addition catalyzed by MBP-YfaU W23V and the subsequent oxidative decarboxylation of *S*-3ea was performed as described above (without adding glycerol for salt solubilization).

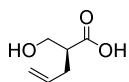
After removing the MeOH under vacuum, H₂O (200 mL) was added to the mixture. The solution was acidified at pH 1.0 (HCl 1 M) and saturated with NaCl. The product was extracted with Et₂O (3x100 mL) and the combined organic phases were dried over anhydrous MgSO₄, filtered and the solvent removed *in vacuo*. The title compound (yellow oil, 354 mg, 76%) was used without any further purification. $[\alpha]^{20}_{\text{D}} = +2.8$ (c = 10 in CHCl₃) [lit: Boeckman Jr, Robert K., 2009, $[\alpha]^{20}_{\text{D}} = -3.0$, c = 10 in CHCl₃, 92% *ee*, *R*].¹⁰² The spectral properties of this product agreed with those reported in the literature.¹⁰² ¹H NMR (400 MHz, CDCl₃) δ 3.82 – 3.73 (m, 2H), 2.62 (p, *J* = 2x7.0, 2x6.9 Hz, 1H), 1.65 (dq, *J* = 13.7, 8.0, 2x7.8 Hz, 1H), 1.51 (dq, *J* = 13.4, 2x6.9, 6.5 Hz, 1H), 1.38 (h, *J* = 3x7.5, 2x7.3 Hz, 2H), 0.92 (t, *J* = 2x7.3 Hz, 3H). ¹³C NMR (101 MHz, CDCl₃) δ 180.6, 62.9, 47.1, 30.3, 20.4, 13.9.

(S)-2-(Hydroxymethyl)hexanoic acid (S-6c)



The title compound (yellow oil, 164 mg, 75%) was prepared following the procedure described for *S*-**6b**. $[\alpha]^{20}_{\text{D}} = -5.9$ (c = 1 in MeOH) [lit: $[\alpha]^{20}_{\text{D}} = +6.5$, c = 1 in MeOH, 99% *ee*, *R*].²⁵⁰ The spectral properties of this product agreed with those reported in the literature.²⁵⁰ ¹H NMR (400 MHz, CDCl₃) δ 3.80 – 3.74 (m, 2H), 2.60 (qd, *J* = 6.8, 2x6.7, 5.3 Hz, 1H), 1.67 (dq, *J* = 15.0, 7.4, 2x7.3 Hz, 1H), 1.54 (dq, *J* = 13.1, 2x7.1, 6.4 Hz, 1H), 1.38 – 1.25 (m, 4H), 0.89 (t, *J* = 2x7.0 Hz, 3H). ¹³C NMR (101 MHz, CDCl₃) δ 180.5, 62.9, 47.3, 29.3, 27.9, 22.5, 13.8.

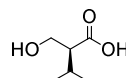
(S)-2-(Hydroxymethyl)pent-4-enoic acid (S-6d)



The title compound (yellow oil, 261 mg, 67%) was prepared following the procedure described for *S*-**6b**. ¹H NMR (400 MHz, CDCl₃) δ 5.77 (ddt, *J* = 17.5, 10.2, 2x7.4 Hz, 1H), 5.17 – 4.88 (m, 1H), 3.79 (d, *J* = 5.8 Hz, 2H), 2.75 – 2.64 (m, 1H), 2.52 – 2.40 (m, 1H), 2.39 – 2.27 (m, 1H). ¹³C NMR (101 MHz, CDCl₃) δ 179.5, 134.4, 117.7, 62.3, 46.7, 32.4.

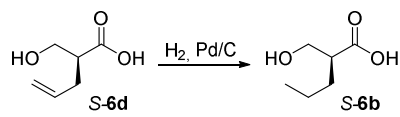
Experimental section

(S)-2-(Hydroxymethyl)-3-methylbutanoic acid (S-6e)

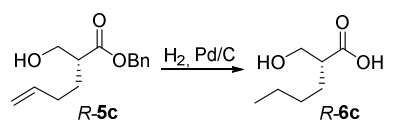
 The title compound (yellow oil, 324 mg, 70%) was prepared following the procedure described for **S-6b**. $[\alpha]_D^{20} = +4.1$ ($c = 4$ in CHCl_3) [lit: $[\alpha]_D^{20} = -5.4$, $c = 4$ in CHCl_3 , 98% *ee*, *R*].¹⁰² The spectral properties of this product agreed with those reported in the literature.¹⁰² ^1H NMR (400 MHz, CDCl_3) δ 3.86 (dd, $J = 11.1, 8.5$ Hz, 1H), 3.78 (dd, $J = 11.2, 4.0$ Hz, 1H), 2.42 (td, $J = 8.1, 7.8, 4.0$ Hz, 1H), 2.12 – 1.96 (m, 1H), 0.99 (d, $J = 4.5$ Hz, 3H), 0.97 (d, $J = 4.4$ Hz, 3H). ^{13}C NMR (101 MHz, CDCl_3) δ 180.0, 61.3, 54.0, 27.6, 20.5, 20.1.

5.6.5 Catalytic hydrogenation of compounds S-6d and R-5c

(S)-2-(Hydroxymethyl)pentanoic acid (S-6b)

 Product **S-6d** (120 mg, 1 mmol) was resuspended with Et_2O (100 mL), the solution was saturated with N_2 and Pd/C (191 mg, 10 mol%, 10% Pd, 50% humidity) was added keeping the reaction under N_2 . Then, H_2 (1 atm) was added under stirring and the reaction was left overnight at room temperature. The crude material was filtered through Celite[®] and the pellet was washed with Et_2O (3x50 mL). Then, the solvent was removed *in vacuo* obtaining the product **S-6b** (yellow oil, 108 mg, 91%) that was used without any further purification. $[\alpha]_D^{20} = +1.8$ ($c = 10$ in CHCl_3) [lit: $[\alpha]_D^{20} = -3.0$, $c = 10$ in CHCl_3 , 92% *ee*, *R*].¹⁰² The spectral properties of this product agreed with the previously obtained **S-6b** and with those reported in the literature.¹⁰²

(R)-2-(hydroxymethyl)hexanoic acid (R-6c)

 The title compound (yellow oil, 145 mg, 94%) was prepared following the procedure described for **S-6b**. $[\alpha]_D^{20} = +6.0$ ($c = 1$ in MeOH) [lit: $[\alpha]_D^{20} = +6.5$, $c = 1$ in MeOH, 99% *ee*, *R*].²⁵⁰ The spectral

properties of this product agreed with *S-6c* and with those reported in the literature.²⁵⁰

5.6.6 Synthesis of racemic mixtures of products

5.6.6.1 Synthesis of racemic mixtures of products 4b–k

Typical procedure: Reactions (3 mL total volume) were conducted at room temperature in a round-bottom flask (100 mL) with magnetic stirring (250 rpm). Substrates **1d–m** (3 mmol, 1 eq, 1 M in the reaction) were dissolved in sodium phosphate buffer (0.15 mL of a 1 M stock solution at pH 7.0, 50 mM in the reaction) and water was added. The reactions were started by adding NiCl₂ (30 μL of a 0.1 M stock solution in water, 1 mM in the reaction) and formaldehyde (**2a**, 0.225 mL of a 13.3 M commercial solution, 3 mmol, 1 eq, 1 M in the reaction). The reactions were monitored by HPLC until no evolution of substrates and products were detected. Decarboxylation of aldol adducts, and the subsequent esterification were performed as described for the enzymatic reaction. The NMR spectra and properties of racemic aldol adducts (*rac-4b–k*) were undistinguishable from those obtained with MBP-YfaU and KPHMT variants.

5.6.6.2 Synthesis of racemic mixtures of products 5a–c

Typical procedure: Aldol addition reaction was performed as described for the racemic phenacyl ester products. Decarboxylation of aldol adducts, and the subsequent esterification were performed as described for the enzymatic reaction. The spectral properties of the racemic products (*rac-5a–c*) agreed with the enzymatically prepared samples **5a–c**.

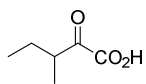
5.7 Synthesis of compounds from section 3.2

5.7.1 Synthesis of 2-oxoacids

The 2-oxoacids were prepared following the general Method A explained in the Section 5.6.1.1.

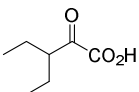
Experimental section

3-Methyl-2-oxopentanoic acid (*rac*-**1n**)



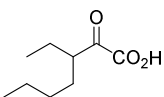
The title compound was prepared following the procedure described for **1e** affording *rac*-**1n** as an oil that crystallized after overnight storage at $-20\text{ }^{\circ}\text{C}$ (3.4 g, isolated yield over two steps: 35%). The spectral properties of this product agreed with those reported in the literature.²⁵¹ ^1H NMR (400 MHz, CDCl_3) δ 3.33 (dq, $J = 13.7, 3 \times 6.9$ Hz, 1H), 1.79 (dq, $J = 14.9, 7.5, 2 \times 7.4, 6.2$ Hz, 1H), 1.55 – 1.40 (m, 1H), 1.16 (d, $J = 6.9$ Hz, 3H), 0.91 (t, $J = 2 \times 7.5$ Hz, 3H). ^{13}C NMR (101 MHz, CDCl_3) δ 199.1, 159.3, 41.6, 25.2, 14.8, 11.3.

3-Ethyl-2-oxopentanoic acid (**1o**)



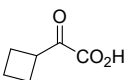
The title compound was prepared following the procedure described for **1e** affording **1o** as an oil that crystallized after overnight storage at $-20\text{ }^{\circ}\text{C}$ (4.1 g, isolated yield over two steps: 34%). ^1H NMR (400 MHz, CDCl_3) δ 3.3 (tt, $J = 2 \times 7.4, 2 \times 5.7$ Hz, 1H), 1.7 (dq, $J = 14.9, 3 \times 7.4$ Hz, 2H), 1.6 (dq, $J = 14.9, 7.5, 2 \times 7.4, 5.7$ Hz, 2H), 0.9 (t, $J = 2 \times 7.5$ Hz, 6H). ^{13}C NMR (101 MHz, CDCl_3) δ 199.3, 159.3, 48.4, 23.2, 11.4.

3-Ethyl-2-oxoheptanoic acid (*rac*-**1p**)



The title compound was prepared following the procedure described for **1e** furnishing *rac*-**1p** as an oil (3.6 g, isolated yield over two steps: 26%). ^1H NMR (400 MHz, CDCl_3) δ 3.31 (tt, $J = 2 \times 7.6, 2 \times 5.7$ Hz, 1H), 1.80 – 1.64 (m, 2H), 1.63 – 1.44 (m, 2H), 1.34 – 1.14 (m, 4H), 0.86 (dt, $J = 7.4, 7.2, 2.7$ Hz, 6H). ^{13}C NMR (101 MHz, CDCl_3) δ 199.4, 159.3, 46.9, 30.0, 29.3, 23.8, 22.6, 13.8, 11.5.

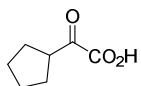
2-Cyclobutyl-2-oxoacetic acid (**1q**)



The title compound was prepared following the procedure described for **1e** affording **1q** as an oil (5.43 g, isolated yield over two steps: 65%). The spectral properties of this product agreed with those reported in the literature.²⁵² ^1H NMR (400 MHz, CDCl_3) δ 3.98 (pd, $J = 4 \times 8.5,$

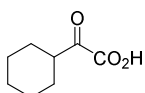
1.2 Hz, 1H), 2.35 – 2.25 (m, 4H), 2.15 – 2.01 (m, 1H), 1.98 – 1.85 (m, 1H). ^{13}C NMR (101 MHz, CDCl_3) δ 195.7, 159.1, 40.6, 24.4, 18.0.

2-Cyclopentyl-2-oxoacetic acid (**1r**)



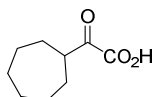
The title compound was prepared following the procedure described for **1e** yielding **1r** as an oil that crystallized after overnight storage at $-20\text{ }^\circ\text{C}$ (4.9 g, isolated yield over two steps: 43%). The spectral properties of this product agreed with those reported in the literature.²⁵² ^1H NMR (400 MHz, CDCl_3) δ 3.64 (tt, $J = 2 \times 9.0, 2 \times 6.9$ Hz, 1H), 2.03 – 1.89 (m, 2H), 1.84 – 1.73 (m, 2H), 1.72 – 1.59 (m, 4H). ^{13}C NMR (101 MHz, CDCl_3) δ 197.7, 159.6, 45.4, 28.8, 26.1.

2-Cyclohexyl-2-oxoacetic acid (**1s**)



The title compound was prepared following the procedure described for **1e** furnishing **1s** as an oil that crystallized after overnight storage at $-20\text{ }^\circ\text{C}$ (7.0 g, isolated yield over two steps: 54%). The spectral properties of this product agreed with those reported in the literature.²⁵² ^1H NMR (400 MHz, CDCl_3) δ 3.22 (dtt, $J = 11.5, 7.9, 7.9, 3.9, 3.9$ Hz, 1H), 2.00 – 1.86 (m, 2H), 1.81 (dq, $J = 12.9, 4.3, 4.0, 4.0$ Hz, 2H), 1.70 (dtt, $J = 13.3, 3.6, 2.0, 2.0$ Hz, 1H), 1.44 – 1.27 (m, 4H), 1.26 – 1.13 (m, 1H). ^{13}C NMR (101 MHz, CDCl_3) δ 198.3, 159.2, 44.4, 27.8, 25.5, 25.2.

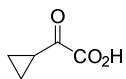
2-Cycloheptyl-2-oxoacetic acid (**1t**)



The title compound was prepared following the procedure described for **1e** furnishing **1t** as an oil that crystallized after overnight storage at $-20\text{ }^\circ\text{C}$ (6.1 g, isolated yield over two steps: 47%). ^1H NMR (400 MHz, CDCl_3) δ 3.39 (tt, $J = 2 \times 8.9, 4.2, 4.2$ Hz, 1H), 1.92 (ddd, $J = 14.8, 6.6, 3.3$ Hz, 2H), 1.73 (ddd, $J = 13.0, 6.5, 3.6$ Hz, 2H), 1.65 – 1.48 (m, 8H). ^{13}C NMR (101 MHz, CDCl_3) δ 198.4, 159.5, 45.4, 29.0, 28.2, 26.4.

Experimental section

2-Cyclopropyl-2-oxoacetic acid (**1u**)



The title compound was prepared following the procedure described for **1e** but adding 0.7 eq of diethyl oxalate. The hydrolysis reaction was performed in TEA buffer (1 M, pH 7.5). The workup procedure consisted on filtering the reaction mixture and adjusting the pH to 8. Then, the aqueous phase was washed with 2-MeTHF (3 x 30 mL). The aqueous phase was adjusted to pH 7.0 and the resulting solution containing **1u** was used without any further purification (10 mL, 1 M, 87%).

5.7.2 Synthesis of hydroxyaldehydes

D And L-lactaldehyde (**2e** and **2f**)

D- And L-lactaldehyde were prepared from L- and D-threonine respectively, following a published procedure,¹⁹³ using acetate buffer instead of citrate. The latter has the capacity to chelate metals and KPHMT, metal cofactor dependent enzyme, can be deactivated by the citrate ions remaining in the product. Indeed, no reaction was detected when using D- and L-lactaldehyde prepared with citrate buffer. D- or L-threonine (25 mmol, 2.98 g, 1 eq), ninhydrin (50 mmol, 9.1 g, 2 eq) and sodium acetate buffer (0.6 L, 0.05 M, pH 5.4) were combined and boiled for 15 min under vigorous stirring. Work-up and purification procedures followed identical published procedures.

D-Threose (**2g**)

D-Threose was prepared following a published procedure²⁰⁶ with some modifications. Reaction (10 mL total volume) was conducted at room temperature in a round-bottom flask (100 mL) with magnetic stirring (250 rpm). Glycolaldehyde (600 mg, 10 mmol, 1 M in the reaction) was dissolved in triethanolamine buffer (20 mM, pH 7.0, 10 mL). The reaction was started by adding FSA A129G (12 mg, 3 mg mL⁻¹ in the reaction), and monitored by HPLC analysis. After 24 h the reaction was transferred onto a 15 mL conical centrifuge tube and centrifuged for 15 min at 6000 rpm. The supernatant was collected and filtered using a Amicon® Ultra 15 mL Centrifugal Filters to

completely remove the enzyme. The product was used without any further purification.

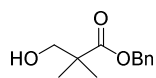
D-Erythrose (2h)

D-Erythrose was commercially available and obtained from TCI (1 g, 70% in water). Preliminary results were obtained using this D-erythrose. To furnish product **7q** D-erythrose from TCI (200 mg, 70% in water) and from Sigma-Aldrich (250 mg, 75% in water) were used and the results were not reproducible. For this reason, D-erythrose from different origins were pooled and absorbed onto silica gel and loaded onto a silica gel column. The solvent system used was A: CH₃CN:AcOEt (1:1) and B: methanol. Product was eluted with a step gradient of 100:0 (500 mL), 95:5 (500 mL), 90:10 (500 mL), 85:15 (500 mL) and 80:20 (500 mL). Pure fractions were pooled and the solvent removed in vacuo affording the title compound.

5.7.3 Enzymatic synthesis of products 7a–j

5.7.3.1 Benzyl esters derivatives

Benzyl 3-hydroxy-2,2-dimethylpropanoate (7a)

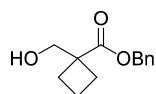


Typical procedure: The aldol addition reaction was performed as described for the product **4a**. The reaction was monitored by HPLC and after 24 h hydrogen peroxide (1.1 mL of a 8.8 M commercial solution, 10 mmol, 5 eq) was added. When the aldol adduct was not detected by HPLC, catalase from bovine liver (50 mg) dissolved in 1 mL of 10 mM sodium phosphate buffer, pH 7.0 was added. The reaction mixture was diluted with methanol (200 mL), filtered through Celite[®] and the pellet was washed with methanol (3x50 mL). The solvent was removed under vacuum. Then, anhydrous DMF (50 mL) and CsCl (168 mg, 1 mmol, 0.5 eq) were added under N₂ atmosphere. The reaction was started by adding BnBr (342 mg, 2 mmol, 1 eq) and heated at 60 °C during 2 h. EtOAc (200 mL) was added to the reaction mixture and washed with H₂O (3x50 mL). The organic phases were pooled, dried over anhydrous MgSO₄, absorbed onto silica gel (100 mL) and loaded

Experimental section

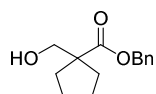
onto a silica gel column. Product was eluted with a step gradient of hexane:AcOEt: 100:0, 200 mL, 90:10, 200 mL, 80:20, 200 mL, 70:30, 400 mL and 60:40, 800mL. Pure fractions were pooled, and the solvent removed in vacuo affording the title compound. The product **7a** was obtained as an oil (218 mg, 53%). ¹H NMR (400 MHz, CDCl₃) δ 7.41 – 7.27 (m, 5H), 5.13 (s, 2H), 3.56 (s, 2H), 1.21 (s, 6H). ¹³C NMR (101 MHz, CDCl₃) δ 177.4, 135.9, 128.6, 128.2, 127.8, 69.7, 66.3, 44.3, 22.1. ESI-TOF m/z for **7a**: Calcd for [M+Na⁺] C₁₂H₁₆O₃Na: 231.0997, found [M+Na⁺]: 231.0991.

Benzyl 1-(hydroxymethyl)cyclobutane-1-carboxylate (**7d**)



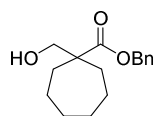
The title compound was prepared using KPHMT I202A following the procedure described for **7a**. The product **7d** was obtained as an oil (160 mg, 36%). ¹H NMR (400 MHz, CDCl₃) δ 7.41 – 7.27 (m, 5H), 5.17 (s, 2H), 3.83 (s, 2H), 2.52 – 2.34 (m, 2H), 2.10 – 1.90 (m, 4H). ¹³C NMR (101 MHz, CDCl₃) δ 135.9, 128.6, 128.2, 127.9, 66.6, 66.4, 48.1, 26.7, 15.9. ESI-TOF m/z for **7d**: Calcd for [M+Na⁺] C₁₃H₁₆O₃Na: 243.0997, found [M+Na⁺]: 243.0996.

Benzyl 1-(hydroxymethyl)cyclopentane-1-carboxylate (**7e**)



The title compound was prepared using KPHMT I202A following the procedure described for **7a**. The product **7e** was obtained as an oil (254 mg, 54%). ¹H NMR (400 MHz, CDCl₃) δ 7.43 – 7.27 (m, 5H), 5.14 (s, 2H), 3.58 (s, 2H), 2.07 – 1.91 (m, 2H), 1.82 – 1.39 (m, 2H). ¹³C NMR (101 MHz, CDCl₃) δ 177.9, 135.9, 128.6, 128.2, 127.8, 67.3, 66.4, 54.9, 33.5, 25.8. ESI-TOF m/z for **7e**: Calcd for [M+Na⁺] C₁₄H₁₈O₃Na: 257.1154, found [M+Na⁺]: 257.1159.

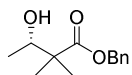
Benzyl 1-(hydroxymethyl)cycloheptane-1-carboxylate (**7f**)



The title compound was prepared using KPHMT I212A/I202A following the procedure described for **7a**. The product **7f** was obtained as an oil (100 mg, 13%). ¹H NMR (400 MHz, CDCl₃) δ 7.43 – 7.27 (m, 5H), 5.15 (s, 2H), 3.55 (s, 2H), 2.05 – 1.92 (m, 2H), 1.66 –

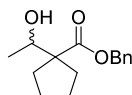
1.40 (m, 10H). ^{13}C NMR (101 MHz, CDCl_3) δ 177.7, 136.0, 128.6, 128.2, 127.8, 67.9, 66.4, 51.3, 32.6, 30.8, 23.5. ESI-TOF m/z for **7f**: Calcd for $[\text{M}+\text{Na}^+]$ $\text{C}_{16}\text{H}_{22}\text{O}_3\text{Na}$: 285.1467, found $[\text{M}+\text{Na}^+]$: 285.1478.

Benzyl 3-hydroxy-2,2-dimethylbutanoate (**7h**)



The title compound was prepared using KPHMT I202A following the procedure described for **7a**. The product **7h** was obtained as an oil (196 mg, 14%). ^1H NMR (400 MHz, CDCl_3) δ 7.40 – 7.28 (m, 5H), 5.13 (s, 2H), 3.88 (q, $J = 3 \times 6.5$ Hz, 1H), 1.19 (d, $J = 1.4$ Hz, 6H), 1.12 (d, $J = 6.4$ Hz, 3H). ^{13}C NMR (101 MHz, CDCl_3) δ 177.5, 135.9, 128.6, 128.2, 127.9, 72.4, 66.4, 47.2, 22.4, 19.7, 17.6. ESI-TOF m/z for **7h**: Calcd for $[\text{M}+\text{Na}^+]$ $\text{C}_{13}\text{H}_{18}\text{O}_3\text{Na}$: 245.1153, found $[\text{M}+\text{Na}^+]$: 245.1158.

Benzyl 1-(1-hydroxyethyl)cyclopentane-1-carboxylate (**7i**)



The title compound was prepared using KPHMT I202A following the procedure described for **7a**. The product **7i** was obtained as an oil (362 mg, 24%). ^1H NMR (400 MHz, CDCl_3) δ 7.44 – 7.25 (m, 5H), 5.14 (d, $J = 2.1$ Hz, 2H), 3.76 (q, $J = 3 \times 6.4$ Hz, 1H), 2.20 – 2.07 (m, 1H), 2.05 – 1.95 (m, 1H), 1.90 – 1.79 (m, 1H), 1.73 – 1.58 (m, 2H), 1.55 – 1.41 (m, 1H), 1.12 (d, $J = 6.4$ Hz, 3H). ^{13}C NMR (101 MHz, CDCl_3) δ 177.3, 135.8, 128.6, 128.3, 128.0, 72.6, 66.5, 59.0, 34.1, 32.8, 26.0, 25.6, 19.4. ESI-TOF m/z for **7i**: Calcd for $[\text{M}+\text{Na}^+]$ $\text{C}_{15}\text{H}_{20}\text{O}_3\text{Na}$: 271.1310, found $[\text{M}+\text{Na}^+]$: 271.1302.

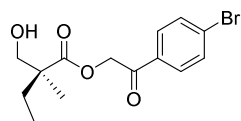
5.7.3.2 Bromophenyl esters derivatives

2-(4-Bromophenyl)-2-oxoethyl (S)-2-(hydroxymethyl)-2-methylbutanoate (7b**) and 2-(4-bromophenyl)-2-oxoethyl (R)-2-methylbutanoate (**R-10**)**

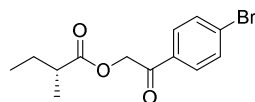
The title compounds were prepared using KPHMT wild-type following the procedure described for **7a**. The esterification was performed by diluting the mixture with DMF (10 mL) and 2,4'-dibromoacetophenone (556 mg, 2.0 mmol, 1 eq) was added. The reaction was followed by HPLC. Then, EtOAc (200 mL) was added to the reaction mixture and washed with H_2O (3x50 mL). The combined organic phases were dried over anhydrous MgSO_4 , absorbed onto

Experimental section

silica gel (100 mL) and loaded onto a silica gel column. Products were eluted with a step gradient of hexane:EtOAc: 100:0, 200 mL, 90:10, 200 mL, 80:20, 200 mL, 70:30, 200 mL, 60:40, 200mL and 50:50, 600 mL. Pure fractions were pooled and the solvent removed under vacuum affording **7b** as a solid (240 mg, 36%) and *R*-**C5** as a solid (327 mg, 54%).

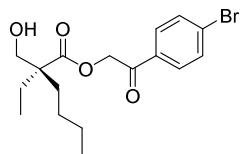


7b: $[\alpha]_D^{20} = -6.1$ ($c = 4$ in CHCl_3). Chiral HPLC analysis isocratic elution: CHIRALPAK[®] IC, hexane/isopropanol 95/5 (v/v), flow rate 1 mL min^{-1} , t_r (*S*) = 51.70, t_r (*R*) = 48.67, 81% *ee*. $^1\text{H NMR}$ (400 MHz, CDCl_3) δ 7.77 (d, $J = 8.6 \text{ Hz}$, 2H), 7.64 (d, $J = 8.5 \text{ Hz}$, 2H), 5.51 (d, $J = 16.5 \text{ Hz}$, 1H), 5.25 (d, $J = 16.5 \text{ Hz}$, 1H), 3.84 (d, $J = 11.3 \text{ Hz}$, 1H), 3.54 (d, $J = 11.4 \text{ Hz}$, 1H), 1.79 (dq, $J = 14.0, 3 \times 7.5 \text{ Hz}$, 1H), 1.52 (dq, $J = 13.9, 3 \times 7.5 \text{ Hz}$, 1H), 1.24 (s, 3H), 0.92 (t, $J = 2 \times 7.5 \text{ Hz}$, 3H). $^{13}\text{C NMR}$ (101 MHz, CDCl_3) δ 192.4, 175.8, 132.4, 132.3, 129.7, 129.3, 69.3, 65.5, 49.4, 27.9, 18.3, 8.5. ESI-TOF m/z for **5b**: Calcd for $[\text{M}+\text{Na}^+]$ $\text{C}_{14}\text{H}_{17}\text{O}_4\text{NaBr}$: 351.0207, found $[\text{M}+\text{Na}^+]$: 351.0212.



R-**C5**: Chiral HPLC analysis isocratic elution: CHIRALPAK[®] IC, hexane/isopropanol 98/2 (v/v), flow rate 1 mL min^{-1} , t_r (*S*) = 12.88, t_r (*R*) = 11.82, 67% *ee*. $^1\text{H NMR}$ (400 MHz, CDCl_3) δ 7.76 (d, $J = 8.6 \text{ Hz}$, 2H), 7.62 (d, $J = 8.6 \text{ Hz}$, 2H), 5.26 (s, 2H), 2.54 (h, $J = 4 \times 7.0 \text{ Hz}$, 1H), 1.77 (ddt, $J = 14.8, 13.8, 2 \times 7.4 \text{ Hz}$, 1H), 1.61 – 1.46 (m, 1H), 1.22 (d, $J = 7.0 \text{ Hz}$, 3H), 0.96 (t, $J = 2 \times 7.4 \text{ Hz}$, 3H). $^{13}\text{C NMR}$ (101 MHz, CDCl_3) δ 191.5, 176.1, 133.0, 132.2, 129.2, 129.0, 65.5, 40.8, 26.7, 16.6, 11.5. ESI-TOF m/z for *R*-**C5**: Calcd for $[\text{M}+\text{Na}^+]$ $\text{C}_{13}\text{H}_{15}\text{O}_3\text{NaBr}$: 321.0102, found $[\text{M}+\text{Na}^+]$: 321.0122.

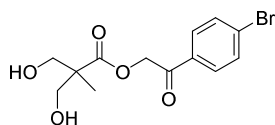
2-(4-bromophenyl)-2-oxoethyl (S)-2-ethyl-2-(hydroxymethyl)hexanoate (**7c**)



The title compound was prepared using KPHMT I202A/V214G following the procedure described for **7b**, affording **7c** as a solid (382 mg, 25%). $[\alpha]_D^{20} = +4.0$ ($c = 4$ in MeOH). $^1\text{H NMR}$ (400 MHz, CDCl_3) δ 7.82 (d, J

= 8.4 Hz, 2H), 7.68 (d, $J = 8.5$ Hz, 2H), 5.42 (d, $J = 2.1$ Hz, 2H), 3.78 (s, 2H), 1.75 (qd, $J = 7.3, 7.2, 7.2, 4.7$ Hz, 2H), 1.67 (m, 2H), 1.41 – 1.30 (m, 3H), 1.30 – 1.27 (m, 1H), 0.93 (q, $J = 7.5, 7.1, 7.1$ Hz, 6H). ^{13}C NMR (101 MHz, CDCl_3) δ 192.5, 175.8, 132.5, 132.4, 132.4, 129.7, 129.4, 129.3, 66.1, 65.5, 52.3, 30.6, 25.9, 24.0, 23.3, 14.0, 8.1. ESI-TOF m/z for **7c**: Calcd for $[\text{M}+\text{Na}^+]$ $\text{C}_{17}\text{H}_{23}\text{O}_4\text{NaBr}$: 393.0677, found $[\text{M}+\text{Na}^+]$: 393.0668.

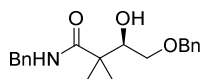
2-(4-Bromophenyl)-2-oxoethyl 3-hydroxy-2-(hydroxymethyl)-2-methylpropanoate (7g)



The title compound was prepared using KPHMT I202A following the procedure described for **7b**, affording **7g** as a solid (311 mg, 48%). ^1H NMR (400 MHz, CD_3OD) δ 7.87 (d, $J = 8.6$ Hz, 2H), 7.70 (d, $J = 8.6$ Hz, 2H), 5.43 (s, 2H), 3.79 – 3.66 (m, 2H), 1.22 (s, 3H). ^{13}C NMR (101 MHz, CD_3OD) δ 192.7, 174.4, 132.9, 131.9, 129.3, 128.6, 65.9, 64.4, 15.9. ESI-TOF m/z for **7g**: Calcd for $[\text{M}+\text{Na}^+]$ $\text{C}_{13}\text{H}_{15}\text{O}_5\text{NaBr}$: 353.0001, found $[\text{M}+\text{Na}^+]$: 353.0009.

5.7.3.3 Amide derivatives

***N*-Benzyl-4-(benzyloxy)-3-hydroxy-2,2-dimethylbutanamide (7j)**



The title compound was prepared using KPHMT wild-type following the procedure described for **7a**. After the decarboxylation and evaporation of MeOH, 100 mL of a saturated solution of bicarbonate was added and washed with EtOAc (3x50 mL). The aqueous phase was acidified to pH 2 with HCl 1M, saturated with NaCl and then extracted with EtOAc (3x50 mL). The organic phase was dried over anhyd MgSO_4 and the solvent removed under vacuum.

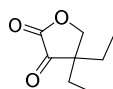
Amidation was performed by diluting the mixture with anh. DMF (80 mL) and cooled to 4°C. HOBt (4.5 mmol, 608 mg, 1.5 eq), EDAC (4.5 mmol, 862 mg, 1.5 eq), benzylamine (3.6 mmol, 385 mg, 1.2 eq) and triethylamine (9 mmol, 910 mg, 3 eq) were added. Reaction was performed over night at 4 °C. Then, the reaction mixture was diluted with AcOEt (300 mL) and washed with citric

Experimental section

acid solution 5% (3x100 mL), bicarbonate solution 5% (3x100 mL) and brine (3x100 mL). The organic phase was dried over anhyd MgSO₄, absorbed onto silica gel (100 mL) and loaded onto a silica gel column. Product was eluted with a step gradient of hexane:EtOAc: 100:0, 500 mL, 90:10, 300 mL, 80:20, 300 mL, 70:30, 300 mL, 60:40, 300 mL and 50:50, 600 mL. Pure fractions were pooled and the solvent removed under vacuum. Two products were detected by NMR and HPLC thus the mixture was reabsorbed onto a KP-C18-HS SNAP Cartridge and purified by Isolera Biotage with step gradient (solvent system used was A: H₂O and B: H₂O:CH₃CN 20:80): 30% of B (3 VC), 30-70% of B (10 VC) and 70% of B (2 VC). After the purification the pure fractions were collected and the solvent removed under vacuum affording the pure compound **7j** as an oil (197 mg, 20%). ¹H NMR (400 MHz, CDCl₃) δ 7.39 – 7.17 (m, 10H), 4.49 (d, *J* = 2.1 Hz, 2H), 4.39 (d, *J* = 5.7 Hz, 2H), 3.77 (dd, *J* = 8.9, 3.0 Hz, 1H), 3.62 (dd, *J* = 9.6, 3.0 Hz, 1H), 3.36 (t, *J* = 2x9.2 Hz, 1H), 1.28 (s, 3H), 1.14 (s, 3H). ¹³C NMR (101 MHz, CDCl₃) δ 176.3, 138.6, 137.6, 128.6, 128.5, 127.9, 127.8, 127.6, 127.3, 75.8, 73.5, 70.9, 43.9, 43.3, 24.4, 21.6. ESI-TOF *m/z* for **7j**: Calcd for [M+Na⁺] C₂₀H₂₅NO₃Na: 350.1732, found [M+Na⁺]: 350.1724.

5.7.4 Enzymatic synthesis of products **8a–g**

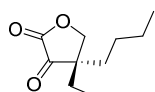
4,4-Diethyldihydrofuran-2,3-dione (**8a**)



Typical procedure: The reaction (25 mL total volume) was conducted at room temperature in a round-bottom flask (250 mL) with magnetic stirring (250 rpm). To a solution of KPHMT I202A (6.5 mL of a 7.7 mg mL⁻¹ stock glycerinated protein solution, 2 mg mL⁻¹ in the reaction, 0.068 mol%), sodium 3-ethyl-2-oxopentanoate (**1o**, 2.5 mL of a 1 M stock solution pH 7.0, 2.5 mmol, 0.1 M in the reaction), plain water (15.7 mL) and CoCl₂ (75 μL of a 0.1 M stock solution, 0.3 mM in the reaction) were added. The reaction was started by adding formaldehyde (**2a**, 188 μL of a 13.3 M commercial solution, 2.5 mmol, 1 eq, 0.1 M in the reaction). After 24 h the reaction mixture was diluted with methanol (200 mL), filtered through Celite®

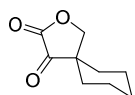
and the pellet was washed with methanol (3x50 mL). Once the MeOH was removed under vacuum, plain water (300 mL) was added. The aqueous phase was acidified to pH 2 with HCl 1 M, saturated with NaCl and extracted with Et₂O (3x100 mL). The organic phases were pooled and washed with NaH₂PO₄ 50 mM pH 7.2 (3x50 mL) to remove the starting substrate. The organic phase was dried over anhydrous MgSO₄ and the solvent removed under vacuum affording **8a** as an oil (112 mg, 26%). ¹H NMR (401 MHz, CDCl₃) δ 4.47 (s, 2H), 1.75 – 1.58 (m, 4H), 0.89 (t, *J* = 2x7.5 Hz, 6H). ¹³C NMR (101 MHz, CDCl₃) δ 198.5, 160.6, 73.4, 48.9, 27.0, 7.8. ESI-TOF *m/z* for **8a**: Calcd for [M+Na⁺] C₈H₁₂O₃Na: 179.0684, found [M+Na⁺]: 179.0688.

4-Butyl-4-ethyldihydrofuran-2,3-dione (**8b**)



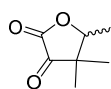
The title compound was prepared using KPHMT I202A/V214G following the procedure described for **8a**. The product **8b** was obtained as an oil (110 mg, 27%). [α]_D²⁰ = + 6.0 (*c* = 4 in MeOH). ¹H NMR (401 MHz, CDCl₃) δ 4.49 (d, *J* = 1.0 Hz, 2H), 1.79 – 1.47 (m, 4H), 1.33 – 1.15 (m, 4H), 0.90 (q, *J* = 2x7.4, 7.3 Hz, 6H). ¹³C NMR (101 MHz, CDCl₃) δ 198.6, 160.7, 74.1, 48.7, 34.0, 27.7, 25.7, 23.0, 13.7, 8.0. ESI-TOF *m/z* for **8b**: Calcd for [M+Na⁺] C₁₀H₁₆O₃Na: 207.0997, found [M+Na⁺]: 207.0990.

2-Oxaspiro[4.5]decane-3,4-dione (**8c**)



The title compound was prepared using KPHMT I212A following the procedure described for **8a**. The product **8c** was obtained as a white solid (71 mg, 19%). ¹H NMR (401 MHz, CDCl₃) δ 4.49 (s, 2H), 1.82 – 1.71 (m, 2H), 1.69 – 1.51 (m, 6H), 1.46 – 1.22 (m, 2H). ¹³C NMR (101 MHz, CDCl₃) δ 197.5, 160.9, 74.9, 31.3, 24.6, 21.4. ESI-TOF *m/z* for **8c**: Calcd for [M+Na⁺] C₉H₁₂O₃Na: 191.0684, found [M+Na⁺]: 191.0691.

4,4,5-Trimethyldihydrofuran-2,3-dione (**8d**)

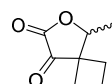


The title compound was prepared using KPHMT wild-type following the procedure described for **8a**. The product **8d** was obtained as a white solid (50 mg, 11%). [α]_D²⁰ = 0 (*c* = 4 in MeOH). ¹H NMR

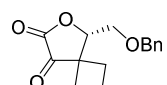
Experimental section

(399 MHz, CDCl₃) δ 4.59 (q, $J = 3 \times 6.6$ Hz, 1H), 1.42 (d, $J = 6.6$ Hz, 3H), 1.25 (s, 3H), 1.11 (s, 3H). ¹³C NMR (100 MHz, CDCl₃) δ 198.8, 160.5, 82.2, 45.9, 20.8, 17.9, 16.0. ESI-TOF m/z for **8d**: Calcd for [M+Na⁺] C₇H₁₀O₃Na: 165.0528, found [M+Na⁺]: 165.0536.

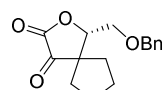
5-Methyl-6-oxaspiro[3.4]octane-7,8-dione (**8e**)

 The title compound was prepared using KPHMT I212A following the procedure described for **8a**. The product **8e** was obtained as a white solid (390 mg, 76%). $[\alpha]^{20}_D = 0$ ($c = 4$ in MeOH). ¹H NMR (400 MHz, CDCl₃) δ 4.80 (q, $J = 3 \times 6.6$ Hz, 1H), 2.49 – 2.35 (m, 1H), 2.33 – 2.20 (m, 3H), 2.20 – 2.10 (m, 1H), 2.01 – 1.90 (m, 1H), 1.48 (d, $J = 6.6$ Hz, 3H). ¹³C NMR (101 MHz, CDCl₃) δ 197.3, 160.2, 81.5, 51.0, 30.0, 25.7, 18.1, 15.3. ESI-TOF m/z for **8e**: Calcd for [M+Na⁺] C₈H₁₀O₃Na: 177.0613, found [M+Na⁺]: 177.0601.

5-((Benzyloxy)methyl)-6-oxaspiro[3.4]octane-7,8-dione (**8f**)

 The title compound was prepared using KPHMT I212A following the procedure described for **8a**. The product **8f** was obtained as a white solid (144 mg, 32%). $[\alpha]^{20}_D = +12.2$ ($c = 4$ in MeOH). ¹H NMR (401 MHz, CDCl₃) δ 7.38 – 7.19 (m, 5H), 4.83 (t, $J = 2 \times 1.8$ Hz, 1H), 4.50 (d, $J = 12.2$ Hz, 1H), 4.36 (d, $J = 12.2$ Hz, 1H), 3.67 (t, $J = 2 \times 1.7$ Hz, 2H), 2.66 – 2.35 (m, 1H), 2.30 – 2.07 (m, 3H), 2.03 – 1.82 (m, 2H). ¹³C NMR (101 MHz, CDCl₃) δ 196.0, 160.7, 136.5, 128.5, 128.0, 127.6, 84.1, 73.6, 67.0, 49.4, 33.1, 24.0, 15.0. ESI-TOF m/z for **8f**: Calcd for [M+Na⁺] C₁₅H₁₆O₄Na: 283.0946, found [M+Na⁺]: 283.0955.

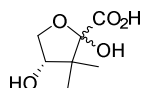
1-((Benzyloxy)methyl)-2-oxaspiro[4.4]nonane-3,4-dione (**8g**)

 The title compound was prepared using KPHMT I202A following procedure described for **8a**. The product **8g** was obtained as a white solid (88 mg, 21%). $[\alpha]^{20}_D = +21.6$ ($c = 4$ in MeOH). ¹H NMR (401 MHz, CDCl₃) δ 7.42 – 7.15 (m, 5H), 4.65 (t, $J = 2 \times 1.8$ Hz, 1H), 4.54 (d, $J = 12.2$ Hz, 1H), 4.42 (d, $J = 12.2$ Hz, 1H), 3.66 (qd, $J = 3 \times 10.8$, 1.7 Hz,

2H), 2.22 (m, 1H), 1.94 (m, 1H), 1.92 – 1.76 (m, 3H), 1.75 – 1.58 (m, 2H), 1.57 – 1.46 (m, 1H). ^{13}C NMR (101 MHz, CDCl_3) δ 195.2, 161.4, 136.5, 128.5, 128.1, 127.6, 84.9, 73.8, 68.0, 56.4, 38.0, 29.3, 25.5, 25.2. ESI-TOF m/z for **8g**: Calcd for $[\text{M}+\text{Na}^+]$ $\text{C}_{16}\text{H}_{18}\text{O}_4\text{Na}$: 297.1103, found $[\text{M}+\text{Na}^+]$: 297.1115.

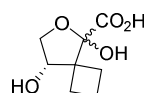
5.7.5 Enzymatic synthesis of products 9a–q

(4S)-2,4-Dihydroxy-3,3-dimethyltetrahydrofuran-2-carboxylic acid (9a)



Typical procedure: The aldol addition reaction was performed as described for the product **4a**. Once the methanol was removed under vacuum, the aqueous residue was purified by ionic exchange chromatography. The purification was performed on Macro-Prep High Q (25 mL, BioRad) stationary phase in HCO_2^- form, packed into a glass column (C16/20, GE S11 Healthcare Life Science). Crude fraction at pH 9 (30 mL, adjusted with NaOH 1 M) was loaded onto the column at 1 mL min^{-1} . The column was washed with water (150 mL) at 3 mL min^{-1} . Product was eluted using a gradient from 0 to 100% of formic acid (1 M) in 150 mL and formic acid (1 M) 90 mL at 3 mL min^{-1} . Typical fraction size was 30 mL. Fractions were lyophilized and analyzed by ^1H NMR. The product **9a** was obtained as an oil (221 mg, 84%). $[\alpha]_D^{20} = 0$ ($c = 5$ in H_2O). **α -anomer**: ^1H NMR (400 MHz, D_2O) δ 4.37 (m, 1H overlapped), 4.07 (dd, $J = 5.3, 2.0$ Hz, 1H), 3.96 (dd, $J = 10.2, 2.0$ Hz, 1H), 1.22 (s, 3H), 0.96 (s, 3H). ^{13}C NMR (101 MHz, D_2O) δ 172.5, 105.8, 78.2, 73.4, 48.1, 22.2, 15.5. **β -anomer**: ^1H NMR (400 MHz, D_2O) δ 4.36 (m, 1H overlapped), 4.27 (dd, $J = 8.8, 7.5$ Hz, 1H), 3.73 (dd, $J = 8.8, 7.1$ Hz, 1H), 1.17 (s, 3H), 0.93 (s, 3H). ^{13}C NMR (101 MHz, D_2O) δ 172.8, 106.0, 76.2, 70.0, 46.6, 19.4, 16.4. ESI-TOF m/z for **9a**: Calcd for $[\text{M}+\text{Na}^+]$ $\text{C}_7\text{H}_{12}\text{O}_5\text{Na}$: 199.0582, found $[\text{M}+\text{Na}^+]$: 199.0575.

(8S)-5,8-Dihydroxy-6-oxaspiro[3.4]octane-5-carboxylic acid (9b)



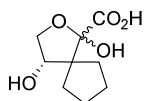
The title compound was prepared using KPHMT wild-type following the procedure described for **9a**. The product **9b** was obtained as an oil (281 mg, 90%). $[\alpha]_D^{20} = +17.8$ ($c = 5$ in H_2O). **α -anomer**: ^1H

Experimental section

NMR (400 MHz, D₂O) δ 4.46 (m, 1H overlapped), 4.16 (d, $J = 4.1$ Hz, 1H), 4.02 (dd, $J = 10.0, 1.5$ Hz, 1H), 2.30 (m, 1H), 2.18 (dd, $J = 7.6, 3.6$ Hz, 1H), 1.95 (m, 1H overlapped), 1.93 (m, 1H overlapped), 1.78 (m, 1H overlapped), 1.75 (m, 1H overlapped). ¹³C NMR (101 MHz, D₂O) δ 173.0, 105.3, 76.4, 73.3, 53.9, 28.2, 21.6, 14.6. **β -anomer:** ¹H NMR (400 MHz, D₂O) δ 4.46 (m, 1H overlapped), 4.13 (dd, $J = 4.1, 0.8$ Hz, 1H), 3.82 (dd, $J = 9.6, 2.8$ Hz, 1H), 2.42 (m, 1H), 2.12 (m, 1H), 1.95 (m, 1H overlapped), 1.90 (m, 1H overlapped), 1.78 (m, 1H overlapped), 1.73 (m, 1H overlapped). ¹³C NMR (101 MHz, D₂O) δ 174.0, 104.5, 76.4, 71.7, 53.7, 25.7, 22.5, 15.1. ESI-TOF m/z for **7b**: Calcd for [M+Na⁺] C₈H₁₂O₅Na: 211.0582, found [M+Na⁺]: 211.0578.

Minor products: **(R)-5-(Hydroxymethyl)-6-oxaspiro[3.4]octane-7,8-dione:** ¹H NMR (400 MHz, D₂O) δ 5.15 (t, $J = 2 \times 2.2$ Hz, 1H), 3.95 (m, 2H), 2.53 – 1.71 (overlapped region, 6H). ¹³C NMR (101 MHz, D₂O) δ 194.5, 163.3, 86.8, 59.3, 49.5, 33.77 – 13.90 (overlapped region, 3C). **(R)-8,8-Dihydroxy-5-(hydroxymethyl)-6-oxaspiro[3.4]octan-7-one:** ¹H NMR (400 MHz, D₂O) δ 4.60 (dd, $J = 8.3, 2.7$ Hz, 1H), 4.10 (d, $J = 2.7$ Hz, 1H), 3.93 (d, $J = 4.4$ Hz, 1H), 2.53 – 1.71 (overlapped region, 6H). ¹³C NMR (101 MHz, D₂O) δ 175.8, 94.4, 86.4, 60.7, 49.2, 33.77 – 13.90 (overlapped region, 3C).

(4S)-1,4-Dihydroxy-2-oxaspiro[4.4]nonane-1-carboxylic acid (9c)

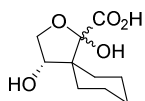


The title compound was prepared using KPHMT I202A following the procedure described for **9a**. The product **9c** was obtained as a white solid (231 mg, 76%). $[\alpha]_D^{20} = +9.3$ ($c = 5$ in H₂O). **α -anomer:** ¹H NMR (400 MHz, D₂O) δ 4.26 (dt, $J = 10.4, 2 \times 5.2$ Hz, 1H), 4.04 (m, 1H), 4.02 (d, $J = 1.2$ Hz, 1H), 2.00 (m, 1H overlapped), 1.85 (m, 1H overlapped), 1.74 – 1.57 (overlapped region, 4H), 1.42 (m, 1H), 1.35 (m, 1H overlapped). ¹³C NMR (101 MHz, D₂O) δ 172.6, 106.2, 77.1, 74.1, 60.4, 33.1, 26.5, 24.6, 24.2. **β -anomer:** ¹H NMR (400 MHz, D₂O) δ 4.27 (dt, $J = 10.4, 2 \times 5.2$ Hz, 1H), 4.21 (m, 1H), 3.73 (dd, $J = 9.0, 4.5$ Hz, 1H), 2.09 (m, 1H overlapped), 1.87 (m, 1H overlapped), 1.74 – 1.57 (overlapped region, 4H), 1.52 (m, 1H overlapped), 1.36 (m, 1H overlapped). ¹³C NMR (101 MHz, D₂O)

δ 174.3, 105.7, 76.8, 71.7, 58.6, 31.4, 27.4, 25.0, 24.7. ESI-TOF m/z for **9c**: Calcd for $[M+Na^+]$ $C_9H_{14}O_5Na$: 225.0739, found $[M+Na^+]$: 225.0741.

Minor products: **(R)-1-(Hydroxymethyl)-2-oxaspiro[4.4]nonane-3,4-dione**: 1H NMR (400 MHz, D_2O) δ 4.96 (t, $J = 2 \times 1.9$ Hz, 1H), 3.89 (d, $J = 1.9$ Hz, 2H), 2.07 (m, 1H overlapped), 1.98 (m, 1H overlapped), 1.90 (m, 1H), 1.82 (m, 1H overlapped), 1.74 – 1.57 (overlapped region, 4H). ^{13}C NMR (101 MHz, D_2O) δ 198.4, 163.4, 87.8, 60.0, 56.5, 37.35, 29.0, 25.2, 24.9. **(R)-4,4-Dihydroxy-1-(hydroxymethyl)-2-oxaspiro[4.4]nonan-3-one**: 1H NMR (400 MHz, D_2O) δ 4.51 (dd, $J = 6.8, 4.5$ Hz, 1H), 3.86 (m, 2H), 1.97 (m, 1H overlapped), 1.68 (m, 1H overlapped), 1.76 – 1.57 (overlapped region, 4H), 1.58 (m, 1H overlapped), 1.54 (m, 1H overlapped). ^{13}C NMR (101 MHz, D_2O) δ 176.1, 95.2, 87.7, 60.7, 55.6, 29.7, 26.5, 24.9, 24.3.

(4S)-1,4-dihydroxy-2-oxaspiro[4.5]decane-1-carboxylic acid (9d)

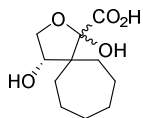


The title compound was prepared using KPHMT I212A following the procedure described for **9a**. The product **9d** was obtained as a white solid (192 mg, 52%). $[\alpha]^{20}_D = +12.1$ ($c = 5$ in H_2O). **α -anomer**: 1H NMR (400 MHz, D_2O) δ 4.49 (d, $J = 4.8$ Hz, 1H), 4.39 (dd, $J = 10.3, 5.0$ Hz, 1H), 4.01 (dd, $J = 10.3, 1.2$ Hz, 1H), 2.05 (dt, $J = 14.1, 2 \times 2.9$ Hz, 1H), 1.71 (m, 1H overlapped), 1.69 (m, 1H overlapped), 1.64 (m, 1H overlapped), 1.44 (m, 1H overlapped), 1.43 (m, 1H overlapped), 1.36 (m, 1H overlapped), 1.34 (m, 1H overlapped), 1.18 (m, 1H overlapped), 1.16 (m, 1H overlapped). ^{13}C NMR (101 MHz, D_2O) δ 172.1, 106.5, 74.3, 72.9, 55.9, 30.7, 29.8, 25.0, 24.7, 21.9. ESI-TOF m/z for **9d**: Calcd for $[M+Na^+]$ $C_{10}H_{16}O_5Na$: 239.0895, found $[M+Na^+]$: 239.0892.

Minor product: **1-(Hydroxymethyl)-2-oxaspiro[4.5]decane-3,4-dione**: 1H NMR (400 MHz, D_2O) δ 5.00 (m, 1H), 3.94 (m, 2H), 1.80 – 1.09 (overlapped region, 10H). ^{13}C NMR (101 MHz, D_2O) δ 198.2, 163.3, 58.7, 50.13, 31.80 – 19.96 (overlapped region, 6C).

Experimental section

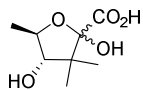
(4S)-1,4-Dihydroxy-2-oxaspiro[4.6]undecane-1-carboxylic acid (9e)



The title compound was prepared using KPHMT I212A following the procedure described for **9a**. The product **9e** was obtained as a white solid (113 mg, 33%). $[\alpha]^{20}_D = +8.7$ ($c = 5$ in H₂O). **α -anomer:** ¹H NMR (400 MHz, D₂O) δ 4.30 (dd, $J = 10.2, 4.8$ Hz, 1H), 4.18 (d, $J = 4.7$ Hz, 1H), 3.98 (dd, $J = 10.2, 1.1$ Hz, 1H), 2.13 (dd, $J = 15.0, 8.9$ Hz, 1H), 1.75 (m, 1H overlapped), 1.72 (m, 1H overlapped), 1.70 (m, 2H overlapped), 1.66 (m, 1H overlapped), 1.52 (m, 1H overlapped), 1.39 (m, 2H overlapped), 1.38 (m, 2H overlapped), 1.35 (m, 1H overlapped). ¹³C NMR (101 MHz, D₂O) δ 172.6, 105.8, 77.7, 73.9, 55.9, 45.9, 33.1, 30.7, 26.0, 23.1, 22.5. ESI-TOF m/z for **9e**: Calcd for $[M+Na^+]$ C₁₁H₁₈O₅Na: 253.1051, found $[M+Na^+]$: 253.1056.

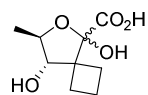
Minor product: **1-(hydroxymethyl)-2-oxaspiro[4.6]undecane-3,4-dione:** ¹H NMR (400 MHz, D₂O) δ 4.94 (t, $J = 2 \times 1.9$ Hz, 1H), 3.94 (m, 2H), 1.82 – 1.26 (overlapped region, 12H). Identified signals: ¹³C NMR (101 MHz, D₂O) δ 198.2, 164.0, 87.1, 59.1.

(4S,5R)-2,4-Dihydroxy-3,3,5-trimethyltetrahydrofuran-2-carboxylic acid (9f)



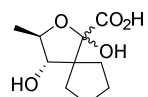
The title compound was prepared using KPHMT wild-type following the procedure described for **9a**. The product **9f** was obtained as a colorless solid (169 mg, 61%). $[\alpha]^{20}_D = -30.4$ ($c = 5$ in H₂O). **β -anomer:** ¹H NMR (400 MHz, D₂O) δ 4.02 (dq, $J = 8.3, 3 \times 6.2$ Hz, 1H), 3.87 (d, $J = 8.3$ Hz, 1H), 1.37 (d, $J = 6.2$ Hz, 3H), 1.16 (s, 3H), 0.93 (s, 3H). ¹³C NMR (101 MHz, D₂O) δ 172.6, 105.0, 81.8, 77.8, 47.2, 19.3, 19.1, 16.2. **α -anomer:** ¹H NMR (400 MHz, D₂O) δ 4.12 (p, $J = 4 \times 6.3$ Hz, 1H), 3.69 (d, $J = 5.6$ Hz, 1H), 1.40 (d, $J = 6.5$ Hz, 3H), 1.11 (s, 3H), 1.01 (s, 3H). ¹³C NMR (101 MHz, D₂O) δ 173.0, 105.0, 82.6, 79.7, 47.5, 22.8, 18.2, 15.7. ESI-TOF m/z for **9f**: Calcd for $[M+Na^+]$ C₈H₁₄O₅Na: 213.0739, found $[M+Na^+]$: 213.0714.

(7*R*,8*S*)-5,8-Dihydroxy-7-methyl-6-oxaspiro[3.4]octane-5-carboxylic acid (9g)



The title compound was prepared using KPHMT I212A following the procedure described for **9a**. The product **9g** was obtained as an oil (194 mg, 72%). $[\alpha]^{20}_{\text{D}} = -15.6$ ($c = 5$ in H_2O). **β -anomer:** ^1H NMR (400 MHz, D_2O) δ 3.97 (d, $J = 7.7$ Hz, 1H), 3.86 (qd, $J = 2 \times 7.2, 6.7, 5.7$ Hz, 1H), 2.45 (m, 1H), 2.27 (m, 1H), 2.02 (m, 1H overlapped), 1.91 (m, 1H overlapped), 1.79 (m, 1 overlapped), 1.80 (m, 1 overlapped), 1.32 (dd, $J = 6.3, 3.2$ Hz, 3H). ^{13}C NMR (101 MHz, D_2O) δ 173.3, 104.2, 80.2, 77.7, 52.7, 24.9, 22.5, 18.4, 14.5. **α -anomer:** ^1H NMR (400 MHz, D_2O) δ 4.06 (m, 1H overlapped), 4.03 (m, 1H overlapped), 2.30 (m, 1H), 2.17 (m, 1H), 2.05 (m, 1H overlapped), 1.93 (m, 1H overlapped), 1.91 (m, 1H overlapped), 1.80 (m, 1H overlapped), 1.32 (dd, $J = 6.3, 3.2$ Hz, 3H). ^{13}C NMR (101 MHz, D_2O) δ 172.9, 104.4, 81.4, 79.7, 53.1, 28.2, 21.3, 17.9, 14.8. ESI-TOF m/z for **9g**: Calcd for $[\text{M}+\text{Na}^+]$ $\text{C}_9\text{H}_{14}\text{O}_5\text{Na}$: 225.0739, found $[\text{M}+\text{Na}^+]$: 225.0736.

(3*R*,4*S*)-1,4-Dihydroxy-3-methyl-2-oxaspiro[4.4]nonane-1-carboxylic acid (9h)

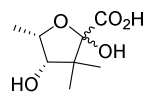


The title compound was prepared using KPHMT I212A following the procedure described for **9a**. The product **9h** was obtained as a colorless oil (143 mg, 50%). $[\alpha]^{20}_{\text{D}} = -20.3$ ($c = 5$ in H_2O). **β -anomer:** ^1H NMR (400 MHz, D_2O) δ 4.02 (d, $J = 8.3$ Hz, 1H), 3.88 (dq, $J = 8.1, 3 \times 6.2$ Hz, 1H), 2.16 (dt, $J = 13.4, 2 \times 6.7$ Hz, 1H), 1.85 (m, 1H overlapped), 1.66 (m, 1H overlapped), 1.63 (m, 1H overlapped), 1.61 (m, 1H overlapped), 1.57 (m, 1H overlapped), 1.54 (m, 1H overlapped), 1.37 (m, 1H overlapped), 1.34 (d, $J = 6.2$ Hz, 3H). ^{13}C NMR (101 MHz, D_2O) δ 173.1, 104.8, 82.1, 77.6, 58.6, 31.4, 26.9, 25.8, 25.1, 18.9. **α -anomer:** ^1H NMR (400 MHz, D_2O) δ 4.14 (qd, $J = 6.6, 2 \times 6.5, 4.4$ Hz, 1H), 3.74 (d, $J = 4.5$ Hz, 1H), 1.92 (m, 1H), 1.87 (m, 1H overlapped), 1.62 (m, 4H overlapped), 1.54 (m, 1H overlapped), 1.49 (m, 1H overlapped), 1.39 (d, $J = 6.6$ Hz, 3H). ^{13}C NMR (101 MHz, D_2O) δ 172.6, 106.2, 77.1, 74.1, 60.4, 34.5, 25.8, 24.3, 24.1, 18.4. ESI-

Experimental section

TOF m/z for **9h**: Calcd for $[M+Na^+]$ $C_{10}H_{16}O_5Na$: 239.0895, found $[M+Na^+]$: 239.0898.

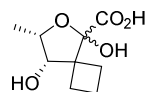
(4*S*,5*S*)-2,4-Dihydroxy-3,3,5-trimethyltetrahydrofuran-2-carboxylic acid (**9i**)



The title compound was prepared using KPHMT wild-type following the procedure described for **9a**. The product **9i** was obtained as a colorless solid (205 mg, 72%). $[\alpha]_D^{20} = +27.3$ ($c = 5$ in H_2O). **β -anomer**: 1H NMR (400 MHz, D_2O) δ 4.57 (m, 1H overlapped), 3.84 (d, $J = 4.2$ Hz, 1H), 1.31 (d, $J = 6.4$ Hz, 3H), 1.24 (s, 3H), 1.03 (s, 3H). ^{13}C NMR (101 MHz, D_2O) δ 172.6, 105.3, 79.8, 78.5, 49.3, 21.9, 16.5, 15.1. **α -anomer**: 1H NMR (400 MHz, D_2O) δ 4.57 (m, 1H overlapped), 4.05 (d, $J = 5.8$ Hz, 1H), 1.25 (d, $J = 6.6$ Hz, 3H), 1.18 (s, 3H), 1.01 (s, 3H). ^{13}C NMR (101 MHz, D_2O) δ 173.3, 105.2, 79.2, 76.5, 47.9, 21.1, 17.8, 14.6. ESI-TOF m/z for **9i**: Calcd for $[M+Na^+]$ $C_8H_{14}O_5Na$: 213.0739, found $[M+Na^+]$: 213.0729.

Minor products: (*S*)-5-((*S*)-1-hydroxyethyl)-4,4-dimethyldihydrofuran-2,3-dione: 1H NMR (400 MHz, D_2O) δ 4.68 (d, $J = 1.1$ Hz, 1H), 4.16 (m, 1H), 1.34 – 1.28 (m, 9H overlapped). ^{13}C NMR (101 MHz, D_2O) δ 198.6, 163.4, 89.9, 64.8, 45.8, 22.8, 18.5, 18.4. (*S*)-3,3-dihydroxy-5-((*S*)-1-hydroxyethyl)-4,4-dimethyldihydrofuran-2(3*H*)-one 1H NMR (400 MHz, D_2O) δ 4.18 (m, 1H), 4.00 (m, 1H), 1.32 (m, 3H overlapped), 1.16 (s, 3H), 0.96 (s, 3H). ^{13}C NMR (101 MHz, D_2O) δ 96.3, 90.1, 66.2, 44.0, 18.3, 17.2, 15.2.

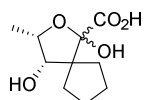
(7*S*,8*S*)-5,8-Dihydroxy-7-methyl-6-oxaspiro[3.4]octane-5-carboxylic acid (**9j**)



The title compound was prepared using KPHMT I212A following the procedure described for **9a**. The product **9j** was obtained as an oil (187 mg, 77%). $[\alpha]_D^{20} = +16.3$ ($c = 5$ in H_2O). **β -anomer**: 1H NMR (400 MHz, D_2O) δ 4.33 (m, 1H overlapped), 4.20 (s, 1H), 2.27 (m, 1H), 2.20 (m, 1H), 1.96 (m, 2H overlapped), 1.82 (m, 1H overlapped), 1.80 (m, 1H overlapped), 1.32 (d, $J = 6.5$ Hz, 3H). ^{13}C NMR (101 MHz, D_2O) δ 173.0, 103.8,

78.4, 77.8, 54.9, 28.5, 22.1, 14.7, 14.3. **α -anomer:** ^1H NMR (400 MHz, D_2O) δ 4.36 (m, 1H overlapped), 4.19 (s, 1H), 2.49 (dt, $J = 11.3, 2 \times 9.1$ Hz, 1H), 2.14 (m, 1H), 1.96 (m, 1H overlapped), 1.90 (m, 1H overlapped), 1.82 (m, 1H overlapped), 1.70 (ddd, $J = 12.1, 7.6, 3.5$ Hz, 1H), 1.28 (d, $J = 6.4$ Hz, 3H). ^{13}C NMR (101 MHz, D_2O) δ 174.0, 105.0, 78.6, 77.2, 55.0, 26.4, 23.0, 15.3, 13.5. ESI-TOF m/z for **9j**: Calcd for $[\text{M}+\text{Na}^+]$ $\text{C}_9\text{H}_{14}\text{O}_5\text{Na}$: 225.0739, found $[\text{M}+\text{Na}^+]$: 225.0733.

(3*S*,4*S*)-1,4-Dihydroxy-3-methyl-2-oxaspiro[4.4]nonane-1-carboxylic acid (7k)



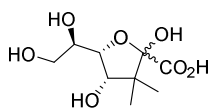
The title compound was prepared using KPHMT I212A following the procedure described for **9a**. The product **9k** was obtained as an oil (169 mg, 65%). $[\alpha]_D^{20} = +20.1$ ($c = 5$ in H_2O).

β -anomer: ^1H NMR (400 MHz, D_2O) δ 4.47 (qd, $J = 3 \times 6.5, 3.6$ Hz, 1H), 3.82 (d, $J = 3.7$ Hz, 1H), 2.09 (m, 1H overlapped), 1.87 (m, 1H overlapped), 1.71 (m, 2H overlapped), 1.61 (m, 2H overlapped), 1.48 (m, 2H overlapped), 1.33 (d, $J = 6.2$ Hz, 3H). ^{13}C NMR (101 MHz, D_2O) δ 172.6, 105.8, 79.1, 78.5, 61.4, 32.8, 27.3, 24.7, 24.0, 15.0. **α -anomer:** ^1H NMR (400 MHz, D_2O) δ 4.52 (qd, $J = 6.3, 2 \times 6.1, 3.2$ Hz, 1H), 3.84 (d, $J = 3.8$ Hz, 1H), 2.10 (m, 1H overlapped), 1.99 (m, 1H), 1.71 (m, 2H overlapped), 1.61 (m, 2H overlapped), 1.49 (m, 1H overlapped), 1.36 (m, 1H overlapped), 1.26 (d, $J = 6.4$ Hz, 3H). ^{13}C NMR (101 MHz, D_2O) δ 172.6, 105.0, 79.0, 78.0, 60.0, 31.9, 28.6, 24.3, 24.1, 14.0. ESI-TOF m/z for **9k**: Calcd for $[\text{M}+\text{Na}^+]$ $\text{C}_{10}\text{H}_{16}\text{O}_5\text{Na}$: 239.0895, found $[\text{M}+\text{Na}^+]$: 239.0893.

Minor product: **(*S*)-1-((*S*)-1-hydroxyethyl)-2-oxaspiro[4.4]nonane-3,4-dione:** ^1H NMR (400 MHz, D_2O) δ 4.82 (s, 1H), 4.18 (q, $J = 3 \times 6.6$ Hz, 1H), 2.08 (m, 1H overlapped), 1.99 (m, 1H), 1.89 (m, 1H overlapped) 1.84 (m, 3H overlapped), 1.72 (m, 1H overlapped), 1.62 (m, 1H overlapped), 1.32 (d, $J = 6.2$ Hz, 3H). ^{13}C NMR (101 MHz, D_2O) δ 197.5, 164.0, 90.1, 65.6, 61.4, 37.2, 28.5, 24.9, 24.5, 18.1.

Experimental section

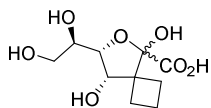
(4*S*,5*R*)-5-((*R*)-1,2-Dihydroxyethyl)-2,4-dihydroxy-3,3-dimethyl-tetrahydrofuran-2-carboxylic acid (**9l**)



The title compound was prepared using KPHMT wild type following the procedure described for **9a**. The product **9l** was obtained as a solid (229 mg, 81%). $[\alpha]^{20}_{\text{D}} = +34.0$ ($c = 5$ in H_2O). **α -anomer:** $^1\text{H NMR}$ (400 MHz, D_2O) δ 4.29 (dd, $J = 7.6, 4.4$ Hz, 1H), 3.99 (ddd, $J = 7.9, 6.7, 3.8$ Hz, 1H), 3.95 (d, $J = 4.4$ Hz, 1H), 3.77 (dd, $J = 11.8, 3.5$ Hz, 1H overlapped), 3.62 (dd, $J = 11.8, 6.5$ Hz, 1H overlapped), 1.21 (s, 3H), 0.98 (s, 3H). $^{13}\text{C NMR}$ (101 MHz, D_2O) δ 172.5, 105.6, 81.6, 78.9, 72.0, 62.6, 49.9, 21.8, 16.2. **β -anomer:** $^1\text{H NMR}$ (400 MHz, D_2O) δ 4.32 (m, 1H), 4.01 (d, $J = 4.2$ Hz, 1H), 3.97 (m, 1H), 3.77 (dd, $J = 11.8, 3.5$ Hz, 1H overlapped), 3.62 (dd, $J = 11.8, 6.5$ Hz, 1H overlapped), 1.14 (s, 3H), 1.02 (s, 3H). $^{13}\text{C NMR}$ (101 MHz, D_2O) δ 172.6, 105.8, 80.2, 79.2, 71.1, 62.6, 48.5, 21.5, 17.6. ESI-TOF m/z for **9l**: Calcd for $[\text{M}+\text{Na}^+]$ $\text{C}_9\text{H}_{16}\text{O}_8\text{Na}$: 259.0794, found $[\text{M}+\text{Na}^+]$: 259.0873.

Minor products: **(2*R*,4*S*)-2,4-dihydroxy-3,3-dimethyltetrahydrofuran-2-carboxylic acid:** $^1\text{H NMR}$ (400 MHz, D_2O) δ 4.35 (m, 1H overlapped), 4.04 (m, 1H), 3.94 (m, 1H), 1.19 (s, 3H), 0.93 (s, 3H). $^{13}\text{C NMR}$ (101 MHz, D_2O) δ 172.9, 105.9, 78.3, 73.6, 48.3, 22.2, 15.8. **(2*S*,4*S*)-2,4-dihydroxy-3,3-dimethyltetrahydrofuran-2-carboxylic acid:** $^1\text{H NMR}$ (400 MHz, D_2O) δ 4.34 (m, 1H overlapped), 4.24 (m, 1H), 3.70 (m, 1H), 1.14 (s, 3H), 0.91 (s, 3H). $^{13}\text{C NMR}$ (101 MHz, D_2O) δ 172.9, 106.1, 76.2, 70.3, 46.9, 19.5, 16.4.

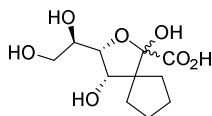
(7*R*,8*S*)-7-((*R*)-1,2-Dihydroxyethyl)-5,8-dihydroxy-6-oxaspiro[3.4]octane-5-carboxylic acid (**9m**)



The title compound was prepared using KPHMT I212A following the procedure described for **9a**. The product **9m** was obtained as a solid (270mg, 91%). $[\alpha]^{20}_{\text{D}} = +20.3$ ($c = 5$ in H_2O). **α -anomer:** $^1\text{H NMR}$ (400 MHz, D_2O) δ 4.33 (d, $J = 3.4$ Hz, 1H), 4.08 (dd, $J = 3.1, 1.9$ Hz, 1H), 4.02 (m, 1H), 3.75 (dd, $J = 5.1, 3.3$ Hz, 1H), 3.64 (m, 1H), 2.36 – 2.23 (m, 1H), 2.23 – 2.13 (m, 1H), 2.04 – 1.88 (m, 4H

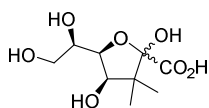
overlapped), 1.87 – 1.71 (m, 3H overlapped). ^{13}C NMR (101 MHz, D_2O) δ 173.0, 105.1, 81.6, 76.6, 71.7, 62.4, 54.9, 28.2, 21.7, 14.6. **β -anomer**: ^1H NMR (400 MHz, D_2O) δ 4.30 (d, $J = 2.7$ Hz, 1H), 4.10 (dd, $J = 3.1, 2.1$ Hz, 1H), 3.98 (m, 1H), 3.79 (dd, $J = 5.0, 3.3$ Hz, 1H), 3.63 (m, 1H), 2.57 – 2.44 (m, 1H), 2.15 – 2.06 (m, 1H), 2.04 – 1.88 (m, 4H overlapped), 1.87 – 1.71 (m, 3H overlapped), 1.70 – 1.62 (m, 1H). ^{13}C NMR (101 MHz, D_2O) δ 174.4, 103.9, 80.9, 77.1, 71.2, 62.3, 55.0, 26.2, 22.6, 15.2. ESI-TOF m/z for **9m**: Calcd for $[\text{M}+\text{Na}^+]$ $\text{C}_{10}\text{H}_{16}\text{O}_7\text{Na}$: 271.0794, found $[\text{M}+\text{Na}^+]$: 271.0789.

(3*R*,4*S*)-3-((*R*)-1,2-Dihydroxyethyl)-1,4-dihydroxy-2-oxaspiro[4.4]nonane-1-carboxylic acid (9n)



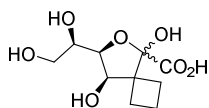
The title compound was prepared using KPHMT I212A following the procedure described for **9a**. The product **9n** was obtained as a solid (192 mg, 73%). $[\alpha]_{\text{D}}^{20} = +26.0$ ($c = 5$ in H_2O). **α -anomer**: ^1H NMR (400 MHz, D_2O) δ 4.21 (dd, $J = 7.7, 3.9$ Hz, 1H), 4.03 (ddd, $J = 7.6, 6.4, 3.4$ Hz, 1H), 3.97 (d, $J = 3.9$ Hz, 1H), 3.78 (ddd, $J = 12.6, 9.5, 3.3$ Hz, 1H overlapped), 3.64 (dd, $J = 11.7, 6.4$ Hz, 1H overlapped), 2.06 (m, 1H overlapped), 1.86 (dq, $J = 13.3, 3 \times 8.3$ Hz, 1H), 1.69 (m, 1H overlapped), 1.65 (m, 2H overlapped), 1.58 (m, 1H overlapped), 1.48 (m, 1H), 1.40 (m, 1H overlapped). ^{13}C NMR (101 MHz, D_2O) δ 172.6, 105.8, 82.1, 77.2, 72.1, 62.4, 61.5, 32.5, 26.9, 24.7, 24.0. **β -anomer**: ^1H NMR (400 MHz, D_2O) δ 4.26 (dd, $J = 7.9, 3.1$ Hz, 1H), 3.98 (m, 1H), 3.90 (d, $J = 3.1$ Hz, 1H), 3.78 (ddd, $J = 12.6, 9.5, 3.3$ Hz, 1H overlapped), 3.64 (dd, $J = 11.7, 6.4$ Hz, 1H overlapped), 2.08 (m, 1H overlapped), 1.97 (m, 1H), 1.69 (m, 2H overlapped), 1.58 (m, 1H overlapped), 1.59 (m, 1H overlapped), 1.43 (m, 1H overlapped), 1.37 (m, 1H overlapped). ^{13}C NMR (101 MHz, D_2O) δ 175.8, 104.9, 81.8, 77.5, 71.5, 62.3, 60.1, 31.6, 26.9, 24.2, 23.9. ESI-TOF m/z for **9n**: Calcd for $[\text{M}+\text{Na}^+]$ $\text{C}_{11}\text{H}_{18}\text{O}_7\text{Na}$: 285.0950, found $[\text{M}+\text{Na}^+]$: 285.0948.

(4*R*,5*S*)-5-((*R*)-1,2-Dihydroxyethyl)-2,4-dihydroxy-3,3-dimethyltetrahydrofuran-2-carboxylic acid (9o)



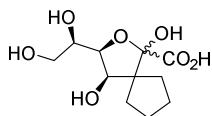
The title compound was prepared using KPHMT V214G following the procedure described for **9a**. The product **9o** was obtained as a white solid (268 mg, 94%). $[\alpha]^{20}_D = -21.9$ ($c = 5$ in H_2O). **α -anomer:** 1H NMR (400 MHz, D_2O) δ 4.24 (d, $J = 7.3$ Hz, 1H), 3.87 (d, $J = 7.6$ Hz, 1H), 3.86 (m, 1H), 3.78 (m, 1H overlapped), 3.64 (m, 1H overlapped), 1.17 (s, 3H), 0.94 (s, 3H). ^{13}C NMR (101 MHz, D_2O) δ 172.6, 105.1, 80.9, 77.3, 72.1, 62.4, 47.6, 18.9, 16.5. **β -anomer:** 1H NMR (400 MHz, D_2O) δ 4.00 (d, $J = 3.3$ Hz, 1H), 3.99 (d, $J = 2.4$ Hz, 1H), 3.98 (m, 1H), 3.78 (m, 1H overlapped), 3.64 (m, 1H overlapped), 1.13 (s, 3H), 0.99 (s, 3H). ^{13}C NMR (101 MHz, D_2O) δ 173.3, 108.0, 83.2, 77.1, 71.6, 62.3, 47.5, 22.5, 15.7. ESI-TOF m/z for **9o**: Calcd for $[M+Na^+]$ $C_9H_{16}O_8Na$: 259.0794, found $[M+Na^+]$: 259.0804.

(7*S*,8*R*)-7-((*R*)-1,2-Dihydroxyethyl)-5,8-dihydroxy-6-oxaspiro[3.4]octane-5-carboxylic acid (9p)



The title compound was prepared using KPHMT I212A following the procedure described for **9a**. The product **9p** was obtained as a white solid (270mg, 91%). $[\alpha]^{20}_D = 0$ ($c = 5$ in H_2O). **α -anomer:** 1H NMR (400 MHz, D_2O) δ 4.37 (m, 1H), 3.89 (m, 1H), 3.86 (m, 1H overlapped), 3.77 (m, 1H), 3.64 (m, 1H overlapped), 2.31 (m, 1H overlapped), 2.20 (m, 1H), 2.02 (m, 1H overlapped), 1.90 (m, 1H overlapped), 1.89 (m, 1H overlapped), 1.79 (m, 1H overlapped). ^{13}C NMR (101 MHz, D_2O) δ 173.2, 104.9, 84.5, 76.6, 71.2, 62.3, 53.5, 28.5, 21.4, 14.6. **β -anomer:** 1H NMR (400 MHz, D_2O) δ 4.39 (m, 1H), 3.85 (m, 1H), 3.82 (m, 1H overlapped), 3.77 (m, 1H), 3.64 (m, 1H overlapped), 2.47 (m, 1H), 2.29 (m, 1H overlapped), 2.00 (m, 1H overlapped), 1.90 (m, 1H overlapped), 1.82 (m, 1H overlapped), 1.79 (m, 1H overlapped). ^{13}C NMR (101 MHz, D_2O) δ 173.2, 104.6, 81.6, 76.0, 72.1, 62.3, 52.9, 25.0, 22.2, 14.7. ESI-TOF m/z for **9p**: Calcd for $[M+Na^+]$ $C_{10}H_{16}O_7Na$: 271.0794, found $[M+Na^+]$: 271.0792.

(3*S*,4*R*)-3-((*R*)-1,2-Dihydroxyethyl)-1,4-dihydroxy-2-oxaspiro[4.4]nonane-1-carboxylic acid (9q**)**

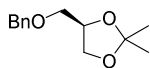


The title compound was prepared using KPHMT I212A following the procedure described for **9a**. The product **9q** was obtained as a white solid (104mg, 48%). $[\alpha]_{\text{D}}^{20} = -6.4$ ($c = 5$ in H_2O). **α -anomer:** $^1\text{H NMR}$ (400 MHz, D_2O) δ 4.40 (d, $J = 7.9$ Hz, 1H), 3.87 (m, 1H), 3.79 (m, 1H overlapped), 3.78 (m, 1H overlapped), 3.64 (m, 1H overlapped), 2.16 (m, 1H), 1.90 (m, 1H), 1.68 (m, 1H overlapped), 1.67 (m, 1H overlapped), 1.65 (m, 1H overlapped), 1.57 (m, 1H overlapped), 1.56 (m, 1H overlapped), 1.39 (m, 1H). $^{13}\text{C NMR}$ (101 MHz, D_2O) δ 173.1, 104.9, 80.9, 77.7, 72.8, 62.5, 59.0, 31.1, 27.3, 25.8, 25.2. **β -anomer:** $^1\text{H NMR}$ (400 MHz, D_2O) δ 3.99 (m, 2H overlapped), 3.96 (m, 1H), 3.80 (m, 1H overlapped), 3.63 (m, 1H overlapped), 1.99 (m, 1H), 1.83 (m, 1H), 1.64 (m, 4H overlapped), 1.49 (m, 2H). $^{13}\text{C NMR}$ (101 MHz, D_2O) δ 173.2, 105.7, 84.8, 76.9, 71.6, 62.8, 59.4, 34.2, 26.0, 24.5, 23.9. ESI-TOF m/z for **9q**: Calcd for $[\text{M}+\text{Na}^+]$ $\text{C}_{11}\text{H}_{18}\text{O}_7\text{Na}$: 285.0950, found $[\text{M}+\text{Na}^+]$: 285.0958.

5.8 Synthesis of compounds from section 3.3

5.8.1 Synthesis of intermediates C11–16

(*R*)-4-((Benzyloxy)methyl)-2,2-dimethyl-1,3-dioxolane (C11b)

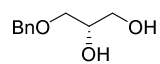


A dried three-necked round bottomed flask was charged with DMF (100 mL) and NaH (544 mg, 22.7 mmol, 1.2 eq, 60% dispersion in mineral oil) was added under N_2 atmosphere. A solution of (*R*)-(2,2-dimethyl-1,3-dioxolan-4-yl)methanol (**C11a**, 2.5 g, 18.9 mmol, 1.0 eq) and BnBr (3.24 g, 18.9 mmol, 1.0 eq) in DMF (50 mL) was added drop-wise over the course of 30 min at 4 °C. The solution was stirred at room temperature overnight. The reaction was quenched by the addition of water (50 + 500 mL) and extracted with EtOAc (3 x 100 mL). The organic phases were collected, washed with brine (3 x 100 mL), dried over anhydrous magnesium sulfate, filtered and the solvent removed in vacuo. Compound **C11b** was afforded in

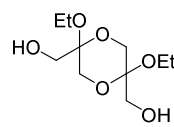
Experimental section

quantitative yields as an orange oil (4.3 g). ^1H NMR (401 MHz, CDCl_3) δ 7.33 – 7.21 (m, 5H), 4.51 (d, $J = 5.9$ Hz, 2H), 4.27 – 4.19 (m, 1H), 3.99 (dd, $J = 8.3$, 6.4 Hz, 1H), 3.67 (dd, $J = 8.3$, 6.3 Hz, 1H), 3.49 (dd, $J = 9.8$, 5.7 Hz, 1H), 3.40 (dd, $J = 9.8$, 5.5 Hz, 1H), 1.35 (s, 3H), 1.30 (s, 3H). ^{13}C NMR (101 MHz, CDCl_3) δ 138.0, 128.4, 128.4, 127.8, 127.8, 109.4, 74.8, 73.5, 71.1, 66.9, 26.8, 25.4.

(S)-3-(Benzyloxy)propane-1,2-diol (C11c)

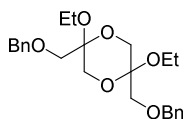
 Compound **C11b** (4.2 g, 18.9 mmol) was dissolved in a solution composed by MeOH:HCl 1 M (100 mL, 1:1, v/v) and stirred at room temperature overnight. The mixture was concentrated *in vacuo*, the aqueous phase saturated with NaCl and extracted with EtOAc (3 x 50 mL). The organic phases were collected, washed with brine (50 mL), dried over anhydrous magnesium sulfate, filtered and the solvent removed in *vacuo*. Compound **C11c** was afforded in quantitative yields (3.5 g). ^1H NMR (401 MHz, CDCl_3) δ 7.34 – 7.21 (m, 5H), 4.49 (s, 3H), 3.83 (ddt, $J = 6.1$, 5.4, 3.9 Hz, 1H), 3.64 (dd, $J = 11.4$, 3.9 Hz, 1H), 3.57 (dd, $J = 11.4$, 5.4 Hz, 1H), 3.52 (dd, $J = 9.7$, 4.0 Hz, 1H), 3.47 (dd, $J = 9.7$, 6.2 Hz, 1H).

(2,5-Diethoxy-1,4-dioxane-2,5-diyl)dimethanol (C13b)

 To an oven-dry 1 L round-bottom flask were added anhydrous ethanol (500 mL), concentrated sulfuric acid (3 mL, 56 mmol, 0.4 eq), and triethyl orthoformate (105 mL, 631 mmol, 4.5 eq). This solution was refluxed for 30 min under nitrogen. The solution was then cooled to 4 °C and dihydroxyacetone dimer (**C13a**, 4.23 g, 23.5 mmol) was added every 12 h over 3 days (total 25.4 g, 141 mmol, 1.0 eq). After the final addition of dihydroxyacetone dimer, the solution was stirred for an additional 1 day and anhydrous sodium bicarbonate (19.0 g, 226 mmol) was added. After stirring for 30 min at 4 °C, the reaction mixture was warmed to room temperature and filtered through a 5 cm pad of an equal mixture of Celite and silica gel (230–400 mesh), and then the filter cake was washed with EtOH. The filtrate was concentrated, and the residue was mixed with ethyl acetate

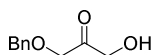
(100 mL) and concentrated. Hexane (400 mL) was then added and the white solid formed was filtered, washed with hexane (100 mL), and dried in vacuum desiccator to afford **C13b** (32.4 g, 97.0%) as a white solid. $^1\text{H NMR}$ (399 MHz, CDCl_3) δ 3.91 (d, $J = 11.7$ Hz, 2H), 3.79 (d, $J = 12.2$ Hz, 2H), 3.72 – 3.66 (m, 2H), 3.64 – 3.49 (m, 6H), 1.23 (t, $J = 7.1$ Hz, 3H), 1.19 (t, $J = 7.0$ Hz, 3H).

2,5-Bis((benzyloxy)methyl)-2,5-diethoxy-1,4-dioxane (**C13c**)



A dried three-necked round bottomed flask was charged with DMF (40 mL) and NaH (1 g, 44.4 mmol, 1.2 eq, 60% dispersion in mineral oil) was added under N_2 atmosphere. A solution of **C13b** (5 g, 21.2 mmol, 1.0 eq) in DMF (40 mL) was added at 4 °C. After 1 h, BnBr (7.24 g, 42.3 mmol, 2.0 eq) was slowly added and the mixture was stirred overnight at room temperature. Water (400 mL) was added and the mixture was extracted with EtOAc (3 x 100 mL). The organic phases were collected, washed with brine (3 x 100 mL), dried over anhydrous magnesium sulfate, filtered and the solvent removed in vacuo. The solid residue was resuspended in EtOH warming the solution with a heat gun. The solution was cooled at -20 °C over weekend. After that time, the solvent was discarded, and the pellet dried in vacuum. The compound **C13c** was afforded as a white solid (9.5 g, 90%). $^1\text{H NMR}$ (400 MHz, CDCl_3) δ 7.34 – 7.16 (m, 10H), 4.56 – 4.37 (m, 4H), 3.75 (dd, $J = 11.9, 6.9$ Hz, 2H), 3.65 – 3.35 (m, 8H), 3.29 (dd, $J = 10.5, 9.8$ Hz, 2H), 1.21 – 1.03 (m, 6H).

1-(Benzyloxy)-3-hydroxypropan-2-one (**C13d**)

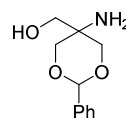


Compound **C13c** was dissolved in a cold solution of THF/ H_2SO_4 8 M (200 mL, 1:1 v/v) and was stirred 1 h. Water (100 mL) was added and the organic phase was evaporated in vacuum. Then, the aqueous phase was extracted with DCM (3 x 100 mL). The organic phases were collected, washed with 5% solution of NaHCO_3 (3 x 100 mL) and with brine (3 x 100 mL), dried over anhydrous magnesium sulfate and filtered. The product was absorbed onto silica gel (100 mL) and loaded onto a silica gel column. Product was eluted with a step gradient of hexane:EtOAc: 100:0, 300 mL,

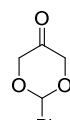
Experimental section

90:10, 300 mL, 80:20, 300 mL, 70:30, 300 mL, 60:40, 300mL and 50:50, 600 mL. Pure fractions were pooled, and the solvent removed in vacuo affording **C13d** (2.57 g, 60%). ¹H NMR (400 MHz, CDCl₃) δ 7.45 – 7.30 (m, 5H), 4.62 (s, 2H), 4.50 (d, *J* = 4.9 Hz, 2H), 4.20 (s, 2H). ¹³C NMR (101 MHz, CDCl₃) δ 208.6, 136.6, 128.7, 128.3, 127.9, 73.8, 73.3, 66.7.

(5-Amino-2-phenyl-1,3-dioxan-5-yl)methanol (**C14b**)

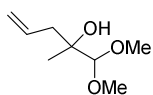
 A dried three-necked round bottomed flask was charged with DMF (100 mL) and tris(hydroxymethyl)aminomethane hydrochloride (20.7 g, 131.4 mmol, 2 eq) and TsOH (1.25 g, 6.6 mmol, 0.1 eq) were added. Then benzaldehyde dimethyl acetal (**C14a**, 10 g, 65.7 mmol, 1 eq) was added in one portion. The resulting solution was stirred overnight. After that time, a solution of KH₂PO₄ (600 mL, 0.3 M) was added and the mixture was washed with Et₂O (3 x 200 mL). Then the pH of the solution was adjusted to pH 12.0 with NaOH 1 M. The aqueous phase was extracted with Et₂O (3 x 200 mL) and with DCM (3 x 200 mL). The organic phases were collected, washed with brine (3 x 100 mL), dried over anhydrous magnesium sulfate, filtered and the solvent removed in vacuo. The compound **C14b** was afforded as a white solid (8.33 g, 61%). ¹H NMR (400 MHz, CDCl₃) δ 7.58 – 7.46 (m, 5H), 7.44 – 7.34 (m, 5H), 5.48 (s, 1H), 5.45 (s, 1H), 4.13 (d, *J* = 11.1 Hz, 2H), 4.00 – 3.86 (m, 4H), 3.60 (d, *J* = 11.2 Hz, 2H), 3.42 (s, 2H). ¹³C NMR (101 MHz, CDCl₃) δ 137.7, 137.7, 129.2, 129.1, 128.4, 128.4, 126.1, 126.0, 102.0, 101.7, 74.4, 73.4, 64.7, 64.7, 51.0, 49.1.

2-Phenyl-1,3-dioxan-5-one (**C14c**)

 To a cold solution (4 °C) containing **C14b** (4 g, 19.1 mmol, 1 eq) and KH₂PO₄ (2.6 g, 19.1 mmol, 1 eq) in water (65 mL), a solution of NaIO₄ (4.1 g, 19.1 mmol, 1 eq) was added dropwise during 3 hours. Upon completion, the mixture was allowed to stir for an additional hour at 4 °C and then overnight at room temperature. Na₂S₂O₃ (3 g, 19.1 mmol, 1 eq) was next added, and the solution was stirred an additional 15 min. The mixture was extracted with DCM (10 x 100 mL) and EtOAc (3 x 100 mL). The organic

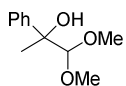
phases were collected, washed with brine (3 x 100 mL), dried over anhydrous magnesium sulfate, filtered and the solvent removed in vacuo. The compound **C14c** was afforded as a white solid (3.3 g, 97%). ¹H NMR (400 MHz, DMSO) δ 7.54 – 7.31 (m, 10H), 6.03 (s, 1H), 5.46 (s, 1H), 4.68 – 4.59 (m, 2H), 4.59 – 4.45 (m, 2H), 3.79 (dt, *J* = 11.3, 1.5 Hz, 2H), 3.67 (dq, *J* = 11.2, 1.4 Hz, 2H). ¹³C NMR (101 MHz, DMSO) δ 205.1, 138.8, 137.8, 129.5, 129.0, 128.7, 128.4, 126.7, 126.6, 100.6, 98.6, 86.6, 74.6, 73.5.

1,1-Dimethoxy-2-methylpent-4-en-2-ol (**C15b**)



A dried three-necked round bottomed flask was charged with THF (100 mL) and pyruvic aldehyde dimethylacetal (**C15a**, 3 g, 25.4 mmol, 1 eq) was added. The solution was cooled to $-78\text{ }^{\circ}\text{C}$ and allylmagnesium bromide (7.38 g, 50.8 mL, 50.8 mmol, 2 eq) was added dropwise. The reaction was stirred at room temperature overnight. The reaction was quenched by the slow addition of NH_4Cl saturated solution (200 mL). The organic phase was separated, and the aqueous phase was extracted with EtOAc (3 x 100 mL). The organic phases were collected, washed with brine (3 x 100 mL), dried over anhydrous magnesium sulfate, filtered and the solvent removed in vacuo affording the compound **C15b** (3.2 g, 79%). ¹H NMR (400 MHz, CDCl_3) δ 5.93 (ddt, *J* = 16.8, 10.5, 7.4 Hz, 1H), 5.18 – 5.05 (m, 2H), 4.06 (s, 1H), 3.58 (s, 3H), 3.57 (s, 3H), 2.30 (qd, *J* = 13.9, 7.3 Hz, 2H), 1.17 (s, 3H). ¹³C NMR (101 MHz, CDCl_3) δ 133.8, 118.1, 110.5, 74.3, 58.4, 58.1, 41.7, 21.6.

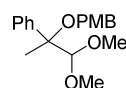
1,1-Dimethoxy-2-phenylpropan-2-ol (**C15c**)



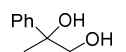
The title compound was prepared following the procedure described for **C15b** affording **C15c** (3.13 g, 63%). ¹H NMR (400 MHz, CDCl_3) δ 7.58 – 7.51 (m, 2H), 7.42 – 7.33 (m, 2H), 7.33 – 7.25 (m, 1H), 4.24 (s, 1H), 3.47 (s, 3H), 3.38 (s, 3H), 1.57 (s, 3H). ¹³C NMR (101 MHz, CDCl_3) δ 144.0, 127.9, 127.0, 125.8, 110.9, 75.9, 58.2, 58.0, 23.6.

Experimental section

1-(((1,1-Dimethoxy-2-phenylpropan-2-yl)oxy)methyl)-4-methoxybenzene (C15f)

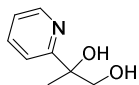
 A dried three-necked round bottomed flask was charged with DMF (50 mL) and NaH (440 mg, 11 mmol, 1.2 eq, 60% dispersion in mineral oil) was added under N₂ atmosphere. A solution of **C15c** (1.8 g, 9.2 mmol, 1.0 eq) was added at 4 °C. After 30 min, PMBCl (1.6 g, 10 mmol, 1.1 eq) and (*n*Bu)₄NBr (295 mg, 0.9 mmol, 0.1 eq) were added and the mixture was stirred overnight at room temperature. Water (400 mL) was added and the mixture was extracted with EtOAc (3 x 100 mL). The organic phases were collected, washed with brine (3 x 100 mL), dried over anhydrous magnesium sulfate and filtered. The product was absorbed onto silica gel (100 mL) and loaded onto a silica gel column. Product was eluted with a step gradient of hexane:EtOAc: 100:0, 300 mL, 95:5, 300 mL, 90:10, 300 mL and 85:15, 900 mL. Pure fractions were pooled, and the solvent removed in vacuo affording **C15f** (2.4 g, 81%). ¹H NMR (400 MHz, CDCl₃) δ 7.55 – 7.48 (m, 2H), 7.43 – 7.25 (m, 5H), 6.95 – 6.86 (m, 2H), 4.38 (d, *J* = 11.0 Hz, 1H), 4.23 (s, 1H), 4.12 (d, *J* = 11.0 Hz, 1H), 3.83 (s, 3H), 3.57 (s, 3H), 3.20 (s, 3H), 1.73 (s, 3H). ¹³C NMR (101 MHz, CDCl₃) δ 158.8, 141.9, 131.5, 128.6, 127.9, 127.5, 127.3, 113.6, 111.1, 82.3, 64.0, 58.1, 57.8, 55.3, 16.5.

2-Phenylpropane-1,2-diol (C16b)

 A dried three-necked round bottomed flask was charged with THF (100 mL) and hydroxyacetone (**C16a**, 1.5 g, 1.54 mL, 20.25 mmol, 1 eq) was added. The solution was cooled to -78 °C and phenylmagnesium bromide (9.18 g, 16.9 mL, 50.6 mmol, 2.5 eq) was added dropwise. The reaction was stirred vigorously at room temperature overnight. The reaction was quenched by the slow addition of NH₄Cl saturated solution (200 mL). The organic phase was separated, and the aqueous phase was extracted with EtOAc (3 x 100 mL). The organic phases were collected, washed with brine (3 x 100 mL), dried over anhydrous magnesium sulfate, filtered and the solvent removed in vacuo affording the compound **C16b** (2.6 g, 86%). ¹H NMR (400 MHz, CDCl₃) δ 7.52

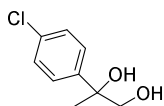
– 7.45 (m, 2H), 7.43 – 7.36 (m, 2H), 7.34 – 7.26 (m, 1H), 3.83 (dd, $J = 11.2$, 4.0 Hz, 1H), 3.66 (dd, $J = 11.1$, 7.8 Hz, 1H), 1.56 (s, 3H). ^{13}C NMR (101 MHz, CDCl_3) δ 144.9, 128.5, 127.2, 125.1, 74.9, 71.1, 26.1.

2-(Pyridin-2-yl)propane-1,2-diol (C16c)



A dried three-necked round bottomed flask was charged with THF (100 mL) and 2-bromopyridine (13.44 g, 85 mmol, 2.1 eq) was added. The solution was cooled to $-78\text{ }^\circ\text{C}$ and $n\text{BuLi}$ (5.45 g, 85 mmol, 2.1 eq) was added dropwise. The reaction was stirred during 30 minutes. After that time, hydroxyacetone (**C16a**, 3 g, 40.5 mmol, 1 eq) was added. The reaction was stirred at room temperature overnight. The reaction was quenched by the slow addition of a saturated solution of NaHCO_3 (200 mL). The organic phase was separated, and the aqueous phase was extracted with EtOAc (10 x 100 mL). The organic phases were collected, dried over anhydrous magnesium sulfate and filtered. The product was absorbed onto silica gel (100 mL) and loaded onto a silica gel column. Product was eluted with a 10% step gradient of hexane:EtOAc from 0 to 100% of EtOAc, in 200 mL fractions. Pure fractions were pooled, and the solvent removed in vacuo affording **C16c** (3.0 g, 49%). ^1H NMR (400 MHz, CDCl_3) δ 8.54 (ddd, $J = 4.8$, 1.8, 0.9 Hz, 1H), 7.76 (td, $J = 7.7$, 1.8 Hz, 1H), 7.45 (dt, $J = 8.0$, 0.9 Hz, 1H), 7.31 – 7.22 (m, 1H), 3.83 (d, $J = 11.1$ Hz, 1H), 3.75 (d, $J = 11.1$ Hz, 1H), 1.52 (s, 3H). ^{13}C NMR (101 MHz, CDCl_3) δ 162.9, 147.5, 137.3, 122.4, 119.7, 74.3, 70.6, 25.2.

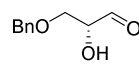
2-(4-Chlorophenyl)propane-1,2-diol (C16d)



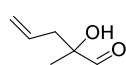
The title compound was prepared following the procedure described for **C16c** affording **C16d** (5.4 g, 71%). ^1H NMR (400 MHz, CDCl_3) δ 7.46 – 7.31 (m, 4H), 3.78 (dd, $J = 11.1$, 4.9 Hz, 1H), 3.65 (dd, $J = 11.1$, 7.6 Hz, 1H), 1.54 (s, 3H). ^{13}C NMR (101 MHz, CDCl_3) δ 143.5, 133.1, 128.5, 126.7, 74.6, 70.9, 26.1.

5.8.2 Synthesis of aldehydes 2m–q

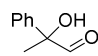
(*R*)-3-(benzyloxy)-2-hydroxypropanal (**2m**)

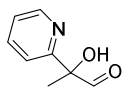

 NaHCO₃ (1.15 g, 13.7 mmol, 5 eq) and catalytic TEMPO (4.3 mg, 27.4 mmol, 0.01 eq) were added to a solution of the alcohol (**C11c**, 0.5 g, 2.75 mmol, 1 eq) in DCM (20 mL). The solution was stirred and cooled to 4 °C and trichloroisocyanuric acid (255 mg, 1.1 mmol, 0.4 eq) was added. The reaction was followed by TLC. When no evolution of reactants and products was detected, another batch of trichloroisocyanuric acid (255 mg, 1.1 mmol, 0.4 eq) was added. When the alcohol was consumed, the reaction mixture was filtered on Celite, washing the filter with DCM (3 x 50 mL). The organic phases were collected, washed with a saturated solution of Na₂CO₃ (3 x 50 mL), followed by brine (3 x 50 mL), dried over anhydrous magnesium sulfate and filtered. DMF (2 mL) were added prior to evaporation of the solvent to avoid total dryness and prevent polymerization of the aldehyde. Compound **2m** was afforded as a solution in DMF (2 mL, 1 M, 73%).

2-hydroxy-2-methylpent-4-enal (**2n**)

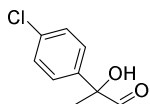

 The dimethylacetal precursor (**C15b**, 1 g, 6.24 mmol, 1 eq) was dissolved in a solution of Et₂O:HCl 1 M (100 mL, 1:1, v/v) and the resulting solution was stirred overnight. After that time, the organic layer was separated, and the aqueous phase was washed with Et₂O (3 x 50 mL). The organic phases were collected, washed with a 5% solution of Na₂CO₃ (3 x 50 mL), dried over anhydrous magnesium sulfate and filtered. DMF (5 mL) was added prior to evaporation of the solvent to avoid total dryness and prevent polymerization of the aldehyde. Compound **2n** was afforded as a solution in DMF (5 mL, 1 M, 80%).

2-Hydroxy-2-phenylpropanal (**2o**)

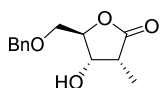

 The title compound was prepared following the procedure described for **2m**, using **C16b** as a precursor and affording **2o** as a solution in DMF (3 mL, 2 M, 65%).

2-Hydroxy-2-(pyridin-2-yl)propanal (2p)

The title compound was prepared following the procedure described for **2o** affording **2p** as a solution in DMF (4 mL, 0.5 M, 22%).

2-(4-Chlorophenyl)-2-hydroxypropanal (2q)

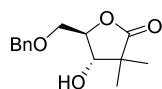
The title compound was prepared following the procedure described for **2m** affording **2o** as a solution in DMF (10 mL, 1 M, 75%).

5.8.3 Enzymatic synthesis of products 11a–d**(3R,4S,5R)-5-((Benzyloxy)methyl)-4-hydroxy-3-methyldihydrofuran-2(3H)-one (11a)**

Typical procedure: The aldol addition reaction was performed as described for the product **4a**. The reaction was monitored by HPLC and after 24 h, MeOH (100 mL) was added. The mixture was filtered on Celite washing the filter with MeOH (3 x 50 mL) and the solvent removed under vacuum. The aqueous phase was transferred into a three-necked round bottomed flask and water (10 mL) and hydrogen peroxide (1.1 mL of a 8.8 M commercial solution, 10 mmol, 10 eq) were added. The reaction was refluxed (100 °C) during 90 min. The reaction was followed by HPLC. Then, a 5% solution of NaHCO₃ (50 mL) was added and the solution washed with EtOAc (3x50 mL). The organic phases were collected, dried over anhydrous MgSO₄, absorbed onto silica gel (100 mL) and loaded onto a silica gel column. Product was eluted with a step gradient from 0% to 100% of EtOAc in hexane, 200 mL each fraction. Pure fractions were pooled, and the solvent removed in vacuo affording the title compound **11a** (96 mg, 40%). ¹H NMR (400 MHz, MeOD) δ 7.39 – 7.24 (m, 5H), 4.42 (td, *J* = 3.5, 1.0 Hz, 1H), 4.33 (dd, *J* = 6.1, 1.1 Hz, 1H), 3.69 (d, *J* = 3.5 Hz, 2H), 2.90 (qd, *J* = 7.4, 6.1 Hz, 1H), 1.16 (d, *J* = 7.5 Hz, 3H). ¹³C NMR (101 MHz, MeOD) δ 180.3, 137.8, 128.1, 127.5, 127.4, 85.7, 73.1, 71.0, 69.2, 39.7, 7.2.

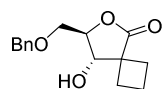
Experimental section

(4*S*,5*R*)-5-((Benzyloxy)methyl)-4-hydroxy-3,3-dimethyldihydrofuran-2(3*H*)-one (11b)



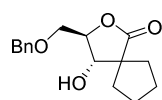
The title compound was prepared using KPHMT wild-type following the procedure described for **11a** affording the product **11b** (130 mg, 52%). ¹H NMR (400 MHz, CDCl₃) δ 7.43 – 7.29 (m, 5H), 4.62 (s, 2H), 4.26 (dt, *J* = 7.9, 4.6 Hz, 1H), 4.18 – 4.05 (m, 1H), 3.82 (dd, *J* = 10.6, 4.6 Hz, 1H), 3.76 (dd, *J* = 10.6, 4.7 Hz, 1H), 2.23 (d, *J* = 4.7 Hz, 3H), 1.29 (s, 1H), 1.22 (s, 3H). ¹³C NMR (101 MHz, CDCl₃) δ 179.5, 137.4, 128.6, 128.0, 127.8, 79.7, 73.8, 69.0, 43.5, 22.7, 17.8.

(7*R*,8*S*)-7-((Benzyloxy)methyl)-8-hydroxy-6-oxaspiro[3.4]octan-5-one (11c)



The title compound was prepared using KPHMT I212A following the procedure described for **11a** affording the product **11c** (170 mg, 65%). ¹H NMR (400 MHz, CDCl₃) δ 7.43 – 7.29 (m, 5H), 4.57 (s, 2H), 4.29 – 4.17 (m, 2H), 3.73 (dd, *J* = 10.4, 3.9 Hz, 1H), 3.63 (dd, *J* = 10.5, 4.6 Hz, 1H), 2.59 – 2.49 (m, 1H), 2.48 – 2.37 (m, 1H), 2.31 (m, 1H), 2.21 (m, 2H), 2.16 – 2.02 (m, 1H), 2.03 – 1.89 (m, 1H). ¹³C NMR (101 MHz, CDCl₃) δ 179.3, 137.3, 128.6, 127.9, 81.6, 75.5, 73.8, 69.0, 48.0, 28.4, 23.5, 16.3.

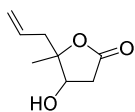
(3*R*,4*S*)-3-((Benzyloxy)methyl)-4-hydroxy-2-oxaspiro[4.4]nonan-1-one (11d)



The title compound was prepared using KPHMT I202A/I212A following the procedure described for **11a** affording the product **11d** (118 mg, 43%). ¹H NMR (400 MHz, CDCl₃) δ 7.45 – 7.30 (m, 5H), 4.61 (s, 2H), 4.27 – 4.15 (m, 2H), 3.81 (dd, *J* = 10.3, 4.6 Hz, 1H), 3.72 (dd, *J* = 10.4, 5.0 Hz, 1H), 2.33 – 2.12 (m, 2H), 1.89 – 1.64 (m, 6H). ¹³C NMR (101 MHz, CDCl₃) δ 180.2, 137.4, 128.6, 128.1, 127.8, 80.4, 73.8, 69.1, 53.4, 35.4, 29.7, 26.1, 26.0.

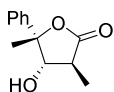
5.8.4 Enzymatic synthesis of products 12a–e

5-Allyl-4-hydroxy-5-methyldihydrofuran-2(3H)-one (12a)



The aldol addition reaction was performed as described for the product **4a**, using MBP-YfaU wt as catalyst. The reaction was monitored by HPLC and after 24 h, hydrogen peroxide (568 μ L, 5 mmol, 5 eq) was added and the solution stirred at room temperature for 90 min. Then MeOH (100 mL) was added. The mixture was filtered on Celite washing the filter with MeOH (3 x 50 mL) and the solvent removed under vacuum. The aqueous residue was purified by ionic exchange chromatography following the same procedure for the product **9a**. Fractions were lyophilized rendering the product as a mixture of the open carboxylate form and the lactone. The total lactonization of the product was achieved by dissolving the product in HCO₂H (1 M) and lyophilizing (this process was repeated three times) rendering the compound **12a** (70 mg, 35%). **Major diastereomer:** ¹H NMR (400 MHz, CDCl₃) δ 5.98 – 5.73 (m, 1H), 5.35 – 5.12 (m, 2H), 4.35 (dd, J = 7.0, 4.5 Hz, 1H), 2.96 – 2.89 (m, 1H), 2.76 – 2.52 (m, 1H), 2.47 (dd, J = 14.2, 6.9 Hz, 1H), 2.39 (dd, J = 14.1, 7.7 Hz, 1H), 1.44 (s, 3H). ¹³C NMR (101 MHz, CDCl₃) δ 174.4, 131.6, 120.2, 88.5, 72.0, 43.9, 38.0, 19.2. **Minor diastereomer:** ¹H NMR (400 MHz, CDCl₃) δ 5.98 – 5.73 (m, 1H), 5.35 – 5.12 (m, 2H), 4.27 (dd, J = 6.2, 2.4 Hz, 1H), 2.98 (dd, J = 12.9, 5.1 Hz, 1H), 2.76 – 2.52 (m, 1H), 2.39 (dd, J = 14.1, 7.7 Hz, 1H), 1.37 (s, 3H). ¹³C NMR (101 MHz, CDCl₃) δ 174.7, 132.6, 119.8, 88.6, 73.6, 39.3, 38.4, 23.5.

(3*S*,4*S*,5*S*)-4-Hydroxy-3,5-dimethyl-5-phenyldihydrofuran-2(3H)-one (12b)

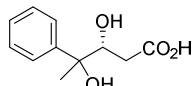


The title compound was prepared using MBP-YfaU wt following the procedure described for **11a** affording the product **12b** (36 mg, 18%). ¹H NMR (400 MHz, CDCl₃) δ 7.46 – 7.30 (m, 5H), 4.46 (t, J = 4.9 Hz, 1H), 2.71 – 2.56 (m, 1H), 2.44 (d, J = 5.3 Hz, 1H), 1.76 (s, 3H), 1.24 (d, J = 7.3

Experimental section

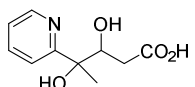
Hz, 3H). ^{13}C NMR (101 MHz, CDCl_3) δ 178.2, 142.5, 128.8, 127.9, 124.2, 88.8, 77.8, 39.7, 23.3, 8.1.

(3R)-3,4-Dihydroxy-4-phenylpentanoic acid (12c)



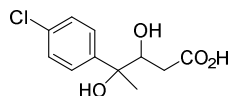
The title compound was prepared using MBP-YfaU wt following the procedure described for **12a** affording the product **12c** (116 mg, 50%). **Major diastereomer:** ^1H NMR (400 MHz, MeOD) δ 7.55 – 7.19 (m, 5H), 4.16 (dd, J = 10.2, 2.5 Hz, 1H), 2.36 (dd, J = 15.8, 10.2 Hz, 1H), 2.17 (dd, J = 15.8, 2.5 Hz, 1H), 1.58 (s, 3H). ^{13}C NMR (101 MHz, MeOD) δ 175.0, 146.1, 127.7, 126.3, 125.0, 75.6, 74.6, 36.4, 25.3, 24.5. **Minor diastereomer:** ^1H NMR (400 MHz, MeOD) δ 7.55 – 7.19 (m, 5H), 4.16 (dd, J = 10.2, 2.5 Hz, 1H), 2.54 (dd, J = 15.7, 2.5 Hz, 1H), 2.04 (dd, J = 15.7, 10.2 Hz, 1H), 1.58 (s, 3H). ^{13}C NMR (101 MHz, MeOD) δ 174.8, 145.0, 127.4, 126.4, 125.8, 75.3, 75.0, 36.7, 24.5.

3,4-Dihydroxy-4-(pyridin-2-yl)pentanoic acid (12d)



The title compound was prepared using MBP-YfaU wt following the procedure described for **12a** affording the product **12d** (107 mg, 46%). ^1H NMR (400 MHz, MeOD) δ 8.57 – 8.44 (m, 1H), 7.93 – 7.79 (m, 1H), 7.78 – 7.69 (m, 1H), 7.39 – 7.28 (m, 1H), 4.34 (dd, J = 10.1, 2.7 Hz, 1H), 2.39 (dd, J = 15.6, 10.0 Hz, 1H), 2.20 (dd, J = 15.6, 2.7 Hz, 1H), 1.58 (s, 3H). ^{13}C NMR (101 MHz, MeOD) δ 174.6, 164.6, 147.3, 137.4, 122.1, 120.5, 75.9, 73.8, 36.3, 23.5.

4-(4-Chlorophenyl)-3,4-dihydroxypentanoic acid (12e)

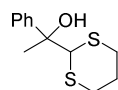


The title compound was prepared using MBP-YfaU wt following the procedure described for **12a** affording the product **12e** (151 mg, 62%). **Major diastereomer:** ^1H NMR (400 MHz, MeOD) δ 7.56 – 7.43 (m, 2H), 7.39 – 7.28 (m, 2H), 4.13 (dd, J = 9.9, 2.8 Hz, 1H), 2.35 (dd, J = 15.7, 9.9 Hz, 1H), 2.23 (dd, J = 15.7, 2.7 Hz, 1H), 1.56 (s, 3H). ^{13}C NMR (101 MHz, MeOD) δ 174.8, 145.1, 132.2, 127.6, 126.9, 75.2, 74.4, 36.4, 24.8. **Minor diastereomer:** ^1H NMR (400 MHz, MeOD) δ 7.56 –

7.43 (m, 2H), 7.39 – 7.28 (m, 2H), 4.13 (dd, $J = 9.9, 2.8$ Hz, 1H), 2.57 (dd, $J = 15.7, 2.6$ Hz, 1H), 2.00 (dd, $J = 15.7, 10.1$ Hz, 0H), 1.57 (s, 3H). ^{13}C NMR (101 MHz, MeOD) δ 174.8, 144.0, 132.0, 127.6, 126.9, 74.9, 74.8, 36.7, 24.9.

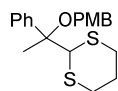
5.8.5 Synthesis of intermediates C17–21

1-(1,3-Dithian-2-yl)-1-phenylethan-1-ol (C17b)



A dried three-necked round bottomed flask was charged with THF (50 mL) and 1,3-dithiane (3.0 g, 25 mmol, 1.2 eq) was added. The solution was cooled to -78 °C and *n*BuLi (1.6 g, 25 mmol, 1.2 eq) was added dropwise. The reaction was stirred for 2 hours. After that time, acetophenone (C17a, 2.5 g, 20.8 mmol, 1 eq) in THF (30 mL) was added. The reaction was stirred at -78 °C for 3 hours. The reaction was quenched by the slow addition of a saturated solution of NH_4Cl (200 mL). The organic phase was separated, and the aqueous phase was extracted with EtOAc (3 x 100 mL). The organic phases were collected, dried over anhydrous magnesium sulfate and filtered. The product was absorbed onto silica gel (100 mL) and loaded onto a silica gel column. Product was eluted with a 10% step gradient of hexane:EtOAc from 0 to 30% of EtOAc, in 200 mL fractions. Pure fractions were pooled, and the solvent removed in vacuo affording C17b (4.6 g, 92%). ^1H NMR (400 MHz, CDCl_3) δ 7.57 – 7.51 (m, 2H), 7.44 – 7.37 (m, 2H), 7.36 – 7.30 (m, 1H), 4.47 (s, 1H), 2.92 – 2.75 (m, 4H), 2.12 – 2.00 (m, 1H), 1.92 – 1.80 (m, 1H), 1.78 (s, 3H). ^{13}C NMR (101 MHz, CDCl_3) δ 144.5, 128.1, 127.6, 125.4, 76.5, 60.1, 30.5, 27.3, 25.4.

2-(1-((4-Methoxybenzyl)oxy)-1-phenylethyl)-1,3-dithiane (C17c)

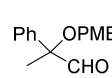


The title compound was prepared following the same procedure described for C15f affording C17c (3 g, 73%). ^1H NMR (400 MHz, CDCl_3) δ 7.58 – 7.51 (m, 2H), 7.47 – 7.27 (m, 5H), 6.95 – 6.84 (m, 2H), 4.49 (s, 1H), 4.34 (d, $J = 11.1$ Hz, 1H), 4.19 (d, $J = 11.2$ Hz, 1H), 3.82 (s, 3H), 2.96 – 2.85 (m, 2H), 2.82 – 2.73 (m, 2H), 2.12 – 2.00 (m, 1H), 1.91 (s, 3H), 1.88 –

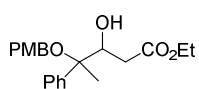
Experimental section

1.77 (m, 1H). ^{13}C NMR (101 MHz, CDCl_3) δ 158.9, 142.1, 131.1, 128.6, 128.1, 128.0, 127.1, 113.8, 81.5, 65.0, 60.2, 55.3, 31.0, 30.8, 26.0, 20.5.

2-((4-Methoxybenzyl)oxy)-2-phenylpropanal (**C18**)

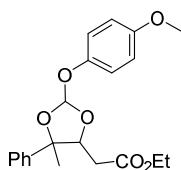
 To a solution of *N*-bromosuccinimide (2 g, 11.1 mmol, 8 eq) in acetone:H₂O (96:4, v/v, 80mL) at $-5\text{ }^\circ\text{C}$ was slowly added a solution of **C17c** (500 mg, 1.4 mmol, 1 eq) in acetone (40 mL). The reaction was stirred 10 min. After that time, a saturated solution of Na_2SO_3 (100 mL) was added and the acetone removed in vacuum. A saturated solution of Na_2SO_3 (100 mL) was added and the resulting solution was extracted with Et_2O (3 x 100 mL). The organic phases were collected, washed with brine (3 x 100 mL), dried over anhydrous magnesium sulfate, filtered and the solvent removed in vacuum. The product **C18** was obtained without any further purification (235 mg, 63%). ^1H NMR (400 MHz, CDCl_3) δ 9.62 (s, 1H), 7.55 – 7.47 (m, 2H), 7.48 – 7.41 (m, 2H), 7.40 – 7.31 (m, 3H), 6.97 – 6.89 (m, 2H), 4.44 (s, 2H), 3.84 (s, 3H), 1.80 (s, 3H). ^{13}C NMR (101 MHz, CDCl_3) δ 199.9, 159.3, 138.0, 130.1, 129.2, 128.9, 128.4, 126.8, 113.9, 84.2, 65.5, 55.3, 18.7.

Ethyl 3-hydroxy-4-((4-methoxybenzyl)oxy)-4-phenylpentanoate (**C19a**)

 A dried three-necked round bottomed flask was charged with THF (40 mL) and LDA (1.7 g, 15.6 mmol, 6.5 eq) and a solution of EtOAc (1.27 g 14.4 mmol, 6 eq) in THF (20 mL) was added dropwise at $-78\text{ }^\circ\text{C}$. The solution was stirred for 30 min. After that time, the aldehyde **C18** was slowly added and the solution stirred for 2 h. The reaction was quenched by adding a saturated solution of NH_4Cl (200 mL). The organic phase was separated, and the aqueous phase was extracted with EtOAc (3 x 100 mL). The organic phases were collected, dried over anhydrous magnesium sulfate and filtered. The product was absorbed onto silica gel (100 mL) and loaded onto a silica gel column. Product was eluted with a 10% step gradient of hexane:EtOAc from 0 to 40% of EtOAc, in 200 mL fractions. Pure fractions were pooled, and the solvent removed in vacuo affording **C19a** (825 mg, 96%). ^1H NMR (400 MHz, CDCl_3) δ 7.52 – 7.22 (m, 7H), 6.97 – 6.87 (m, 2H), 4.38

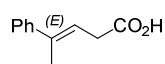
(d, $J = 10.8$ Hz, 1H), 4.20 (d, $J = 10.7$ Hz, 1H), 4.17 – 4.11 (m, 1H), 4.11 – 4.02 (m, 2H), 3.84 (s, 3H), 2.43 (dd, $J = 15.9, 9.9$ Hz, 1H), 2.34 – 2.24 (m, 1H), 1.75 (s, 3H), 1.23 (t, $J = 7.2$ Hz, 3H). ^{13}C NMR (101 MHz, CDCl_3) δ 172.8, 159.0, 142.4, 130.9, 128.9, 128.4, 127.9, 127.6, 127.3, 81.1, 75.6, 64.6, 60.6, 55.3, 36.6, 18.6, 14.2.

Ethyl 2-(2-(4-methoxyphenoxy)-5-methyl-5-phenyl-1,3-dioxolan-4-yl) acetate (C19b)



To a solution of **C19a** (825 mg, 2.3 mmol, 1 eq) in $\text{CH}_2\text{Cl}_2:\text{H}_2\text{O}$ (9:1, v/v), DDQ (783 mg, 3.45 mmol, 1.5 eq) was added. The solution was stirred for 1 h at room temperature. The reaction mixture was filtered, and the filter washed with CH_2Cl_2 (3 x 50 mL). Then a saturated solution of NaHCO_3 (100 mL) was added and the resulting solution was extracted with EtOAc (3 x 100 mL). The organic phases were collected, washed with brine (3 x 100 mL), dried over anhydrous magnesium sulfate and filtered. The product was absorbed onto silica gel (100 mL) and loaded onto a silica gel column. Product was eluted with a 10% step gradient of hexane:EtOAc from 0 to 50% of EtOAc, in 200 mL fractions. Pure fractions were pooled, and the solvent removed in vacuo affording **C19b** (255 mg, 30%). ^1H NMR (400 MHz, CDCl_3) δ 7.64 – 7.23 (m, 7H), 7.05 – 6.91 (m, 2H), 6.09 (s, 1H), 4.61 (dd, $J = 8.2, 5.3$ Hz, 1H), 4.06 (ddt, $J = 11.0, 7.1, 3.6, 3.6$ Hz, 2H), 3.87 (s, 3H), 2.19 (dd, $J = 16.3, 8.1$ Hz, 1H), 2.05 (dd, $J = 16.3, 5.3$ Hz, 1H), 1.87 (s, 3H), 1.18 (t, $J = 7.2, 7.2$ Hz, 3H). ^{13}C NMR (101 MHz, CDCl_3) δ 170.8, 160.4, 142.0, 129.2, 128.3, 128.2, 127.5, 126.1, 125.2, 113.8, 101.6, 83.7, 82.4, 60.6, 55.3, 38.1, 24.9, 14.1.

(E)-4-Phenylpent-3-enoic acid (C20b)

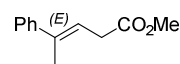


2-Phenylpropanal (**C20a**, 10 g, 74.5 mmol, 1 eq) and malonic acid (11.6 g, 111.8 mmol, 1.5 eq) in triethylamine (150 mL) were heated to reflux for 4 h. The reaction mixture was then diluted with water (100 mL) and the pH adjusted to 9 with NaOH (1 M). The solution was washed with Et₂O (3 x 100 mL). Then the pH was adjusted to 3 with fuming acid (37%)

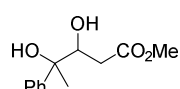
Experimental section

and the solution extracted with Et₂O (3 x 100 mL). The combined organic layer was dried over MgSO₄ and the solvent evaporated under reduced pressure affording **C20b** (11.4 g, 87%). ¹H NMR (400 MHz, CDCl₃) δ 7.50 – 7.17 (m, 5H), 5.96 (tq, *J* = 7.1, 1.5 Hz, 1H), 3.34 (d, *J* = 6.1 Hz, 2H), 2.10 (s, 3H). ¹³C NMR (101 MHz, CDCl₃) δ 178.1, 142.9, 138.8, 128.3, 127.2, 125.8, 118.3, 34.1, 16.3.

Methyl (*E*)-4-phenylpent-3-enoate (**C20c**)

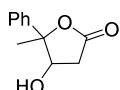
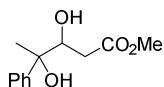
 The compound **C20b** (3 g, 17 mmol, 1 eq) was resuspended in acetone (150 mL) and K₂CO₃ (9.4 g, 68 mmol, 4 eq) and MeI (9.67 mg, 68 mmol, 4 eq) were added. The mixture was heated to reflux overnight. Then, the solution was filtered, the solvent removed in vacuum and the pellet resuspended in EtOAc (250 mL). The solution was washed with a saturated solution of NaHCO₃ (3 x 100 mL) and brine (3 x 100 mL). The organic layer was dried over anhydrous MgSO₄ and filtered. The product was absorbed onto silica gel (100 mL) and loaded onto a silica gel column. Product was eluted with a 5% step gradient of hexane:EtOAc from 0 to 20% of EtOAc, in 500 mL fractions. Pure fractions were pooled, and the solvent removed in vacuo affording **C20c** (2.1 g, 65%). ¹H NMR (400 MHz, CDCl₃) δ 7.48 – 7.25 (m, 5H), 5.97 (td, *J* = 7.2, 1.5 Hz, 1H), 3.75 (s, 3H), 3.29 (dd, *J* = 7.3, 1.2 Hz, 2H), 2.09 (s, 3H). ¹³C NMR (101 MHz, CDCl₃) δ 172.3, 143.1, 138.1, 128.2, 127.1, 125.8, 119.2, 51.9, 34.3, 16.2.

Methyl 3,4-dihydroxy-4-phenylpentanoate (**C20d**)

 The compound **C20c** was resuspended in a solution citric acid (455 mg, 2.4 mmol, 1 eq) in *t*BuOH:H₂O (1:1, v/v, 50 mL). Then, potassium osmate (78.6 mg, 0.236 mmol, 0.1 eq) and 4-methylmorpholine *N*-oxide (304 mg, 2.6 mmol, 1.1 eq) were added. The reaction was stirred over night at room temperature. *t*BuOH was removed on a rotary evaporator, and H₂O (100 mL) was added to the aqueous residue. The resulting solution, which had a pH around 4, was extracted with EtOAc (3 x 100 mL). The organic layers were washed with a 5% solution of NaHCO₃ (3 x

100 mL). The organic layer was dried over anhydrous MgSO_4 and filtered. The product was absorbed onto silica gel (100 mL) and loaded onto a silica gel column. Product was eluted with a 10% step gradient of hexane:EtOAc from 0 to 60% of EtOAc, in 300 mL fractions. Pure fractions were pooled, and the solvent removed in vacuo affording **C20d** (356 mg, 67%). ^1H NMR (400 MHz, CDCl_3) δ 7.57 – 7.23 (m, 5H), 4.29 (dt, $J = 9.6, 3.3, 3.3$ Hz, 1H), 3.70 (s, 3H), 2.58 (dd, $J = 16.4, 3.1$ Hz, 1H), 2.50 (dd, $J = 16.4, 9.6$ Hz, 1H), 1.55 (s, 3H). ^{13}C NMR (101 MHz, CDCl_3) δ 173.5, 144.8, 128.4, 127.4, 125.5, 75.8, 74.4, 51.9, 35.7, 24.1.

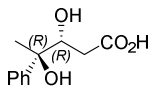
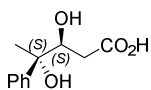
Methyl 3,4-dihydroxy-4-phenylpentanoate (C20f) and 4-hydroxy-5-methyl-5-phenyldihydrofuran-2(3H)-one (C20g)



A dried three-necked round bottomed flask was charged with CH_2Cl_2 (80 mL) and the compound **C20c** (650 mg, 3.4 mmol, 1 eq). MCPBA (737 mg, 7.3 mmol, 1.25 eq) was added at 4 °C and the solution was stirred for 3 h at room temperature. After that time, the solution was washed with a 5% solution of NaHCO_3 (3 x 50 mL). The organic layer was dried over anhydrous MgSO_4 and filtered. The product was absorbed onto silica gel (100 mL) and loaded onto a silica gel column. Product was eluted with a 5% step gradient of hexane:EtOAc from 0 to 60% of EtOAc, in 200 mL fractions. Pure fractions were pooled, and the solvent removed in vacuo affording **C20f** and **C20g** (62:38, 380 mg, 53%). **C20f**: ^1H NMR (400 MHz, CDCl_3) δ 7.52 – 7.30 (m, 5H), 4.20 (dd, $J = 10.2, 2.6$ Hz, 1H), 3.66 (s, 3H), 2.45 (dd, $J = 16.9, 10.1$ Hz, 1H), 2.14 (dd, $J = 16.9, 2.5$ Hz, 1H), 1.67 (s, 3H). ^{13}C NMR (101 MHz, CDCl_3) δ 174.3, 142.7, 128.8, 128.0, 124.1, 75.7, 74.1, 51.9, 35.6, 27.5. **C20g**: ^1H NMR (400 MHz, CDCl_3) δ 7.52 – 7.30 (m, 5H), 4.57 (dd, $J = 5.8, 2.7$ Hz, 1H), 2.73 (dd, $J = 17.7, 5.9$ Hz, 1H), 2.54 (dd, $J = 17.7, 2.7$ Hz, 1H), 1.76 (s, 3H). ^{13}C NMR (101 MHz, CDCl_3) δ 174.3, 144.0, 128.4, 127.1, 124.9, 90.0, 75.3, 37.7, 22.6.

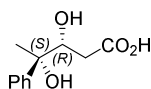
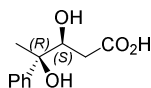
Experimental section

(3*S*,4*S*) and (3*R*,4*R*)-3,4-dihydroxy-4-phenylpentanoic acid (**C21a**)



The compound **C20d** (70 mg, 0.31 mmol, 1eq) was resuspended in a solution of MeOH:H₂O (3:1, v/v, 40 mL) and LiOH (37.4 mg, 1.56 mmol, 5 eq) was added. The solution was stirred at 5 °C overnight. After that time, H₂O (100 mL) was added and the pH of the solution adjusted to pH 5 with HCl (1 M). The MeOH was removed under vacuum. The pH of the resulting solution was basified, and the mixture washed with EtOAc (3 x 50 mL). The pH of the aqueous solution was acidified and extracted with Et₂O (3 x 50 mL). The combined organic layers were dried over MgSO₄ and the solvent evaporated under reduced pressure affording **C21a** (41 mg, 63%). ¹H NMR (400 MHz, MeOD) δ 7.59 – 7.16 (m, 5H), 4.15 (dd, *J* = 10.2, 2.5 Hz, 1H), 2.52 (dd, *J* = 15.7, 2.6 Hz, 1H), 2.03 (dd, *J* = 15.7, 10.2 Hz, 1H), 1.56 (s, 3H). ¹³C NMR (101 MHz, MeOD) δ 174.8, 145.0, 127.4, 126.4, 125.8, 75.3, 75.0, 36.7, 24.4.

(3*S*,4*R*) and (3*R*,4*S*)-3,4-dihydroxy-4-phenylpentanoic acid (**C21b**)



The title compound was prepared following the same procedure described for **C21a** affording **C21b** (338 mg, 79%). ¹H NMR (400 MHz, MeOD) δ 7.43 – 7.05 (m, 5H), 4.04 (dd, *J* = 10.2, 2.5 Hz, 1H), 2.23 (dd, *J* = 15.8, 10.2 Hz, 1H), 2.05 (dd, *J* = 15.8, 2.5 Hz, 1H), 1.46 (s, 3H). ¹³C NMR (101 MHz, MeOD) δ 175.0, 146.1, 127.7, 126.3, 125.0, 75.6, 74.6, 36.4, 25.3.

BIBLIOGRAPHY

1. Nelson, D. L.; Cox, M. M.; Lehninger, A. L., *Principles of biochemistry*. 4th ed.; Freeman: New York, 2008.
2. Voet, D.; Voet, J. G., *Biochemistry*. 4th ed.; John Wiley & Sons Inc: New York, 2011.
3. Purich, D. L., *Enzyme kinetics: catalysis and control: a reference of theory and best-practice methods*. 1st ed.; Elsevier: London, 2010.
4. Jimenez-Morales, D.; Liang, J.; Eisenberg, B., Ionizable side chains at catalytic active sites of enzymes. *Eur. Biophys. J.* **2012**, *41* (5), 449-460.
5. Hudlicky, T.; Reed, J. W., Applications of biotransformations and biocatalysis to complexity generation in organic synthesis. *Chem. Soc. Rev.* **2009**, *38* (11), 3117-3132.
6. Faber, K., *Biotransformations in organic chemistry*. 6th ed.; Springer-Verlag: Berlin, 2011.
7. Alcalde, M.; Ferrer, M.; Plou, F. J.; Ballesteros, A., Environmental biocatalysis: from remediation with enzymes to novel green processes. *Trends Biotechnol.* **2006**, *24* (6), 281-287.
8. Simon, R. C.; Mutti, F. G.; Kroutil, W., Biocatalytic synthesis of enantiopure building blocks for pharmaceuticals. *Drug Discov. Today Technol.* **2013**, *10* (1), 37-44.
9. Wu, S.; Snajdrova, R.; Moore, J. C.; Baldenius, K.; Bornscheuer, U. T., Biocatalysis: Enzymatic synthesis for industrial applications. *Angew. Chem. Int. Ed.* **2020**, *60*, 88-119.
10. Voet, D.; Voet, J. G.; Pratt, C. W., *Fundamentals of biochemistry: life at the molecular level*. 5th ed.; John Wiley & Sons: New York, 2016.
11. Koeller, K. M.; Wong, C.-H., Enzymes for chemical synthesis. *Nature* **2001**, *409* (6817), 232-240.
12. Sheldon, R. A.; Woodley, J. M., Role of biocatalysis in sustainable chemistry. *Chem. Rev.* **2018**, *118* (2), 801-838.
13. Basso, A.; Serban, S., Industrial applications of immobilized enzymes—A review. *Mol. Catal.* **2019**, *479*, 110607.
14. Choi, J.-M.; Han, S.-S.; Kim, H.-S., Industrial applications of enzyme biocatalysis: Current status and future aspects. *Biotechnol. Adv.* **2015**, *33* (7), 1443-1454.
15. Neto, W.; Schürmann, M.; Panella, L.; Vogel, A.; Woodley, J. M., Immobilisation of ω -transaminase for industrial application: Screening and characterisation of commercial ready to use enzyme carriers. *J. Mol. Catal. B Enzym.* **2015**, *117*, 54-61.

16. Wachtmeister, J.; Rother, D., Recent advances in whole cell biocatalysis techniques bridging from investigative to industrial scale. *Curr. Opin. Biotechnol.* **2016**, *42*, 169-177.
17. de Souza, R. O.; Miranda, L. S.; Bornscheuer, U. T., A retrosynthesis approach for biocatalysis in organic synthesis. *Chem. Eur. J.* **2017**, *23* (50), 12040-12063.
18. Liu, Q.; Xun, G.; Feng, Y., The state-of-the-art strategies of protein engineering for enzyme stabilization. *Biotechnol. Adv.* **2019**, *37* (4), 530-537.
19. Eriksen, D. T.; Lian, J.; Zhao, H., Protein design for pathway engineering. *J. Struct. Biol.* **2014**, *185* (2), 234-242.
20. Madhavan, A.; Sindhu, R.; Binod, P.; Sukumaran, R. K.; Pandey, A., Strategies for design of improved biocatalysts for industrial applications. *Bioresour. Technol.* **2017**, *245*, 1304-1313.
21. Chowdhury, R.; Maranas, C. D., From directed evolution to computational enzyme engineering—A review. *AIChE J.* **2020**, *66* (3), e16847.
22. Obexer, R.; Godina, A.; Garrabou, X.; Mittl, P. R.; Baker, D.; Griffiths, A. D.; Hilvert, D., Emergence of a catalytic tetrad during evolution of a highly active artificial aldolase. *Nat. Chem.* **2017**, *9* (1), 50-56.
23. Quin, M. B.; Schmidt-Dannert, C., Engineering of biocatalysts: from evolution to creation. *ACS Catal.* **2011**, *1* (9), 1017-1021.
24. Dick, M.; Sarai, N. S.; Martynowycz, M. W.; Gonen, T.; Arnold, F. H., Tailoring tryptophan synthase TrpB for selective quaternary carbon bond formation. *J. Am. Chem. Soc.* **2019**, *141* (50), 19817-19822.
25. Packer, M. S.; Liu, D. R., Methods for the directed evolution of proteins. *Nat. Rev. Genet.* **2015**, *16* (7), 379-394.
26. Leung, D. W., A method for random mutagenesis of a defined DNA segment using a modified polymerase chain reaction. *Technique* **1989**, *1*, 11-15.
27. Stemmer, W. P., Rapid evolution of a protein in vitro by DNA shuffling. *Nature* **1994**, *370* (6488), 389-391.
28. Greener, A.; Callahan, M.; Jerpseth, B., An efficient random mutagenesis technique using an *E. coli* mutator strain. *Mol. Biotechnol.* **1997**, *7* (2), 189-195.
29. Wong, T. S.; Tee, K. L.; Hauer, B.; Schwaneberg, U., Sequence saturation mutagenesis (SeSaM): a novel method for directed evolution. *Nucleic Acids Res.* **2004**, *32* (3), e26-e26.
30. Dominy, C. N.; Andrews, D. W., Site-directed mutagenesis by inverse PCR. In *E. coli Plasmid Vectors*, Springer: 2003; pp 209-223.

31. Hemsley, A.; Arnheim, N.; Toney, M. D.; Cortopassi, G.; Galas, D. J., A simple method for site-directed mutagenesis using the polymerase chain reaction. *Nucleic Acids Res.* **1989**, *17* (16), 6545-6551.
32. Manual, I., QuikChange® Site-Directed Mutagenesis Kit. **1998**.
33. Vallette, F.; Mege, E.; Reiss, A.; Adesnik, M., Construction of mutant and chimeric genes using the polymerase chain reaction. *Nucleic Acids Res.* **1989**, *17* (2), 723-733.
34. Xu, X.; Kang, S.-H.; Heidenreich, O.; Li, Q.; Nerenberg, M., Rapid PCR method for site-directed mutagenesis on double-stranded plasmid DNA. *BioTechniques* **1996**, *20* (1), 44-46.
35. Ling, M. M.; Robinson, B. H., Approaches to DNA mutagenesis: an overview. *Anal. Biochem.* **1997**, *254* (2), 157-178.
36. Rouwendal, G. J.; Wolbert, E. J.; Zwiers, L.-H.; Springer, J., Ligase chain reaction for site-directed in vitro mutagenesis. *In Vitro Mutagenesis Protocols* **1996**, 149-156.
37. Tomic, M.; Sunjevaric, I.; Savtchenko, E.; Blumenberg, M., A rapid and simple method for introducing specific mutations into any position of DNA leaving all other positions unaltered. *Nucleic Acids Res.* **1990**, *18* (6), 1656.
38. Owen, J.; Hay, C.; Schuster, D.; Rashtchian, A., A highly efficient method of site-directed mutagenesis using PCR and UDG cloning. *Focus* **1994**, *16*, 39-44.
39. Higuchi, R.; Krummel, B.; Saiki, R., A general method of in vitro preparation and specific mutagenesis of DNA fragments: study of protein and DNA interactions. *Nucleic Acids Res.* **1988**, *16* (15), 7351-7367.
40. Gibson, D. G.; Young, L.; Chuang, R.-Y.; Venter, J. C.; Hutchison, C. A.; Smith, H. O., Enzymatic assembly of DNA molecules up to several hundred kilobases. *Nat. Methods* **2009**, *6* (5), 343-345.
41. Kammann, M.; Laufs, J. r.; Schell, J.; Gronenborn, B., Rapid insertional mutagenesis of DNA by polymerase chain reaction (PCR). *Nucleic Acids Res.* **1989**, *17* (13), 5404.
42. Sarkar, G.; Sommer, S. S., The " megaprimer" method of site-directed mutagenesis. *BioTechniques* **1990**, *8* (4), 404-407.
43. Clapes, P.; Garrabou, X., Current trends in asymmetric synthesis with aldolases. *Adv. Synth. Catal.* **2011**, *353* (13), 2263-2283.
44. Borodin, A., Ueber die Einwirkung des Natriums auf Valeraldehyd. *J. Prakt. Chem.* **1864**, *93* (1), 413-425.
45. Podlech, J., "Try and Fall Sick..."—The Composer, Chemist, and Surgeon Aleksandr Borodin. *Angew. Chem. Int. Ed.* **2010**, *49* (37), 6490-6495.

46. Heathcock, C. H., The aldol reaction: Acid and general base catalysis. **1991**, 133-179.
47. Palomo, C.; Oiarbide, M.; García, J. M., The aldol addition reaction: an old transformation at constant rebirth. *Chem. Eur. J.* **2002**, 8 (1), 36-44.
48. Heathcock, C. H.; White, C. T.; Morrison, J. J.; VanDerveer, D., Acyclic stereoselection. 11. Double stereodifferentiation as a method for achieving superior Cram's rule selectivity in aldol condensations with chiral aldehydes. *J. Org. Chem.* **1981**, 46 (7), 1296-1309.
49. Mukaiyama, T.; Banno, K.; Narasaka, K., New cross-aldol reactions. Reactions of silyl enol ethers with carbonyl compounds activated by titanium tetrachloride. *J. Am. Chem. Soc.* **1974**, 96 (24), 7503-7509.
50. Mukaiyama, T.; Matsuo, J. I., Boron and silicon enolates in crossed aldol reaction. In *Modern Aldol Reactions*, Mahrwald, R., Ed. 2004; pp 127-160.
51. Zimmerman, H. E.; Traxler, M. D., The stereochemistry of the Ivanov and Reformatsky reactions. I. *J. Am. Chem. Soc.* **1957**, 79 (8), 1920-1923.
52. Heathcock, C. H.; Davidsen, S. K.; Hug, K. T.; Flippin, L. A., Acyclic stereoselection. 36. Simple diastereoselection in the Lewis acid mediated reactions of enol silanes with aldehydes. *J. Org. Chem.* **1986**, 51 (15), 3027-3037.
53. Evans, D. A., Studies in Asymmetric Synthesis. The Development of Practical Chiral Enolate Synthons. *Aldrichimica Acta* **1982**, 15 (2), 23-32.
54. Evans, D. A.; Urpi, F.; Somers, T. C.; Clark, J. S.; Bilodeau, M. T., New procedure for the direct generation of titanium enolates. Diastereoselective bond constructions with representative electrophiles. *J. Am. Chem. Soc.* **1990**, 112 (22), 8215-8216.
55. Heravi, M. M.; Zadsirjan, V.; Farajpour, B., Applications of oxazolidinones as chiral auxiliaries in the asymmetric alkylation reaction applied to total synthesis. *RSC Adv.* **2016**, 6 (36), 30498-30551.
56. Evans, D. A.; Rieger, D. L.; Bilodeau, M. T.; Urpi, F., Stereoselective aldol reactions of chlorotitanium enolates. An efficient method for the assemblage of polypropionate-related synthons. *J. Am. Chem. Soc.* **1991**, 113 (3), 1047-1049.
57. Mahrwald, R.; Ziemer, B., Insight into the mechanism of direct catalytic aldol addition mediated by ambifunctional titanium complexes. *Tetrahedron Lett.* **2002**, 43 (25), 4459-4461.
58. Palomo, C.; Oiarbide, M.; García, J. M., Current progress in the asymmetric aldol addition reaction. *Chem. Soc. Rev.* **2004**, 33 (2), 65-75.
59. Machajewski, T. D.; Wong, C. H., The catalytic asymmetric aldol reaction. *Angew. Chem. Int. Ed.* **2000**, 39 (8), 1352-1375.

60. Yamada, Y. M.; Yoshikawa, N.; Sasai, H.; Shibasaki, M., Direct catalytic asymmetric aldol reactions of aldehydes with unmodified ketones. *Angew. Chem., Int. Ed. Engl.* **1997**, *36* (17), 1871-1873.
61. Gaunt, M. J.; Johansson, C. C.; McNally, A.; Vo, N. T., Enantioselective organocatalysis. *Drug Discov. Today* **2007**, *12* (1-2), 8-27.
62. Mandal, S.; Mandal, S.; Ghosh, S. K.; Ghosh, A.; Saha, R.; Banerjee, S.; Saha, B., Review of the aldol reaction. *Synth. Commun.* **2016**, *46* (16), 1327-1342.
63. Yamashita, Y.; Yasukawa, T.; Yoo, W.-J.; Kitanosono, T.; Kobayashi, S., Catalytic enantioselective aldol reactions. *Chem. Soc. Rev.* **2018**, *47* (12), 4388-4480.
64. Notz, W.; List, B., Catalytic asymmetric synthesis of anti-1, 2-diols. *J. Am. Chem. Soc.* **2000**, *122* (30), 7386-7387.
65. Mahrwald, R., *Aldol Reactions*. Springer Science & Business Media: Berlin, 2009.
66. Clapés, P.; Fessner, W.-D.; Sprenger, G. A.; Samland, A. K., Recent progress in stereoselective synthesis with aldolases. *Curr. Opin. Chem. Biol.* **2010**, *14* (2), 154-167.
67. Hernández, K.; Szekrenyi, A.; Clapés, P., Nucleophile promiscuity of natural and engineered aldolases. *ChemBioChem* **2018**, *19* (13), 1353-1358.
68. Clapés, P., Aldol Reactions. In *Biocatalysis in Organic Synthesis* Faber, K.; Fessner, W.-D.; Turner, N. J., Eds. Georg Thieme Verlag KG: Stuttgart (Germany), 2015; Vol. 2, pp 31-92.
69. Fessner, W.-D.; Walter, C., Enzymatic CC bond formation in asymmetric synthesis. *Bioorg. Chem.* **1996**, 97-194.
70. Helmchen, G., *Asymmetric synthesis with chemical and biological methods*. 1st ed.; John Wiley & Sons: Weinheim, 2007.
71. Gefflaut, T.; Blonski, C.; Perie, J.; Willson, M., Class I aldolases: substrate specificity, mechanism, inhibitors and structural aspects. *Prog. Biophys. Mol. Biol.* **1995**, *63* (3), 301-340.
72. Cronan, J. E.; Littel, K.; Jackowski, S., Genetic and biochemical analyses of pantothenate biosynthesis in *Escherichia coli* and *Salmonella typhimurium*. *J. Bacteriol. Res.* **1982**, *149* (3), 916-922.
73. Sugantino, M.; Zheng, R.; Yu, M.; Blanchard, J. S., Mycobacterium tuberculosis ketopantoate hydroxymethyltransferase: Tetrahydrofolate-independent hydroxymethyltransferase and enolization reactions with α -keto acids. *Biochemistry* **2003**, *42* (1), 191-199.
74. Rubio, A.; Downs, D., Elevated levels of ketopantoate hydroxymethyltransferase (PanB) lead to a physiologically significant

- coenzyme A elevation in *Salmonella enterica* serovar Typhimurium. *J. Bacteriol. Res.* **2002**, *184* (10), 2827-2832.
75. Teller, J. H.; Powers, S.; Snell, E. E., Ketopantoate hydroxymethyltransferase. I. Purification and role in pantothenate biosynthesis. *J. Biol. Chem.* **1976**, *251* (12), 3780-3785.
76. Hunter, B. K.; Nicholls, K. M.; Sanders, J. K., Formaldehyde metabolism by *Escherichia coli*. In vivo carbon, deuterium, and two-dimensional NMR observations of multiple detoxifying pathways. *Biochemistry* **1984**, *23* (3), 508-514.
77. McIntosh, E. N.; Purko, M.; Wood, W., Ketopantoate formation by a hydroxymethylation enzyme from *Escherichia coli*. *J. Biol. Chem.* **1957**, *228* (1), 499-510.
78. Stover, P.; Schirch, V., Serine hydroxymethyltransferase catalyzes the hydrolysis of 5, 10-methenyltetrahydrofolate to 5-formyltetrahydrofolate. *J. Biol. Chem.* **1990**, *265* (24), 14227-14233.
79. von Delft, F.; Inoue, T.; Saldanha, S. A.; Ottenhof, H. H.; Schmitzberger, F.; Birch, L. M.; Dhanaraj, V.; Witty, M.; Smith, A. G.; Blundell, T. L., Structure of *E. coli* ketopantoate hydroxymethyl transferase complexed with ketopantoate and Mg²⁺, solved by locating 160 selenomethionine sites. *Structure* **2003**, *11* (8), 985-996.
80. Chaudhuri, B. N.; Sawaya, M. R.; Kim, C.-Y.; Waldo, G. S.; Park, M. S.; Terwilliger, T. C.; Yeates, T. O., The crystal structure of the first enzyme in the pantothenate biosynthetic pathway, ketopantoate hydroxymethyltransferase, from *M. tuberculosis*. *Structure* **2003**, *11* (7), 753-764.
81. Badger, J.; Sauder, J.; Adams, J.; Antonysamy, S.; Bain, K.; Bergseid, M.; Buchanan, S.; Buchanan, M.; Batiyenko, Y.; Christopher, J., Structural analysis of a set of proteins resulting from a bacterial genomics project. *Proteins* **2005**, *60* (4), 787-796.
82. Baugh, L.; Gallagher, L. A.; Patrapuvich, R.; Clifton, M. C.; Gardberg, A. S.; Edwards, T. E.; Armour, B.; Begley, D. W.; Dieterich, S. H.; Dranow, D. M., Combining functional and structural genomics to sample the essential *Burkholderia* structome. *PloS one* **2013**, *8* (1).
83. Webb, M. E.; Smith, A. G.; Abell, C., Biosynthesis of pantothenate. *Nat. Prod. Rep.* **2004**, *21* (6), 695-721.
84. Schmitzberger, F.; Smith, A. G.; Abell, C.; Blundell, T. L., Comparative analysis of the *Escherichia coli* ketopantoate hydroxymethyltransferase crystal structure confirms that it is a member of the ($\beta\alpha$) 8 phosphoenolpyruvate/pyruvate superfamily. *J. Bacteriol. Res.* **2003**, *185* (14), 4163-4171.

85. Rea, D.; Hovington, R.; Rakus, J. F.; Gerlt, J. A.; Fülöp, V.; Bugg, T. D.; Roper, D. I., Crystal structure and functional assignment of YfaU, a metal ion dependent class II aldolase from *Escherichia coli* K12. *Biochemistry* **2008**, *47* (38), 9955-9965.
86. Rea, D.; Fülöp, V.; Bugg, T. D.; Roper, D. I., Structure and mechanism of HpcH: a metal ion dependent class II aldolase from the homoprotocatechuate degradation pathway of *Escherichia coli*. *J. Mol. Biol* **2007**, *373* (4), 866-876.
87. Rakus, J. F.; Fedorov, A. A.; Fedorov, E. V.; Glasner, M. E.; Hubbard, B. K.; Delli, J. D.; Babbitt, P. C.; Almo, S. C.; Gerlt, J. A., Evolution of enzymatic activities in the enolase superfamily: L-rhamnonate dehydratase. *Biochemistry* **2008**, *47* (38), 9944-9954.
88. Izard, T.; Blackwell, N. C., Crystal structures of the metal-dependent 2-dehydro-3-deoxy-galactarate aldolase suggest a novel reaction mechanism. *EMBO J.* **2000**, *19* (15), 3849-3856.
89. Desmons, S.; Fauré, R.; Bontemps, S., Formaldehyde as a promising C1 source: The instrumental role of biocatalysis for stereocontrolled reactions. *ACS Catal.* **2019**, *9* (10), 9575-9588.
90. Hernandez, K.; Bujons, J.; Joglar, J. s.; Charnock, S. J.; Dominguez de Maria, P.; Fessner, W. D.; Clapés, P., Combining aldolases and transaminases for the synthesis of 2-amino-4-hydroxybutanoic acid. *ACS Catal.* **2017**, *7* (3), 1707-1711.
91. Hernández, K.; Gómez, A.; Joglar, J.; Bujons, J.; Parella, T.; Clapés, P., 2-Keto-3-Deoxy-l-Rhamnonate Aldolase (YfaU) as Catalyst in Aldol Additions of Pyruvate to Amino Aldehyde Derivatives. *Adv. Synth. Catal.* **2017**, *359* (12), 2090-2100.
92. Hernández, K.; Joglar, J.; Bujons, J.; Parella, T.; Clapés, P., Nucleophile Promiscuity of Engineered Class II Pyruvate Aldolase YfaU from *E. Coli*. *Angew. Chem. Int. Ed.* **2018**, *57* (14), 3583-3587.
93. Roush, W. R.; Palkowitz, A. D.; Ando, K., Acyclic diastereoselective synthesis using tartrate ester-modified crotylboronates. Double asymmetric reactions with. α -methyl chiral aldehydes and synthesis of the C (19)-C (29) segment of rifamycin S. *J. Am. Chem. Soc.* **1990**, *112* (17), 6348-6359.
94. Paterson, I.; Florence, G. J.; Gerlach, K.; Scott, J. P., Total Synthesis of the Antimicrotubule Agent (+)-Discodermolide Using Boron-Mediated Aldol Reactions of Chiral Ketones. *Angew. Chem.* **2000**, *112* (2), 385-388.
95. Mickel, S. J.; Sedelmeier, G. H.; Niederer, D.; Daeffler, R.; Osmani, A.; Schreiner, K.; Seeger-Weibel, M.; Bérod, B.; Schaer, K.; Gamboni, R., Large-scale synthesis of the anti-cancer marine natural product (+)-discodermolide. Part 1: synthetic strategy and preparation of a common precursor. *Org. Process Res. Dev.* **2004**, *8* (1), 92-100.

96. Reddy, S. V.; Kumar, K. P.; Ramakrishna, K. V.; Sharma, G. V., Approaches towards the total synthesis of carolacton: synthesis of C1–C16 fragment. *Tetrahedron Lett.* **2015**, *56* (15), 2018-2022.
97. Klar, U.; Buchmann, B.; Schwede, W.; Skuballa, W.; Hoffmann, J.; Lichtner, R. B., Total synthesis and antitumor activity of ZK-EPO: the first fully synthetic epothilone in clinical development. *Angew. Chem. Int. Ed.* **2006**, *45* (47), 7942-7948.
98. Barbie, P.; Kazmaier, U., Total synthesis of cyclomarins A, C and D, marine cyclic peptides with interesting anti-tuberculosis and anti-malaria activities. *Org. Biomol. Chem.* **2016**, *14* (25), 6036-6054.
99. Zhou, J.; Gao, B.; Xu, Z.; Ye, T., Total synthesis and stereochemical assignment of callyspongiolide. *J. Am. Chem. Soc.* **2016**, *138* (22), 6948-6951.
100. Trost, B. M.; Sieber, J. D.; Qian, W.; Dhawan, R.; Ball, Z. T., Asymmetric total synthesis of soraphen A: A flexible alkyne strategy. *Angew. Chem. Int. Ed.* **2009**, *48* (30), 5478-5481.
101. Defosseux, M.; Blanchard, N.; Meyer, C.; Cossy, J., Total synthesis of zincophorin and its methyl ester. *J. Org. Chem.* **2004**, *69* (14), 4626-4647.
102. Boeckman Jr, R. K.; Miller, J. R., Direct Enantioselective Organocatalytic Hydroxymethylation of Aldehydes Catalyzed by α , α -Diphenylprolinol Trimethylsilyl Ether. *Org. Lett.* **2009**, *11* (20), 4544-4547.
103. Bruckner, S.; Bilitewski, U.; Schobert, R., Synthesis and antibacterial activity of four stereoisomers of the spider-pathogenic fungus metabolite torrubiellone D. *Org. Lett.* **2016**, *18* (5), 1136-1139.
104. Galletti, P.; Quintavalla, A.; Ventrice, C.; Giannini, G.; Cabri, W.; Penco, S.; Gallo, G.; Vincenti, S.; Giacomini, D., Azetidinones as Zinc-Binding Groups to Design Selective HDAC8 Inhibitors. *ChemMedChem* **2009**, *4* (12), 1991-2001.
105. Hu, X.; Nguyen, K. T.; Verlinde, C. L.; Hol, W. G.; Pei, D., Structure-based design of a macrocyclic inhibitor for peptide deformylase. *J. Med. Chem.* **2003**, *46* (18), 3771-3774.
106. Yu, L.; Zhou, W.; Wang, Z., Synthesis and in vitro antibacterial activity of oxazolidine LBM-415 analogs as peptide deformylase inhibitors. *Bioorg. Med. Chem. Lett.* **2011**, *21* (5), 1541-1544.
107. McKinnell, R. M.; Fatheree, P.; Choi, S.-K.; Gendron, R.; Jendza, K.; Olson Blair, B.; Budman, J.; Hill, C. M.; Hegde, L. G.; Yu, C., Discovery of TD-0212, an Orally Active Dual Pharmacology AT1 Antagonist and Nephilysin Inhibitor (ARNI). *ACS Med. Chem. Lett.* **2018**, *10* (1), 86-91.
108. van Leeuwen, P. W. N. M.; Claver, C., *Rhodium Catalyzed Hydroformylation*. Kluwer: Dordrecht, 2000.

109. Yu, Z.; Eno, M. S.; Annis, A. H.; Morken, J. P., Enantioselective Hydroformylation of 1-Alkenes with Commercial Ph-BPE Ligand. *Org. Lett.* **2015**, *17* (13), 3264-3267.
110. Wei, Y.; Shi, M., Recent advances in organocatalytic asymmetric morita–baylis–hillman/aza-morita–baylis–hillman reactions. *Chem. Rev.* **2013**, *113* (8), 6659-6690.
111. Shimizu, H.; Saito, T.; Kumobayashi, H., Synthesis of novel chiral benzophospholanes and their application in asymmetric hydrogenation. *Adv. Synth. Catal.* **2003**, *345* (1-2), 185-189.
112. Wassenaar, J.; Kuil, M.; Reek, J. N., Asymmetric Synthesis of the Roche Ester and its Derivatives by Rhodium-INDOLPHOS-Catalyzed Hydrogenation. *Adv. Synth. Catal.* **2008**, *350* (10), 1610-1614.
113. Rütthlein, E.; Classen, T.; Dobnikar, L.; Schölzel, M.; Pietruszka, J., Finding the selectivity switch—a rational approach towards stereocomplementary variants of the ene reductase YqjM. *Adv. Synth. Catal.* **2015**, *357* (8), 1775-1786.
114. Nett, N.; Duewel, S.; Richter, A. A.; Hoebenreich, S., Revealing additional stereocomplementary pairs of old yellow enzymes by rational transfer of engineered residues. *ChemBioChem* **2017**, *18* (7), 685-691.
115. Walton, A. Z.; Conerly, W. C.; Pompeu, Y.; Sullivan, B.; Stewart, J. D., Biocatalytic reductions of Baylis–Hillman adducts. *ACS Catal.* **2011**, *1* (9), 989-993.
116. Stueckler, C.; Winkler, C. K.; Bonnekessel, M.; Faber, K., Asymmetric synthesis of (R)-3-hydroxy-2-methylpropanoate ('Roche ester') and derivatives via biocatalytic C=C-bond reduction. *Adv. Synth. Catal.* **2010**, *352* (14-15), 2663-2666.
117. Boeckman Jr, R. K.; Biegasiewicz, K. F.; Tusch, D. J.; Miller, J. R., Organocatalytic enantioselective α -hydroxymethylation of aldehydes: mechanistic aspects and optimization. *J. Org. Chem.* **2015**, *80* (8), 4030-4045.
118. Yasui, Y.; Benohoud, M.; Sato, I.; Hayashi, Y., Asymmetric Aldol Reaction of Formaldehyde Catalyzed by Diarylprolinol. *Chem. Lett.* **2014**, *43* (4), 556-558.
119. Lang, K.; Buehler, K.; Schmid, A., Multistep Synthesis of (S)-3-Hydroxyisobutyric Acid from Glucose using *Pseudomonas taiwanensis* VLB120 B83 T7 Catalytic Biofilms. *Adv. Synth. Catal.* **2015**, *357* (8), 1919-1927.
120. Bueschleb, M.; Dorich, S.; Hanessian, S.; Tao, D.; Schenthal, K. B.; Overman, L. E., Synthetic strategies toward natural products containing contiguous stereogenic quaternary carbon atoms. *Angew. Chem. Int. Ed.* **2016**, *55* (13), 4156-4186.

121. Hu, P.; Chi, H. M.; DeBacker, K. C.; Gong, X.; Keim, J. H.; Hsu, I. T.; Snyder, S. A., Quaternary-centre-guided synthesis of complex polycyclic terpenes. *Nature* **2019**, *569* (7758), 703-707.
122. Stockdale, T. P.; Williams, C. M., Pharmaceuticals that contain polycyclic hydrocarbon scaffolds. *Chem. Soc. Rev.* **2015**, *44* (21), 7737-7763.
123. Yoshimura, F.; Itoh, R.; Torizuka, M.; Mori, G.; Tanino, K., Asymmetric total synthesis of Brasilicardins. *Angew. Chem. Int. Ed.* **2018**, *57* (52), 17161-17167.
124. Liu, Y.; Han, S.-J.; Liu, W.-B.; Stoltz, B. M., Catalytic enantioselective construction of quaternary stereocenters: assembly of key building blocks for the synthesis of biologically active molecules. *Acc. Chem. Res.* **2015**, *48* (3), 740-751.
125. Lovering, F.; Bikker, J.; Humblet, C., Escape from flatland: increasing saturation as an approach to improving clinical success. *J. Med. Chem.* **2009**, *52* (21), 6752-6756.
126. Li, C.; Ragab, S. S.; Liu, G.; Tang, W., Enantioselective formation of quaternary carbon stereocenters in natural product synthesis: a recent update. *Nat. Prod. Rep.* **2020**, *37* (2), 276-292.
127. Pierrot, D.; Marek, I., Synthesis of Enantioenriched Vicinal Tertiary and Quaternary Carbon Stereogenic Centers within an Acyclic Chain. *Angew. Chem. Int. Ed.* **2020**, *59* (1), 36-49.
128. Li, L.; Yang, Q.; Wang, Y.; Jia, Y., Catalytic Asymmetric Total Synthesis of (-)-Galanthamine and (-)-Lycoramine. *Angew. Chem. Int. Ed.* **2015**, *54* (21), 6255-6259.
129. Ni, D.; Wei, Y.; Ma, D., Thiourea-Catalyzed Asymmetric Michael Addition of Carbazolones to 2-Chloroacrylonitrile: Total Synthesis of 5, 22-Dioxokopsane, Kopsinidine C, and Demethoxycarbonylkopsin. *Angew. Chem.* **2018**, *130* (32), 10364-10368.
130. He, W.; Hu, J.; Wang, P.; Chen, L.; Ji, K.; Yang, S.; Li, Y.; Xie, Z.; Xie, W., Highly Enantioselective Tandem Michael Addition of Tryptamine-Derived Oxindoles to Alkynones: Concise Synthesis of Strychnos Alkaloids. *Angew. Chem.* **2018**, *130* (14), 3868-3871.
131. Zhang, H.; Hong, L.; Kang, H.; Wang, R., Construction of vicinal all-carbon quaternary stereocenters by catalytic asymmetric alkylation reaction of 3-bromooxindoles with 3-substituted indoles: total synthesis of (+)-perophoramidine. *J. Am. Chem. Soc.* **2013**, *135* (38), 14098-14101.
132. Dalpozzo, R., Recent Catalytic Asymmetric Syntheses of 3, 3-Disubstituted Indolin-2-ones and 2, 2-Disubstituted Indolin-3-ones. *Adv. Synth. Catal.* **2017**, *359* (11), 1772-1810.

133. Ma, S.; Han, X.; Krishnan, S.; Virgil, S. C.; Stoltz, B. M., Catalytic Enantioselective Stereoablative Alkylation of 3-Halooxindoles: Facile Access to Oxindoles with C3 All-Carbon Quaternary Stereocenters. *Angew. Chem.* **2009**, *121* (43), 8181-8185.
134. Zhou, F.; Zhu, L.; Pan, B.-W.; Shi, Y.; Liu, Y.-L.; Zhou, J., Catalytic enantioselective construction of vicinal quaternary carbon stereocenters. *Chem. Sci.* **2020**, *11* (35), 9341-9365.
135. Cao, Z.-Y.; Wang, W.; Liao, K.; Wang, X.; Zhou, J.; Ma, J., Catalytic enantioselective synthesis of cyclopropanes featuring vicinal all-carbon quaternary stereocenters with a CH₂F group; study of the influence of C–F…H–N interactions on reactivity. *Org. Chem. Front.* **2018**, *5* (20), 2960-2968.
136. Tao, Z.; Robb, K. A.; Zhao, K.; Denmark, S. E., Enantioselective, Lewis Base-Catalyzed Sulfenocyclization of Polyenes. *J. Am. Chem. Soc.* **2018**, *140* (10), 3569-3573.
137. Peifer, M.; Berger, R. I.; Shurtleff, V. W.; Conrad, J. C.; MacMillan, D. W., A general and enantioselective approach to pentoses: a rapid synthesis of PSI-6130, the nucleoside core of sofosbuvir. *J. Am. Chem. Soc.* **2014**, *136* (16), 5900-5903.
138. Coelho, P. S.; Brustad, E. M.; Kannan, A.; Arnold, F. H., Olefin cyclopropanation via carbene transfer catalyzed by engineered cytochrome P450 enzymes. *Science* **2013**, *339* (6117), 307-310.
139. Seitz, M.; Syrén, P. O.; Steiner, L.; Klebensberger, J.; Nestl, B. M.; Hauer, B., Synthesis of heterocyclic terpenoids by promiscuous squalene-hopene cyclases. *ChemBioChem* **2013**, *14* (4), 436-439.
140. Harms, V.; Kirschning, A.; Dickschat, J. S., Nature-driven approaches to non-natural terpene analogues. *Nat. Prod. Rep.* **2020**, *37* (8), 1080-1097.
141. Guinan, M.; Benckendorff, C.; Smith, M.; Miller, G. J., Recent advances in the chemical synthesis and evaluation of anticancer nucleoside analogues. *Molecules* **2020**, *25* (9), 2050.
142. Pruijssers, A. J.; Denison, M. R., Nucleoside analogues for the treatment of coronavirus infections. *Curr. Opin. Virol.* **2019**, *35*, 57-62.
143. Thomson, J. M.; Lamont, I. L., Nucleoside analogues as antibacterial agents. *Front. Microbiol.* **2019**, *10*, 952.
144. Lapponi, M. J.; Rivero, C. W.; Zinni, M. A.; Britos, C. N.; Trelles, J. A., New developments in nucleoside analogues biosynthesis: a review. *J. Mol. Catal. B Enzym.* **2016**, *133*, 218-233.
145. Seley-Radtke, K. L.; Yates, M. K., The evolution of nucleoside analogue antivirals: A review for chemists and non-chemists. Part 1: Early structural modifications to the nucleoside scaffold. *Antivir. Res.* **2018**, *154*, 66-86.

146. Jordheim, L. P.; Durantel, D.; Zoulim, F.; Dumontet, C., Advances in the development of nucleoside and nucleotide analogues for cancer and viral diseases. *Nat. Rev. Drug Discov.* **2013**, *12* (6), 447-464.
147. Walwick, E.; Roberts, W.; Dekker, C., Cyclisation during the phosphorylation of uridine and cytidine by polyphosphoric acid-A new route to the O-2, 2'-cyclonucleosides. *J. Chem. Soc.* **1959**, (3), 84-84.
148. Hertel, L.; Kroin, J.; Misner, J.; Tustin, J., Synthesis of 2-deoxy-2, 2-difluoro-D-ribose and 2-deoxy-2, 2'-difluoro-D-ribofuranosyl nucleosides. *J. Org. Chem.* **1988**, *53* (11), 2406-2409.
149. Brown, K.; Dixey, M.; Weymouth-Wilson, A.; Linclau, B., The synthesis of gemcitabine. *Carbohydr. Res.* **2014**, *387*, 59-73.
150. Shelton, J.; Lu, X.; Hollenbaugh, J. A.; Cho, J. H.; Amblard, F.; Schinazi, R. F., Metabolism, biochemical actions, and chemical synthesis of anticancer nucleosides, nucleotides, and base analogs. *Chem. Rev.* **2016**, *116* (23), 14379-14455.
151. Charlton, M.; Gane, E.; Manns, M. P.; Brown Jr, R. S.; Curry, M. P.; Kwo, P. Y.; Fontana, R. J.; Gilroy, R.; Teperman, L.; Muir, A. J., Sofosbuvir and ribavirin for treatment of compensated recurrent hepatitis C virus infection after liver transplantation. *Gastroenterology* **2015**, *148* (1), 108-117.
152. Clark, J. L.; Hollecker, L.; Mason, J. C.; Stuyver, L. J.; Tharnish, P. M.; Lostia, S.; McBrayer, T. R.; Schinazi, R. F.; Watanabe, K. A.; Otto, M. J., Design, synthesis, and antiviral activity of 2'-deoxy-2'-fluoro-2'-C-methylcytidine, a potent inhibitor of hepatitis C virus replication. *J. Med. Chem.* **2005**, *48* (17), 5504-5508.
153. Azuma, A.; Nakajima, Y.; Nishizono, N.; Minakawa, N.; Suzuki, M.; Hanaoka, K.; Kobayashi, T.; Tanaka, M.; Sasaki, T.; Matsuda, A., Nucleosides and nucleotides. 122. 2'-C-Cyano-2'-deoxy-1- β -D-arabinofuranosylcytosine and its derivatives. A new class of nucleoside with a broad antitumor spectrum. *J. Med. Chem.* **1993**, *36* (26), 4183-4189.
154. Yin, Z.; Chen, Y.-L.; Schul, W.; Wang, Q.-Y.; Gu, F.; Duraiswamy, J.; Kondreddi, R. R.; Niyomrattanakit, P.; Lakshminarayana, S. B.; Goh, A., An adenosine nucleoside inhibitor of dengue virus. *Proc. Natl. Acad. Sci.* **2009**, *106* (48), 20435-20439.
155. Yates, M. K.; Seley-Radtke, K. L., The evolution of antiviral nucleoside analogues: A review for chemists and non-chemists. Part II: Complex modifications to the nucleoside scaffold. *Antivir. Res.* **2019**, *162*, 5-21.
156. Kirby, K. A.; Michailidis, E.; Fetterly, T. L.; Steinbach, M. A.; Singh, K.; Marchand, B.; Leslie, M. D.; Hagedorn, A. N.; Kodama, E. N.; Marquez, V. E., Effects of substitutions at the 4' and 2 positions on the bioactivity of 4'-

- ethynyl-2-fluoro-2'-deoxyadenosine. *Antimicrob. Agents Chemother.* **2013**, *57* (12), 6254-6264.
157. Salie, Z. L.; Kirby, K. A.; Michailidis, E.; Marchand, B.; Singh, K.; Rohan, L. C.; Kodama, E. N.; Mitsuya, H.; Parniak, M. A.; Sarafianos, S. G., Structural basis of HIV inhibition by translocation-defective RT inhibitor 4'-ethynyl-2-fluoro-2'-deoxyadenosine (EFdA). *Proc. Natl. Acad. Sci.* **2016**, *113* (33), 9274-9279.
158. Kohgo, S.; Yamada, K.; Kitano, K.; Iwai, Y.; Sakata, S.; Ashida, N.; Hayakawa, H.; Nameki, D.; Kodama, E.; Matsuoka, M., Design, efficient synthesis, and anti-HIV activity of 4'-C-cyano-and 4'-C-ethynyl-2'-deoxy purine nucleosides. *Nucleosides, Nucleotides and Nucleic Acids* **2004**, *23* (4), 671-690.
159. Nawrat, C. C.; Whittaker, A. M.; Huffman, M. A.; McLaughlin, M.; Cohen, R. D.; Andreani, T.; Ding, B.; Li, H.; Weisel, M.; Tschaen, D. M., Nine-Step Stereoselective Synthesis of Islatravir from Deoxyribose. *Org. Lett.* **2020**, *22* (6), 2167-2172.
160. Fukuyama, K.; Ohru, H.; Kuwahara, S., Synthesis of EFdA via a diastereoselective aldol reaction of a protected 3-keto furanose. *Org. Lett.* **2015**, *17* (4), 828-831.
161. McLaughlin, M.; Kong, J.; Belyk, K. M.; Chen, B.; Gibson, A. W.; Keen, S. P.; Lieberman, D. R.; Milczek, E. M.; Moore, J. C.; Murray, D., Enantioselective synthesis of 4'-ethynyl-2-fluoro-2'-deoxyadenosine (EFdA) via enzymatic desymmetrization. *Org. Lett.* **2017**, *19* (4), 926-929.
162. Kageyama, M.; Nagasawa, T.; Yoshida, M.; Ohru, H.; Kuwahara, S., Enantioselective total synthesis of the potent anti-HIV nucleoside EFdA. *Org. Lett.* **2011**, *13* (19), 5264-5266.
163. Huffman, M. A.; Fryszkowska, A.; Alvizo, O.; Borra-Garske, M.; Campos, K. R.; Devine, P. N.; Duan, D.; Forstater, J. H.; Grosser, S. T.; Halsey, H. M., Design of an in vitro biocatalytic cascade for the manufacture of islatravir. *Science* **2019**, *366* (6470), 1255-1259.
164. Patel, N. R.; Huffman, M. A.; Wang, X.; Ding, B.; McLaughlin, M.; Newman, J. A.; Andreani, T.; Maloney, K. M.; Johnson, H. C.; Whittaker, A. M., Five-Step Enantioselective Synthesis of Islatravir via Asymmetric Ketone Alkynylation and an Ozonolysis Cascade. *Chem. Eur. J.* **2020**, *26* (62), 14118-14123.
165. Hansen, B. A.; Lane, R. S.; Dekker, E. E., Formaldehyde Binding by 2-Keto-4-hydroxyglutarate Aldolase: FORMATION AND CHARACTERIZATION OF AN INACTIVE ALDOLASE-FORMALDEHYDE-CYANIDE ADDUCT. *J. Biol. Chem.* **1974**, *249* (15), 4891-4896.

166. Vagenende, V.; Yap, M. G.; Trout, B. L., Mechanisms of protein stabilization and prevention of protein aggregation by glycerol. *Biochemistry* **2009**, *48* (46), 11084-11096.
167. Wang, W.; Seah, S. Y., Purification and biochemical characterization of a pyruvate-specific class II aldolase, HpaI. *Biochemistry* **2005**, *44* (27), 9447-9455.
168. Hixon, M.; Sinerius, G.; Schneider, A.; Walter, C.; Fessner, W.-D.; Schloss, J. V., Quo vadis photorespiration: a tale of two aldolases. *FEBS Lett.* **1996**, *392* (3), 281-284.
169. Labbé, G.; de Groot, S.; Rasmusson, T.; Milojevic, G.; Dmitrienko, G. I.; Guillemette, J. G., Evaluation of four microbial Class II fructose 1, 6-bisphosphate aldolase enzymes for use as biocatalysts. *Protein Expr. Purif.* **2011**, *80* (2), 224-233.
170. Laurent, V.; Uzel, A.; Helaine, V.; Nauton, L.; Traïkia, M.; Gefflaut, T.; Salanoubat, M.; de Berardinis, V.; Lemaire, M.; Guérard-Hélaine, C., Exploration of Aldol Reactions Catalyzed by Stereoselective Pyruvate Aldolases with 2-Oxobutyric Acid as Nucleophile. *Adv. Synth. Catal.* **2019**, *361* (11), 2713-2717.
171. Brewitz, L.; Nakashima, Y.; Schofield, C. J., Synthesis of 2-oxoglutarate derivatives and their evaluation as cosubstrates and inhibitors of human aspartate/asparagine- β -hydroxylase. *Chem. Sci.* **2021**, *12* (4), 1327-1342.
172. Baker, P.; Seah, S. Y., Rational design of stereoselectivity in the class II pyruvate aldolase BphI. *J. Am. Chem. Soc.* **2012**, *134* (1), 507-513.
173. Cooper, A. J.; Ginos, J. Z.; Meister, A., Synthesis and properties of the alpha-keto acids. *Chem. Rev.* **1983**, *83* (3), 321-358.
174. Lopalco, A.; Dalwadi, G.; Niu, S.; Schowen, R. L.; Douglas, J.; Stella, V. J., Mechanism of decarboxylation of pyruvic acid in the presence of hydrogen peroxide. *J. Pharm. Sci.* **2016**, *105* (2), 705-713.
175. Hendrickson, J. B.; Kandall, C., The phenacyl protecting group for acids and phenols. *Tetrahedron Lett.* **1970**, *11* (5), 343-344.
176. Song, Y.; Li, J.; Shin, H.-d.; Liu, L.; Du, G.; Chen, J., Biotechnological production of alpha-keto acids: current status and perspectives. *Bioresour. Technol.* **2016**, *219*, 716-724.
177. Angajala, G.; Pavan, P.; Subashini, R., Lipases: an overview of its current challenges and prospectives in the revolution of biocatalysis. *Biocatal. Agric. Biotechnol.* **2016**, *7*, 257-270.
178. Luo, Z.; Yu, S.; Zeng, W.; Zhou, J., Comparative analysis of the chemical and biochemical synthesis of keto acids. *Biotechnol. Adv.* **2021**, 107706.

179. McKinley, J.; Aponick, A.; Raber, J. C.; Fritz, C.; Montgomery, D.; Wigal, C. T., Reactions of alkyllithium and grignard reagents with benzoquinone: Evidence for an electron-transfer mechanism. *J. Org. Chem.* **1997**, *62* (14), 4874-4876.
180. Mathew, L.; Warkentin, J., The cyclopropylmethyl free-radical clock. Calibration for the range 30-89 °C. *J. Am. Chem. Soc.* **1986**, *108* (25), 7981-7984.
181. Künding, E. P.; Perret, C., Low Temperature Grignard Reactions with Pure Mg Slurries. Trapping of cyclopropylmethyl and benzocyclobutenylmethyl Grignard reagents with CO₂. *Helv. Chim. Acta* **1981**, *64* (8), 2606-2613.
182. Cushman, M.; Yang, D.; Gerhardt, S.; Huber, R.; Fischer, M.; Kis, K.; Bacher, A., Design, synthesis, and evaluation of 6-carboxyalkyl and 6-phosphonoxyalkyl derivatives of 7-oxo-8-ribitylaminolumazines as inhibitors of riboflavin synthase and lumazine synthase. *J. Org. Chem.* **2002**, *67* (16), 5807-5816.
183. Lissel, M., Phase Transfer Catalysis for Preparation and Alkylation of Ethyl 1, 3-Dithiane-2-carboxylate. *Synth. Commun.* **1981**, *11* (4), 343-346.
184. Morrison, K. L.; Weiss, G. A., Combinatorial alanine-scanning. *Curr. Opin. Chem. Biol.* **2001**, *5* (3), 302-307.
185. Hammes, G. G.; Morrell, M. L., A study of nickel (II) and cobalt (II) phosphate complexes. *J. Am. Chem. Soc.* **1964**, *86* (8), 1497-1502.
186. Senanayake, C. H.; Larsen, R. D.; Bill, T. J.; Liu, J.; Corley, E. G.; Reider, P. J., Enantioselective synthesis of 1, 3-dioxygen-substituted chiral building blocks. *Synlett* **1994**, *1994* (03), 199-200.
187. Tokutake, N.; Hiratake, J.; Katoh, M.; Irie, T.; Kato, H.; Oda, J. i., Design, synthesis and evaluation of transition-state analogue inhibitors of Escherichia coli γ -glutamylcysteine synthetase. *Bioorg. Med. Chem.* **1998**, *6* (10), 1935-1953.
188. Ortiz, C.; Ferreira, M. L.; Barbosa, O.; dos Santos, J. C.; Rodrigues, R. C.; Berenguer-Murcia, Á.; Briand, L. E.; Fernandez-Lafuente, R., Novozym 435: the "perfect" lipase immobilized biocatalyst? *Catal. Sci. Technol.* **2019**, *9* (10), 2380-2420.
189. Holm, T.; Crossland, I.; Richley, H., *Grignard Reagents: New Developments*. 2000.
190. Inoue, A.; Kitagawa, K.; Shinokubo, H.; Oshima, K., Simple and efficient TiCl₄-mediated synthesis of biaryls via arylmagnesium compounds. *Tetrahedron* **2000**, *56* (49), 9601-9605.
191. Suh, Y.; Lee, J.-s.; Kim, S.-H.; Rieke, R. D., Direct preparation of benzylic manganese reagents from benzyl halides, sulfonates, and phosphates

and their reactions: applications in organic synthesis. *J. Organomet. Chem.* **2003**, *684* (1-2), 20-36.

192. Li, X.; Li, D.; Li, Y.; Chang, H.; Gao, W.; Wei, W., Homocoupling of heteroaryl/aryl/alkyl Grignard reagents: I 2-promoted, or Ni-or Pd-or Cu-or nano-Fe-based salt catalyzed. *RSC Adv.* **2016**, *6* (90), 86998-87002.

193. Zagalak, B.; Frey, P. A.; Karabatsos, G.; Abeles, R. H., The stereochemistry of the conversion of D and L 1, 2-propanediols to propionaldehyde. *J. Biol. Chem.* **1966**, *241* (13), 3028-3035.

194. Serianni, A. S.; Pierce, J.; Huang, S. G.; Barker, R., Anomerization of furanose sugars: kinetics of ring-opening reactions by proton and carbon-13 saturation-transfer NMR spectroscopy. *J. Am. Chem. Soc.* **1982**, *104* (15), 4037-4044.

195. Angyal, S. J., The composition and conformation of sugars in solution. *Angew. Chem., Int. Ed. Engl.* **1969**, *8* (3), 157-166.

196. Gordon, E. M.; Duncton, M. A.; Gallop, M. A., Orally absorbed derivatives of the β -lactamase inhibitor avibactam. Design of novel prodrugs of sulfate containing drugs. *J. Med. Chem.* **2018**, *61* (22), 10340-10344.

197. Lee, D.-Y.; Hou, Y.-C.; Yang, J.-S.; Lin, H.-Y.; Chang, T.-Y.; Lee, K.-H.; Kuo, S.-C.; Hsieh, M.-T., Synthesis, anticancer activity, and preliminary pharmacokinetic evaluation of 4, 4-disubstituted curcuminoid 2, 2-bis (hydroxymethyl) propionate derivatives. *Molecules* **2020**, *25* (3), 479.

198. Athawale, P. R.; Kumari, N.; Dandawate, M. R.; Kashinath, K.; Srinivasa Reddy, D., Synthesis of Chiral Tetrahydrofuran Building Blocks from Pantolactones: Application in the Synthesis of Empagliflozin and Amprenavir Analogs. *Eur. J. Org. Chem.* **2019**, *2019* (30), 4805-4810.

199. Hajare, A. K.; Ravikumar, V.; Khaleel, S.; Bhuniya, D.; Reddy, D. S., Synthesis of molluscicidal agent cyanolide A macrolactone from D-(-)-pantolactone. *J. Org. Chem.* **2011**, *76* (3), 963-966.

200. Muthusamy, S.; Gnanaprakasam, B., Imidazolium salts as phase transfer catalysts for the dialkylation and cycloalkylation of active methylene compounds. *Tetrahedron Lett.* **2005**, *46* (4), 635-638.

201. De Meo, C.; Jones, B. T., Chemical Synthesis of Glycosides of N-Acetylneuraminic Acid. *Adv. Carbohydr. Chem. Biochem.* **2018**, *75*, 215-316.

202. Varki, A., Diversity in the sialic acids. *Glycobiology* **1992**, *2* (1), 25.

203. Varki, A., Glycan-based interactions involving vertebrate sialic-acid-recognizing proteins. *Nature* **2007**, *446* (7139), 1023-1029.

204. Wang, Y.; Ren, H.; Zhao, H., Expanding the boundary of biocatalysis: design and optimization of in vitro tandem catalytic reactions for biochemical production. *Crit. Rev. Biochem. Mol. Biol.* **2018**, *53* (2), 115-129.

205. Oroz-Guinea, I.; García-Junceda, E., Enzyme catalysed tandem reactions. *Curr. Opin. Chem. Biol.* **2013**, *17* (2), 236-249.
206. Szekrenyi, A.; Garrabou, X.; Parella, T.; Joglar, J.; Bujons, J.; Clapés, P., Asymmetric assembly of aldose carbohydrates from formaldehyde and glycolaldehyde by tandem biocatalytic aldol reactions. *Nat. Chem.* **2015**, *7* (9), 724.
207. Moreno, C. J.; Hernández, K.; Charnok, S. J.; Gittings, S.; Bolte, M.; Joglar, J. s.; Bujons, J.; Parella, T.; Clapés, P., Synthesis of γ -Hydroxy- α -amino Acid Derivatives by Enzymatic Tandem Aldol Addition–Transamination Reactions. *ACS Catal.* **2021**, *11*, 4660-4669.
208. Hocek, M., C-nucleosides: Synthetic strategies and biological applications. *Chem. Rev.* **2009**, *109* (12), 6729-6764.
209. Bouton, J.; Van Hecke, K.; Van Calenbergh, S., Efficient diastereoselective synthesis of a new class of azanucleosides: 2'-homoazanucleosides. *Tetrahedron* **2017**, *73* (30), 4307-4316.
210. De Luca, L.; Giacomelli, G.; Porcheddu, A., A very mild and chemoselective oxidation of alcohols to carbonyl compounds. *Org. Lett.* **2001**, *3* (19), 3041-3043.
211. Henderson, I.; Sharpless, K. B.; Wong, C. H., Synthesis of carbohydrates via tandem use of the osmium-catalyzed asymmetric dihydroxylation and enzyme-catalyzed aldol addition reactions. *J. Am. Chem. Soc.* **1994**, *116* (2), 558-561.
212. Hubschwerlen, C., A convenient synthesis of L-(S)-glyceraldehyde acetone from L-ascorbic acid. *Synthesis* **1986**, (11), 962-964.
213. Richter, N.; Neumann, M.; Liese, A.; Wohlgemuth, R.; Weckbecker, A.; Eggert, T.; Hummel, W., Characterization of a whole-cell catalyst co-expressing glycerol dehydrogenase and glucose dehydrogenase and its application in the synthesis of l-glyceraldehyde. *Biotechnol. Bioeng.* **2010**, *106* (4), 541-552.
214. Castillo, J. A.; Guérard-Hélaine, C.; Gutiérrez, M.; Garrabou, X.; Sancelme, M.; Schürmann, M.; Inoue, T.; Hélaine, V.; Charmantray, F.; Gefflaut, T., A mutant D-fructose-6-phosphate aldolase (Ala129Ser) with improved affinity towards dihydroxyacetone for the synthesis of polyhydroxylated compounds. *Adv. Synth. Catal.* **2010**, *352* (6), 1039-1046.
215. Bolduc, M.; Bergeron, J.; Michaud, A.; Pelchat, N.; Morin, P.; Dasser, M.; Chênevert, R., Chemoenzymatic enantioselective synthesis of 2-substituted glycerol derivatives. *Tetrahedron Asymmetry* **2012**, *23* (6-7), 428-433.
216. Loertscher, B. M.; Young, P. R.; Evans, P. R.; Castle, S. L., Diastereoselective Synthesis of Vicinal Tertiary Diols. *Org. Lett.* **2013**, *15* (8), 1930-1933.

217. Jung, S.-H.; Jeong, J.-H.; Miller, P.; Wong, C.-H., An efficient multigram-scale preparation of dihydroxyacetone phosphate. *J. Org. Chem.* **1994**, *59* (23), 7182-7184.
218. Yuasa, H.; Hashimoto, H.; Abe, Y.; Kajimoto, T.; Wong, C.-H., Studies on the Unusual Stability of cis-2, 5-Diethoxy-2, 5-bis (hydroxymethyl)-1, 4-dioxane. *Tetrahedron* **1999**, *55* (8), 2193-2204.
219. Enders, D.; Voith, M.; Ince, S. J., Preparation and reactions of 2, 2-dimethyl-1, 3-dioxan-5-one-SAMP-hydrazone: a versatile chiral dihydroxyacetone equivalent. *Synthesis* **2002**, *2002* (12), 1775-1779.
220. Forbes, D. C.; Ene, D. G.; Doyle, M. P., Stereoselective synthesis of substituted 5-hydroxy-1, 3-dioxanes. *Synthesis* **1998**, *1998* (06), 879-882.
221. Kim, J. H.; Coric, I.; Palumbo, C.; List, B., Resolution of diols via catalytic asymmetric acetalization. *J. Am. Chem. Soc.* **2015**, *137* (5), 1778-1781.
222. Ikeuchi, K.; Murasawa, K.; Ohara, K.; Yamada, H., p-Methylbenzyl Group: Oxidative Removal and Orthogonal Alcohol Deprotection. *Org. Lett.* **2019**, *21* (17), 6638-6642.
223. Dieckmann, M.; Menche, D., Stereoselective Synthesis of 1, 3-anti Diols by an Ipc-Mediated Domino Aldol-Coupling/Reduction Sequence. *Org. Lett.* **2013**, *15* (1), 228-231.
224. Mootoo, D. R.; Fraser-Reid, B., The pyranosidic homologation route to the nine contiguous chiral centers of streptovaricin A1. *Tetrahedron* **1990**, *46* (1), 185-200.
225. Sun, J.; Dong, Y.; Cao, L.; Wang, X.; Wang, S.; Hu, Y., Highly efficient chemoselective deprotection of O, O-acetals and O, O-ketals catalyzed by molecular iodine in acetone. *J. Org. Chem.* **2004**, *69* (25), 8932-8934.
226. Nagase, H.; Watanabe, A.; Harada, M.; Nakajima, M.; Hasebe, K.; Mochizuki, H.; Yoza, K.; Fujii, H., Novel synthesis of a 1, 3, 5-trioxazatriquinane skeleton using a nitrogen clamp. *Org. Lett.* **2009**, *11* (3), 539-542.
227. McHale, W. A.; Kutateladze, A. G., An Efficient Photo-SET-Induced Cleavage of Dithiane- Carbonyl Adducts and Its Relevance to the Development of Photoremovable Protecting Groups for Ketones and Aldehydes. *J. Org. Chem.* **1998**, *63* (26), 9924-9931.
228. Kuwajima, I.; Minami, N.; Sato, T., A convenient method for the preparation of β -hydroxy esters. *Tetrahedron Lett.* **1976**, *17* (26), 2253-2256.
229. Paquette, L. A.; Chang, J.; Liu, Z., Synthetic Studies Aimed at (-)-Cochleamycin A. Evaluation of Late-Stage Macrocyclization Alternatives. *J. Org. Chem.* **2004**, *69* (19), 6441-6448.

230. Madala, M.; Raman, B.; Sastry, K.; Musulla, S., A concise stereoselective total synthesis of verbalactone. *Monatsh. Chem.* **2016**, *147* (11), 1985-1990.
231. Martin, S. F.; Hida, T.; Kym, P. R.; Loft, M.; Hodgson, A., The asymmetric synthesis of erythromycin B. *J. Am. Chem. Soc.* **1997**, *119* (13), 3193-3194.
232. Drikermann, D.; Mößel, R. S.; Al-Jammal, W. K.; Vilotijevic, I., Synthesis of Allylboranes via Cu (I)-Catalyzed B–H Insertion of Vinyl diazoacetates into Phosphine–Borane Adducts. *Org. Lett.* **2020**, *22* (3), 1091-1095.
233. Dupau, P.; Epple, R.; Thomas, A. A.; Fokin, V. V.; Sharpless, K. B., Osmium-catalyzed dihydroxylation of olefins in acidic media: Old process, new tricks. *Adv. Synth. Catal.* **2002**, *344* (3-4), 421-433.
234. Corey, E.; Székely, I.; Shiner, C. S., Synthesis of 6, 9 α -oxido-11 α , 15 α -dihydroxyprosta-(E) 5,(E) 13-dienoic acid, an isomer of PGI₂ (vane's PGX). *Tetrahedron Lett.* **1977**, *18* (40), 3529-3532.
235. Afon'kin, A.; Kostrikin, L.; Shumeiko, A.; Popov, A.; Matveev, A.; Matvienko, V.; Zabudkin, A., Regio- and stereoselective methods for the conversion of (2 S, 3 R)- β -phenylglycidic acid esters to taxoids and other enantiopure (2 R, 3 S)-phenylisoserine esters. *Russ. Chem. Bull.* **2012**, *61* (11), 2149-2162.
236. Qi, J.; Xie, X.; He, J.; Zhang, L.; Ma, D.; She, X., N-Heterocyclic carbene-catalyzed cascade epoxide-opening and lactonization reaction for the synthesis of dihydropyrene derivatives. *Org. Biomol. Chem.* **2011**, *9* (17), 5948-5950.
237. Greene, T. W.; Wuts, P. G., Protective groups in organic synthesis. **1999**.
238. Lu, H.; Yu, S.; Qin, F.; Ning, W.; Ma, X.; Tian, K.; Li, Z.; Zhou, K., A secretion-based dual fluorescence assay for high-throughput screening of alcohol dehydrogenases. *Biotechnol. Bioeng.* **2021**, *118* (4), 1605-1616.
239. Szekrenyi, A.; Soler, A.; Garrabou, X.; Guérard-Hélaine, C.; Parella, T.; Joglar, J.; Lemaire, M.; Bujons, J.; Clapés, P., Engineering the Donor Selectivity of D-Fructose-6-Phosphate Aldolase for Biocatalytic Asymmetric Cross-Aldol Additions of Glycolaldehyde. *Chem. Eur. J.* **2014**, *20* (39), 12572-12583.
240. Altschul, S. F.; Gish, W.; Miller, W.; Myers, E. W.; Lipman, D. J., Basic local alignment search tool. *J. Mol. Biol.* **1990**, *215* (3), 403-410.
241. Laemmli, U. K., Cleavage of structural proteins during the assembly of the head of bacteriophage T4. *nature* **1970**, *227* (5259), 680-685.

242. Simpson, R. J., Disruption of cultured cells by nitrogen cavitation. *Cold Spring Harbor Protocols* **2010**, 2010 (11), pdb. prot5513.
243. Zhang, Z.; Marshall, A. G., A universal algorithm for fast and automated charge state deconvolution of electrospray mass-to-charge ratio spectra. *J. Am. Soc. Mass Spectrom.* **1998**, 9 (3), 225-233.
244. Lebarillier, L.; Outurquin, F.; Paulmier, C., Synthesis and Reactivity of α - and β -Chloro- α -phenylselenanyl Esters. *Tetrahedron* **2000**, 56 (38), 7495-7502.
245. Rapf, R. J.; Perkins, R. J.; Yang, H.; Miyake, G. M.; Carpenter, B. K.; Vaida, V., Photochemical synthesis of oligomeric amphiphiles from alkyl oxoacids in aqueous environments. *J. Am. Chem. Soc.* **2017**, 139 (20), 6946-6959.
246. Wong, M.-K.; Chung, N.-W.; He, L.; Wang, X.-C.; Yan, Z.; Tang, Y.-C.; Yang, D., Investigation on the regioselectivities of intramolecular oxidation of unactivated C–H bonds by dioxiranes generated in situ. *J. Org. Chem.* **2003**, 68 (16), 6321-6328.
247. Berryhill, S.; Price, T.; Rosenblum, M., . beta.-Lactam synthesis using organoiron intermediates. Preparation of 3-carbomethoxycarbapenam. *J. Org. Chem.* **1983**, 48 (2), 158-162.
248. Barton, D. H.; Chern, C.-Y.; Jaszberenyi, J. C., The invention of radical reactions. Part XXXIV. Homologation of carboxylic acids to α -keto carboxylic acids by Barton-ester based radical chain chemistry. *Tetrahedron* **1995**, 51 (7), 1867-1886.
249. Qiu, M.; Wang, D.-Y.; Hu, X.-P.; Huang, J.-D.; Yu, S.-B.; Deng, J.; Duan, Z.-C.; Zheng, Z., Asymmetric synthesis of chiral Roche ester and its derivatives via Rh-catalyzed enantioselective hydrogenation with chiral phosphine-phosphoramidite ligands. *Tetrahedron Asymmetry* **2009**, 20 (2), 210-213.
250. Hu, B.; Prasad, M.; Har, D.; Prasad, K.; Repič, O.; Blacklock, T. J., An efficient synthesis of (R)-2-butyl-3-hydroxypropionic acid. *Org. Process Res. Dev.* **2007**, 11 (1), 90-93.
251. Lin, D. W.; Masuda, T.; Biskup, M. B.; Nelson, J. D.; Baran, P. S., Synthesis-guided structure revision of the sarcodonin, sarcoviolin, and hydnellin natural product family. *J. Org. Chem.* **2011**, 76 (4), 1013-1030.
252. Luyten, M. A.; Bur, D.; Wynn, H.; Parris, W.; Gold, M.; Friesen, J. D.; Jones, J. B., An evaluation of the substrate specificity, and of its modification by site-directed mutagenesis, of the cloned L-lactate dehydrogenase from *Bacillus stearothermophilus*. *J. Am. Chem. Soc.* **1989**, 111 (17), 6800-6804.